Long-Run Incremental Cost Pricing for Improving Voltage Profiles of Distribution Networks in a Deregulated Environment

Matlotse, Edwin

Award date:
2010

Awarding institution:
University of Bath

UNIVERSITY OF

BATH

Long-Run Incremental Cost Pricing for Improving Voltage Profiles of Distribution Networks in a Deregulated Environment

by
Edwin Matlotse
BEng, MSc

Thesis submitted for the degree of
Doctor of Philosophy
in
The Department of
Electronic and Electrical Engineering
University of Bath
September 2010

Signature: Date:

Abstract

Electricity network pricing approaches play a fundamental role in establishing whether providing the network service function is economically beneficial to both the network operators and other stakeholders, namely, network users. Many pricing methodologies have been developed since the late 80's. The earlier approaches were not based on economic principle while the latest are directed to being more based on economic principle as the shift is towards deregulated and privatized electric power industry as opposed to the earlier vertically regulated regime. As a result, many such methodologies based on economic principle have emerged and these reflect the investment cost incurred in circuits and transformers to support real and reactive power flow. However, to reflect investment cost incurred for maintaining network voltages in network charges has received very little attention in network charges. Therefore, this research work is aimed to create a charging approach to recover investment cost, by the network operator, for maintaining the network voltages.

This thesis presents a new long-run incremental cost (LRIC) pricing approach for distribution networks and demonstrates the course of action of evaluating and allocating the network asset cost in the context of maintaining network voltages. Also, it should be noted that this approach can be used for transmission networks. Firstly, the LRIC-voltage network pricing approach for reflecting the future network VAr compensation assets is proposed. Then, this approach is extended to consider n-1 contingency situation as per statutory requirement that the network should be able to withstand such contingencies in order to enhance reasonable security and reliability in its network. Lastly, this LRIC-voltage network charging methodology is again extended to reflect the charges for existing network VAr compensation assets. In addition, this LRIC-voltage network pricing approach is improved to reflect better the nodal charges as the respective nodal voltage degradation rates, given corresponding load growth rate, are determined based on the P-V curve concept. The advantages of all these incorporate the ability to reflect correct forward-looking charges, to recognize both real and reactive powers, to provide locational charges and to provide charges for both generation and demand customers.

In addition, two fundamental studies were conducted to demonstrate the trend in which the LRIC-voltage network charges would follow given different networks and different load growth rates. What set apart the LRIC-voltage network charges are those two parameters. Moreover, with regard to different networks, this was a defining moment as to how the aforementioned charges should be sought given transmission and distribution networks.

A pricing software package utilizing load-flow has been developed implementing the proposed LRIC-voltage network pricing methodology and, its extensions. This software can well be utilized by transmission and distribution companies for analyzing their cost.

The LRIC-voltage network pricing methodology and its extensions, are all demonstrated on the IEEE 14-bus test system and a practical distribution test network in the South Wales area of England, UK.

Acknowledgements

I would like to direct my well deserved sincere thanks and appreciation to my supervisor, Dr. Furong Li, for her endless guidance and support which resulted in helping me to maintain my motivation all the way through my research work.

Also, I would like to thank my colleague, Hui Yi Heng, to have shared information with me time and, time again and as such helped me to progress. In addition, I would like to thank my ex-colleagues, the whole power group, the industrialists (who are linked to this power group) and the rest of the electronic & electrical department staff for the support they have afforded me until to the end.

Also, I would like to thank my lovely wife, Mrs. Pelonomi Beatrice Matlotse, and my son, Taolo Liam Matlotse, for the support and courage they have afforded me especially at times when I mostly needed such. Furthermore, I would like to direct my gratitude to my niece and nephews, Yolanda Modumedisi, Leatso Modumedisi and Katlo Matlotse, since they kept asking me to tell them as to when would I be coming back home for good. This, in turn, was enough motivation to propel myself to work hard, finish and return home.

Lastly, I am delighted to dedicate this thesis to my mother, Mrs Emily Magadi Matlotse, who supported me throughout my youth life and beyond, against all the odds, particularly after the passing of my father.

Contents

List of Figures

List of Tables

List of Abbreviations

AC – Alternating Current

AHP – Analytical Hierachical Process

AIC – Average Incremental Cost

ARR – Annual Revenue Requirements

DC – Direct Current

DCLF – DC load flow

DGs – Distribution Generations

DISCOs – Distribution Companies

DNA – Deoxyribo Nucleic Acid

DNO – Distribution Network Owner

DRM – Distribution Reinforcement Model

EAs – Evolutionary Algorithms

EGs – Embedded Generators

EP – Evolutionary Programming

FACTS – Flexible AC Transmission Systems

FR & FC – Fixed Reactor & Fixed Capacitor

GAs – Genetic Algorithms

GENCOs – Generating Companies

GMM – Generation Meter Multipliers

GRG – Generalised Reduced Gradient

GTO – Gate Turn Off

HM – Heuristic Method

ICRP – Investment Cost-Related Pricing

IEEE – Institute of Electrical and Electronics Engineers

ISOs – Independent System Operators

kW – kilowatts

kWh – kiloWatt hour

LP – Linear Programming

LRIC – Long-Run Incremental Cost

LRMC – Long-Run Marginal Cost

MIP - Mixed Integer Programming

MSC – Mechanically Switched Capacitors

MVAr- MegaVArs

MW – MegaWatts

NEDL – Northern Electric Distribution Ltd

NETA – New Electricity Trading Arrangements

NLP – Non Linear Programming

OFGEM – Office of Gas and Electricity Markets

O&M – Operation & Maintenance

POOLCO – Pool Company

PV – Present Value

P-V curve – Power-Voltage Curve

PWRR – Present Worth Revenue Requirement

RETAILCOs – Retail Companies

RPP – Reactive Power Planning

R/X ratios – Resistance/Reactance ratios

SA – Simulated Annealing

SCC – Self-Commutated Converter Compensator

SDM – Simultaneous Maximum Demand

SQP – Successive Quadratic Programming

SR – Saturable Reactor

SRMC – Short-Run Marginal Cost

SSSC – Solid-State Series Compensator

SRIC – Short-Run Incremental Cost

STATCOM – Static Synchronous Compensation

SVCs – Static VAr Compensators

SVS – Solid-State Synchronous Voltage Source

TCR – Thyristor-Controlled Reactor

TCT – Thyristor Controlled Transformer

TNUoS – Transmission Network Use of System

TRANSCOs – Transmission Companies

UK – United Kingdom

UPFC – Unified Power Flow Converter

VAr – Reactive Power

WPD – Western Power Distribution

List of Symbols

a_1 - Coefficient of a quadratic equation

a_2 - Coefficient of a linear equation

a_3 - Coefficient of a piecewise linear equation

a_4 - Coefficient of a piecewise linear equation

AIC - Average incremental cost

$AssetCost$ - Cost of asset in sterling pounds

$Asset\ Cost_{CbL}$ - Node b modern equivalent asset cost to cater for supporting voltage due to lower voltage limit violation in sterling pounds

$Asset\ Cost_{CbH}$ - Node b modern equivalent asset cost to cater for supporting voltage due to upper voltage limit violation in sterling pounds

b - Network node index

B' - Negative of network admittance matrix

b_1 - Coefficient of a quadratic equation

b_2 - Coefficient of a linear equation

b_3 - Coefficient of a piecewise linear equation

b_4 - Coefficient of a piecewise linear equation

bH - Total number of affected nodal upper voltage limits

bL - Total number of affected nodal lower voltage limits

BMC_i - Basic marginal cost at bus i

B_t - Set of network buses involved in transaction t

C - Cost of a power transaction

$\bar{c}$ - expansion constant in £/MW/km/yr

$C_{c\max}$ - Maximum reactive power support possible to add in pu

c_1 - Coefficient of a quadratic equation

CF_L - Nodal contingency factor with respect to the corresponding lower voltage limit

CF_H - Nodal contingency factor with respect to the corresponding upper voltage limit

d - Discount rate

$dC(P)$ - Cost change due to marginal power change

$DICRP$ - Distribution ICRP

$DICRP_N$ - Distribution ICRP at node N

$d(P_i)$ - Marginal power change at bus i

ΔD_y - Load increment in year y

$\tilde{e}_{ij}$ - Vector with its elements zero, except for the element that corresponds to node i, equals +1, and the element that corresponds to node j, which equals -1

f - Bus index

$F_{j,t}$ - Maximum flow on facility j for transaction t

f_{ij} - Power flow on branch between bus i and bus j

i - Index for a bus

IC_i - Incremental Cost at bus i

ΔIC_N - Reinforcement costs at node N

IV_{bL} - Annualized incremental cost of the network nodal items associated with node b with respect to the lower voltage limit

IV_{bH} - Annualized incremental cost of the network nodal items associated with node b with respect to the upper voltage limit

j - Index for a bus

l - Transmission line index

l_{ij} - length of line between bus i and bus j

$LRIC_N$ - Long-Run Incremental Cost at bus N

$LRIC\_V_{N,L}$ - LRIC-V network charges at node N with respect to the lower voltage limit

$LRIC\_V_{N,H}$ - LRIC-V network charges at node N with respect to the upper voltage limit

$LRMC_i$ - Long-Run Marginal Cost at bus i

MC_i - Marginal cost at bus i

N - Node index

n - Time horizon in years

n_1 - Time horizon after nodal perturbation in years

n_{bL} - Node b lower voltage limit number of years

n_{bH} - Node b upper voltage limit number of years

n_{bLnew} - Node b lower voltage limit number of years after nodal perturbation

n_{bHnew} - Node b upper voltage limit number of years after nodal perturbation

NG - Number of generating buses

NL - Number of load buses

ΔOC - Operating cost change

ΔOC_N - Operating cost change at node N

$\Delta OCost_y$ - added operational costs in year y

P - Power before incremental/marginal change

P' - Real power injections vector

P_1 - Quadratic equation power in pu

P_2 - Linear equation power in pu

P_3 - Piecewise linear equation power in pu

P_4 - Piecewise linear equation power in pu

p - total MW.km of egn. (2.13)

P_{AB} - real power from busbars, A to B

ΔP_{bIn} - Real power injection/withdrawal at bus b in MW

P_C - Nodal power collapse point, in MW, with the corresponding voltage collapse point, V_C

P_D - Power demand in MW

P_{Di} - Power demand at bus i in MW

P_{di} - Real power demand at bus i in pu

P_{gi} - Real power generation at bus i in pu

$P_{gi}^{\min}$ - Real power generation lower limit at bus i in pu

$P_{gi}^{\max}$ - Real power generation upper limit at bus i in pu

P_H - Nodal power at the upper nodal voltage limit, V_H in pu

P_i - Net real power injection at bus i in MW (peak demand conditions)

$P_{i,t}$ - Injected power at bus i due to transaction t

ΔP_i - Total power injected at bus i

ΔP_{iN} - Power injected at node N

P_{ij} - Power transfer on line between bus i and bus j in pu

P_L - Nodal power at the lower nodal voltage limit, V_L, pu

ΔP_N - Real power change at bus N

P_O - Nodal power at the original nodal loading level at the corresponding nodal

voltage, V_O, in pu

P_{O_L} - Nodal power between P_O and P_L at the corresponding nodal voltage, V_{O_L}, pu

P_{O_H} - Nodal power (pu) between P_H and P_O at the corresponding nodal voltage, V_{O_H}, in pu

P_{peak} - Entire system load at the time of system peak load

P_t - Transaction t load

$P_{T\max}$ - Maximum power transfer limit in pu

PV - Present value without increment

PV_1 - Present value with increment

PV_{bL} - Present value at bus b with respect to the lower voltage limit

PV_{bH} - Present value at bus b with respect to the upper voltage limit

PV_{bLnew} - New present value at bus b with respect to lower voltage limit consequent to perturbation at this bus

PV_{bHnew} - New present value at bus b with respect to upper voltage limit consequent to perturbation at this bus

ΔPV_{bL} - Present value change at bus b with respect to the lower voltage limit consequent to nodal withdrawal/injection $\Delta P_{bIn}/\Delta Q_{bIn}$

ΔPV_{bH} - Present value change at bus b with respect to the upper voltage limit consequent to nodal withdrawal/injection $\Delta P_{bIn}/\Delta Q_{bIn}$

ΔPV - Nodal present value change

PX_t - MW-mile value of transaction t

Q_{AB} - reactive power from busbars, A to B

ΔQ_{bIn} - Reactive power injection/withdrawal at bus b in MVAr

Q_{ci} - Reactive power support from new capacitor at bus i in pu

Q_{di} - Reactive power demand at bus i in pu

Q_{gen} - Generated SVC reactive power in MVAr

Q_{gi} - Reactive power generation at bus i in pu

$Q_{gi}^{\min}$ - Reactive power generation lower limit at of bus i in pu

$Q_{gi}^{\max}$ - Reactive power generation upper limit at of bus i in pu

$Q_{\min}$ - Minimum reactive power limit in MVAr

$Q_{\max}$ - Maximum reactive power limit in MVAr

ΔQ_N - VAr change at bus N

R - line resistance

R_t - Price for transaction t

S_B - System power base in MVA

SMC - Surrogate Marginal Cost

$SRMC_f$ - Short-Run Marginal Cost at bus f

$\Delta SInv_y$ - system investment in year y

T - Time horizon in years of the expansion plan

t - Transacted power

TC - Total network charges

TIC - Total incremental cost

TU_t - System capacity use by transaction t in MW-mile

$UnitCost$ - Unit cost

V - Busbar current voltage level in pu

v - Nodal voltage degradation rate given a constant load growth (%)

V_1 - Nodal voltage attained after increment in pu

V_A - busbar A voltage

ΔV_{AB} - voltage difference between bus A and bus B

V_b - Voltage at bus b

$V_{b_{CF_L}}$ - New nodal voltage limit for the lower bus voltage limit in pu

$V_{b_{CFH}}$ - New nodal voltage limit for the upper bus voltage limit in pu

$V_{b_{SVC}}$ - Resulting node voltage corresponding to Q_{gen} in pu

ΔV_{bL} - Voltage change consequent upon an additional $\Delta P_{bIn}/\Delta Q_{bIn}$ withdrawal/injection at node b with respect to the lower voltage limit

ΔV_{bH} - Voltage change consequent upon an additional $\Delta P_{bIn}/\Delta Q_{bIn}$ withdrawal/injection at node b with respect to the upper voltage limit

V_C - Nodal voltage collapse point in pu

V_H - Upper nodal voltage limit in pu

ΔV_H - Additional nodal voltage with respect to the corresponding upper voltage limit due to the most severe n-1 contingency condition in pu

V_i - Voltage at node i in pu

$V_i^{\min}$ - Lower voltage limit on bus i in pu

$V_i^{\max}$ - Upper voltage limit on bus i pu

V_j - Voltage at node j in pu

V_L - Nodal lower voltage limit in pu

ΔV_L - Additional nodal voltage with respect to the corresponding lower voltage limit due to the most severe n-1 contingency condition in pu

V_{Limit} - Nodal voltage limit in pu

V_O - Nodal voltage at the original nodal loading level in pu

V_{O_L} - Nodal voltage between V_O and V_L in pu

V_{O_H} - Nodal voltage between V_O and V_H in pu

w - Total MW.km of egn. (2.18)

w^* - Local minimum w

W_j - Weight of the capacity use of facility j

X - Line reactance

x_{ij} - Reactance of line between bus i and bus j in pu

Y - Time horizon in years of the expansion plan

Y_{ij} - Element of network admittance matrix between buses *i* and *j* in pu

α - Responsibility of distribution system in terms of zone associated with transmission network

β - Responsibility of network user to the distribution system capacity peak hour

β_t - Factor including the discount rate in year t

δ_i - Voltage angle at bus i in radians

δ_j - Voltage angle at bus *j* in radians

∂p - Change in p

∂P - Change in P

∂P_D - Change in P_D

∂P_{Di} - Change in P_{Di}

$\partial \theta$ - Change in θ

∂w^* - Change in w^*

∂P_{Di} - Change in P_{Di}

θ - Voltage phase angle vector (reference node excluded)

θ_i - Voltage phase angle at node i

θ_{ij} - Phase angle of Y_{ij}

θ_j - Voltage phase angle at node j

$\bar{\lambda^T}$ - Differential of eqn. (2.17) with respect to P_D vector

λ_i - Lagrange multiplier at bus i

Chapter 1

Introduction

In this chapter, the background information about the electricity network pricing, power system reactive power (VAr) and reactive power planning (RPP) and pricing are introduced. Next, the motivation of this research, which is focussed on Long-Run Incremental Cost (LRIC) pricing for improving the voltage profile of distribution network, is outlined. Thereafter, the main contributions of this study are also summarized. Finally, this thesis layout is presented.

1.1 Background

1.1.1 Deregulation and Restructuring of the Electricity Power Industry

Many developing and industrialized countries have been undergoing liberalization as a major trend in the reform of their respective electricity power industries, since the late 20th century. The idea was to introduce competition – where competition was deemed possible, and to regulate – where competition was not considered practicable [2]. Consequent to this power industry restructuring and decentralization, electricity is a commodity to be traded by generators, suppliers and other traders.

Compared to telecommunication and transportation sectors, the electricity power industry is transforming from being state-owned monopolies to competitive entities. In accordance to this electricity market's hierarchy and architecture, these companies were disaggregated into a number of individual business functions carrying out one or more of the newly defined industry functions, namely,

- generation (transmission connected)
- transmission
- distribution
- supply (energy retail)

Generating companies (GENCOs) are responsible for the generation function while the transmission companies (TRANSCOs) and distribution companies (DISCOs) are responsible for transmission and distribution functions, respectively.

In the above mentioned structure, generation and supply then became the pivot having potential to develop into competitive business functions, whereas ownership and operation of the transmission and distribution networks were viewed as natural monopolies and, as such, their actions and business revenue inevitably required independent centrally administered regulation. Also, for the latter business functions, with regulation, open, non-discriminatory access to the grid for all market participants was to be ensured. Moreover, these latter functions are charged with the responsibility to develop and maintain an efficient, co-ordinated and economical system of electricity transport. In addition, to facilitate competition in generation and supply of electricity, and facilitate a mechanism to charge for the use of and connection to their systems employing rational methodologies which reflect, as far as reasonably practicable, the costs incurred [3, 4, 5]. Suppliers (RETAILCOs) are organisations who buy electricity and other related services, and sell them to customers. Even though these companies are separate legal entities, they are interconnected into an electrical system as shown below in figure 1.1.

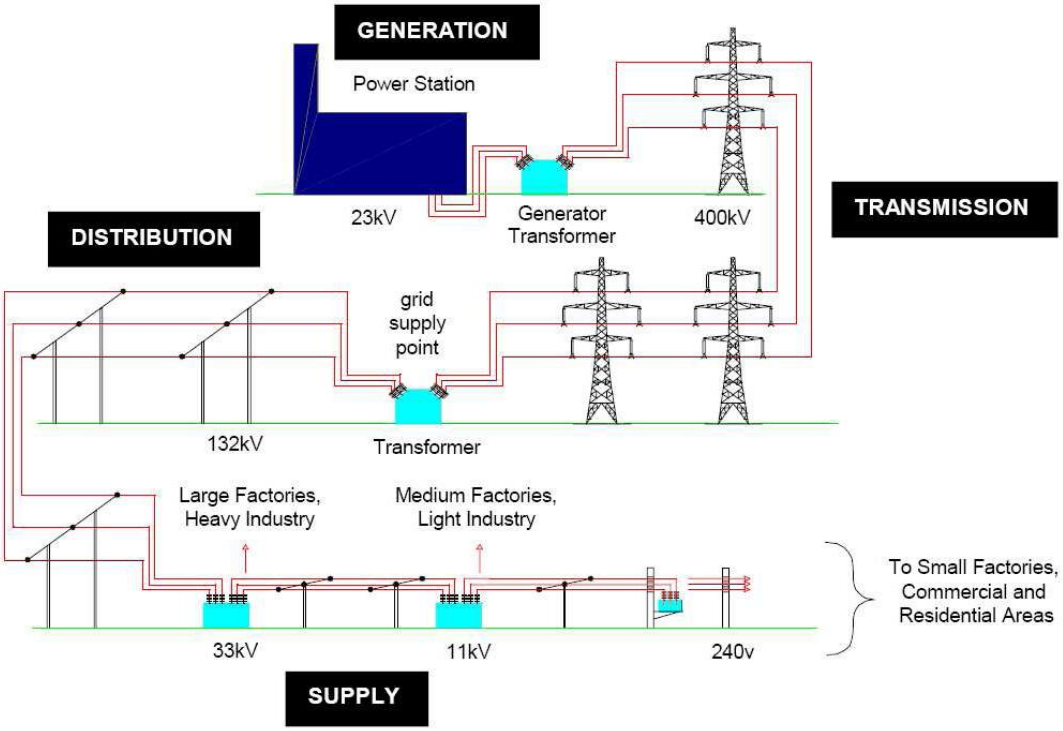

Figure 1.1: An integrated electricity system [6]

The deregulation and restructuring took effect for the first time in Chile in the late 1970's. This model was regarded as successful in the context of being rational and transparent to power pricing. Though this model was highly regarded, it had some large incumbents holding market power and suffered from the attendant structural problems. Argentina was next and they adopted the Chilian model which they improved by enhancing reliability. This was achieved by imposing stringent limits on the concentration of the market by improving the structure of payments to units held in reserve. This propagation of deregulation into Argentina improved the reliability of their system since under the government monopoly, it suffered a number of disruptions due to the bad condition of the generating units [7]. Thereafter, many countries followed by introducing deregulation and restructuring.

In 1990 privatisation was introduced in the United Kingdom (England and Wales) in a bid to increase efficiency and reduce costs in the electric power industry. The UK model propagated into other countries such as Australia, New Zealand, e.t.c. This deregulation process took different shapes and forms as it propagated but the underlying principles and concepts remain the same. Specifically, for the UK, this operated as electricity pool for the production and trading of the wholesale electricity arrangements. Later, the electricity pool setup was reformed to become New Electricity Trading Arrangements (NETA) in which energy could be traded bilaterally among generators and supplies. Moreover, capacity could be traded in daily, weekly, monthly and even annually, in advance. This arrangement was competitive and for the interest of customer, as it was recorded [8] for the period April 2001 to February 2002, peak prices fell by 27% and base load prices fell by 20%. In April 2005, NETA became the British Electricity Trading Transmission Arrangements (BETTA), thus expanding to being the single Great Britain electricity market of England, Wales and Scotland.

1.1.2 Reactive Power

Overhead lines, underground lines, transformers and shunt devices (reactors and capacitors) are components of an AC electrical distribution system. These components display the following characteristics:

- capacitance -which provides a good measure of how a plant item can store electrical charge.
- resistance -which provides a good measure of how a plant item can absorb a electrical power and convert it to heat.
- inductance -which provides a good measure of how a plant item can create a magnetic field due to electrical current passing through it.

The capacitive and inductive instances of the power system produce the charging and magnetising currents, respectively, which result in reactive power. The current waveform is 90˚ out of phase with the voltage across its terminals when pure reactive loads are connected. The current can be resolved into two parts in complex loads, one in phase with the voltage and the other 90˚ out of phase with the voltage [9, 10].

Real power can be converted into mechanical and other forms (useful work) and reactive power can not. In essence real power is the transfer of physical energy across an electrical power system and its unit of measurement is megawatts (MW) and reactive power is measured in megavars (MVAr). In contrast, reactive power bounces back and forth across the system (every half cycle) propagating between the magnetic field of inductors and the electric fields of capacitors.

The equation below shows the relation between the scalar voltage difference between two nodes in a network and, the flow of reactive power and real power [10].

$$\Delta V_{AB} = \frac{RP_{AB} + XQ_{AB}}{V_A} + j\frac{XP_{AB} - RQ_{AB}}{V_A} \tag{1.1}$$

The transmission angle is defined by this relation:

$$\partial\theta = \frac{XP - RQ}{V} \tag{1.2}$$

Since for the distribution systems, the ratio of X to R is approximately small, therefore from eqn. 1.1, it can clearly be seen that the voltage difference can be varied by controlling the flow of both reactive and real powers [9].

The above relation depicted by eqn. 1.1 has a significant influencing on the power system operation. In order to guarantee the quality and reliability of a power system, the load bus voltages should be maintained within their acceptable limits. This latter factor is ensured

by having a sufficient supply of reactive power readily available to the system operator [9]. This is due to the fact that, if there is a deficiency or surplus of reactive power at a node the voltage at that node will fall or rise, respectively. This instance of installing plant item on a power system for providing or drawing reactive power is termed as reactive power compensation. The next section will outline why reactive power compensation is important.

1.1.3 Why reactive power compensation

The profile of power generation and reactive power support are changing continuously, therefore, there is always a need for reactive power compensation since the instantaneous reactive power of a system is continuously changing due to number of challenges, as listed below.

- **Temporal cycles**

  Changing VAr needs are due to the daily and seasonal changes in the system loading and load type. Usually during daytime, the power systems are heavily loaded, therefore, the voltage decreases. This is as a consequent of overhead lines which generate reactive power when lightly loaded or otherwise absorb reactive power when fully loaded. Given this scenario inevitably this is one of the operational instances and, therefore, has attracted the attention of reactive power dispatch and optimization communities employing techniques described by [11].

- **Topographic/profile changes**

  Considering the distribution system over a horizon of a number of years, there are two fundamental considerations that must take effect. Firstly, the physical structure of the system is continuously changing. For instance, major demand centres change as industrial or domestic areas expand or contract and generation sets may be commissioned or decommissioned. Secondly, with the processes of privatisation getting more and more refined, and movement towards free markets for real and reactive power supply, market forces affect the choice of generators (in essence shifting the power flow pattern across the system). This calls for stringent planning considerations and, therefore, the system operator requires to be constantly evaluating and predicting the shape of the future needs for reactive power and ensuring those needs are met when the time is right.

- **Contingencies**

  Contingency is failure of plant item. This refers to loss of a generator, loss of a line, e.t.c. With or without credible contingencies, the power system has to be secure and stable, as a statutory requirement. During a contingent action, busbar voltages and line power flows can instantly and significantly change as

the loading of the lines change to cover demand. This results with different reactive power needs to support the voltage.

In essence, there must be enough reactive power capability (from generators and compensation devices) on the system to ensure that an acceptable voltage profile can be maintained for normal and contingent conditions of operation.

1.1.4 Network Voltage Control and Pricing

Although the process of worldwide structuring of the electricity power industry has many substantial benefits (as outlined above), however, it introduced some inherent few problems and, one such, has been the network voltage instability which at times led to several major voltage collapse incidents in the world. Owing to this restructuring, voltage instability is due to power systems being operated closer to their transmission capability limits due to economic and environmental concerns. The problem is often compounded by delays in developing transmission lines resulting from lengthy and complex approval process, particularly to interconnect independent power systems. These aforementioned effects, makes it difficult to control the reactive power demand and, hence difficult to retain network nodal voltages within prescribed limits.

Given the above voltage problem, it is imperative to formulate some stringent measures to ensure that the network nodal voltages are kept within required limits. The natural way of dealing with the problem is to have distributed VAr resources through out the network, with static (reactors and capacitor banks) and dynamic (generators, synchronous condensors, SVCs, STATCOM e.t.c) sources balanced through out the entire network resulting from the reactive power planning process. In addition, the network voltage control could be enhanced by developing an economic charging paradigm to price for the improvement of the network voltage profile.

The network (transmission and distribution systems) is expected to operate securely and efficiently as this is the key to the electricity market efficiency. Specifically, distribution network owners (DNOs) are charged with the responsibility for developing, operating and maintaining their electrical systems, to maintain a certain acceptable degree of reliability and availability. Also, distribution companies are required to deal with distribution network power quality and outage issues. In turn, the transmission and distribution systems charge users for the use of their electricity networks. In this regard, the pricing methodologies play a pivotal role in establishing whether or not providing “wires” is economically viable and sustainable to both the utilities and other market players. The current trends are such that, the power sector is based upon economic efficiency which would inherently lead to technical efficiency as its basis for decision-making. To that end, the network prices should be able to facilitate fair and equitable competition in the trading of energy and services. Also, these prices should be a reasonable economic indicator utilized by the market to make informed decisions on resource allocation, system expansion and reinforcement. In addition to this economic consideration, market and political concerns also plays a major part in the overall process of network asset prices [6, 12]. As a measure of checks and balances, the activities of the network companies have to be independently regulated since transmission and distribution systems are natural

monopolies. Such regulatory body in the UK, is the Office of Gas and Electricity Markets (OFGEM).

Based upon the above, therefore, the dominant intention in the deregulated and privatized electric power industry has been to generate new efforts to create appropriate frameworks to encourage efficient utilization of network assets. Maintaining the security and quality of supply is one of the key issues required for the network operators. Specifically, this requires the network operators (NOs) to ensure that their network nodal voltages are within specified lower and upper limits. This can be achieved by the use of the reactive power compensation devices in supporting the nodal voltages whilst transporting real power thus improving the efficiency of the network.

On the other hand, reactive power support can be categorized as a component that supports real power shipment, supplies reactive loads and provides reserve for maintaining voltage profiles under steady state and following credible contingencies. To this effect, network operators are required to secure adequate balanced reactive power support through-out their networks to assist real power shipment coupled with improving network security. The process of ensuring adequate VAr support on the network is referred to as reactive power planning (RPP). The reactive power support in a network comes from three sources:

- generators that can generate reactive power
- networks for carrying and producing reactive power for maintaining the security and quality of supply
- suppliers who affect consumers' reactive power consumption expressed by [13] in terms of lines and transformers

The fundamental requirement for any efficient charging methodology from the view point of regulatory authorities, is to develop a scheme which will ensure that the concerned network asset investment is cost effective and, also, it is best utilized. To this effect, significant amount of research into methodologies to establish the resulting charges has been carried-out, however, these reflect the investment cost incurred in circuits and transformers to support real and reactive power flow, as would be reflected in chapters 3 and 4. These methodologies are based on the "extent of use" of a network by the network users in which as a result the cost of the network is assigned. Unfortunately, to reflect investment cost incurred for maintaining network voltages in network charges has received very little attention in network charges. In addition, power factor (pf) penalty approach, which is currently used to recover charges for generator operating costs, has been seen as inconsistent (no basis for the choice of pf penalty threshold as a number of network companies have different pf thresholds) and inadequate by many researchers [14, 15, 16, 17, 18] and it is also not based on economic principle. Moreover, pf penalty approach only penalise network users operating at power factor below the preset threshold and fails to incentive those users who otherwise operating above the required pf threshold. Furthermore, every network user impacts on the network during either nodal withdrawal or injection and, therefore, that impact should be evaluated and, finally, be allocated to network users in an equitable manner.

Therefore, it is against the aforementioned background that this particular research is directed at formulating a scheme for charging to price the network cost for improving the overall network voltage profile. Given the prevailing current renewed sense of purpose in tackling environmental issues entailed in many government policies, which were motivated by the Kyoto protocol as mentioned by [19-21], renewable energy generation sources, e.g. wind power generators in the UK, are sought to provide the solution for the most part. In turn, SVCs are sought to be the network VAr compensation assets to be mostly used since they are able to effectively regulate the fast voltage changes due to uncertain wind power outputs [6, 22, 23, 24]. To this end, UK has pledged to increase the renewable power energy sources by 10% in 2010, 20% by 2020 and, finally, by 60% by 2050 [23].

1.2 Motivation

Most research in reactive power pricing [14, 25-35] reflects the benefits from generation, reflecting the operational cost due to new customers, i.e. how they might change network losses. This research work is concerned with the support from the network, particularly, the pricing of reactive power devices in the network in maintaining the network voltage profiles within acceptable limits as per statutory requirement.

The investment costs of maintaining network voltages within acceptable limits should be recovered from generators, large industrial customers and suppliers. A scheme for network charging to reflect the potential impact on network voltages needs to satisfy two fundamental purposes:

1. to recover capital, operation and maintenance costs of the network VAr compensation assets thus enabling the concerned network establishments to gain a reasonable rate of return on the capital invested

2. to provide forward-looking, economically efficient signals that reflect both the extent of the network VAr compensation assets required to service withdrawal and/or injection and at the degree of network VAr compensation asset use. This aims to influence the future use of the system by the network users to better the system voltage profiles.

Most of the network pricing approaches satisfy the first purpose while ignoring the latter as the resulting charges are not forward-looking and do not influence the future use of the system to benefit the network.

Research work objectives:

- To Formulate the LRIC-voltage network charging approach to price for the future network SVCs.

- To extend the LRIC-voltage network approach to support the network given n-1 circuit contingency situation.

- To conduct studies to establish the trends assumed by LRIC-voltage network charges given different networks and different demand growth rates.

- To extend the LRIC-voltage network charging approach to price for the existing network SVCs.

- To formulate the improved version of the LRIC-voltage network charges.

- To undertake a comprehensive literature review of transmission and distribution network pricing methodologies concerning circuits and transformers. This is to be executed in view of setting the scene for the new proposed LRIC-voltage network approach to be undertaken.

1.3 Contribution

The main thrust of this research was to establish a novel long-run incremental cost (LRIC) pricing methodology for charging for the future and existing network reactive power (VAr) compensation assets. Even though this LRIC pricing methodology was meant to be utilized for the distribution networks, it may, however be utilized for the transmission networks, as well. Consequently, this aforementioned pricing paradigm was demonstrated in evaluating network asset costs in improving the overall network voltage profile and, subsequently, apportioning these costs equitably among the network users.

The major contributions in this research work are as follows:

- LRIC-voltage network charging pricing for future network SVCs

The LRIC-voltage network charging pricing for future network SVCs is the proposed long-run incremental cost pricing principle based on nodal voltage to reflect the additional investment cost in network reactive power (VAr) compensation assets when accommodating new generation/demand, reflecting the cost to the network in ensuring that nodal voltages are within statutory limits. This proposed approach makes use of spare capacity or headroom of nodal voltage of an existing network (distribution and transmission systems) to provide the time to invest in reactive power compensation devices. A nodal power withdrawal or injection will impact on system voltages, which as a result will defer or advance the future investment costs of VAr compensation devices. The LRIC-voltage network charge aims to reflect the impact on network voltage profiles consequent upon nodal power perturbation. This approach provides forward-looking signals that reflect both the voltage profiles of an existing network and the associated indicative future network cost of VAr compensation assets. The forward-looking LRIC-voltage charges can be used to influence the location of future generation/demand for bettering network security. Comparing this proposed approach with the currently used power factor (pf) penalty, it is found that it outweighs the currently used approach. The proposed charging approach is able to penalise the users

who advance closer the network investment horizons and reward those that defer the network investment horizons in the context of the network nodal future VAr compensation assets. The currently used power factor penalty approach can only penalise the defaulters who operate below the set power factor threshold but fails to reward those users who otherwise operate above this set pf. Practically, every network users has an impact on the network whether positive or negative as depicted by the proposed novel approach. This aforementioned impact by the user should be evaluated and, therefore, be accounted for in any associated charging approach.

- LRIC-voltage network charging pricing principle to support a network given n-1 circuit contingencies

The LRIC-voltage network charging pricing for future network SVCs was extended to withstand n-1 contingency situation, as per statutory requirement. Therefore, to ensure system security and reliability practically, the resulting network nodal voltage limits have to be determined given n-1 contingencies. It should be noted that, during these n-1 contingencies, the nodal bus margins are reduced and if these are allowed to be operated at full capacity, the system security and reliability would be compromised if one of these contingencies occurred. The results showed that the respective charges follow the same pattern as the LRIC-voltage network charges without considering n-1 contingencies but are increased since the nodal busbar voltage margins are reduced to these specific types of contingencies.

It should be noted that, for electrical corridors having single circuits, their contingency factors would be unity for the sake of not compromising the integrity of the concerned network in terms of causing any network constraint violations (nodal voltages, line currents, line power flows, e.t.c.). This means that, the n-1 contingencies would not be carried out for such circuits. This refers mostly to radial networks. It should also be noted that, even for densely meshed networks, where a concerned n-1 contingency compromises the integrity of the network, such a contingency should be guarded against.

- LRIC-voltage network charging pricing principle for charging for existing network SVCs

The LRIC-v network charging pricing for future network SVCs was further extended to cater for pricing existing network SVCs. It should be noted that when an SVC is sited at a node, provided the SVC is operated within its VAr capability range, the voltage at that particular node remains constant at a preset value. Since the strength of the LRIC-v network charging principle for future network SVCs is based on changing voltage at a particular node, this charging approach could not work for pricing the existing network SVCs. It should be also noted that, at an SVC connected node, only the SVC VAr loading varies while this device is performing its voltage controlling task. Ultimately, at the SVC installed node, the SVC VAr lower limit was mapped to the nodal voltage lower limit while the SVC VAr upper limit was mapped to the nodal voltage upper limit. Consequently, the impact induced on the particular SVCs given nodal perturbation could then be successfully measured and, therefore, priced as well.

- LRIC-voltages network charges on the system with different R/X ratios

Studies were conducted on different networks to establish the trends assumed by LRIC-v network charges given these kinds of networks. Specifically, different networks represented a practical reality ranging from transmission to distribution systems, in that these networks have different circuit R/X ratios. The advantages of this comprehensive charging principle include the ability to reflect forward-looking costs, to recognize both real and reactive power perturbations, to distinguish network nodal costs and to reflect the costs/credits incurred by generation/demand. This proposed LRIC-v network charging principle better reflects the impact caused by users as compared to the currently used approach based on power factor penalty [6, 15, 25, 26, 27]. The power factor penalty approach is inadequate and not cost reflective as after charging the remaining costs are recovered by harmonising them among all network users, which may result in cross-subsidization among the users. The results show that when the network circuit Xs are atleast ten times more than their R counterparts, only MVAr nodal perturbations should be considered. When the network circuit Rs, on the other hand, are atleast ten folds more than their Xs counterparts, then, only MW nodal perturbations should be considered. Finally, when the network circuit Xs and their corresponding Rs are comparable, both MVAr and MW nodal perturbations should be considered.

- LRIC-voltage network charges with different demand load growth rates

Also, studies were conducted on different load growths to establish the trends assumed by LRIC-v network charges given different load growths of 1%, 1.6% and 2%. Specifically, there are different LRIC-v charges for different load growths. The results show that the LRIC-v network charges given different load growth rates are a function of the system nodal voltage loading levels.

- Improved implementation for LRIC- voltage network charges

This improvement emanates from the premise that the voltage change at a node and its corresponding power (MVA) change are related to each other by the P-V curve. As such, the best approximation of this relationship was used to execute the nodal voltage degradation rates resulting from the load growth rate and, finally, the improved LRIC-v network charges were sought. The results show that improved LRIC-v network charges are less than the LRIC-v network charges since the nodal voltage degradation rates for the latter are less than those of the former.

- Rigorous literature review

Moreover, in this thesis, a comprehensive literature review of transmission and distribution network pricing methodologies concerning circuits and transformers is undertaken. Most

of those pricing approaches are explained. Most emphasis was on the pricing approaches for UK transmission and distribution network companies. In addition, rigorous reviews of VAr compensation assets and optimisation techniques for these assets are undertaken.

The proposed comprehensive LRIC-voltage network charging principle is demonstrated on the IEEE-14 bus test system and, finally, a practical distribution test network in the South Wales area of England.

1.4 Thesis Layout

This thesis is organized as follows:

Chapter 2 discusses the various methods of pricing the network use of the system.

Chapter 3 discusses the network pricing in the UK and other countries, currently in use. Lastly, the concept of LRIC in pricing of reactive power compensation devices is briefly introduced.

Chapter 4 deals, in more pronounced details, with the formulation and explanation of the novel approach of long-run incremental cost (LRIC)-voltage network pricing methodology, which forms the core of this research work.

In **chapter 5**, the proposed LRIC-voltage network pricing methodology formulated and explained in the chapter 5 is extended to reflect the true burden on a power system to support network voltages under n-1 contingencies, as per statutory requirement.

In **chapter 6**, studies were performed to analyse the trend of LRIC-voltage network charges on different types of networks and different demand load growths. These undertakings provide insights into how charges would change with different network circuit resistance/reactance (R/X) ratios and different demand load growths, respectively.

In **chapter 7**, the LRIC-voltage network charging principle for pricing the use of future SVCs which was discussed in chapter 5, is extended to price, also, for the use of existing network SVCs.

In **chapter 8**, an improved version of the LRIC-v network charges is formulated and explained.

Finally, **chapter 9**, is composed of the final conclusions and future work.

Chapter 2

Network Pricing Theory

This chapter starts by introducing the network pricing methodology objectives. Next, the existing network pricing methodologies are reviewed. These methodologies are segregated into three distinctive main categories of embedded, incremental and composite embedded/incremental paradigms. Also, the pros and cons of each of the methodologies are outlined. Finally, the long-run incremental pricing methodologies under the incremental paradigm are further discussed, since they are advanced methodologies in use, in the UK.

2.1 Network Pricing Methodology Objectives

The most fundamental principle of any network pricing methodology is to apportion all or part of the existing and new cost of a network system to the network users. Since the basis of the operation of the electricity market is the result of the policies and directives set by respective government in each respective country, the network pricing methodologies should adopt similar objectives, those include cost reflectivity, encourage efficient use of existing network, simplicity, transparency, predictability and minimizing investment in serving increasing load [6]. These objectives are outlined below.

Cost reflectivity: Any network pricing paradigm used should reflect the costs incurred by network operators (TRANSCOs or DISCOs) in their transmission or distribution business functions [36]. This factor is stipulated as one of the conditions of the transmission or distribution license and advocates that the pricing approaches should be driven by the network asset costs. In addition, the revenue recovered from the tariffs charged for the usage of network services should be adequate to recover all the expense incurred in the investment, operation and maintenance, and also a regulated level of profit. This cost recovery exercise is usually termed as "revenue reconciliation".

Encouraging efficient network use: The price should provide incentives to encourage efficient use of the electricity network. This network efficient usage can be attributed to technical efficiency which minimizes network losses and minimize future network investment. Also, efficient use means the price should provide locational signals to customers to make an economic choice whether to buy or not.

Simplicity: The pricing approach should be as simple as possible to be easily understandable. Even though the implementation of the respective pricing methodologies may not be so easy but the pricing scheme should be easily understandable.

Transparency: This means everybody has access to information that helps them to understand the process. The pricing approaches should be to discharge the correct economic signals to all network participants. It should be fair and justifiable.

Predictability: The concerned pricing scheme should produce a tariff following a correct economic prediction as this is important for all network participants to forecast the possible future cost.

Minimize investment: The prices and the dividends paid to various network owners should provide an incentive for the investment in new infrastructure as and when necessary.

It should be noted that cost reflectivity remains an essential driver for pricing schemes. Other factors like encouraging efficient use, simplicity, transparency and predictability are expected to benefit GENCOs and RETAILCOs. TRANSCOs and DISCOs will benefit from incentives for improved efficiency and reduced cost. In addition to all above, there are more potential benefit functions, such as independence, competition facilitation, e.t.c.

2.2 Network Pricing Paradigms

Most existing and proposed network models are cost based. The intention of these pricing schemes is to allocate and/or assign all or part of the existing and the new cost of the network system to network users for the use of the network. The pricing models are employed to facilitate the process of translating network costs into overall network charges [37]. The main distinct paradigms are:

(i) rolled-in paradigm

(ii) incremental paradigm

(iii) composite embedded / incremental paradigm

2.2.1 Rolled-in Paradigm

In rolled-in paradigm, the new operating and investment costs and all existing costs are summed-up (rolled-in) into a single value. This cost is divided among different users of the network in accordance to the extent of use of the system. There are different network pricing methodologies under this paradigm, each outlining and evaluating this extent of use. These are outlined below.

2.2.1.1 Postage stamp methodology

Given this methodology, network charges are allocated (existing or rolled-in) based in the transacted power. The magnitude of the transacted power for a particular network transaction is measured at the time of system peak load condition and the equation below relates all the parameters involved.

$$R_t = TC * \frac{P_t}{P_{peak}} \tag{2.1}$$

This methodology is best applicable for a system operated centrally in an integrated setup. The strong hold of this approach is that, it is very simple to implement. Owing to the fact that this approach oversees the actual system operation, it is most probably likely to send incorrect economic signal to customers.

2.2.1.2 Contract path methodology

In contract path methodology, a selected path between delivery and receipt points is established for a transaction by the utility and the wheeling customer, without any use of the power flow study to establish the impact on the facilities involved. Part or all charges associated with the transaction in the contract path are allocated to the wheeling customer.

This approach also ignores the actual system operation, therefore, also incorrect economic signals will be sent to wheeling customers and uneconomic transactions may effect.

2.2.1.3 Distance based MW-mile methodology

In distance based MW-mile methodology, existing or rolled-in network charges are allocated to wheeling customers based on the magnitude of the transacted power using the measure of distance between the point of delivery and that of receipt. In fact, this is a product of power magnitude (MW) and the distance (mile) as shown, below, by the relation:

$$R_t = TC * \frac{PX_t}{\sum_t PX_t} \tag{2.2}$$

This methodology, also, disregard actual system operation, therefore, incorrect economic signals are likely to dominate.

2.2.1.4 Power Flow based MW-mile (facility-by-facility) methodology

This methodology allocates the charges for each network facility to transactions based on the extent of use of that facility. All the allocated charges are added all over the concerned network assets to constitute the total price for the use of the network system. The flow is computed based on simulating the operation of the system employing the use of the power flow model and the transaction's forecasted loads and generation configuration. The network system capacity use for the transaction t is, therefore, calculated as the weighted sum of the capacity use of individual assets, as shown below

$$TU_t = \sum_j W_j * F_{j,t} \tag{2.3}$$

Then, the transmission price for the network for transaction t is

$$R_t = TC * \frac{TU_t}{\sum_t TU_t} \tag{2.4}$$

Since this approach allocates charges facility by facility based on the maximum use of each facility, it constitutes the actual planning process for system reinforcements as opposed to peak conditions for the entire system.

This model is most popular owing to its simplicity to implement. Figure 2.1 shows the basic outline of the rolled-in paradigm. This model is regarded as economically inefficient as it ignores network scarcity.

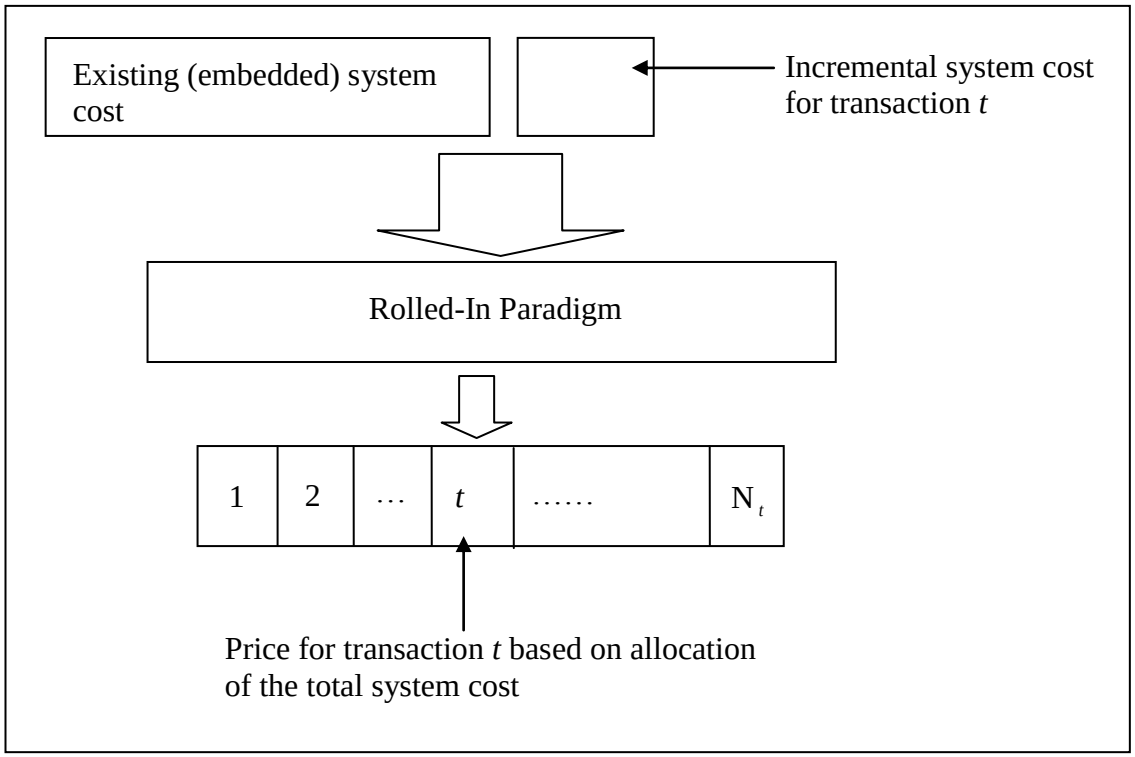

Figure 2.1: Rolled-in pricing paradigm [37]

2.2.2 Incremental Pricing Paradigm

For this paradigm, only new network costs due to new customers are considered for effecting network charges for these particular customers. The existing system costs are allocated to utilities' present customers. The methodologies involved are:

2.2.2.1 Short-Run Incremental Cost (SRIC) Pricing Methodology

The operating costs involved with a new network transaction are evaluated and assigned to that particular transaction. The network transaction operating costs can be assumed by

employing the use of an optimal power flow model that entails all the operating constraints, namely, network system (static or dynamic) constraints and generating scheduling constraints [37, 38].

There are a number of issues regarding the SRIC pricing methodology. Firstly, being to provide timely economic signals to network customers, there should be some forecasted operating costs. This involves forecasting future operating conditions resulting in less and less accuracy as the forecast time horizon extends further into the future. Secondly, it is related to the SRIC allocation among several transactions that collectively influence for changes in operating costs. Lastly, issues involved with instability of network prices which could be resolved by the use of long-term transactions. All these concerns would make it difficult to make efficient economic decision for long-term network transaction employing this methodology. In a nutshell, this methodology caters for the system operating costs and this would discourage host utilities from expanding their network.

2.2.2.2 Long-Run Incremental Cost (LRIC) Pricing

This methodology caters for the evaluation of all long-run costs (operating and reinforcement costs) required to accommodate a network transaction and assigning such costs to that transaction. The operating costs component maybe evaluated by the method entailed in SRIC [37-40].

The reinforcement cost component of a network transaction can be established employing changes caused in long-term network plans due to the transaction. Similar to SRIC, reinforcement costs could be negative indicating that the transaction has resulted in the deferral of planned network reinforcements.

Even though the issue of reinforcement costs is straight forward to evaluate, it is involving as it requires computing the least cost expansion problem. As reflected for SRIC case, the issue concerned with the allocation of the costs among multiple transactions that collectively cause such costs surfaces.

2.2.2.3 Short-Run Marginal Cost (SRMC) Pricing Methodology

The marginal operating cost of the system resulting from transaction is computed. This cost is the cost of accommodating a marginal increase in the transacted power. The marginal operating cost per MW of transacted power is constituted by the difference in the optimal cost of power at all points of delivery and receipt of the transaction [37, 38, 39, 41, 42, 43, 44, 45]. This cost is then multiplied by the value of the transacted power to give the SRMC for the network as shown, below

$$SRMC_f = \sum_{i \varepsilon B_t} BMC_i * P_{i,t} \tag{2.5}$$

SRMC shares the same concerns as SRIC pricing approach as the issue of reinforcement costs are ignored.

2.2.2.4 Long-Run Marginal Cost (LRMC) Pricing Methodology [37, 38, 40]

The marginal operating and reinforcement costs of the power system are used to establish the prices for a network transaction. Marginal operating costs are evaluated as in SRMC.

Following a long time horizon of a number of years, all the network expansion projects are identified and costed. This cost is then divided over the total power magnitude of all new planned transactions to evaluate the marginal reinforcement cost. The issues highlighted in the LRIC pricing approach, also, apply in this approach. Figure 2.2 illustrates the basic outline of this paradigm.

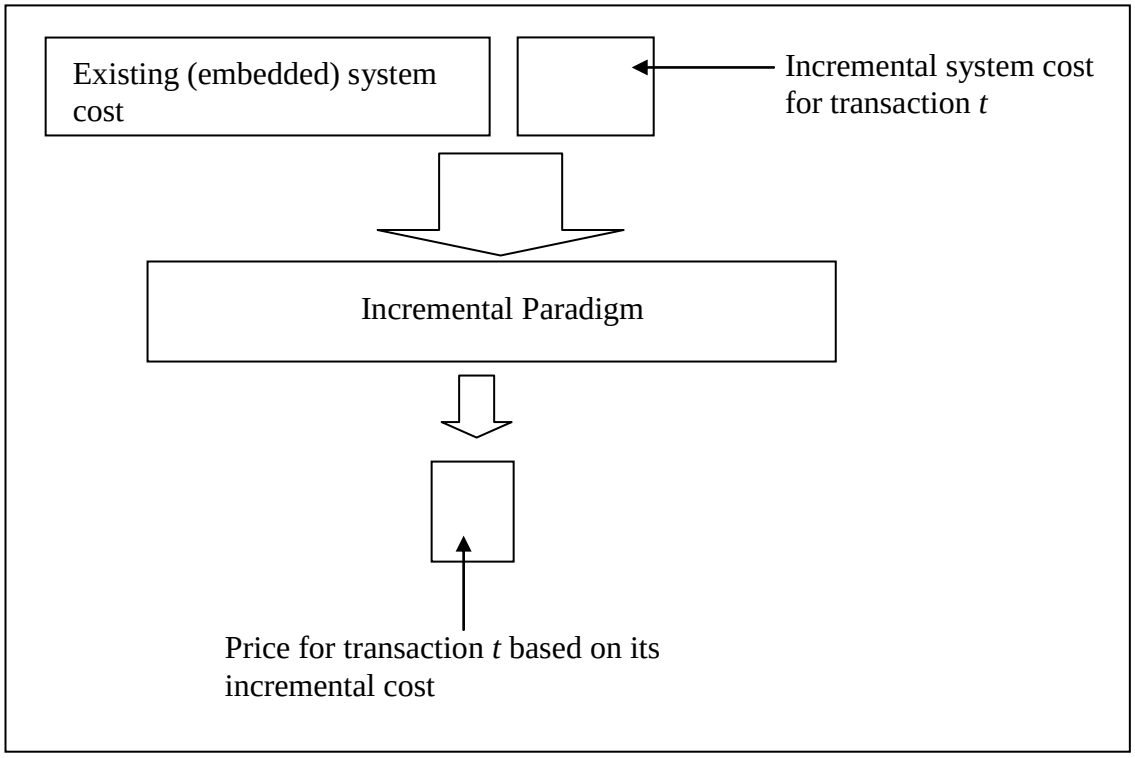

Figure 2.2: Incremental pricing paradigm [37]

This paradigm is believed to promote economic efficiency, however, it is hard to implement. Also, many methodologies of this paradigm consider an approximation of actual cost resulting in an inaccurate cost evaluation.

2.2.3 Composite embedded / Incremental Paradigm

This paradigm considers both the existing system and the incremental costs of transactions in the construction of the overall network charges. The composite embedded / incremental paradigm is meant to address the discrepancies visible in the rolled-in and incremental paradigms. Figure 2.3, below, shows an outline of this paradigm.

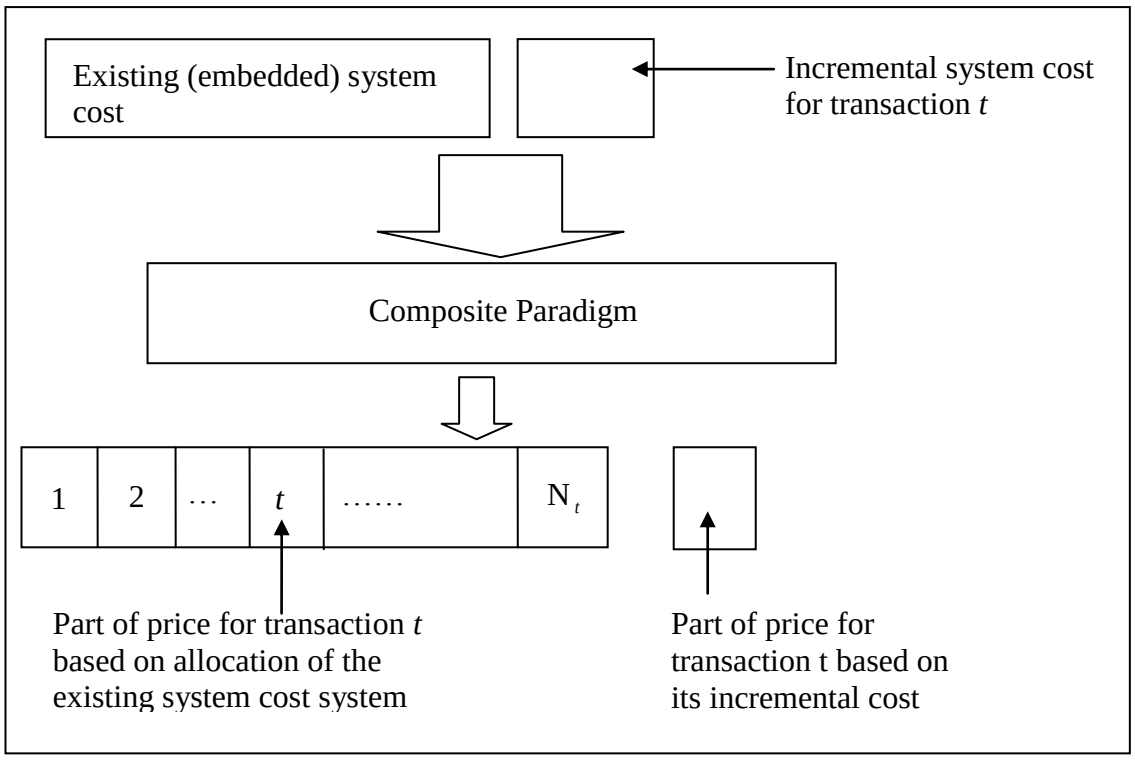

Figure 2.3: Composite embedded / incremental pricing paradigm [37]

This pricing paradigm can address many of the shortfalls associated with either the rolled-in or the incremental pricing paradigm. The main disadvantage is that it is a bit complex.

2.3 Long-Run Cost Pricing Methodologies

This research work involves evaluating network VAr compensation assets costs over a long term planning period, which is a function of any of the long-run cost pricing methodologies, these aforementioned pricing methodologies involved would be reviewed, in this section.

In these particular approaches, as earlier explained, the customer accounts for the full cost for any new facilities that the transaction need while the existing ones are still the responsibility of the old customer. The incremental pricing approach is considered to promote economic efficiency, but, is a very complex undertaking. In determining the incremental prices, on a long term basis, there are two distinct methods which can be employed, namely,

- Long-run incremental cost pricing (LRIC)
- Long-run marginal cost pricing (LRMC)

As opposed to long-run approach, short-run approach assumes a fixed network capacity, whereas long-run assumes that new facilities can be build. This means that the long-run marginal or incremental costs are composed of operating, reinforcement and expansion

costs. The marginal costs are a product of the unit cost of the additional transaction (obtained using a power system linearized model) and the size of the transaction. On the other hand, incremental cost is evaluated by looking at system costs before and after a transaction. All these are expressed in the equations, below:

$$IC_i = C(P + \Delta P_i) - C(P) \tag{2.6}$$

$$MC_i = \frac{dC(P)}{d(P_i)} \tag{2.7}$$

As it can be observed from the above equations, incremental cost accounts for the additional cost of the transaction while marginal cost account for the change of the total cost $C(P)$ for a given change in the output. These approaches are discussed in the next chapter.

2.3.1 Long-Run Incremental Cost (LRIC) Pricing Methodology

The incremental methodology differs from the marginal methodology as regard to cost evaluation. LRIC is employed to calculate and assign all long-run costs (operating and reinforcement) due to new network transaction [37]. In that regard, this approach can be described as evaluating revenue required to account for any new facilities that are attributed to the service customer [40]. LRIC also, just like LRMC, accounts for the change in total costs, which are investment costs for reinforcements and the change in operating costs.

The reinforcement cost component is usually evaluated based on changes resulting in long-term plans caused by a transaction. While, on the other hand, the operating cost can be estimated by employing the use of an optimal power flow model operating within system (dynamic or static security) constraints and generation scheduling constraints.

There are two distinct LRIC approaches which will be discussed and these are, standard long-run incremental cost (standard LRIC) pricing and the long-run fully incremental cost pricing [46].

2.3.1.1 Standard Long-Run Incremental Cost Pricing

This approach employs the use of traditional system planning approach to establish the reinforcement needed for both before and after the increment and the difference between the costs constitutes the cost due to the increment. Each increment is allocated its own costs in accordance [46-48]. This approach has four distinct cost allocation methods, which are

(i) £ per MW allocation

(ii) £ per MW.km allocation

(iii) Interface Flow allocation by region

(iv) One-by-one allocation

The exact representation of the future costs of investment are accounted for by the stream of annual revenue requirements (ARR) for each reinforcement project and their present worth revenue requirement (PWRR) but before everything else, reinforcement projects in a given time horizon have to be identified together with the corresponding capital costs involved. The flow chart below shows how these relate:

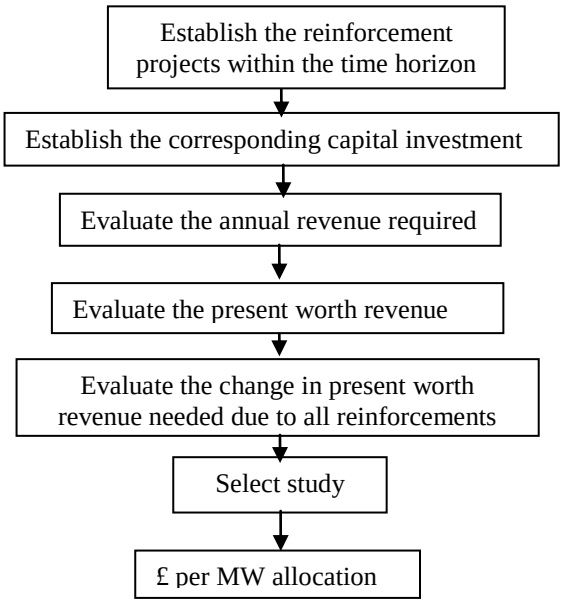

Figure 2.4: Standard LRIC pricing methodology

This whole process is demonstrated in the equations below:

$$\Delta IC_N = \Delta PV * AnnuityFactor * \frac{\Delta P_{iN}}{\Delta P_i} \tag{2.8}$$

$$\Delta OC_N = \Delta OC * \frac{\Delta P_{iN}}{\Delta P_i} \tag{2.9}$$

Lastly,

$$LRIC_N = \Delta IC_N + \Delta OC_N \tag{2.10}$$

2.3.1.2 Long-Run Fully Incremental Cost Pricing Methodology

In this approach when headroom or capacity of an asset is all used up by the increment, reinforcement is required. Given that each increment is studied individually, the reinforcement cost does not have to be allocated. This particular approach was used for this project work.

2.3.2 Long-Run Marginal Cost (LRMC) Pricing Methodology

LRMC comprises of reinforcements and operating costs to constitute a transaction tariff in a given power system. The marginal reinforcement cost is derived from all expansion projects in question and are costed over a defined time horizon of several years. This cost is, thereafter, divided over the total power magnitude of all new planned transactions to evaluate the marginal reinforcement cost. Regarding marginal operating cost, this cost is evaluated as cost per MW of transacted power which is a cost for accommodating a marginal increase in the transacted power. This is estimated as the difference in the optimal cost of the power at all points of delivery and receipt of the concerned transaction [49]. Also, "Long-run marginal cost based pricing seeks to determine the present value of future investments required to support a marginal increase in demand at different locations in the system, based on peak scenarios of future demand and supply growth. The users pay a charge that is geographically differentiated to the provider of the service [50]."

It is involving to accurately evaluate LRMC transaction as it is based on a number of assumptions about the future. An approximation of this is suitably executed in practice [51].

There are two distinct LRMC methods, namely, DC load flow (DCLF) ICRP pricing and Investment Cost-Related Pricing (ICRP) methodologies.

2.3.2.1 DC load Flow investment Cost-Related Pricing Methodology

This model is for long-run transmission capacity cost analysis having an additional feature of sensitivity analysis [50]. The main distinction between DCLF and ICRP is that the former satisfies Kirchhoff's laws.

Therefore the equations are as follows:

$$\min \quad p = \left(\sum_{ij} l_{ij} \frac{S_B}{x_{ij}} \left| \theta_i - \theta_j \right| \right) \text{ [MW.km]} \tag{2.13}$$

$$\text{and} \quad \frac{P_i}{S_B} = \sum_j \frac{1}{x_{ij}}(\theta_i - \theta_j) \quad \text{for bus } i \tag{2.14}$$

Given that this model offers no generation re-dispatch, as such, the reference node generation has its voltage phase angle preset to zero.

Equations (2.13) and (2.14) are reduced employing vector notation

$$\min \quad p = \left(\sum_{ij} l_{ij} \frac{S_B}{x_{ij}} \tilde{e}_{ij}^{T} \right) \theta \quad \text{[MW.km]} \tag{2.15}$$

$$\text{and} \qquad B^{'}.\theta = \frac{1}{S_B} P \tag{2.16}$$

This resulted [51] as

$$\lambda^{\bar{T}} = \frac{\partial p}{\partial P_D}$$

$$= -\frac{\partial p}{\partial P}$$

$$= -(\sum_{ij} l_{ij} \frac{S_B}{x_{ij}} \tilde{e}_{ij}^{T}) * \frac{\partial \theta}{\partial P}$$

$$= -(\sum_{ij} \frac{l_{ij}}{x_{ij}} \tilde{e}_{ij}^{T}) * (B^{'}) \tag{2.17}$$

Equation 2.17 gives nodal LRMC in £/MW/yr.

2.3.2.2 Contract Path Investment Cost-Related Pricing Methodology

[51, 52] Relate some of the fundamental assumptions for the evaluation of LRMC under an environment of minimum cost network (optimum network). The assumptions are as follows:

- Peak conditions are assumed. The maximum system stress take place under peak demand conditions.

- The line capacity is taken to equal to the power transported from generators to loads at peak demand conditions. The needed network redundancy (N-1 or higher) is not observed and no discrete network expansion quantities.

- Optimum network is constructed employing the use of only the existing routes of the exact network, in question.

- All the lines are homogenous and of the same type. Their corresponding cost is proportional to their length. The length of the cable is scaled up to reflect their higher price relative to that of the overhead lines.

- Electric power can be routed freely on the existing corridors. Power flow respects the real power balance equations. Kirchhoff's voltage law is not observed and shorter routes are being used.

The optimum network is derived from evaluating the optimisation problem

$$\min \quad w = \left(\sum_{ij} l_{ij} \left| f_{ij} \right|\right) \qquad \text{MW.km]} \tag{2.18}$$

$$\text{and} \quad P_i = \sum_j f_{ij} \qquad \text{for bus } i \tag{2.19}$$

Multiplying the total MW-km with the network expansion constant $\bar{c}$ [£/MW/km/yr] yields annualised network construction cost.

The LRMC of transporting electric power to node i is defined by the Lagrange multiplier λ_i related to equation (2.19). The resulting relation is the optimum network construction cost with respect to the power demand at node i [48].

$$\lambda_i = \frac{\partial w^*}{\partial P_{Di}} \qquad \text{[km]} \tag{2.20}$$

Therefore, the LRMC is

$$LRMC_i = \bar{c}\lambda_i \quad \text{[£/MW/yr]} \tag{2.21}$$

A 1 MW increase in the demand of node i is supplied by total MW.km of reinforcement of the optimum network expressed by λ_i. This means that an equal increase of the reference node generation will supply demand increase at node i. The addition of 1 MW of transport capacity from all branches from the reference node to i mark the much needed reinforcement. Therefore, λ_i is the distance between the reference node and node i.

2.4 Chapter Conclusions

All the approaches discussed (either in use or have been used) in this chapter, do not cater for the network VAr compensation asset pricing. The concept of the long-run fully incremental costs was employed for the network VAr compensation asset pricing for this project work, as it offers the features that are required. This LRIC methodology will be employed bearing in mind that the nodal voltage change is influenced by the real and reactive power flows (as explained in chapter 1). The methodology for this project would be introduced in the next chapter.

Chapter 3

Network Pricing in the United Kingdom and other countries

This chapter reviews the network pricing in use in the UK. The transmission and distribution network pricing methodologies are treated differently. Further, the network pricing approaches in Brazil, Norway, New Zealand and other countries are reviewed. Finally, the proposed LRIC-voltage network pricing methodology for pricing the use of network VAr compensation resources, is introduced. This latter pricing methodology is employed for this research work.

3.1 Chapter Introduction

Power industry deregulation and re-structuring process has set in motion the transmission and distribution pricing action in a number of countries. The electricity market has been established based on the instances of open access and non-discriminatory use of the network assets. In turn, network business remains as a natural monopoly hence economic regulation is inevitable. This change in the whole power market was destined to benefit network users. This chapter relates the network pricing in actual use in the UK, Brazil, California, Norway and other countries.

3.2 Network Pricing in UK

Since transmission and distribution systems are fully independent business functions in the UK, the charging for the use of their networks are also executed separately and independently. In this regard, they would be treated separately in the following sections.

3.2.1 Transmission Network Pricing

In April 2004 National Grid commissioned the employment of DC Loadflow (DCLF) ICRP as the use of system charging methodology [3, 53]. This transport model caters for the differentiation of the basic nodal costs to be established and, also, provides for sensitivity analysis accounting for alternative developments of generation and demand to be executed.

The basis for charging the use of the transmission network is the Investment Cost Related Pricing (ICRP) methodology which was introduced in 1993/1994 for England and Wales [3, 53]. This paradigm assumes that power flows along the shortest path, while with the DCLF ICRP, the power flow is established based on the DC power flow equations. In a nutshell, that means the circuit reactance is considered for the DCLF ICRP transport paradigm [54].

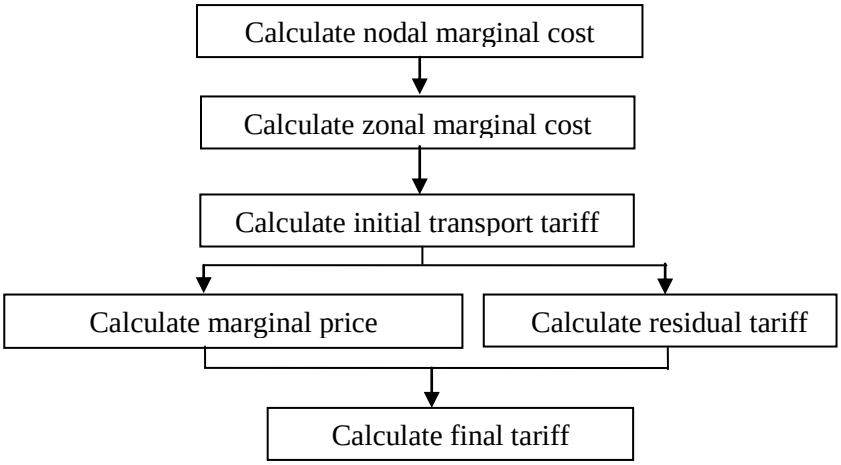

Figure 3.1: Flow chart showing how TNUoS charges are evaluated

Fig. 3.1 shows the flow chart relating to the calculation of the transmission network use of system (TNUoS) charges for the UK's three transmission licenses. The nodal marginal km is compounded into zones by weighting them accordingly by generation and demand capacity. In the DCLF transport algorithm, it has been assumed that the value of circuit impedance equates to the value of circuit reactance.

3.2.2 Distribution Network Pricing

The Distribution Reinforcement Model (DRM) was introduced in the 1980's and, ever since, it has been used for the distribution tariffs for all Distribution Networks in England and Wales. The basic principle of the model is to apportion the asset costs of the representative incremental network between customers with reference to their contribution to the demand that necessitates the assets [4]. The model has gone through a series of changes over time to be current in terms of policy and to ascertain accuracy and relevance of its representation.

For a change, Western Power Distribution (WPD) uses long-run incremental costs (LRIC), as of April 2007 [4], for their EHV networks and for LV networks they still employ the use of DRM. While this is the case with WPD, companies like CE Electric and EDF still employ the use of DRM throughout their networks [4]. Appendix B-1 and appendix B-2 show examples of LRIC and yardstick methodologies, respectively, for WPD.

The DRM denotes an independent network designed as an extension to the existing network. This model assumes that there is a need of supplying electricity to an additional 500MW of demand at each voltage level represented in the model [2]. Due to the 500MW value this model is often called "500MW model".

3.2.2.1 Yardstick Tariff

The main purpose of the DRM is to simulate a scaled down network as opposed to the real network. In a sense, the model evaluates the marginal costs, the 500MW figure become particularly insignificant. The significance of 500MW is that its value is large enough to have a noticeable impact on the voltage levels in the network, but none-the-less small enough to dilute the benefit of using a scaled model [2].

The DRM evaluates a full set of annuitized rates for user groups. The resulting outcomes are usually called 'yardstick' tariff with yardsticks being products for different voltage level of demand connections. Summing all items of plant required, this constitutes costs for availing the network at each voltage level.

The main setback with DRM is that, while it takes account for the cost of providing a distribution network, it is lacking in fully representing the physical electrical capability of performance of the network. Usually, the electrical capability is derived from using simple, static, load information and equipment ratings in this model.

3.3 Network Pricing in Brazil

The method in Brazil is the investment cost-related pricing (ICRP) approach for determining the marginal costs for the network users [55]. This approach has a similar economic pricing principles compared with the UK model, but look forward a number of years.

Given the new environment, the above planning rationale remained uncertain. This was compounded specifically by new regulation orders and the quality criteria of electricity supply as defined by [56]. This led to marginal\incremental cost pricing being proposed for distribution networks [55]. This arrangement was substituted by average incremental cost (*AIC*).

$$AIC = \frac{\sum_{y=1}^{Y} \beta_y (\Delta SInv_y + \Delta OCost_y)}{\sum_{y=1}^{Y} \beta_y \Delta D_y} \tag{3.1}$$

For the tariff assessment, the incremental cost associated with each network user is

$$TIC_{jik} = \alpha_{ki} SMC_k + \beta_{ij} AIC_i \tag{3.2}$$

3.4 Network Pricing in California

The approach in California puts main emphasis to losses and congestion to determine the price signals, with congestion given more attention [53, 57, 58]. This is in relation to the

fact that there is a growing concern that congestion could demarcate the proposed market into two portions, therefore, compromising the instance of competition.

The losses are captured employing generation meter multipliers (GMM). Power to cover losses is the product of the location generation and the corresponding GMM. The interzonal congestion card employs a DC load flow paradigm for simplicity and for reliable, robust marginal cost calculation [59]. The summation of the flow the network users induce on each corridor multiplied by the marginal value of the capacity of the corridor constitutes the congestion charges.

This paradigm provides short-term signals, instances of time of use and location to load and generation, to network users. It is lacking in an instance of providing future investment signals.

3.5 Network Pricing in Norway

In the Norwegian structure, the central grid charges comprise of four components: two realised from short-run utilisation of the network and two which are fixed on an annual basis. The former are for compensation for losses and congestion fees [58, 60].

The congestion pricing of the system is evaluated at the base case (with no bottlenecks). Congestion charge is considered only when there is congestion between two zones. This charge is the difference between the system price and the regional price (evaluated for corresponding price in that particular region).

On the other hand, pricing of losses reflect short-run marginal cost as a result of energy wheeling. The grid operator purchases power at the current spot prices to account for losses. In that regard, losses are a cost suffered by the grid. Network users have to account for charge equating approximately to the marginal cost they induce to the grid. A marginal load factor is derived by estimating the separated regions' marginal loss rates for three typical load functions, namely, winter day, winter/weekend and summer. The product of power consumed, the spot price of electricity at a specific hour and the marginal loss factor is the rate accounted for by the network users.

The grid future investment is accounted for in two ways, through a construction contribution and tariff elements. Grid users pay the contribution charge to the concerned grid that they are connected to and it is a one-off payment [58].

Like the Californian tariff structure, the Norwegian central grid tariff structure lacks in promoting locational price signals for investment, however, it promotes the day-to-day utilisation of the grid [58, 60].

3.6 Network Pricing in New Zealand, Japan, Spain and other countries

For the case of New Zealand, generation and demand levy the same price at each node in a spot pricing theory implementation. These spot prices are equal nodal marginal costs and when the difference in prices with and without the scheme equals the cost of the scheme then system expansion is justified. In addition, investment can be effected only if a group of users are accepting to pay for it [60].

The Spanish network pricing involves charging for congestion and losses. The grid owner can be penalised if the corresponding owner avails the network less time frame than the prescribed time. This approach obviously does not provide enough signals for investments [58].

For the Japanese situation, a charge of per kWh has to be levied by independent generators being a cost to cover for the use of the network and their corresponding losses.

Summary of network pricing in other countries in South America are depicted in table 3.1 below, showing their allocation approach, which time period the charging is calculated and the quantity that each network user is charged for.

Table 3.1: Schemes of allocation of payments [61]

Country	Argentina	Bolivia	Chile	Colombia	Peru
Allocation of payments	Based on use of network, given incremental charges	Based on use of network, given incremental charges	Based on use of network, given incremental charges	Based on use of network, given incremental charges	Based on postage stamp Scheme
Usage Measured	At peak Conditions	Different operating conditions	At peak Conditions	At conditions of maximum transmission charge	
Pro-rata of Payments based on	Maximum transmitted flow	Generators' peaking capacity and consumers' peak demand	Maximum transmitted Flow	Transmitted flow with additional adjustment to allocate 50% to consumers	Generators' Peak capacity

3.7 Recent developments in long-run network charging

In this section, a new methodology for charging the use of network reactive power assets is going to be introduced. This method would be appropriate because the charging of these assets were accounted (UK) for in the calculation of residual tariff. This charging is lacking in that it does not fully represent the physical electrical capability of system performance induced by each individual users. Since nodal voltage is associated to reactive power flow in a system, that relationship is going to be the basis for charging for the use of network reactive power assets.

In addition, some other issues relating to the problem scope as regard to network pricing will be outlined.

3.7.1 Time of Use, Location Specific (TULS) Model

This model added a dimension to the DRM as regard to adding distributed generation, which was previously not catered for. It analyses power flow during maximum load minimum generation at a secured amount as prescribed by P2/6 (security standard documentation), and during minimum load maximum rated generation.

The critical loading of each asset and circuit is determined by employing the use of a DC load flow equivalent to that of the transmission DCLF ICRP transport model. When the loading is highest during maximum load condition, this scenario is referred to as demand dominated and load will be charged accordingly while generation will be rewarded. Otherwise, the scenario is termed as generation dominated in which generation will be charged and load rewarded. Thereafter, an annuitized forward looking investment costs (£/kW/yr) are, then, evaluated and allocated amongst the nodes. Consequently, this methodology provides demand and generation prices on a consistent basis and the prices reflect the location. In addition, the prices are derived from either crediting or debiting the cost of upstream assets as regard to whether they are generation or demand dominated. This latter point ensures significant gross payments are made from generators to load or vice versa. One setback is that this model does not account for system security. Also, DC load flow does not consider limitations resulting from voltage, fault levels and reactive power prices are not provided on a consistent basis. The model entails confidential data, therefore, not easier to place it in the public domain.

3.7.2 Distribution ICRP

This pricing approach was established by Bath University conducted for Ofgem to establish the benefits, thereafter, from charging models based on economic principles in

2005. This model has some added dimensions in relation to the transmission pricing paradigm to satisfy the distribution network properties. For this model, each grid supply point is effectively a slack node [62]. In that regard, any withdrawal or injection at this particular supply point will have a zero charge.

This model is a derivative of injecting a 1 MW of load or generation at each node and the power flow at each circuit caused by that injection is compared to the original power flow before injection. The equations below hold

$$UnitCost = \frac{AssetCost}{LC} \tag{3.3}$$

$$DICRP_N = \sum_l (UnitCost * \Delta P_l * L_l) \tag{3.4}$$

3.7.3 Original Long-run Incremental Cost (LRIC) for voltage pricing

Since this is the model to be used in this work, it is worthwhile to introduce it so as an insight can be drawn from it.

Furong Li et al [47] suggested that LRIC model reflects the asset costs of supporting an increment, in which lines and cables are a function of distance and, also, the horizon when the investment will be needed. Employing the concept in [44], the relationship below then holds:

$$n = \frac{\log V_{Limit} - \log V}{\log(1+v)} \tag{3.5}$$

The above relation (eqn. (3.5)) states that, for a given voltage degradation rate, v, the time horizon, n, will be the time frame for the voltage to grow from current voltage loading level, V, to full loading level, V_{Limit}.

Calculating the time horizon for the case with and without the increment, n and n_1 can be established where there are time horizons for with and without increment, respectively. This results into the relations below

$$PV = \frac{AssetCost}{(1+d)^n} \tag{3.6}$$

$$n_1 = \frac{\log V_{Limit} - \log V_1}{\log(1+v)} \tag{3.7}$$

$$PV_1 = \frac{AssetCost}{(1+d)^{n_1}} \tag{3.8}$$

$$\Delta PV = PV_1 - PV \tag{3.9}$$

Lastly, the long-run incremental cost (LRIC) is as follows:

$$LRIC_N = \frac{\sum \Delta PV}{\Delta P_N / \Delta Q_N} \tag{3.10}$$

The LRIC approach accounts for the VAr compensation assets and, also, recognises both the distance and the utilization of the asset. This approach is fully formulated and explained, in the next chapter.

3.8 Chapter Conclusions

In this chapter, network pricing in UK and other countries are outlined. Further, recent developments in long-run network charging in the UK were also outlined since the method employed in this research work involves this kind of charging principle. Furthermore, proposed LRIC methodology, which is employed for this research work, is introduced. Any of the pricing approaches (those in actual use) studied in this chapter do not cater for network VAr compensation assets they instead reflect the investment costs incurred in circuits and transformers to support real and reactive power flow. Even though these assets are catered for in the whole charging methodology but their charges do not necessarily represent the actions of each individual user.

It should be noted that most research in reactive power pricing [25-35] reflects the benefits from generation, reflecting the operational cost due to new customers, that is, how they might change network losses, however, they fail to reflect the network VAr compensation asset investment costs to support real and reactive power flow.

It is then against this background that the LRIC methodology is proposed and it is able to reflect both the existing and future network VAr compensation asset costs and it is based on the spare nodal voltage capacity of an existing network. This aforementioned proposed approach fully represents the action of each individual user on the network, therefore, it provides the correct economic signals for each respective user. This approach is also forward looking, locational and, integrating demand and generation.

Chapter 4

LRIC-Voltage Network Pricing Reflecting Future VAr Compensation Assets

The novel approach of long-run incremental cost (LRIC)-voltage network pricing methodology is formulated and explained in this chapter. This approach is based on the network nodal voltage calculations given the impact resulting from either withdrawal/injection of incremental real power/reactive power into or from the system. To demonstrate this formulation, IEEE 14 bus standard test system and the practical distribution test system are employed. The results show that the customers (generators and loads) are charged according to the impact they impose on the system voltage profiles. The charges reflect how the customer may either advance or defer the investment in future network reactive power (VAr) compensation asset investments, which are used to support the network nodal voltages.

4.1 Chapter Introduction

Over the years, it has been shown from the review for both transmission and distribution pricing methodologies in chapters 2 and 3, that, these have evolved and progressed to become more cost reflective and complex. However, majority of these network charging methodologies reflect the investment costs incurred in circuits and transformers to support real and reactive power flow. To reflect the investment costs incurred for maintaining network voltages in network charges has received very little attention. Other approaches in reactive power pricing tend to reflect the operational cost from new customers, e.g. how they might change the network losses but they do not reflect the capital investment of the network VAr compensation devices as they are responsible for ensuring that network voltages are within statutory requirements. It is against this background that LRIC-voltage network charging approach was proposed in this research work.

The LRIC-voltage network charging principle [63], is based on an economic principle, which is intended to reflect the charges in investment costs of the VAr compensation assets to maintain the network voltages within acceptable limits from nodal power perturbations. These costs are to be recovered from generators, large industrial customers and supplies. The most attraction with this approach is that, it provides forward-looking, economically efficient signals that reflect both the extent of the network VAr compensation assets required to service withdrawal and/or injection and do present voltage profiles. This, in turn, aims to influence the future use of the system to better the network voltage profiles. This pricing approach is tested on the IEEE 14 bus test system and on the distribution practical test system. Thereafter, the results are presented and analyzed.

4.2 LRIC-voltage network pricing principle formulation

The LRIC-v network charging principle is based upon the premise that for an assumed nodal generation/load growth rate there will be an associated rate of busbar voltage degradation. Given this assumption, the time horizon for a busbar to reach its upper/lower voltage limit can be evaluated. Once the limit has been reached, a pseudo compensation device will be placed at the node as the future network reinforcement to support the network voltage profiles. A nodal demand/generation increment would affect the future investment horizon. The nodal voltage charge would then be the difference in the present value of the future reinforcement consequent to voltage with and without the nodal perturbation.

The following steps outlined below can be utilized to implement this charging model:

1) Evaluating the future investment cost of network VAr compensation assets to support existing customers

If a network node b, has lower voltage limit, V_L and upper voltage limit V_H, and holds a voltage level of V_b, then the number of years for the voltage to grow from V_b to V_L/V_H for a given voltage degradation rate *v* can be evaluated from (4.1a) or (4.1b).
If V_L is critical, that is, bus voltage is closer to V_L than V_H and less than target voltage, 1 pu :

$$V_L = V_b * (1-v)^{n_{bL}} \tag{4.1a}$$

On the other hand if V_H is critical, that is, bus voltage is closer to V_H than V_L and more than target voltage, 1 pu :

$$V_H = V_b * (1-v)^{n_{bH}} \tag{4.1b}$$

where: n_{bL} and n_{bH} are the respective numbers of years that takes V_b to reach V_L/V_H.

Reconfiguring equations (4.1a) and (4.1b) constitute:

$$(1-v)^{n_{bL}} = \frac{V_L}{V_b} \tag{4.2a}$$

or

$$(1+v)^{n_{bH}} = \frac{V_H}{V_b} \tag{4.2b}$$

Taking the logarithm of equations (4.2a) and (4.2b) on both sides gives

$$n_{bL} * \log(1-v) = \log V_L - \log V_b \tag{4.3a}$$

or

$$n_{bH} * \log(1+v) = \log V_H - \log V_b \tag{4.3b}$$

then the values of n_{bL}/n_{bH} are

$$n_{bL} = \frac{\log V_L - \log V_b}{\log(1-v)} \tag{4.4a}$$

or

$$n_{bH} = \frac{\log V_H - \log V_b}{\log(1+v)} \tag{4.4b}$$

The assumption is that when the node reaches its limit the reinforcement will take effect. This means that investment will be effected in n_{bL}/n_{bH} years when the node utilization

reaches V_L/V_H , respectively. At this point an installation of a VAr compensation asset is regarded as the future investment that will be needed at the node to support the voltage.

2) Determining the present value of future investment cost

For a given discount rate of d, the present value of the future investment in n_{bL}/n_{bH} years will be:

$$PV_{bL} = \frac{Asset\ Cost_{CbL}}{(1+d)^{nbL}} \tag{4.5a}$$

or

$$PV_{bH} = \frac{Asset\ Cost_{CbH}}{(1+d)^{nbH}} \tag{4.5b}$$

where: $Asset\ Cost_{CbL}$ and $Asset\ Cost_{CbH}$ are the modern equivalent asset cost to cater for supporting voltage due to lower voltage limit and upper voltage limit violations.

3). Deriving the incremental cost as a result of an additional power injection or withdrawal at node N

If the nodal voltage change is $\Delta V_{bL}/\Delta V_{bH}$ consequent upon an additional $\Delta P_{bIn}/\Delta Q_{bIn}$ withdrawal/injection at node N, this will bring forward/delay the future investment from year n_{bL}/n_{bH} to n_{bLnew}/n_{bHnew} and when V_L is critical

for withdrawal

$$V_L = (V_b - \Delta V_{bL}) * (1-v)^{n_{bLnew}} \tag{4.6a}$$

or

for injection

$$V_L = (V_b + \Delta V_{bH}) * (1-v)^{n_{bLnew}} \tag{4.6b}$$

and when V_H is critical

for withdrawal

$$V_H = (V_b - \Delta V_{bL}) * (1-v)^{n_{bHnew}} \tag{4.6c}$$

or

for injection

$$V_H = (V_b + \Delta V_{bH}) * (1-v)^{n_{bHnew}} \tag{4.6d}$$

Equations (4.7a), (4.7b), (4.7c) and (4.7d) give the new investment horizons as

$$n_{bLnew} = \frac{\log V_L - \log(V_b - \Delta V_{bL})}{\log(1-v)} \tag{4.7a}$$

or

$$n_{bLnew} = \frac{\log V_L - \log(V_b + \Delta V_{bH})}{\log(1-v)} \tag{4.7b}$$

$$n_{bHnew} = \frac{\log V_H - \log(V_b - \Delta V_{bL})}{\log(1+v)} \tag{4.7c}$$

or

$$n_{bHnew} = \frac{\log V_H - \log(V_b + \Delta V_{bH})}{\log(1+v)} \tag{4.7d}$$

then the new present values of the future investments are

$$PV_{bLnew} = \frac{Asset\ Cost_{CbL}}{(1+d)^{nbnewL}} \tag{4.8a}$$

or

$$PV_{bHnew} = \frac{Asset\ Cost_{CbH}}{(1+d)^{nbnewH}} \tag{4.8b}$$

The changes in the present values as consequent of the nodal withdrawal/injection $\Delta P_{bIn}/\Delta Q_{bIn}$ are given by (4.9a) and (4.9b)

$$\Delta PV_{bL} = PV_{bLnew} - PV_{bL} = Asset\ Cost_{CbL}\left(\frac{1}{(1+d)^{n_{bLnew}}} - \frac{1}{(1+d)^{n_{bL}}}\right) \tag{4.9a}$$

or

$$\Delta PV_{bH} = PV_{bHnew} - PV_{bH} = Asset_{CbH}\left(\frac{1}{(1+d)^{n_{bHnew}}} - \frac{1}{(1+d)^{n_{bH}}}\right) \tag{4.9b}$$

The annualized incremental cost of the network items associated with component b is the difference in the present values of the future investments due to the reactive power magnitude change $\Delta P_{bIn}/\Delta Q_{bIn}$ at node N multiplied by an annuity factor

$$IV_{bL} = \Delta PV_{bL} * annuity\ factor \tag{4.10a}$$

or

$$IV_{bH} = \Delta PV_{bH} * annuity\ factor \tag{4.10b}$$

4) Evaluating the long-run incremental cost

If there are a total of bL busbars' lower limits and bH busbars' upper limits that are affected by a nodal increment from N, then the LRIC-V network charges at node N will be the aggregation of the changes in present value of future incremental costs over all affected nodes:

$$LRIC\_V_{N,L} = \frac{\sum_{bL} IV_{bL}}{\Delta P_{In} / \Delta Q_{In}} \tag{4.11a}$$

or

$$LRIC\_V_{N,H} = \frac{\sum_{bH} IV_{bH}}{\Delta P_{In} / \Delta Q_{In}} \tag{4.11b}$$

It should be noted that, in order to understand the above outlined methodology fully, reference [63] uses the same methodology for a simple 4-bus system in establishing LRIC-voltage network charges.

4.3 Results and Analysis

The results are presented and analysed below, consequent to the LRIC-voltage network pricing approach being tested on the IEEE-14 bus test system and a distribution test system chosen from the South Wales distribution network, in the UK.

4.3.1 IEEE-14 Bus Test System

As it can be observed, below on figure 4.1, this particular test system comprises of fourteen buses, fifteen lines, three transformers, two generators and three synchronous condensers. The buses and circuits drawn in red are at 132kV voltage level while those in blue are at 33kV voltage level. The other generation is accounted for by the slack bus which is at bus 1. The network data can be found from reference [64].

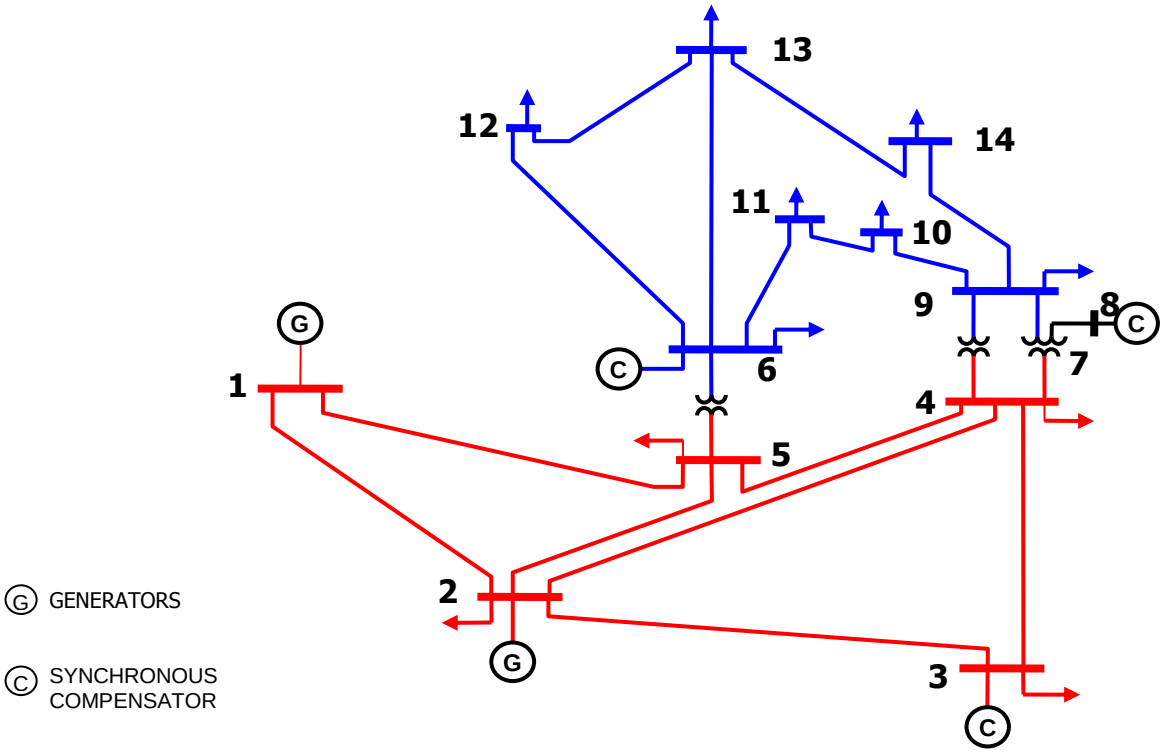

Figure 4.1: IEEE 14-bus test system

The compensation assets (SVCs) have the investment costs of £1, 452,000 and £696, 960 at the 275-kV and 132-kV voltage levels, respectively. Bus 1 is the slack bus. The voltage limits are assumed to be$1 \pm 6\%$ pu. The use of power flow was employed to capture the nodal voltages while performing nodal withdrawals/injections on the system. The annual load growth for this test network is assumed to be 1.6% while the discount rate is assumed to be 6.9%. The assumed annual growth rate and discount rate are the figures used in the UK [65].

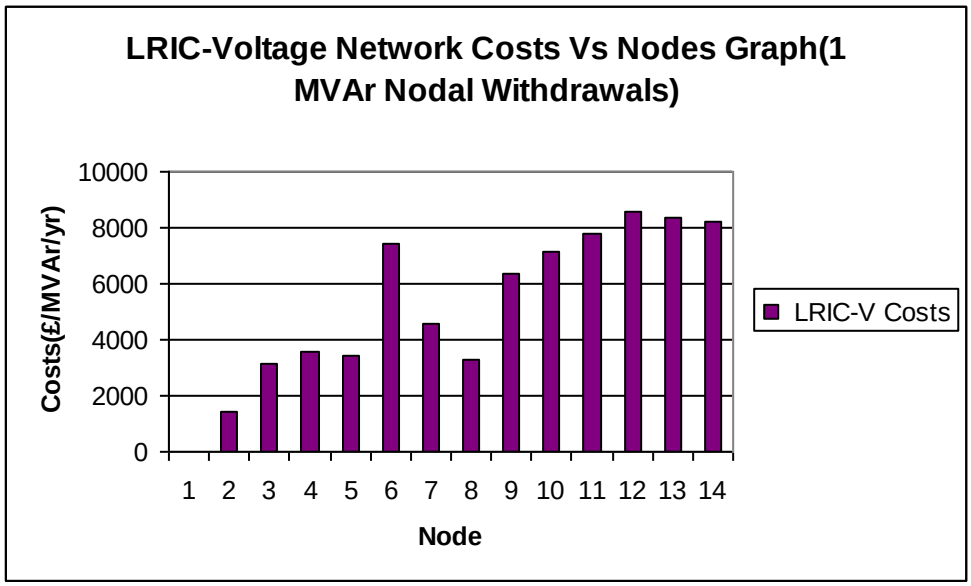

Figure 4.2: LRIC-voltage network charges per 1 MVAr nodal withdrawal on the IEEE 14 bus test system

Table 4.1: LRIC-voltage network charges due to MVAr nodal withdrawals on the IEEE 14 bus test system.

Bus	Voltage Before MVAr Withdrawal	Voltage Difference (pu)	LRIC-V Charges (£/MVAr/yr)	Distancce from slack bus (km)
1	1.030	0.000E+00	0	0
2	1.020	-5.000E-04	1397.86	38
3	0.996	-1.526E-03	3154.75	108
4	0.988	-1.018E-03	3577.28	95
5	0.995	-9.290E-04	3422.21	82
6	0.982	-2.647E-03	7410.18	82
7	1.008	-2.337E-03	4588.71	95
8	1.048	-3.709E-03	3311.04	95
9	0.981	-2.604E-03	6370.51	95
10	0.974	-3.100E-03	7127.37	97
11	0.974	-3.399E-03	7758.26	88
12	0.967	-4.096E-03	8597.2	93
13	0.963	-3.431E-03	8374.03	87
14	0.954	-4.112E-03	8237.87	101

Figure 4.2 and table 4.1 show Base LRIC-voltage charges for each node of the system. Further, Table 4.1 gives additional information to explain the variations in charges, they include the distances of each bus from the slack bus, the voltage levels before each MVAr withdrawal and voltage differences (voltages after nodal perturbations – voltages before nodal perturbations).

It can be observed from the results that buses 2, 7 and 8 have their initial voltages greater than the target voltage of 1 pu while the rest of buses excluding the slack bus have their initial voltages below 1 pu. Withdrawing reactive power would help buses 2, 7, and 8 to be closer to the target voltage, thus should be rewarded for increasing the margins of the already critical busbar upper voltage limits. Customers at these buses are incentivized to take reactive power from the network as the investment horizons of the VAr compensation assets at the respective bus are deferred. While the rest of the buses excluding the slack bus are penalized for reactive power withdrawal as it decrease the margins to the lower voltage limits since this action advance the investment horizons of the VAr compensation assets at the study bus. Although individual busbars may have charges or credits against the same nodal withdrawal, the nodal LRIC-voltage price in this system is a charge against each node, since the price accounts for the system wide effects from a nodal withdrawal, the credits from buses 2, 7 and 8 are far less that the accumulated charges from the rest of the busbars.

It can also be observed that the LRIC-voltage charges generally increase with increasing distance reflecting the worsening voltage profile over long distance. Bus 3 has the largest distance but the charge is comparably small, this is because the bus is connected with a synchronous condenser which boosts the voltage at that bus. The same occurs at bus 6 and 8. The charge at bus 8 is smaller that at bus 7 since bus 8 has its voltage boosted. Even though Bus 14 has a larger distance than buses 12 and 13, as withdrawing from this node has a larger impact to buses 7 and 8 which earn larger credit contributing to reduced overall charge. The same applies to bus 13 since it is closer to buses 7 and 8 than bus 12.

Bus 12 under the aforementioned circumstances attracts the most charge since it is further from buses 7 and 8 than buses 13 and 14 resulting in less credit at buses 7 and 8 in contribution to the overall higher charge at this bus. Bus 2 has the least charge since it is closer to the slack bus.

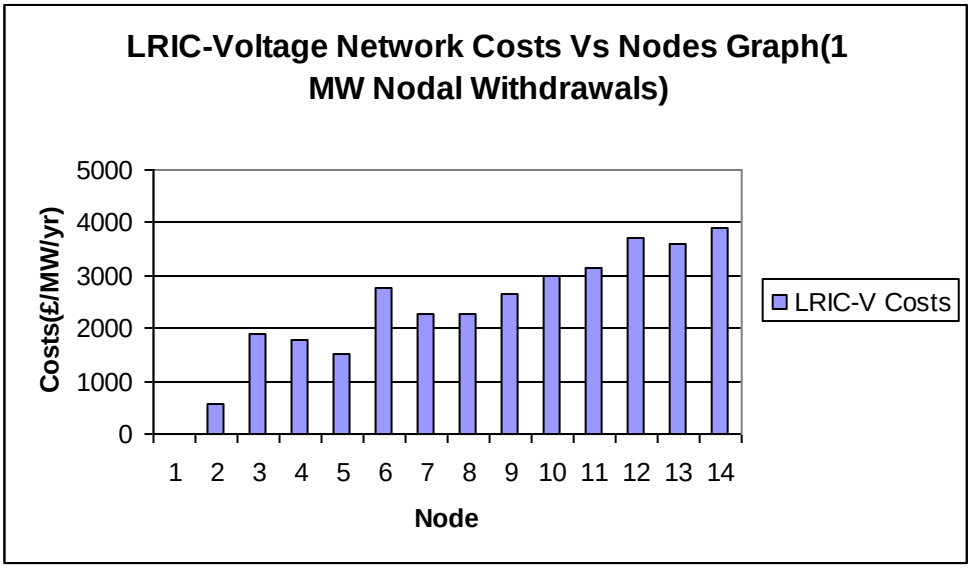

Figure 4.3: LRIC-voltage network charges per 1 MW nodal withdrawals on the IEEE 14 bus test system

Table 4.2: LRIC-voltage network charges due to 1 MW nodal withdrawals on the IEEE 14 bus test system.

Bus	Voltage Before MW Withdrawal	Voltage Difference (pu)	LRIC-V Charges (£/MW/yr)	Distancce from slack bus (km)
1	1.03	0.000E+00	0	0
2	1.02	-2.880E-04	584.14	38
3	0.996	-1.254E-03	1882.62	108
4	0.988	-1.220E-04	1775.89	95
5	0.995	-3.940E-04	1521.07	82
6	0.982	-3.920E-04	2762.76	82
7	1.008	-7.240E-04	2279.48	95
8	1.048	-3.750E-04	2286.02	95
9	0.981	-5.870E-04	2643.38	95
10	0.974	-1.600E-03	2977.46	97
11	0.974	-1.014E-03	3138.4	88
12	0.967	-1.653E-03	3708.92	93
13	0.963	-1.293E-03	3590.62	87
14	0.954	-2.027E-03	3900.97	101

Figure 4.3 and table 4.2 show the costs given 1 MW nodal withdrawals. As it can be

observed from this figure and table, the LRIC-v charges follow the same pattern as those of MVAr nodal withdrawals in figure 4.2 and table 4.1. Since the network is the same with respect to nodal distances from the slack bus. However, during the MW withdrawals, the nodal voltages are degraded less than in the case with MVAr withdrawals and, hence, lowering LRIC-v costs. This owes to the fact that the test network has the circuit reactances (Xs) are more the corresponding network circuit resistances (Rs).

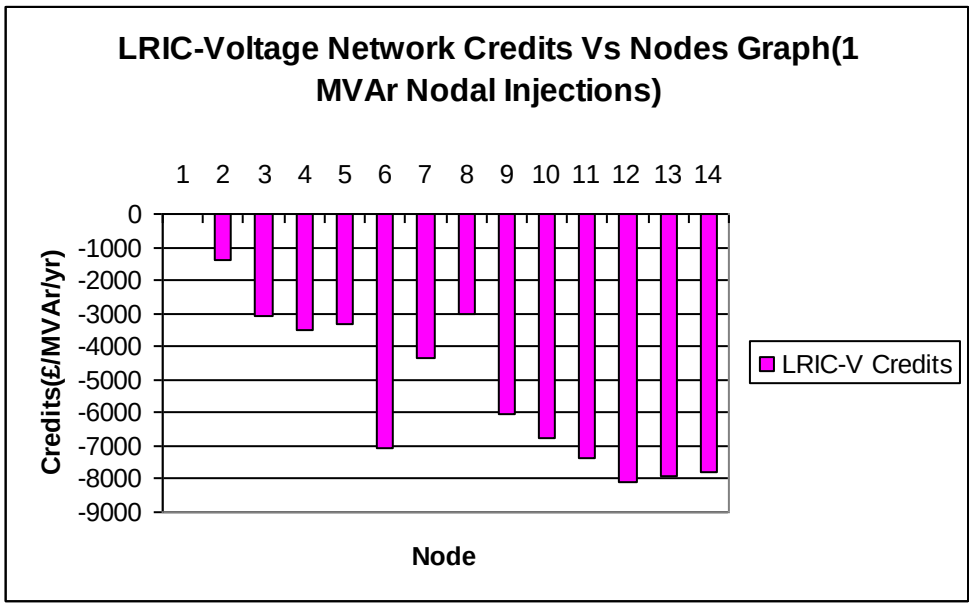

Figure 4.4: LRIC-voltage network charges per 1 MVAr nodal injections on the IEEE 14 bus test system

Table 4.3: LRIC-voltage network charges due to 1 MVAr nodal injections on the IEEE 14 bus test system.

Bus	Voltage Before MVAr Withdrawal	Voltage Difference (pu)	LRIC-V Charges (£/MVAr/yr)	Distancce from slack bus (km)
1	1.03	0.000E+00	0	0
2	1.020	4.990E-04	-1370.13	38
3	0.996	1.521E-03	-3068.19	108
4	0.988	1.016E-03	-3478.5	95
5	0.995	9.260E-04	-3336.72	82
6	0.982	2.633E-03	-7066.96	82
7	1.008	2.326E-03	-4342.58	95
8	1.048	3.685E-03	-3026.64	95
9	0.981	2.589E-03	-6044.51	95
10	0.974	3.078E-03	-6748.56	97
11	0.974	3.373E-03	-7351.67	88
12	0.967	4.058E-03	-8113.58	93
13	0.963	3.403E-03	-7929.68	87
14	0.954	4.073E-03	-7763.94	101

Figure 4.4 and table 4.3 show benefits against buses given 1 MVAr nodal injections. In addition, table 4.3 shows the shortest distances of buses from the slack bus, the voltage levels before each MVAr injection and voltage differences (voltages after nodal perturbations – voltages before nodal perturbations).

During nodal injections, the buses (2, 7 & 8) having their initial voltages above 1 pu are penalized for degrading the already critical busbar upper voltage limits while the rest except the slack bus are credited for relieving the already critical busbar lower voltage limits. The same reasons as for nodal MVAr withdrawals hold as the overall result is that all buses earn credits. Also, observed, is that the credits increase as distances increase. The conditions in this case are the same as for the previous case of figure 4.1, therefore, the same pattern is observed, in that, Bus 12 attracts the most credit while Bus 2 attracts the least.

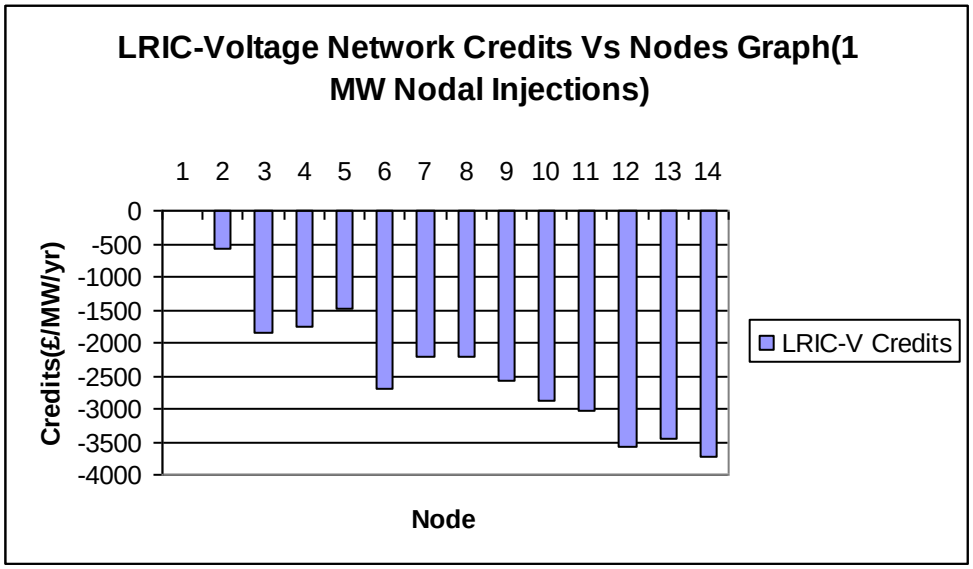

Figure 4.5: LRIC-voltage network charges due to 1 MW nodal injections on the IEEE 14 bus test system

Table 4.4: LRIC-voltage network charges due to 1 MW injection at each node.

Bus	Voltage Before MW Withdrawal	Voltage Difference (pu)	LRIC-V Charges (£/MW/yr)	Distancce from slack bus (km)
1	1.03	0.000E+00	0	0
2	1.02	1.170E-04	-578.48	38
3	0.996	3.420E-04	-1842.03	108
4	0.988	8.790E-04	-1745.09	95
5	0.995	4.300E-04	-1499.18	82
6	0.982	1.369E-03	-2684.34	82
7	1.008	7.130E-04	-2217.2	95
8	1.048	1.009E-03	-2211.01	95
9	0.981	1.263E-03	-2561.02	95
10	0.974	7.500E-04	-2877.01	97
11	0.974	1.652E-03	-3030.38	88
12	0.967	2.245E-03	-3561.5	93
13	0.963	1.619E-03	-3464.96	87
14	0.954	1.770E-03	-3741.85	101

It can also be observed from figure 4.5 and table 4.4, that the LRIC-v charges follow the same pattern as those of MVAr nodal injections, but with less LRIC-v credits for the same reasons relating to the differences depicted above for the MVAr and MW withdrawals.

4.4.2 Distribution Test System

To demonstrate the practicability of this LRIC-voltage network charging principle, a practical network is opted as the test network. The reason for this choice being that this particular network should in absolute terms reflect the configuration of a practical distribute network. In this regard, the practical system to be employed shall be the Pembroke network in Wales under the ownership of Western Power Distribution (WPD). The geographic map of this system is shown below in figure 4.6.

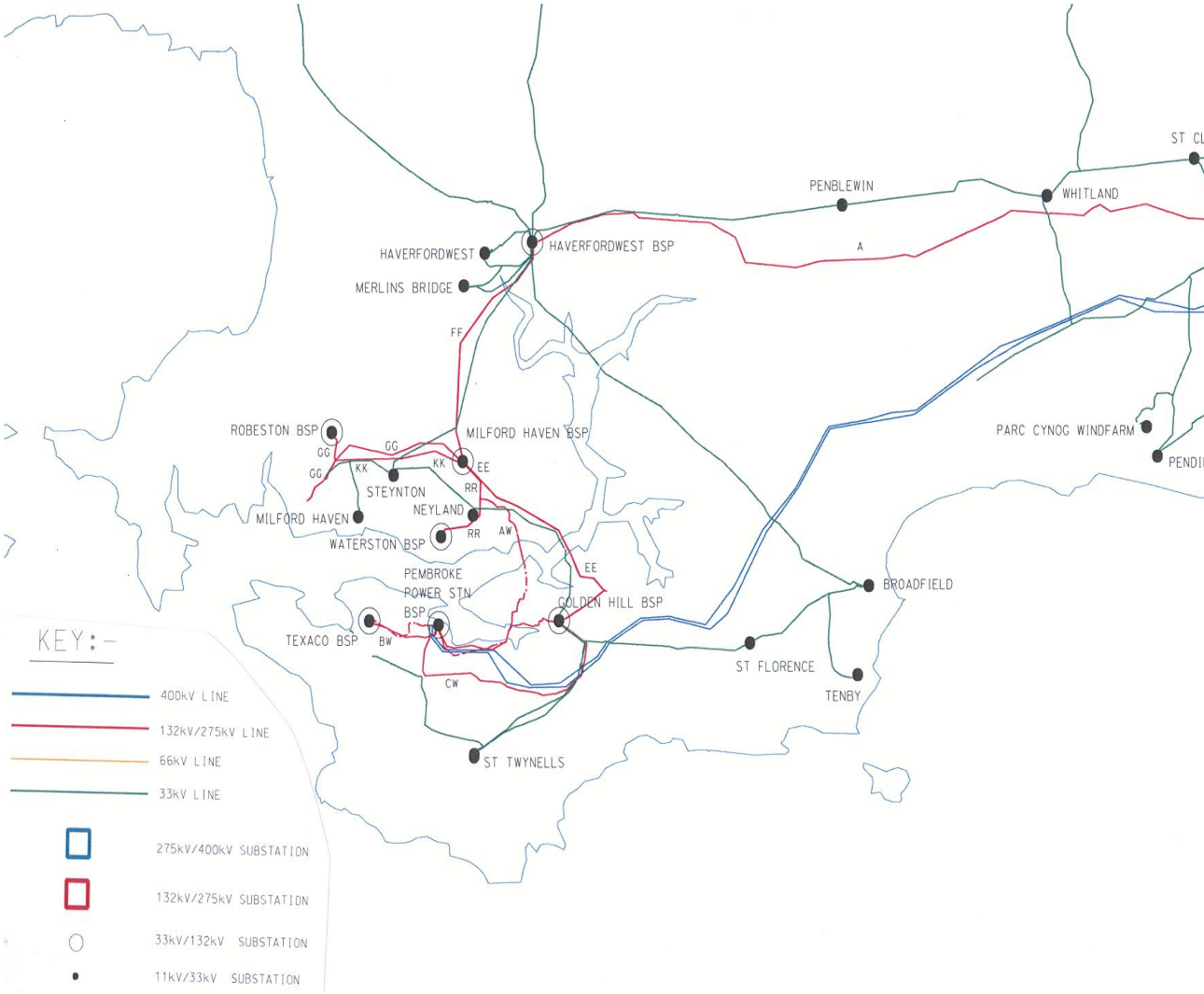

Figure 4.6: Pembroke network (Wales) [66]

This network is apportioned into two zones: zone 1 and zone 2. Zone 1 is a rural area comprising of 23 lines and 29 transformers. On the other hand, zone 2 is a central area comprising of 33 lines, 25 transformers.

The SVCs have the investment costs of £696,960.00, £174,240.00, £116,100.00, £58,058.00 and £696.00 at the 132-kV, 33-kV, 22-kV, 11-kV and 0.415-kV voltage levels, respectively. Bus 5140 is the slack bus. The voltage limits are assumed to be $1 \pm 6\%$ pu on the 11-kV, 22-kV and 33-kV levels. While the voltage limits are (1-6% & 1+10%) pu on the 0.415-kV level and $1 \pm 10\%$ pu on the 132-kV level as detailed by [122]. The use of power flow was employed to capture the nodal voltage charges while performing nodal withdrawals/injections on the system. Also, the annual load growth for this test network is assumed to be 1.6% while the discount rate is assumed to be 6.9%.

Table 4.5: LRIC-voltage network charges due to 1 MVAr withdrawal at each node on the Pembroke practical test system.

Bus	Initial Voltage (pu)	Voltage Difference (pu)	LRIC-V Charges (£/MVAr/yr)	Distance from slack Bus (km)	Bus	Initial Voltage (pu)	Voltage Difference (pu)	LRIC-V Charges (£/MVAr/yr)	Distance from slack Bus (km)	Bus	Initial Voltage (pu)	Voltage Difference (pu)	LRIC-V Charges (£/MVAr/yr)	Distance from slack Bus (km)
2005	0.997	-1.774E-03	2843.64	7.2	** 3084	0.958	-9.855E-03	**8011.74**	**50.3**	2041	1.025	-6.160E-04	1270.02	12.4
2015	1.000	-1.188E-03	2795.95	21.7	3087	0.998	-8.856E-03	3939.08	24.3	2045	0.991	-3.379E-03	1320.08	10.8
3003	1.002	-1.072E-02	6566.01	37.8	3090	0.976	-3.122E-03	3762.26	24.3	2046	0.991	-3.380E-03	1320.09	10.8
3006	0.964	-5.151E-03	6394.27	37.8	3093	0.999	-1.647E-02	6763.53	20.9	2047	0.992	-3.393E-03	1333.73	12.4
3009	0.992	-1.037E-02	6008.73	42.8	3096	0.954	-5.812E-03	6367.47	20.9	2048	0.992	-3.394E-03	1333.74	12.4
3012	0.958	-4.325E-03	5745.4	42.8	3099	0.995	-1.823E-03	2880.05	23.8	2620	1.025	-5.210E-04	1269.96	12.4
3015	1.009	-1.091E-02	5898.11	42	3102	0.965	-5.133E-03	6388.06	37.9	2621	1.025	-5.220E-04	1270.95	12.4
3018	0.962	-5.491E-03	5860.04	42	3105	0.960	-4.243E-03	5809.63	20.9	2630	1.025	-5.580E-04	1270.58	12.4
3021	0.990	-6.674E-03	3029.79	7.2	20051	0.997	-1.266E-02	2877.57	7.2	2631	1.026	-5.160E-04	1227.89	10.8
3024	1.005	-6.827E-03	2868.71	24.7	20052	0.997	-2.603E-02	2922.22	7.2	2640	1.023	-6.710E-04	1271.62	12.4
3027	0.997	-1.895E-03	2812.24	24.7	20151	1.000	-1.904E-02	2854.32	21.9	2641	1.022	-6.620E-04	1268.4	12.4
3030	0.993	-2.020E-03	2885.6	25.1	20152	1.000	-2.475E-02	2874.29	21.9	2650	1.023	-7.170E-04	1271.68	12.4
3033	0.999	-7.118E-03	3027.7	26	2000	1.026	-5.780E-04	1226.68	12.6	2651	1.022	-7.070E-04	1267.56	12.4
3036	0.996	-2.469E-03	2849.49	26	2001	1.029	-4.600E-04	1116.22	7.2	*** 5140	0.990	0.000E+00	**0**	**Slack bus**
3039	0.993	-2.368E-03	2903.78	23.8	2010	1.021	-7.240E-04	1495.86	21.9	5148	1.030	-4.250E-04	1069.03	0
3042	0.990	-1.455E-02	4495.97	24.3	2011	1.021	-7.250E-04	1488.68	22	5149	1.030	-4.240E-04	1069.23	0
3045	0.969	-4.631E-03	4088.92	24.3	2020	1.022	-6.940E-04	1271.88	12.4	5150	1.030	-4.240E-04	1068.33	0
* 3048	1.030	-3.047E-02	**6275.63**	**55.9**	2021	1.021	-6.850E-04	1269.07	12.4	*** 5151	0.990	-3.210E-08	**0**	**0**
* 3051	0.965	-1.034E-02	**6660.56**	**55.9**	2025	1.000	-3.425E-03	1379.12	12.4	*** 5152	0.990	-3.220E-08	**0**	**0**
3054	0.991	-2.247E-02	4486.25	19.7	2026	0.996	-3.541E-03	1425.73	12.4	5153	1.030	-3.020E-04	516.98	0
3057	0.981	-3.066E-03	3584.32	19.7	2027	0.996	-3.542E-03	1425.76	12.4	5154	1.030	-3.100E-04	517.06	0
3060	0.992	-1.393E-02	4538.01	27.1	2030	1.030	-5.040E-04	1063.56	0	20251	1.000	-4.220E-02	1450.9	12.4
3063	0.964	-6.568E-03	4208.93	27.1	2031	1.030	-4.470E-04	1066.67	0	20262	0.996	-4.271E-02	1506.14	12.4
3066	0.987	-2.977E-02	6633.58	16.6	2032	1.030	-5.130E-04	1063.25	0	20351	1.012	-1.835E-01	1346.27	0
3069	0.969	-3.777E-03	5053.04	16.6	2033	1.030	-4.580E-04	1066.34	0	20352	1.012	-1.835E-01	1346.27	0
3072	0.992	-1.335E-02	3100.48	15.6	2035	1.012	-3.179E-03	1050.86	0	20373	1.011	-1.698E-01	1345.58	0
3075	0.996	-4.181E-03	2919.98	15.6	2036	1.012	-3.180E-03	1050.85	0	20374	1.011	-1.694E-01	1344.86	0
3078	0.994	-4.517E-03	2935.46	15.6	2037	1.011	-2.914E-03	1070.05	0	20451	0.991	-4.134E-02	1398.7	10.8
** 3081	1.000	-3.335E-02	**9209.59**	**50.3**	2040	1.026	-5.730E-04	1227.53	10.8	20472	0.992	-4.135E-02	1412.5	12.4

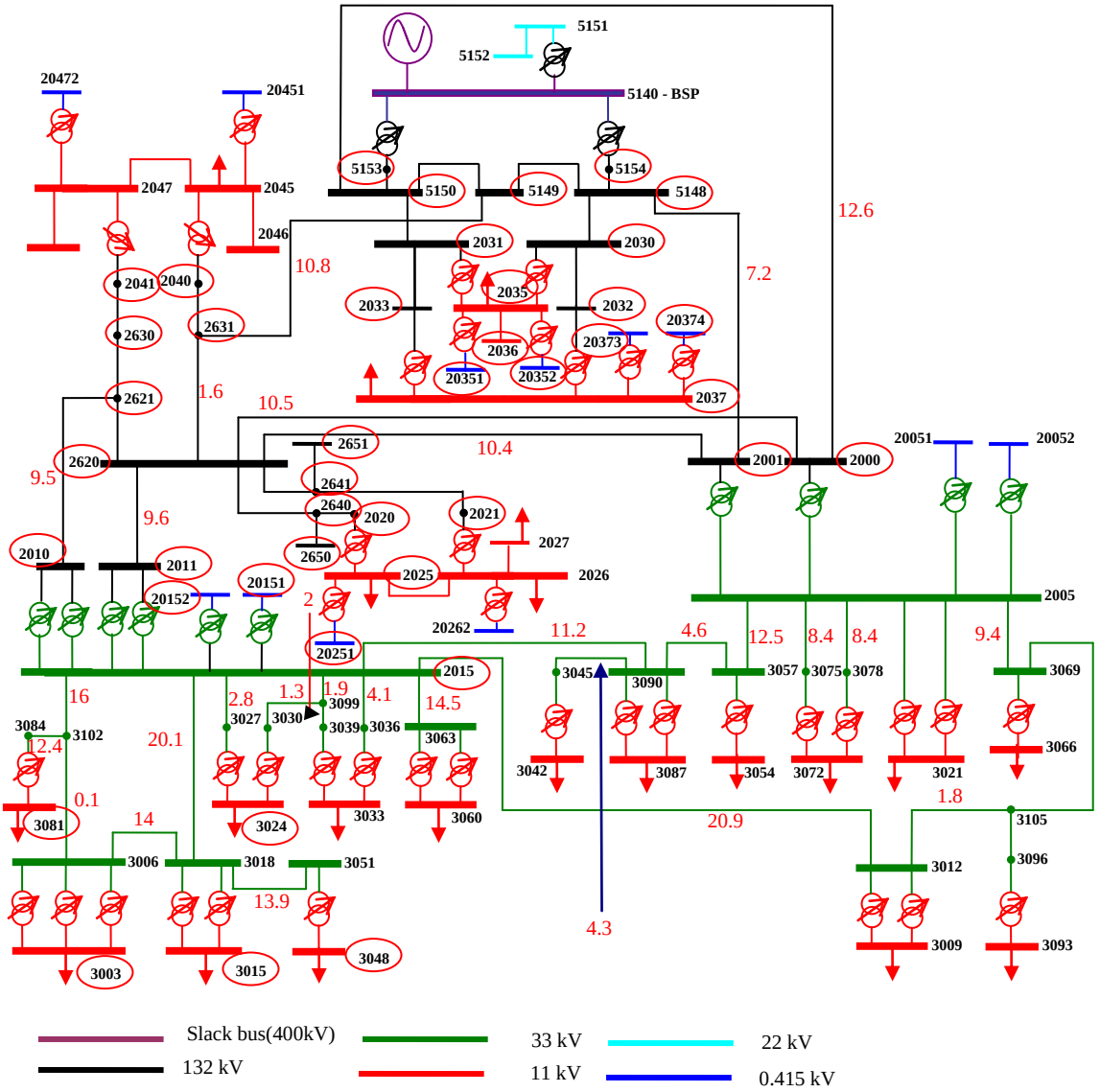

Figure 4.7: Circuit diagram of the Pembroke network

Table 4.5 shows the LRIC-v network charges owing to 1 MVAr nodal withdrawals. Specifically, columns 1-5, show bus name, voltage before withdrawal, voltage difference (voltage after nodal perturbation – voltage before nodal perturbation), LRIC-v charges and bus distance from the slack bus, respectively. While figure 4.7 shows the circuit diagram of the Pembroke network. All the red circled busbars have their voltages before withdrawals above 1 pu (that is, upper bus voltage limits critical) and while the rest have their voltages below 1 pu (that is, lower bus voltage limits critical).

For the buses with critical upper voltage limits, during MVAr withdrawals, their voltage upper margins would be increased as the voltage would be reduced on these particular buses. As a result, these buses would earn credits while on the other hand, the buses with critical lower voltage limits would be penalised as these would earn a costs for degrading their already critical bus lower margins. Since there are 42 critical upper bus limits, therefore, the

critical lower bus limits dominate hence during withdrawals the results are nodal costs as can be seen in table 4.5.

Generally, the costs increase as bus distance increases from the slack bus. However, bus 3081 attracts the most cost even though bus 3048 is the furthest from the slack bus. This is due to the fact that, bus 3048 has its upper voltage limit critical and as such during withdrawal at this bus, it attracts credit since this upper limit margin would be increased, therefore, delaying VAr device investment at this bus. This, in turn, result in the overall LRIC-voltage cost reduced due to this perturbation, at this bus. Since bus 3051 is the same distance from the slack bus as bus 3048, its overall costs are reduced, as well, since even though it itself attracts a cost but since it is closest to bus 3048 which attracts a significant credit during withdrawal at bus 3048. It should be noted, as well, that bus 3051 attracts more cost than bus 3048, consequent to the latter reason. Buses 3081 and 3084 attract the largest costs, respectively. The cost for bus 3081 is more than that of bus 3084 as the latter supplies the former, through a transformer, with power requirement and as a result there is a voltage drop across the transformer. It should be noted that voltage is 1 pu at bus 3081, before withdrawal, such that, during withdrawal it attracts a cost since this action would degrade its lower voltage limit margin, therefore, advancing the VAr asset investment horizon at this bus to a closer date. It should be noted that the resulting distances for these respective buses from the slack bus are quoted to be the same but their costs are different. The earlier stated reasoning applies to other buses with the same distances from the slack bus but with different costs. The slack bus, buses 5151 and 5152 attract no costs as their respective voltages for the slack bus did not change while those for buses 5151 and 5152 slightly change since they are close to the slack bus.

Table 4.6: LRIC-voltage network charges due to 1 MW withdrawal at each node on the Pembroke practical test system.

Bus	Initial Voltage (pu)	Voltage Difference (pu)	LRIC-V Charges (£/MW/yr)	Distance from slack Bus (km)	Bus	Initial Voltage (pu)	Voltage Difference (pu)	LRIC-V Charges (£/MW/yr)	Distance from slack Bus (km)	Bus	Initial Voltage (pu)	Voltage Difference (pu)	LRIC-V Charges (£/MW/yr)	Distance from slack Bus (km)
2005	0.997	-3.580E-04	507.81	7.2	** 3084	0.958	-7.082E-03	**4756.23**	**50.3**	2041	1.025	-1.230E-04	179.65	12.4
2015	1.000	-2.370E-04	453.33	21.7	3087	0.998	-2.855E-03	1712.88	24.3	2045	0.991	-2.540E-04	180.66	10.8
3003	1.002	-4.854E-03	3961.97	37.8	3090	0.976	-1.678E-03	1293.92	24.3	2046	0.991	-2.540E-04	180.67	10.8
3006	0.964	-3.526E-03	3489.16	37.8	3093	0.999	-6.307E-03	4327.63	20.9	2047	0.992	-2.510E-04	183.81	12.4
3009	0.992	-4.469E-03	3835.05	42.8	3096	0.954	-3.957E-03	3544.78	20.9	2048	0.992	-2.510E-04	183.81	12.4
3012	0.958	-2.845E-03	3030.16	42.8	3099	0.995	-6.880E-04	548.85	23.8	2620	1.025	-8.200E-05	180.03	12.4
3015	1.009	-5.278E-03	3672.85	42	3102	0.965	-3.508E-03	3479.42	37.9	2621	1.025	-8.300E-05	180.1	12.4
3018	0.962	-3.881E-03	3145.47	42	3105	0.960	-2.728E-03	3038.47	20.9	2630	1.025	-9.800E-05	179.93	12.4
3021	0.990	-1.292E-03	926.77	7.2	20051	0.997	-4.350E-04	537.54	7.2	2631	1.026	-7.700E-05	157.02	10.8
3024	1.005	-1.466E-03	801.02	24.7	20052	0.997	-6.790E-04	573.19	7.2	2640	1.023	-1.470E-04	186.54	12.4
3027	0.997	-9.470E-04	491.56	24.7	20151	1.000	-4.110E-04	499.75	21.9	2641	1.022	-1.440E-04	186.21	12.4
3030	0.993	-1.115E-03	564.13	25.1	20152	1.000	-5.280E-04	514.3	21.9	2650	1.023	-1.680E-04	186.6	12.4
3033	0.999	-1.704E-03	941.52	26	2000	1.026	-1.080E-04	163.82	12.6	2651	1.022	-1.640E-04	185.86	12.4
3036	0.996	-8.800E-04	528.08	26	2001	1.029	-5.200E-05	109.34	7.2	*** 5140	0.990	0.000E+00	**0**	**Slack bus**
3039	0.993	-9.770E-04	581.38	23.8	2010	1.021	-1.720E-04	288.2	21.9	5148	1.030	-3.600E-05	85.38	0
3042	0.990	-5.192E-03	2114.41	24.3	2011	1.021	-1.720E-04	280.91	22	5149	1.030	-3.600E-05	85.41	0
3045	0.969	-3.401E-03	1701.16	24.3	2020	1.022	-1.580E-04	187.54	12.4	5150	1.030	-3.500E-05	85.3	0
* 3048	1.030	-1.359E-02	**4488.24**	**55.9**	2021	1.021	-1.550E-04	187.64	12.4	*** 5151	0.990	-1.503E-09	**0**	**0**
* 3051	0.965	-7.506E-03	**3631.54**	**55.9**	2025	1.000	-4.810E-04	375.74	12.4	*** 5152	0.990	-1.340E-09	**0**	**0**
3054	0.991	-6.562E-03	1922.21	19.7	2026	0.996	-6.260E-04	445.2	12.4	5153	1.030	-1.200E-05	26	0
3057	0.981	-1.417E-03	1109.92	19.7	2027	0.996	-6.260E-04	445.25	12.4	5154	1.030	-1.300E-05	26.03	0
3060	0.992	-7.043E-03	2429.75	27.1	2030	1.030	-6.600E-05	84.56	0	20251	1.000	-1.295E-03	425.64	12.4
3063	0.964	-4.635E-03	1806.69	27.1	2031	1.030	-5.000E-05	84.61	0	20262	0.996	-1.462E-03	497.53	12.4
3066	0.987	-7.994E-03	3471.09	16.6	2032	1.030	-6.600E-05	84.58	0	20351	1.012	-1.177E-02	324.76	0
3069	0.969	-2.163E-03	2314.88	16.6	2033	1.030	-5.100E-05	84.63	0	20352	1.012	-1.177E-02	324.76	0
3072	0.992	-3.219E-03	758.86	15.6	2035	1.012	-2.920E-04	172.78	0	20373	1.011	-1.027E-02	239.33	0
3075	0.996	-1.524E-03	566.54	15.6	2036	1.012	-2.920E-04	172.78	0	20374	1.011	-1.023E-02	239	0
3078	0.994	-3.086E-03	613.19	15.6	2037	1.011	-1.450E-04	93.28	0	20451	0.991	-1.042E-03	227.45	10.8
** 3081	1.000	-1.288E-02	**5881.11**	**50.3**	2040	1.026	-1.020E-04	157.06	10.8	20472	0.992	-1.039E-03	231.03	12.4

Table 4.6 shows the LRIC-v charges given 1 MW nodal withdrawals. The columns 1-5 show the same parameters as in the previous table 4.5. It can be observed that the charges takes the same pattern as 1 MVAr nodal withdrawals but are reduced since the resulting network circuit X is more than the corresponding R. In that regard, bus 3081 attracts most cost. The same issue holds, since, during MW withdrawals the critical upper bus voltage margins are increased while the lower bus voltage margins are reduced, thereby, these earning credits and costs, respectively. The increase and degradation of the respective margins occur in a small way as reflected by the bus voltage changes in tables 4.6 as compared to table 4.5.

Table 4.7: LRIC-voltage network charges due to 1 MVAr injection at each node on the Pembroke practical test system

Bus	Initial Voltage (pu)	Voltage Difference (pu)	LRIC-V Charges (£/MVAr/yr)	Distance from slack Bus (km)	Bus	Initial Voltage (pu)	Voltage Difference (pu)	LRIC-V Charges (£/MVAr/yr)	Distance from slack Bus (km)	Bus	Initial Voltage (pu)	Voltage Difference (pu)	LRIC-V Charges (£/MVAr/yr)	Distance from slack Bus (km)
2005	0.997	1.767E-03	-2602.09	7.2	** 3084	0.958	9.610E-03	**-5616.43**	**50.3**	2041	1.025	6.140E-04	-1178.33	12.4
2015	1.000	1.184E-03	-2479.5	21.7	3087	0.998	8.695E-03	-3184.02	24.3	2045	0.991	3.356E-03	-1209	10.8
3003	1.002	1.048E-02	-4801.13	37.8	3090	0.976	3.099E-03	-3311.93	24.3	2046	0.991	3.357E-03	-1209	10.8
3006	0.964	5.084E-03	-4961.93	37.8	3093	0.999	1.592E-02	-4889.21	20.9	2047	0.992	3.370E-03	-1220.82	12.4
3009	0.992	1.015E-02	-4867.17	42.8	3096	0.954	5.728E-03	-5191.26	20.9	2048	0.992	3.371E-03	-1220.83	12.4
3012	0.958	4.279E-03	-4844.7	42.8	3099	0.995	1.816E-03	-2534.73	23.8	2620	1.025	5.200E-04	-1178.89	12.4
3015	1.009	1.066E-02	-4467.4	42	3102	0.965	5.068E-03	-4958.26	37.9	2621	1.025	5.210E-04	-1179.75	12.4
3018	0.962	5.414E-03	-4660.03	42	3105	0.960	4.199E-03	-4885.2	20.9	2630	1.025	5.580E-04	-1179.19	12.4
3021	0.990	6.583E-03	-2717.94	7.2	20051	0.997	1.235E-02	-2575.96	7.2	2631	1.026	5.140E-04	-1142.06	10.8
3024	1.005	6.734E-03	-2461.32	24.7	20052	0.997	2.473E-02	-2545.87	7.2	2640	1.023	6.700E-04	-1178.27	12.4
3027	0.997	1.886E-03	-2487.66	24.7	20151	1.000	1.834E-02	-2437.77	21.9	2641	1.022	6.600E-04	-1175.08	12.4
3030	0.993	2.010E-03	-2537.33	25.1	20152	1.000	2.358E-02	-2425.06	21.9	2650	1.023	7.150E-04	-1178.22	12.4
3033	0.999	7.015E-03	-2407.29	26	2000	1.026	5.770E-04	-1144.41	12.6	2651	1.022	7.060E-04	-1174.03	12.4
3036	0.996	2.457E-03	-2491.57	26	2001	1.029	4.600E-04	-1046.42	7.2	*** 5140	0.990	0.000E+00	**0**	**Slack bus**
3039	0.993	2.355E-03	-2539	23.8	2010	1.021	7.230E-04	-1377.13	21.9	5148	1.030	4.240E-04	-1003.88	0
3042	0.990	1.411E-02	-3529.32	24.3	2011	1.021	7.230E-04	-1370.06	22	5149	1.030	4.240E-04	-1004.04	0
3045	0.969	4.576E-03	-3545.23	24.3	2020	1.022	6.940E-04	-1178.17	12.4	5150	1.030	4.240E-04	-1003.24	0
* 3048	1.030	2.864E-02	**-3593.66**	**55.9**	2021	1.021	6.840E-04	-1175.44	12.4	*** 5151	0.990	3.200E-08	**0**	**0**
* 3051	0.965	1.006E-02	**-4987.73**	**55.9**	2025	1.000	3.401E-03	-1233.9	12.4	*** 5152	0.990	3.210E-08	**0**	**0**
3054	0.991	2.146E-02	-3010.14	19.7	2026	0.996	3.515E-03	-1286.01	12.4	5153	1.030	3.030E-04	-499.05	0
3057	0.981	3.045E-03	-3202	19.7	2027	0.996	3.516E-03	-1286.03	12.4	5154	1.030	3.100E-04	-499.09	0
3060	0.992	1.352E-02	-3414.05	27.1	2030	1.030	5.030E-04	-997.77	0	20251	1.000	3.891E-02	-1191.59	12.4
3063	0.964	6.461E-03	-3522.7	27.1	2031	1.030	4.480E-04	-1001.39	0	20262	0.996	3.932E-02	-1241.72	12.4
3066	0.987	2.803E-02	-4072.92	16.6	2032	1.030	5.120E-04	-997.42	0	20351	1.012	1.328E-01	-801.37	0
3069	0.969	3.743E-03	-4351.44	16.6	2033	1.030	4.570E-04	-1001.02	0	20352	1.012	1.328E-01	-801.37	0
3072	0.992	1.299E-02	-2621.34	15.6	2035	1.012	3.157E-03	-959.12	0	20373	1.011	1.257E-01	-840.98	0
3075	0.996	4.143E-03	-2641.74	15.6	2036	1.012	3.158E-03	-959.11	0	20374	1.011	1.255E-01	-841.17	0
3078	0.994	4.467E-03	-2647.94	15.6	2037	1.011	2.897E-03	-999.08	0	20451	0.991	3.815E-02	-1168.81	10.8
** 3081	1.000	3.115E-02	**-4660.56**	**50.3**	2040	1.026	5.710E-04	-1141.35	10.8	20472	0.992	3.816E-02	-1180.23	12.4

Table 4.7 shows LRIC-V charges consequent to 1 MVAr nodal injections. Columns 1-5 show all the parameters shown in the previous tables, 4.5 and 4.6.

During nodal injections, the reverse is true, in the context of what transpires during nodal withdrawals. That is, the buses with critical lower limits attract credits during nodal injections since the respective margins of these buses are increased, therefore, users who cause this effect have to be incentivized since this benefit the network. On the other hand, the buses with critical upper limits attract costs during nodal injections since the respective margins of these buses are degraded further and in that regard the investment horizons of the VAr compensation assets are advanced forward, therefore, users who cause this effect have to be penalized.

From table 4.7, it can be observed that the results follow a similar pattern to the ones for MVAr withdrawals but they are in a negative sense since the MVAr injections attract credits for a system with dominating critical lower bus limits. However, in this case, bus 3084 attracts the most credit, because during injection at node 3081, this bus attracts cost as its upper limit margin is degraded resulting in overall reduced credit at bus 3081. On the other hand, an injection at bus 3084 attracts a credit at this bus with less significant perturbation propagated at bus 3081 thus less cost at this bus and finally contributing to more overall credit at bus 3084 to bus 3081. Slack bus, buses 5151 and 5152 attract no credits for the same aforementioned reasons.

Table 4.8: LRIC-Voltage Network Charges Due To 1 MW Injection At Each Node

Bus	Initial Voltage (pu)	Voltage Difference (pu)	LRIC-V Charges (£/MW/yr)	Distance from slack Bus (km)	Bus	Initial Voltage (pu)	Voltage Difference (pu)	LRIC-V Charges (£/MW/yr)	Distance from slack Bus (km)	Bus	Initial Voltage (pu)	Voltage Difference (pu)	LRIC-V Charges (£/MW/yr)	Distance From slack Bus (km)
2005	0.997	3.540E-04	-492.36	7.2	** 3084	0.958	6.875E-03	**-3440.04**	**50.3**	2041	1.025	1.220E-04	-175.05	12.4
2015	1.000	2.350E-04	-433.53	21.7	3087	0.998	2.757E-03	-1529.26	24.3	2045	0.991	2.420E-04	-169.36	10.8
3003	1.002	4.687E-03	-3064.54	37.8	3090	0.976	1.662E-03	-1215.77	24.3	2046	0.991	2.420E-04	-169.36	10.8
3006	0.964	3.470E-03	-2809.94	37.8	3093	0.999	5.948E-03	-3447.69	20.9	2047	0.992	2.400E-04	-172.25	12.4
3009	0.992	4.311E-03	-3259.99	42.8	3096	0.954	3.887E-03	-3014.8	20.9	2048	0.992	2.400E-04	-172.25	12.4
3012	0.958	2.807E-03	-2679.19	42.8	3099	0.995	6.830E-04	-520.85	23.8	2620	1.025	8.200E-05	-175.69	12.4
3015	1.009	5.096E-03	-2935.18	42	3102	0.965	3.454E-03	-2803.2	37.9	2621	1.025	8.200E-05	-175.75	12.4
3018	0.962	3.816E-03	-2604.98	42	3105	0.960	2.692E-03	-2681.66	20.9	2630	1.025	9.800E-05	-175.48	12.4
3021	0.990	1.242E-03	-864.53	7.2	20051	0.997	2.770E-04	-463.7	7.2	2631	1.026	7.600E-05	-153.48	10.8
3024	1.005	1.415E-03	-726.23	24.7	20052	0.997	3.400E-05	-429.32	7.2	2640	1.023	1.480E-04	-181.54	12.4
3027	0.997	9.410E-04	-465.1	24.7	20151	1.000	6.200E-05	-389.24	21.9	2641	1.022	1.430E-04	-181.15	12.4
3030	0.993	1.108E-03	-532.95	25.1	20152	1.000	-5.500E-05	-375.38	21.9	2650	1.023	1.670E-04	-181.48	12.4
3033	0.999	1.645E-03	-823.97	26	2000	1.026	1.070E-04	-160.57	12.6	2651	1.022	1.640E-04	-180.67	12.4
3036	0.996	8.740E-04	-497.41	26	2001	1.029	5.300E-05	-107.81	7.2	*** 5140	0.990	0.000E+00	**0**	**Slack bus**
3039	0.993	9.690E-04	-548.2	23.8	2010	1.021	1.710E-04	-279.14	21.9	5148	1.030	3.500E-05	-84.45	0
3042	0.990	4.923E-03	-1824.85	24.3	2011	1.021	1.710E-04	-272.05	22	5149	1.030	3.500E-05	-84.48	0
3045	0.969	3.354E-03	-1544.39	24.3	2020	1.022	1.580E-04	-182.43	12.4	5150	1.030	3.600E-05	-84.37	0
* 3048	1.030	1.235E-02	**-3087.78**	**55.9**	2021	1.021	1.540E-04	-182.47	12.4	*** 5151	0.990	1.520E-09	**0**	**0**
* 3051	0.965	7.284E-03	**-2823.25**	**55.9**	2025	1.000	4.690E-04	-354.45	12.4	*** 5152	0.990	1.523E-09	**0**	**0**
3054	0.991	5.967E-03	-1625.49	19.7	2026	0.996	6.130E-04	-420.06	12.4	5153	1.030	1.300E-05	-25.79	0
3057	0.981	1.404E-03	-1050.58	19.7	2027	0.996	6.130E-04	-420.1	12.4	5154	1.030	1.200E-05	-25.81	0
3060	0.992	6.730E-03	-1988.32	27.1	2030	1.030	6.500E-05	-83.4	0	20251	1.000	-3.420E-04	-308.18	12.4
3063	0.964	4.543E-03	-1554.26	27.1	2031	1.030	5.100E-05	-83.6	0	20262	0.996	-2.190E-04	-371.21	12.4
3066	0.987	6.992E-03	-2789.93	16.6	2032	1.030	6.500E-05	-83.41	0	20351	1.012	-1.118E-02	-17.63	0
3069	0.969	2.137E-03	-2105.67	16.6	2033	1.030	5.000E-05	-83.6	0	20352	1.012	-1.118E-02	-17.63	0
3072	0.992	3.023E-03	-657.49	15.6	2035	1.012	2.810E-04	-163.57	0	20373	1.011	-9.980E-03	54.73	0
3075	0.996	1.501E-03	-532.39	15.6	2036	1.012	2.810E-04	-163.57	0	20374	1.011	-9.936E-03	54.42	0
3078	0.994	3.047E-03	-564.15	15.6	2037	1.011	1.360E-04	-87.08	0	20451	0.991	-5.450E-04	-124.16	10.8
** 3081	1.000	1.149E-02	**-3675.4**	**50.3**	2040	1.026	1.010E-04	-153.36	10.8	20472	0.992	-5.470E-04	-126.63	12.4

Table 4.8 shows LRIC-V charges consequent to 1 MW nodal injections. Columns 1-5 show all the parameters shown in the previous tables, 4.5, 4.6 and 4.7.

The results are similar to the case involving MVAr nodal injections but they are smaller. This is consequent to the fact that the resulting network circuit X is more that the corresponding resulting network circuit R. Here, again, bus 3081 attracts most credit while the slack bus and buses 5151 and 5152 attract no credits.

4.5 Chapter Conclusions

In this chapter, the principle of LRIC-voltage network charges is presented and demonstrated on the IEEE 14 bus test system and the 87-bus practical distribution test system. The LRIC-voltage network charging principle is to reflect the additional investment cost in network reactive power (VAr) compensation assets when accommodating new generation/demand, reflecting the cost to the network in ensuring that nodal voltages are within statutory limits. This approach makes use of spare capacity or headroom of nodal voltage of an existing network (distribution and transmission systems) to provide the time to invest in reactive power compensation devices. A nodal power withdrawal or injection will impact on system voltages, which as a result will defer or advance the future investment costs of VAr compensation devices. The LRIC-voltage network charge aims to reflect the impact on network voltage profiles consequent upon nodal power perturbation. This approach provides forward-looking economic signals that reflect both the voltage profiles of an existing network and the associated indicative future network cost of VAr compensation assets. The forward-looking LRIC-voltage network charges can be used to influence the location of future generation/demand for bettering network security and, consequently, minimize the cost of future investment in VAr compensation. Moreover, the real power and reactive power withdrawals/injections have being taken into account to derive the LRIC-V network charges in this study since both play a major role in impacting on the network nodal voltages.

Given this novel charging approach, true burden on the system, in terms of future network VAr compensation asset costs and network nodal voltages can be known to both network operators and the users. Finally, the users can exercise some economic choices whether their reactive power is to be supplied by the network reactive power or to install VAr compensation devices. This, in turn, can benefit the network by working towards the improvement of the network voltage profile. This LRIC-v network charging approach provide correct price signals as opposed to the currently used power factor penalty approach which many researchers view as inconsistent and inadequate as it would be apparently outlined below.

Comparing the proposed approach with the currently used power factor (pf) penalty, it is found that the proposed approach outweighs the currently used approach. The proposed charging approach is able to penalise the users who advance closer the network investment horizons and reward those that defer the network investment horizons in the context of the network nodal future VAr compensation assets. The currently used power factor penalty approach can only penalise the defaulters who operate below the set power factor threshold but fails to reward those users who otherwise operate above this set pf. Practically, every

network users has an impact on the network whether positive or negative as depicted by the proposed novel approach. This aforementioned impact by the user should be evaluated and, therefore, be accounted for in any associated charging approach. Further, it should be noted that WPD [68] has its power factor threshold set at 0.9. While Central Networks, the distribution company covering central England, has set a power factor threshold at 0.95 [69] and Scottish Hydro Electric Power Distribution, the distribution company covering Northern Scotland, has a power factor threshold set at 0.8 [70]. Based on the above various preset pf penalty thresholds, it is evident that there is no solid basis as to why these are chosen and, therefore, it is not cost reflective but a compromise reflecting costs and material constraints, as outlined by [71]. In addition, the pf penalty approach was proposed several years ago and, therefore, it is outdated as described by [71]. For example, if we consider two loads 200 MW + j50.1 MVAr (pf = 0.97) and 20 MW + j19 MVAr (pf = 0.72). If these two loads are connected to the above distribution networks, the larger load would not be penalised by any of the distribution networks since its pf is above the trigger pf threshold of all of them while the smaller load would be penalised since its pf is below the trigger pf threshold of all the distribution companies. This would be unfair as the larger load draws some considerable real and reactive powers from the network. Regarding the proposed novel LRIC-voltage network charging principle, both the loads would be charged in accordance to the exact proportion as the amounts of real and reactive powers consumed by each, which results in an equitable sharing of cost burden. Moreover, the proposed approach shows the nodal charges owing to the nodal perturbations as every network user impact on the network but not only the users having pf less than the chosen threshold as it is suggested by the currently used approach. The charges by this proposed novel approach obviously provide forward-looking cost-reflective correct price signals to both the loads and, moreover, this principle can easily be understood by the network users than the pf penalty approach. In this regard, the considered loads (network users) would exercise an economic choice whether to source network VAr or provide their own VAr. This, in turn, would benefit the network as the overall result being the improved network voltage profile. Furthermost, unlike the pf penalty approach, this approach directly utilizes the actual parameter (nodal voltage) which is being monitored to ensure that the network nodal voltages are within the lower and upper limits. Also, the pf penalty approach was designed specifically to recover charges for generator operating costs.

Chapter 5

LRIC-Voltage Network Pricing To Support Network Voltages Under N-1 Contingencies

The proposed LRIC-voltage network pricing methodology formulated and explained in the previous chapter is extended to reflect the true burden on a system to support network voltages under n-1 contingencies. The need for considering n-1 contingencies being that, during these, the nodal voltage loadings would be reduced to accommodate them. Again, to demonstrate this extension, IEEE 14 bus standard test system and the practical distribution test system would be once again employed. The results show that the respective charges follow the same pattern but are increased since the nodal busbar voltage margins are reduced to accommodate n-1 contingencies.

5.1 Chapter Introduction

The investment cost-related pricing (ICRP) charging model [72] used in the UK, for recovering investment costs of network circuits and transformers, does not consider the network security requirement, but, it relies on post-processing through a full-contingency analysis to give an average security factor of 1.86 for all concerned network assets. On other works related to investment costs of circuits and transformers, authors of [65] demonstrated a simplistic approach to network security based on the assumption that reinforcement is required when a branch reaches 50% utilization. Authors of [73]-[76] considered the n-1 contingency analysis into their charging principles and all of these were for pricing of network circuits and transformers. It is against this background that the n-1 contingency conditions were factored into the previously mentioned charging principles coupled with the fact that in reality the network is required to be able to withstand these, that these contingencies must be factored into the LRIC-voltage network charging principle.

The LRIC-Voltage Network Charges, as explained earlier, do not reflect the practical reality of the network being subjected to n-1 contingency situation, as required, to ensure that the system is secured and reliable under these. To ensure system security and reliability practically, the resulting network nodal voltage limits have to be determined given n-1 contingencies. It should be noted that, during these n-1 contingencies, the nodal bus margins are reduced and if these are allowed to be operated at full capacity, the system security and reliability would be compromised. As a result, the actual network nodal voltage loadings should be determined considering n-1 contingencies and, consequently, the resulting charges due to this consideration should be determined. The charges considering n-1 contingencies are referred to as CF LRIC-voltage network charges.

In this chapter, the nodal busbar contingency factors for both lower and upper bus limits are determined and, thereafter, the resulting new nodal busbar lower and upper limits are determined. Finally, the CF LRIC-Voltage Network Charges are evaluated to reflect the true burden on the system to support n-1 contingencies.

This charging extension of the LRIC-Voltage Network Charging principle is, once again, finally tested on the IEEE 14 bus test system and lastly on the distribution test system. Thereafter, the results are presented and analyzed.

5.2 Impact To Network Voltage When Considering N-1 Contingencies

If a network node b supports voltage V_b under the normal state and has to carry an additional voltage of ΔV_L due to the most severe n-1 contingency situation, then the contingency factor at that node can be determined by (5.1)

$$CF_L = \frac{V_b + \Delta V_L}{V_b} \tag{5.1}$$

Given the node has to withstand additional voltage disturbance, where the magnitude of the disturbance is indicated by contingency factor, CF_L, the system cannot be allowed to operate to its limits. Instead, the maximum allowed voltage level at each busbar has to be modified to cater for potential contingencies. This new nodal voltage limit for the lower bus voltage limit can be determined by (5.2)

$$V_{b_{CF_L}} = \frac{V_L}{CF_L} \tag{5.2}$$

On the other hand, if a network node b supports voltage V_b under normal state and has to carry an additional voltage of ΔV_H due to the most severe n-1 contingency situation, then the contingency factor at that node can be determined by (5.3)

$$CF_H = \frac{V_b + \Delta V_H}{V_b} \tag{5.3}$$

Given the node has to withstand additional voltage disturbance, where the magnitude of the disturbance is indicated by contingency factor, CF_H, the system cannot be allowed to operate to its limits. Instead, the maximum allowed voltage level at each busbar has to be modified to cater for potential contingencies. This new nodal voltage limit for the higher bus voltage limit can be determined by (5.4)

$$V_{b_{CF_H}} = \frac{V_H}{CF_H} \tag{5.4}$$

5.3 Contingency Factor (CF) LRIC-Voltage Network Charges

Given the newly determined effective network lower bus limit, $V_{b_{CF_L}}$, and higher bus limit, $V_{b_{CFH}}$, to support n-1 contingencies, these can be utilized in the LRIC-v charging principle to formulate the CF LRIC-voltage network charges by replacing V_L by the former new limit while replacing V_H by the latter new limit in the relevant equations ranging from (4.1a) to (4.11a) in the previous chapter.

5.4 Results and Analysis

The results are presented and analysed below, they show the contingency factors for the nodal lower and upper voltage limits, the resulting nodal lower and upper voltage limits and finally, LRIC-voltage network charges considering n-1 contingencies or CF LRIC-voltage network charges. Once again, the IEEE-14 bus test system and a distribution test system used, in the previous chapter, are utilised to demonstrate what pattern the charges followed.

5.4.1 IEEE-14 Bus Test System

This test system was introduced in chapter 4. All the data introduced earlier remains the same, namely, the nodal voltage limits, economic data and, loading and generation conditions of this test system.

1. Contingency Factor Terms

The nodal contingency factors reflect additional voltage change that would be incurred following the worst n-1 contingency. Since every network bus has both the lower and upper limits, the contingency factors to cater for both these limits on each bus were determined, subject to n-1 contingencies.

Figure 5.1 and table 5.1 show lower voltage limit contingency factors against nodes. In addition, table 5.1 shows initial, and outage voltages and the resulting lower nodal voltage limits.

On the other hand, Figure 5.2 and table 5.2 show higher voltage limit contingency factors against nodes. In addition, table 5.2 shows initial, and outage voltages and the resulting higher nodal voltage limits.

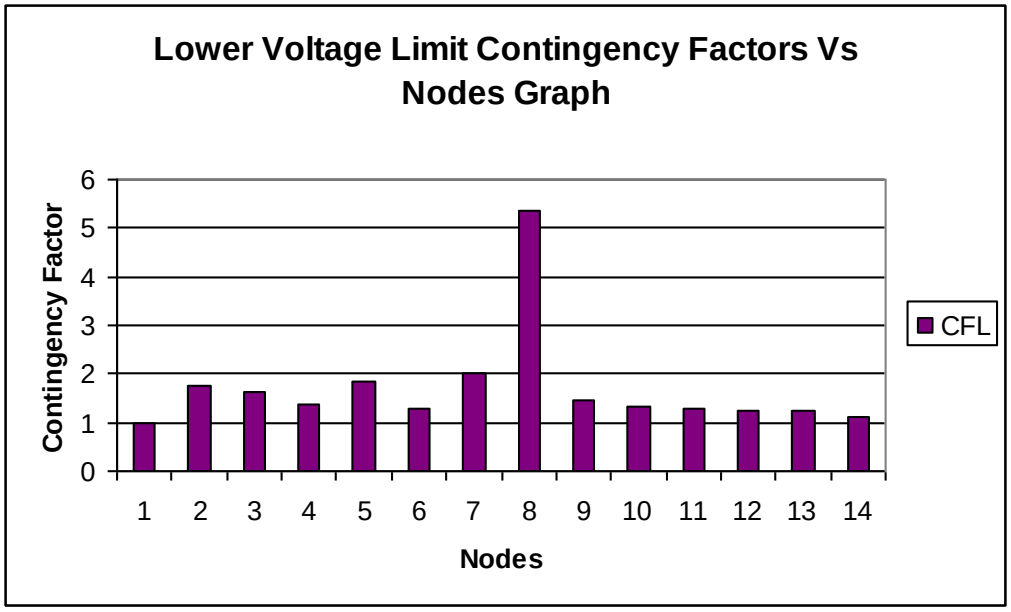

Figure 5.1: IEEE 14 bus system lower voltage limit contingency factors at each node

Table 5.1: Lower nodal voltage limit contingency factors subject to n-1 contingencies on the IEEE 14 bus test system

Bus	Initial Voltage (pu)	Outage Voltage (pu)	CF_L	Resulting VL (pu)
1	1.03	1.03	1	0.94
2	1.02	0.99	1.752	0.992
3	0.996	0.954	1.646	0.987
4	0.988	0.962	1.374	0.973
5	0.995	0.941	1.83	0.994
6	0.982	0.96	1.284	0.967
7	1.008	0.955	2.015	1.000
8	1.048	0.998	5.345	1.038
9	0.981	0.947	1.442	0.977
10	0.974	0.946	1.314	0.969
11	0.974	0.95	1.281	0.966
12	0.967	0.945	1.244	0.964
13	0.963	0.94	1.239	0.963
14	0.954	0.943	1.099	0.951

Figure 5.1 shows a plot of CF_L values against nodes given the most severe n-1 contingency condition impacting on each lower voltage bus limit on the IEEE-14 bus system. Table 5.1 also shows the CF_L values against nodes and in addition the initial voltages before the outages, the outage voltages and the resulting new lower voltage limits.

The largest CF_L is recorded at bus 8. The most severe outage on this bus was when the line between buses 2 and 3 is outaged. This particular line was critical in supplying the necessary apparent power to support the load at bus 3. During this outage, all the apparent power had to be re-routed along the line between buses 3 and 4. This caused the voltage at bus 8 to drop from 1.048 pu to 0.998 pu which corresponds to a bus loading of 9.73% to 52% with respect to the lower voltage limit. The CF_L value at bus 7 is the second largest since both aforementioned buses where severely affected by the same outage. The least CF_L value is at the slack bus since the voltage at this bus remains the same across all the outages.

The results generally show that the more the CF_L values the more reduced the resulting nodal lower voltage limits.

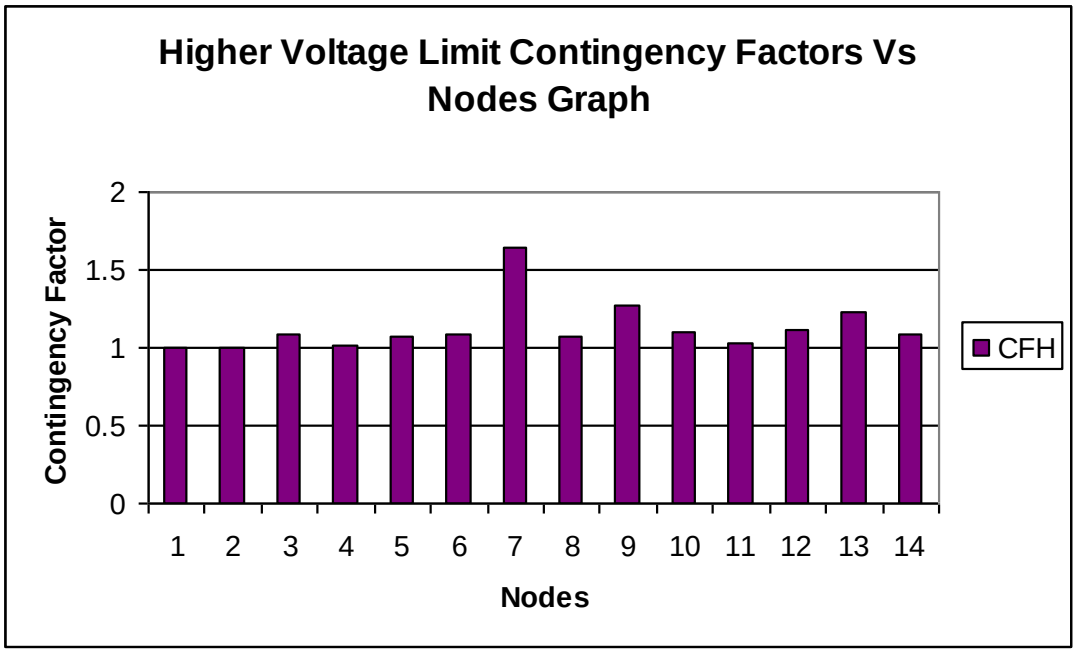

Figure 5.2: IEEE 14 bus system higher voltage limit contingency factors at each node

Table 5.2: Higher nodal voltage limit contingency factors subject to n-1 contingencies on the IEEE 14 bus test system

Bus	Initial Voltage (pu)	Outage Voltage (pu)	CF_H	Resulting VH (pu)
1	1.03	1.03	1	1.06
2	1.02	1.02	1.001	1.060
3	0.996	1	1.081	1.051
4	0.988	0.989	1.02	1.058
5	0.995	0.999	1.07	1.052
6	0.982	0.986	1.088	1.050
7	1.008	1.052	1.644	1.013
8	1.048	1.056	1.068	1.052
9	0.981	0.992	1.268	1.035
10	0.974	0.977	1.097	1.049
11	0.974	0.975	1.029	1.057
12	0.967	0.971	1.12	1.047
13	0.963	0.968	1.222	1.038
14	0.954	0.955	1.089	1.050

Figure 5.2 shows a plot of CF_H values against nodes given the most severe n-1 contingency condition impacting on each higher voltage bus on the ieee 14 bus system. Table 5.2 also shows the CF_H values against nodes and in addition the initial voltages before the outages, the outage voltages and the resulting higher voltage limits.

The largest CF_H value is recorded at bus 7. The most severe outage on this bus is when the line between buses 7 and 9 was taken out. This outage resulted in a large voltage rise at this bus since this line was critical in linking the subtransmission and most of the distribution side of the network. Due to this outage the power was re-routed from the line connecting the slack bus to bus 5 and eventually from bus 5 through to bus 6 through the transformer to other buses. The voltage rised from 1.008 pu to 1.052 pu which constituted bus loading of 56.67% to 93.17% with reference to the higher voltage limit. The least CF_H value is also at the slack bus since the voltage at this bus remains the same across all the outages.

The results generally show that the more the CF_H values the more reduced are the resulting nodal higher voltage limits.

2. CF LRIC-Voltage Network Charges

After calculating the contingency factors for the corresponding lower and higher nodal voltage limits then the CF LRIC-voltage network charges were determined based on those new limits.

Figure 5.3 and table 5.3 show CF LRIC-voltage network charges due to 1 MVAr nodal withdrawals. Also, shown in table 5.3 are the shortest distances from the slack bus to the corresponding buses, nodal voltages before the withdrawals and voltage differences (voltages after nodal perturbations – voltages before nodal perturbations).
.

On the other hand, figure 5.4 and table 5.4 show CF LRIC-voltage network charges due to 1 MW nodal withdrawals. Also, shown in table 5.4 are the shortest distances from the slack bus to the corresponding buses, nodal voltages before the withdrawals and voltage differences (voltages after nodal perturbations – voltages before nodal perturbations).

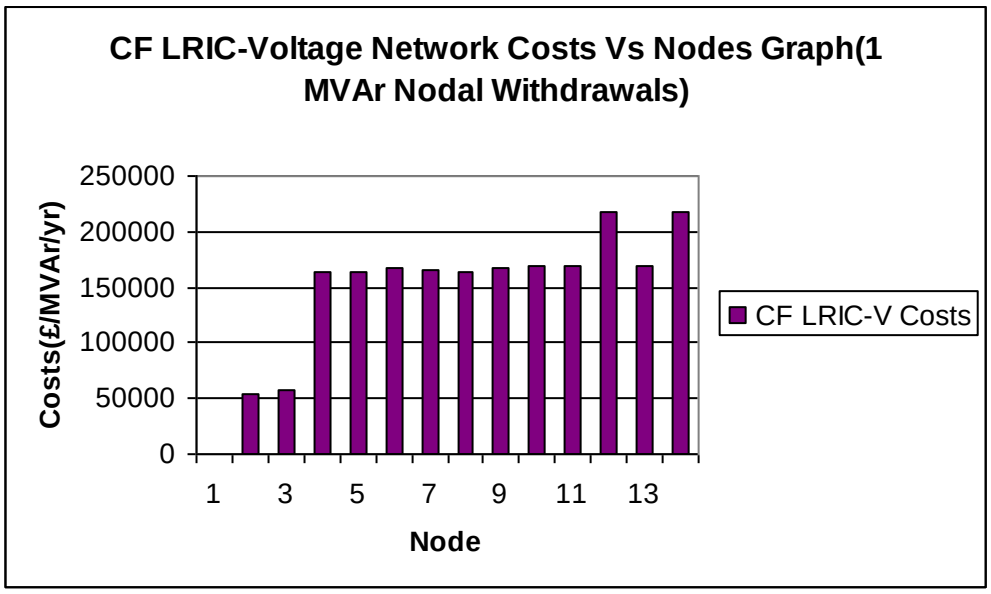

Figure 5.3: CF LRIC-voltage network charges per 1 MVAr withdrawal at each node on the IEEE 14 bus test system

Table 5.3: CF LRIC-Voltage Network Charges due to 1 MVAr withdrawal at each node on the IEEE 14 bus test system

Bus	Initial Voltage pu	Voltage Difference (pu)	LRIC-Charges (£/MVAr/yr)	Distance from slack (km)
1	1.03	0.000E+00	0	0
2	1.020	-5.000E-04	54532.3	38
3	0.996	-1.526E-03	57853.13	108
4	0.988	-1.018E-03	163911.38	95
5	0.995	-9.290E-04	163413.62	82
6	0.982	-2.647E-03	168008.73	82
7	1.008	-2.337E-03	164956.64	95
8	1.048	-3.709E-03	163499.45	95
9	0.981	-2.604E-03	167205.32	95
10	0.974	-3.100E-03	168168.26	97
11	0.974	-3.399E-03	168787.28	88
12	0.967	-4.096E-03	218164.86	93
13	0.963	-3.431E-03	168671.87	87
14	0.954	-4.112E-03	218300.42	101

Since the lower nodal voltage limit margins have been reduced to support n-1 contingencies, during nodal withdrawals, a number of lower voltage limits have been reached therefore reinforcements indications were as follows:

1) During withdrawals at buses 2 and 3, the lower voltage limit at bus 13 was reached therefore a reinforcement cost was attracted at this bus. At other buses during these respective withdrawals, some attracted credits (buses 2, 7 and 8) while the rest excluding the slack bus attracted costs for degrading the respective lower voltage limit margins. Since bus 3 has more distance from the slack bus it attracted more cost than bus 2.

2) During withdrawals at buses 4, 5, 6, 7, 8, 9, 10, 11 & 13 there are lower voltage limit violations at buses 5, and 13 as such these attracted reinforcement costs.

3) During withdrawal at bus 12, buses 5, 12 and 13 had their lower voltage limits reached and as such attracted reinforcement costs.

4) Lastly, during withdrawal at bus 14, buses 5, 13 and 14 had their lower voltage limits reached therefore they attracted some reinforcement costs.

Since buses 12 and 14 attracted three reinforcement costs, they have their costs around £218,000.00 while buses 2 and 3 have the least costs around £55,000.00 and £58,000.00 respectively since they attracted only one reinforcement costs.

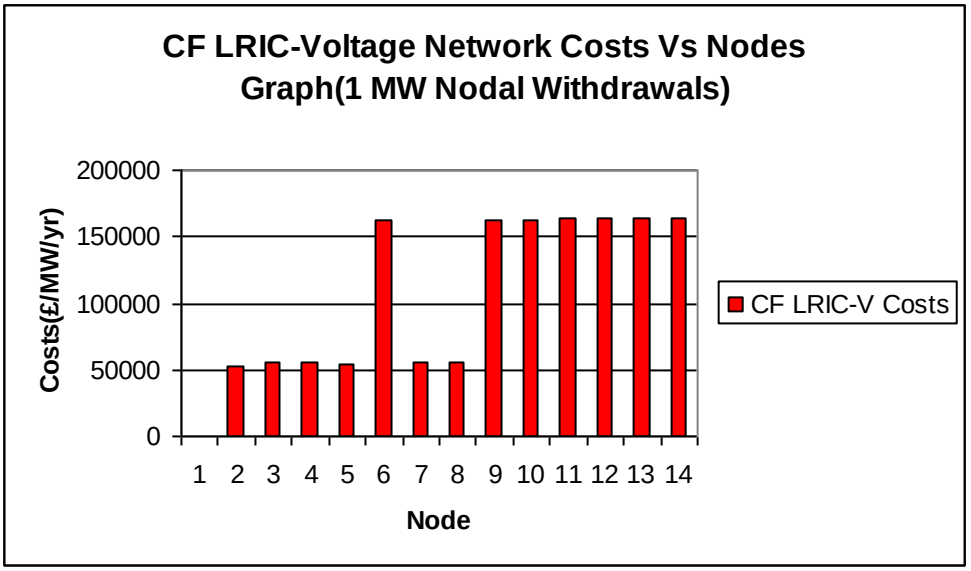

Figure 5.4: CF LRIC-voltage network charges per 1 MW withdrawal at each node on the IEEE 14 bus test system

Table 5.4: CF LRIC-Voltage Network Charges due to 1 MW withdrawal at each node on the IEEE 14 bus test system

Bus	Initial Voltage pu	Voltage Difference (pu)	LRIC-Charges (£/MW/yr)	Distance from slack (km)
1	1.03	0.000E+00	0	0
2	1.020	-2.030E-04	52865.48	38
3	0.996	-8.000E-04	55371.38	108
4	0.988	-5.010E-04	54971.01	95
5	0.995	-4.130E-04	54521.16	82
6	0.982	-8.850E-04	162645.22	82
7	1.008	-7.220E-04	55870	95
8	1.048	-7.000E-04	55881.35	95
9	0.981	-9.300E-04	162679.22	95
10	0.974	-1.182E-03	163107.77	97
11	0.974	-1.341E-03	163252.04	88
12	0.967	-1.962E-03	163762.18	93
13	0.963	-1.465E-03	163350.55	87
14	0.954	-1.911E-03	163955.94	101

During 1 MW nodal withdrawals, the nodal voltage changes were relative smaller than in the MVAr nodal withdrawals' case and, as such, the number of nodal lower voltage limits reached was few, hence, less comparable nodal costs. The following number of nodal lower voltage limits has been reached, therefore, reinforcements indications were as follows:

1) During MW withdrawals at buses 2, 3, 4, 5, 7 and 8, reinforcements were triggered at bus 13.

2) MW withdrawals at buses 6, 9, 10, 11, 12, 13 and 14 triggered reinforcements at buses 5 and 13.

Given the above triggered reinforcements, buses 2, 3, 4, 5, 7 and 8 attract costs around the region of £52, 865.00 to £55, 881.00 since they all triggered one reinforcement investment. On the other hand, the rest of the buses, excluding the slack bus, triggered two reinforcement investments, therefore, comparatively more costs ranging from £162, 645.00 to £163, 955.00. However, the costs are relatively more during the 1 MVAr withdrawals since up to three reinforcement investments were triggered.

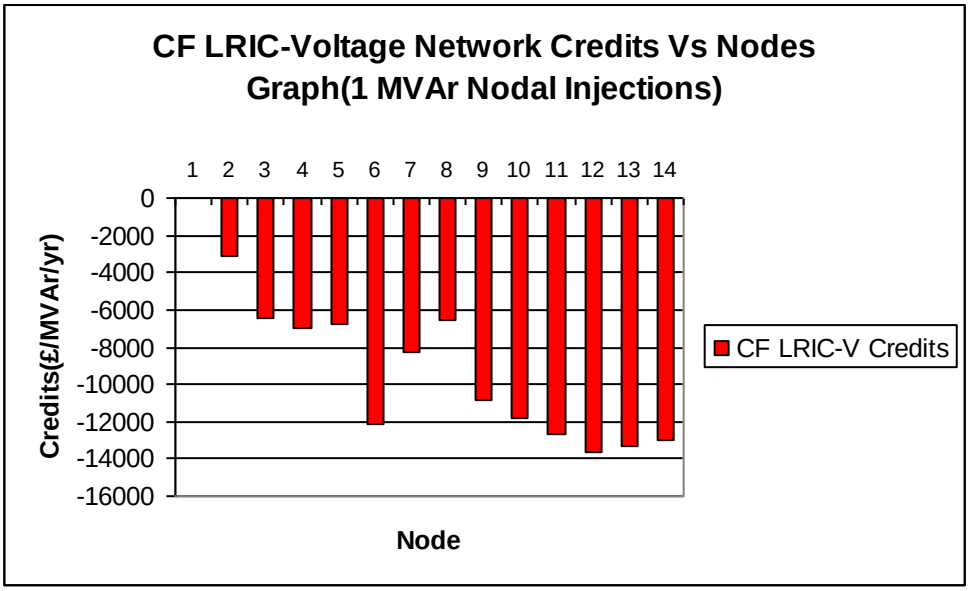

Figure 5.5: CF LRIC-voltage network charges per 1 MVAr withdrawal at each node

Table 5.5: CF LRIC-voltage network charges due to 1 MVAr injection at each node on the IEEE 14 bus test system

Bus	Initial Voltage pu	Voltage Difference (pu)	LRIC-Charges (£/MVAr/yr)	Distancce from slack (km)
1	1.03	0.000E+00	0	0
2	1.020	4.990E-04	-3105.31	38
3	0.996	1.521E-03	-6483.26	108
4	0.988	1.016E-03	-6984.61	95
5	0.995	9.260E-04	-6814.79	82
6	0.982	2.633E-03	-12145.65	82
7	1.008	2.326E-03	-8279.41	95
8	1.048	3.685E-03	-6564.85	95
9	0.981	2.589E-03	-10793.53	95
10	0.974	3.078E-03	-11822.65	97
11	0.974	3.373E-03	-12631.67	88
12	0.967	4.058E-03	-13602.91	93
13	0.963	3.403E-03	-13346	87
14	0.954	4.073E-03	-13007.91	101

During nodal injections, there were not limits reached. It should be noted that the range of nodal voltage limits with contingency factors considered is less than that without contingency factors considered. This factor leads to more nodal credits for CF LRIC-voltage network charges than LRIC-voltage network charges. It should also be noted that the nodal credits follow the same pattern as the case without considering the contingency factors (in the previous chapter) but only increased credits, therefore bus 12 attracts the most credits while bus 2 the least.

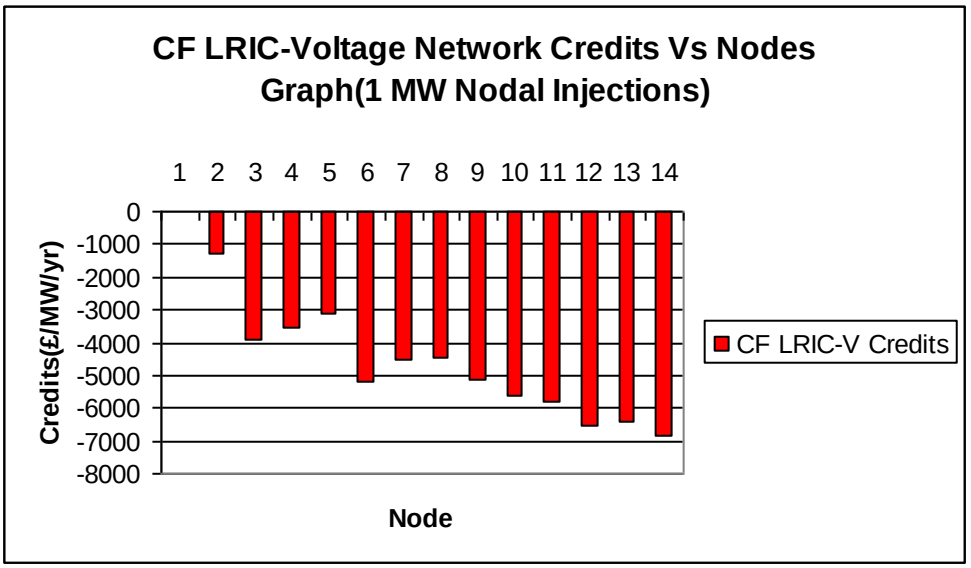

Figure 5.6: CF LRIC-voltage network charges due to 1 MW withdrawal at each node

Table 5.6: CF LRIC-voltage network charges due to 1 MW injection at each node on the IEEE 14 bus test system

Bus	Initial Voltage pu	Voltage Difference (pu)	LRIC-Charges (£/MW/yr)	Distancce from slack (km)
1	1.03	0.000E+00	0	0
2	1.020	2.020E-04	-1303.95	38
3	0.996	7.960E-04	-3928.85	108
4	0.988	5.000E-04	-3569.05	95
5	0.995	4.110E-04	-3096.70	82
6	0.982	8.760E-04	-5219.80	82
7	1.008	7.150E-04	-4500.96	95
8	1.048	6.840E-04	-4488.53	95
9	0.981	9.200E-04	-5137.50	95
10	0.974	1.168E-03	-5622.18	97
11	0.974	1.325E-03	-5799.86	88
12	0.967	1.936E-03	-6542.55	93
13	0.963	1.447E-03	-6419.17	87
14	0.954	1.886E-03	-6841.21	101

It can be seen from figure 5.6 and table 5.6 that the results follow the same pattern as those of figure 4.5 and table 4.5, but, the credits sought in the former case are small than in the latter one since the network resulting reactance (X) is more than the corresponding resulting resistance (R) and hence less network nodal voltage increments.

5.4.2 Pembroke Practical Test System

This practical test system was also introduced in chapter 4. All the data introduced earlier remains the same, namely, the nodal voltage limits, economic data and, loading and generation conditions of this test system.

1. Contingency Factor Terms

The nodal contingency factors reflect additional voltage change that would be incurred following the worst contingency. Since every network bus has both the lower and upper limits, the contingency factors to cater for both these limits on each bus were determined, subject to n-1 contingencies.

Table 5.7 shows lower voltage limit contingency factors against nodes. Columns 1-5 show bus number, initial, and outage voltages and the resulting lower nodal voltage limits, respectively.

On the other hand, table 5.8 shows higher voltage limit contingency factors against nodes. Also, columns 1-5 show bus number, initial, and outage voltages and the resulting higher nodal voltage limits, respectively.

Table 5.7: Lower nodal voltage limit contingency factors subject to n-1 contingencies on Pembroke practical test system.

Bus	Initial Voltage (pu)	Outage Voltage (pu)	CF_L	Resulting VL (pu)	Bus	Initial Voltage (pu)	Outage Voltage (pu)	CF_L	Resulting VL (pu)	Bus	Initial Voltage (pu)	Outage Voltage (pu)	CF_L	Resulting VL (pu)
2005	0.997	0.969	1.445	0.977	3084	0.958	0.943	1.15	0.956	2041	1.025	1.01	1.196	0.933
2015	1	0.986	1.242	0.963	3087	0.998	0.958	1.636	0.987	2045	0.991	0.976	1.223	0.962
3003	1.002	0.96	1.726	0.990	3090	0.976	0.953	1.276	0.966	2046	0.991	0.976	1.223	0.962
3006	0.964	0.949	1.159	0.956	3093	0.999	0.959	1.645	0.987	2047	0.992	0.977	1.216	0.961
3009	0.992	0.949	1.632	0.986	3096	0.954	0.941	1.117	0.953	2048	0.992	0.977	1.216	0.961
3012	0.958	0.942	1.157	0.956	3099	0.995	0.976	1.295	0.967	2620	1.025	1.01	1.195	0.933
3015	1.009	0.943	2.273	1.007	3102	0.965	0.949	1.159	0.956	2621	1.025	1.01	1.195	0.933
3018	0.962	0.947	1.155	0.956	3105	0.96	0.944	1.16	0.957	2630	1.025	1.01	1.195	0.933
3021	0.99	0.962	1.406	0.975	20051	0.997	0.969	1.272	0.974	2631	1.026	1.01	1.22	0.936
3024	1.005	0.99	1.268	0.965	20052	0.997	0.969	1.272	0.974	2640	1.023	1.008	2.159	1.007
3027	0.997	0.977	1.316	0.969	20151	1	0.986	1.145	0.960	2641	1.022	1.007	1.188	0.932
3030	0.993	0.977	1.249	0.964	20152	1	0.986	1.145	0.960	2650	1.023	1.008	2.159	1.007
3033	0.999	0.979	1.327	0.970	2000	1.026	1.015	1.153	0.927	2651	1.022	1.007	1.188	0.932
3036	0.996	0.967	1.439	0.977	2001	1.029	1.009	1.29	0.945	** 5140	0.99	0.99	**1**	**0.900**
3039	0.993	0.969	1.354	0.971	2010	1.021	1.005	1.208	0.934	5148	1.03	1.022	1.125	0.922
3042	0.99	0.951	1.568	0.983	2011	1.021	1.006	1.188	0.932	5149	1.03	1.022	1.125	0.922
3045	0.969	0.946	1.257	0.965	2020	1.022	1.008	2.173	1.008	5150	1.03	1.022	1.124	0.922
* 3048	1.03	0.954	**3.555**	**1.026**	2021	1.021	1.006	1.187	0.932	** 5151	0.99	0.99	**1**	**0.940**
3051	0.965	0.949	1.159	0.957	2025	1	0.985	1.257	0.965	** 5152	0.99	0.99	**1**	**0.940**
3054	0.991	0.941	1.71	0.990	2026	0.996	0.952	1.688	0.989	5153	1.03	1.024	1.09	0.917
3057	0.981	0.959	1.278	0.966	2027	0.996	0.952	1.688	0.989	5154	1.03	1.024	1.083	0.915
3060	0.992	0.975	1.243	0.963	2030	1.03	1.009	1.292	0.945	20251	1	0.985	1.154	0.961
3063	0.964	0.949	1.158	0.956	2031	1.03	1.006	1.346	0.951	20262	0.996	0.952	1.424	0.988
3066	0.987	0.959	1.388	0.974	2032	1.03	1.009	1.292	0.945	20351	1.012	0.99	1.251	0.972
3069	0.969	0.943	1.297	0.967	2033	1.03	1.006	1.345	0.951	20352	1.012	0.99	1.251	0.972
3072	0.992	0.964	1.413	0.975	2035	1.012	0.99	1.459	0.978	20373	1.011	0.998	1.156	0.962
3075	0.996	0.968	1.436	0.976	2036	1.012	0.99	1.459	0.978	20374	1.011	0.998	1.156	0.962
3078	0.994	0.966	1.427	0.976	2037	1.011	0.998	1.285	0.967	20451	0.991	0.976	1.141	0.960
3081	1	0.957	1.713	0.990	2040	1.026	1.01	1.22	0.936	20472	0.992	0.977	1.136	0.959

Table 5.7 shows the lower nodal voltage limit contingency factors subject to n-1 contingencies. In addition, table 5.7 shows the bus numbers, initial voltage before n-1 contingencies, voltage during n-1 contingencies and the resulting lower bus voltage limits.

The results show that bus 3048 was most affected as the contingency factor for this bus, in relation to the lower bus voltage limit, is 3.555 and the resulting lower bus voltage limit being 1.026 pu from 0.94 pu. This was consequent to the outage of a line connecting buses 2015 and 3018. This resulted in power being supplied to bus 3048 and others utilising only line connecting buses 2015 and 3006, therefore, there were a lot of losses experienced and hence lower voltage at bus 3048. Before this aforementioned contingency, the voltage was 1.03 pu and after this contingency the voltage was 0.954 pu which constituted a bus voltage loading of 24.8% to 88.17%, respectively, with respect to the lower bus voltage limit.

The lowest contingency factor was lowest at slack bus, buses 5151 and 5152 as the voltages of theses buses did not change across all contingencies.

Table 5.8: Upper nodal voltage limit contingency factors subject to n-1 contingencies on Pembroke practical test system

Bus	Initial Voltage (pu)	Outage Voltage (pu)	CF_L	Resulting VL (pu)	Bus	Initial Voltage (pu)	Outage Voltage (pu)	CF_L	Resulting VL (pu)	Bus	Initial Voltage (pu)	Outage Voltage (pu)	CF_L	Resulting VL (pu)
2005	0.997	1.001	1.064	1.053	* 3084	0.958	0.985	**2.483**	**0.988**	2041	1.025	1.026	1.007	1.099
2015	1	1.001	1.01	1.059	3087	0.998	0.998	1.008	1.059	2045	0.991	0.992	1.002	1.060
3003	1.002	1.004	1.043	1.055	3090	0.976	0.977	1.013	1.059	2046	0.991	0.992	1.002	1.060
3006	0.964	0.967	1.105	1.049	3093	0.999	1.014	1.255	1.036	2047	0.992	0.992	1.01	1.059
3009	0.992	0.993	1.018	1.058	3096	0.954	0.968	2.017	0.999	2048	0.992	0.992	1.01	1.059
3012	0.958	0.959	1.048	1.054	3099	0.995	0.997	1.033	1.056	2620	1.025	1.025	**1**	**1.100**
3015	1.009	1.009	1.01	1.059	3102	0.965	0.991	2.082	0.998	2621	1.025	1.025	**1**	**1.100**
3018	0.962	0.963	1.028	1.057	3105	0.96	0.974	1.718	1.010	2630	1.025	1.026	1.007	1.099
3021	0.99	0.994	1.073	1.052	20051	0.997	1.001	1.064	1.090	2631	1.026	1.03	1.032	1.094
3024	1.005	1.005	1.009	1.059	20052	0.997	1.001	1.064	1.090	2640	1.023	1.023	1.003	1.099
3027	0.997	1	1.055	1.054	20151	1	1.001	1.01	1.098	2641	1.022	1.022	**1**	**1.100**
3030	0.993	0.997	1.067	1.052	20152	1	1.001	1.01	1.098	2650	1.023	1.023	1.003	1.099
3033	0.999	1	1.01	1.059	2000	1.026	1.027	1.008	1.098	2651	1.022	1.022	**1**	**1.100**
3036	0.996	0.999	1.066	1.053	2001	1.029	1.03	1.008	1.098	5140	0.99	0.99	**1**	**1.100**
3039	0.993	0.997	1.073	1.052	2010	1.021	1.022	1.004	1.099	5148	1.03	1.031	1.01	1.098
3042	0.99	0.991	1.009	1.059	2011	1.021	1.022	1.004	1.099	5149	1.03	1.03	**1**	**1.100**
3045	0.969	0.97	1.016	1.058	2020	1.022	1.023	1.003	1.099	5150	1.03	1.032	1.014	1.097
3048	1.03	1.031	1.007	1.059	2021	1.021	1.021	**1**	**1.100**	5151	0.99	0.99	**1**	**1.060**
3051	0.965	0.965	1.025	1.057	2025	1	1.006	1.103	1.049	5152	0.99	0.99	**1**	**1.060**
3054	0.991	1.003	1.248	1.036	2026	0.996	0.996	**1**	**1.060**	5153	1.03	1.031	1.008	1.098
3057	0.981	0.993	1.292	1.033	2027	0.996	0.996	**1**	**1.060**	5154	1.03	1.031	1.008	1.098
3060	0.992	0.992	1.012	1.059	2030	1.03	1.031	1.009	1.098	20251	1	1.006	1.103	1.085
3063	0.964	0.965	1.025	1.057	2031	1.03	1.032	1.013	1.097	20262	0.996	0.996	**1**	**1.100**
3066	0.987	1.012	1.51	1.019	2032	1.03	1.031	1.009	1.098	20351	1.012	1.012	**1**	**1.100**
3069	0.969	0.993	1.783	1.007	2033	1.03	1.032	1.013	1.097	20352	1.012	1.012	**1**	**1.100**
3072	0.992	0.995	1.07	1.052	2035	1.012	1.012	**1**	**1.060**	20373	1.011	1.011	**1**	**1.100**
3075	0.996	0.999	1.065	1.053	2036	1.012	1.012	**1**	**1.060**	20374	1.011	1.011	**1**	**1.100**
3078	0.994	0.998	1.067	1.052	2037	1.011	1.011	**1**	**1.060**	20451	0.991	0.992	1.002	1.100
3081	1	1.028	1.473	1.021	2040	1.026	1.03	1.032	1.094	20472	0.992	0.992	1.01	1.098

Table 5.8 shows the lower nodal voltage limit contingency factors subject to n-1 contingencies. In addition, table 5.8 shows the bus numbers, initial voltage before n-1 contingencies, voltage during n-1 contingencies and the resulting upper bus voltage limits.

The results show that bus 3084 was most affected as the contingency factor for this bus, in relation to the upper bus voltage limit, is 2.483 and the resulting upper bus voltage limit being 0.988 pu from 1.06 pu. This was consequent to the outage of a line connecting buses 3102 and 3006. This resulted in power being supplied to buses 3006, 3018 and 3051 via line connecting buses 2015 and 3018. This acted as a relief of loading constituted by the aforementioned buses at bus 3102 and hence less voltage drop and therefore voltage rise at this bus and subsequent ones including bus 3084. Before this aforementioned contingency, the voltage was 0.958 pu and after this contingency the voltage was 0.985 pu which constituted a bus voltage loading of 15.07% to 37.5%, respectively, with respect to the upper bus voltage limit.

The lowest contingency factor was lowest at slack bus and other several buses as highlighted in bolded font. This is because the voltages of theses buses did not change across all contingencies.

2. CF LRIC-Voltage Network Charges

After calculating the contingency factors for the corresponding lower and higher nodal voltage limits then the CF LRIC-voltage network charges were determined based on those new limits.

Tables 5.9 and 5.11 show CF LRIC-voltage network charges due to 1 MVAr and 1 MW nodal withdrawals, respectively. Also, shown in these aforementioned tables are the shortest distances from the slack bus to the corresponding buses, the voltage levels before each nodal perturbation and voltage differences (voltages after nodal perturbations – voltages before nodal perturbations). In addition, tables 5.10 and 5.12 show VAr investments which were triggered due to MVAr and MW nodal withdrawals, respectively.

On the other hand, tables 5.13 and 5.14 show CF LRIC-voltage network charges due to 1 MVAr and 1 MW nodal injections, respectively. Also, shown in these aforementioned tables are the shortest distances from the slack bus to the corresponding buses, the voltage levels before each nodal perturbation and voltage differences (voltages after nodal perturbations – voltages before nodal perturbations).

Table 5.9: CF LRIC-Voltage Network Charges due to 1 MVAr withdrawal at each node on Pembroke distribution.

Bus	Initial Voltage (pu)	Voltage Difference (pu)	LRIC-V Charges (£/MVAr/yr)	Distance from slack Bus (km)	Bus	Initial Voltage (pu)	Voltage Difference (pu)	LRIC-V Charges (£/MVAr/yr)	Distance From slack Bus (km)	Bus	Initial Voltage (pu)	Voltage Difference (pu)	LRIC-V Charges (£/MVAr/yr)	Distance from slack Bus (km)
2005	0.997	-1.774E-03	24670.23	7.2	3084	0.958	-9.855E-03	37297	50.3	2041	1.025	-6.160E-04	3746.28	12.4
2015	1.000	-1.188E-03	11521.37	21.7	3087	0.998	-8.856E-03	15172.76	24.3	2045	0.991	-3.379E-03	4031.43	10.8
3003	1.002	-1.072E-02	34141.93	37.8	3090	0.976	-3.122E-03	14367.66	24.3	2046	0.991	-3.380E-03	4031.48	10.8
3006	0.964	-5.151E-03	33352.74	37.8	* 3093	0.999	-1.647E-02	**66686.35**	20.9	2047	0.992	-3.393E-03	4063.05	12.4
* 3009	0.992	-1.037E-02	**66543.22**	22.7	3096	0.954	-5.812E-03	62949.27	20.9	2048	0.992	-3.394E-03	4063.1	12.4
* 3012	0.958	-4.325E-03	**62747.47**	22.7	3099	0.995	-1.823E-03	11892.46	23.8	2620	1.025	-5.210E-04	3739.74	12.4
3015	1.009	-1.091E-02	37727.13	42	3102	0.965	-5.133E-03	33331.52	37.9	2621	1.025	-5.220E-04	3742.16	12.4
3018	0.962	-5.491E-03	37616.34	42	3105	0.960	-4.243E-03	62730.71	20.9	2630	1.025	-5.580E-04	3743.77	12.4
3021	0.990	-6.674E-03	25267.03	7.2	20051	0.997	-1.266E-02	24769.3	7.2	2631	1.026	-5.160E-04	3625.77	10.8
3024	1.005	-6.827E-03	11894.24	24.7	20052	0.997	-2.603E-02	24914.23	7.2	2640	1.023	-6.710E-04	3768.58	12.4
3027	0.997	-1.895E-03	11635.85	24.7	20151	1.000	-1.904E-02	11668.49	21.9	2641	1.022	-6.620E-04	3786.67	12.4
3030	0.993	-2.020E-03	11921.03	25.1	20152	1.000	-2.475E-02	11718.48	21.9	2650	1.023	-7.170E-04	3768.76	12.4
3033	0.999	-7.118E-03	12420.08	26	2000	1.026	-5.780E-04	3629.09	12.6	2651	1.022	-7.070E-04	3785.95	12.4
3036	0.996	-2.469E-03	11951.07	26	2001	1.029	-4.600E-04	3314.12	7.2	** 5140	0.990	0.000E+00	**0**	Slack bus
3039	0.993	-2.368E-03	12050.35	23.8	2010	1.021	-7.240E-04	4275.54	21.9	5148	1.030	-4.250E-04	3181.66	0
3042	0.990	-1.455E-02	19084.51	24.3	2011	1.021	-7.250E-04	4263.13	22	5149	1.030	-4.240E-04	3182.21	0
3045	0.969	-4.631E-03	15235.71	24.3	2020	1.022	-6.940E-04	3773.06	12.4	5150	1.030	-4.240E-04	3179.69	0
3048	1.030	-3.047E-02	49585.97	55.9	2021	1.021	-6.850E-04	3795.49	12.4	** 5151	0.990	-3.210E-08	**0**	0
3051	0.965	-1.034E-02	49273.35	55.9	2025	1.000	-3.425E-03	4584.77	12.4	** 5152	0.990	-3.220E-08	**0**	0
3054	0.991	-2.247E-02	14310.64	19.7	2026	0.996	-3.541E-03	5352.6	12.4	5153	1.030	-3.020E-04	1560.63	0
3057	0.981	-3.066E-03	13955.91	19.7	2027	0.996	-3.542E-03	5352.91	12.4	5154	1.030	-3.100E-04	1561.31	0
3060	0.992	-1.393E-02	14669.48	27.1	2030	1.030	-5.040E-04	3177.06	0	20251	1.000	-4.220E-02	4828.95	12.4
3063	0.964	-6.568E-03	14059.88	27.1	2031	1.030	-4.470E-04	3178.19	0	20262	0.996	-4.271E-02	5629.42	12.4
* 3066	0.987	-2.977E-02	**66671.27**	16.6	2032	1.030	-5.130E-04	3176.73	0	20351	1.012	-1.835E-01	4034.38	0
3069	0.969	-3.777E-03	62489.02	16.6	2033	1.030	-4.580E-04	3177.84	0	20352	1.012	-1.835E-01	4034.38	0
3072	0.992	-1.335E-02	27400.99	15.6	2035	1.012	-3.179E-03	3246.76	0	20373	1.011	-1.698E-01	3901.59	0
3075	0.996	-4.181E-03	25564.57	15.6	2036	1.012	-3.180E-03	3246.76	0	20374	1.011	-1.694E-01	3899.48	0
3078	0.994	-4.517E-03	25715.87	15.6	2037	1.011	-2.914E-03	3192.72	0	20451	0.991	-4.134E-02	4249.43	10.8
3081	1.000	-3.335E-02	42162.53	50.3	2040	1.026	-5.730E-04	3628.53	10.8	20472	0.992	-4.135E-02	4282.31	12.4

Table 5.10: Reinforcements effected during MVAr nodal withdrawals at specific buses on Pembroke practical test system.

MVAr Withdrawal At Bus	Reinforcent At Bus(es)
2005, 3021, 3072, 3075, 3078 & 20051	3054 & 3096
2015, 3024, 3027, 3030, 3033, 3036 & 3039	3054
3003, 3006 & 3102	3015, 3054 & 3084
3009	3009, 3012, 3054, 3069, 3096 & 3105
3012, 3069, 3096 & 3105	3012, 3054, 3069, 3096 & 3105
3015 & 3018	3015, 3048, 3054 & 3084
3042	3042 & 3054
3045, 3054, 3057, 3060, 3063 & 3087	3054
3048 & 3051	3015, 3048, 3051, 3054 & 3084
3066	3012, 3054, 3066, 3069, 3096 & 3105
3081	3015, 3048, 3054, 3081 & 3084
3084	3015, 3054, 3081 & 3084
3090, 3099, 20151 & 20152	3054
3093	3012, 3054, 3069, 3093, 3096 & 3105
20052	3054, 3096 & 20052
20251	20251
20262	20262
20351	20351
20352	20352
20373	20373
20374	20374
20451	20451
20472	20472

Since the lower nodal voltage limit margins have been reduced to support n-1 contingencies, during the MVAr nodal withdrawals, a number of lower voltage limits have been reached as reflected in table 5.10. The most affected, being buses 3009, 3066 and 3096 which each attracted six new VAr asset reinforcements. This resulted in these aforementioned buses attracting the most comparables costs (highlighted in bolded font and the corresponding bus number preceded by an asterisk). Slack bus, buses 5151 and 5152 (highlighted in bolded font and the corresponding bus number preceded by double asterisk) attracted no costs as the voltage at the slack bus did not change, while for the other two, their respective voltages varied slightly amid their closeness to the slack bus.

Table 5.11: CF LRIC-voltage network charges due to 1 MW withdrawal at each node on Pembroke distribution system.

Bus	Initial Voltage (pu)	Voltage Difference (pu)	LRIC-V Charges (£/MVAr/yr)	Distance from slack Bus (km)	Bus	Initial Voltage (pu)	Voltage Difference (pu)	LRIC-V Charges (£/MVAr/yr)	Distance from slack Bus (km)	Bus	Initial Voltage (pu)	Voltage Difference (pu)	LRIC-V Charges (£/MVAr/yr)	Distance from slack Bus (km)
2005	0.997	-3.580E-04	1530.17	7.2	3084	0.958	-7.082E-03	23569.55	50.3	2041	1.025	-1.230E-04	528.59	12.4
2015	1.000	-2.370E-04	1214.36	21.7	3087	0.998	-2.855E-03	8975.38	24.3	2045	0.991	-2.540E-04	541.37	10.8
3003	1.002	-4.854E-03	23813.43	37.8	3090	0.976	-1.678E-03	7807.42	24.3	2046	0.991	-2.540E-04	541.37	10.8
3006	0.964	-3.526E-03	22876.72	37.8	* 3093	0.999	-6.307E-03	**55423.52**	20.9	2047	0.992	-2.510E-04	549.31	12.4
* 3009	0.992	-4.469E-03	**55236.93**	42.8	3096	0.954	-3.957E-03	42710.51	20.9	2048	0.992	-2.510E-04	549.32	12.4
3012	0.958	-2.845E-03	30240.79	42.8	3099	0.995	-6.880E-04	1568.05	23.8	2620	1.025	-8.200E-05	526.69	12.4
3015	1.009	-5.278E-03	28341.56	42	3102	0.965	-3.508E-03	22852.39	37.9	2621	1.025	-8.300E-05	526.86	12.4
3018	0.962	-3.881E-03	15305.52	42	3105	0.960	-2.728E-03	30308.1	20.9	2630	1.025	-9.800E-05	527.56	12.4
3021	0.990	-1.292E-03	2763.06	7.2	20051	0.997	-4.350E-04	1617.03	7.2	2631	1.026	-7.700E-05	462.46	10.8
3024	1.005	-1.466E-03	2256.16	24.7	20052	0.997	-6.790E-04	1721.3	7.2	2640	1.023	-1.470E-04	556.65	12.4
3027	0.997	-9.470E-04	1391.47	24.7	20151	1.000	-4.110E-04	1338.03	21.9	2641	1.022	-1.440E-04	565.91	12.4
3030	0.993	-1.115E-03	1639.24	25.1	20152	1.000	-5.280E-04	1376.78	21.9	2650	1.023	-1.680E-04	556.83	12.4
3033	0.999	-1.704E-03	2685.14	26	2000	1.026	-1.080E-04	485.72	12.6	2651	1.022	-1.640E-04	565.68	12.4
3036	0.996	-8.800E-04	1551.83	26	2001	1.029	-5.200E-05	326.21	7.2	** 5140	0.990	0.000E+00	**0**	Slack bus
3039	0.993	-9.770E-04	1705.34	23.8	2010	1.021	-1.720E-04	791.08	21.9	5148	1.030	-3.600E-05	256.98	0
3042	0.990	-5.192E-03	10073.16	24.3	2011	1.021	-1.720E-04	775.42	22	5149	1.030	-3.600E-05	257.07	0
3045	0.969	-3.401E-03	8892.21	24.3	2020	1.022	-1.580E-04	561.36	12.4	5150	1.030	-3.500E-05	256.74	0
* 3048	1.030	-1.359E-02	**40714.17**	55.9	2021	1.021	-1.550E-04	573.02	12.4	** 5151	0.990	-1.503E-09	**0**	0
3051	0.965	-7.506E-03	16241.83	55.9	2025	1.000	-4.810E-04	1198.34	12.4	** 5152	0.990	-1.340E-09	**0**	0
3054	0.991	-6.562E-03	9152.02	19.7	2026	0.996	-6.260E-04	1469.17	12.4	5153	1.030	-1.200E-05	78.73	0
3057	0.981	-1.417E-03	7304.45	19.7	2027	0.996	-6.260E-04	1469.35	12.4	5154	1.030	-1.300E-05	78.81	0
3060	0.992	-7.043E-03	5303.03	27.1	2030	1.030	-6.600E-05	259.06	0	20251	1.000	-1.295E-03	1365.18	12.4
3063	0.964	-4.635E-03	3883.75	27.1	2031	1.030	-5.000E-05	257.01	0	20262	0.996	-1.462E-03	1665.73	12.4
3066	0.987	-7.994E-03	43751.77	16.6	2032	1.030	-6.600E-05	259.12	0	20351	1.012	-1.177E-02	1006.78	0
3069	0.969	-2.163E-03	29493.42	16.6	2033	1.030	-5.100E-05	257.07	0	20352	1.012	-1.177E-02	1006.78	0
3072	0.992	-3.219E-03	2934.91	15.6	2035	1.012	-2.920E-04	532.31	0	20373	1.011	-1.027E-02	722.44	0
3075	0.996	-1.524E-03	2022.12	15.6	2036	1.012	-2.920E-04	532.31	0	20374	1.011	-1.023E-02	721.46	0
3078	0.994	-3.086E-03	2566.98	15.6	2037	1.011	-1.450E-04	284.16	0	20451	0.991	-1.042E-03	685.06	10.8
3081	1.000	-1.288E-02	28640.23	50.3	2040	1.026	-1.020E-04	464.27	10.8	20472	0.992	-1.039E-03	694.03	12.4

Table 5.12: Reinforcements effected during MW nodal withdrawals at specific buses on Pembroke practical test system

MVAr Withdrawal At Bus	Reinforcement At Bus(es)
3003, 3006, 3084 & 3102	3015 & 3084
3009 & 3093	3012, 3069, 3096 & 3105
3012	3012 & 3096
3015	3015, 3048 & 3084
3018 & 3051	3015 & 3048
3042, 3045, 3054, 3057, 3087 & 3090	3054
3048	3015, 3048, 3051 & 3084
3066 & 3096	3012, 3069 & 3096
3069	3069 & 3096
3081	3015, 3081 & 3084
3105	3012 & 3096

Given the new reduced lower nodal voltage limit margins to support n-1 contingencies, again during MW nodal withdrawals, a number of lower voltage limits have been reached as reflected in table 5.12. The most affected, being buses 3009, 3048 and 3093 which each attracted four new VAr asset reinforcements. This resulted in buses 3009 and 3093 attracting the most comparables costs (highlighted in bolded font and the corresponding bus number preceded by double asterisk) since all occurred at 33-kv level and on the same buses. While, on the other hand, even though bus 3048 triggered reinforcements on four buses as the other two mentioned, it attracted less cost than them as the reinforcements in this case was due at two 11-kV and two 33-kV levels. It should be noted that the SVCs have the investment costs of £174, 240.00 and £58, 058.00 at 33-kV and 11-kV voltage levels, respectively. Slack bus, buses 5151 and 5152 (highlighted in bolded font and the corresponding bus number preceded by double asterisk) attracted no costs for the same reasons as stated above.

Table 5.13: CF LRIC-Voltage Network Charges due to 1 MVAr injections at each node on Pembroke distribution system.

Bus	Initial Voltage (pu)	Voltage Difference (pu)	LRIC-V Charges (£/MVAr/yr)	Distance from slack Bus (km)	Bus	Initial Voltage (pu)	Voltage Difference (pu)	LRIC-V Charges (£/MVAr/yr)	Distance from slack Bus (km)	Bus	Initial Voltage (pu)	Voltage Difference (pu)	LRIC-V Charges (£/MVAr/yr)	Distance from slack Bus (km)
2005	0.997	1.767E-03	-7556.78	7.2	3084	0.958	9.610E-03	-12007.96	50.3	2041	1.025	6.140E-04	-3521.21	12.4
2015	1.000	1.184E-03	-6627.69	21.7	3087	0.998	8.695E-03	-9117.42	24.3	2045	0.991	3.356E-03	-3717.78	10.8
3003	1.002	1.048E-02	-10786.96	37.8	3090	0.976	3.099E-03	-9252.62	24.3	2046	0.991	3.357E-03	-3717.81	10.8
3006	0.964	5.084E-03	-10993.28	37.8	3093	0.999	1.592E-02	-11474.79	20.9	2047	0.992	3.370E-03	-3746.87	12.4
3009	0.992	1.015E-02	-11900.61	42.8	* 3096	0.954	5.728E-03	**-12146.17**	20.9	2048	0.992	3.371E-03	-3746.89	12.4
3012	0.958	4.279E-03	-11610.01	42.8	3099	0.995	1.816E-03	-6906.23	23.8	2620	1.025	5.200E-04	-3516.27	12.4
3015	1.009	1.066E-02	-10318.21	42	3102	0.965	5.068E-03	-10985.53	37.9	2621	1.025	5.210E-04	-3518.42	12.4
3018	0.962	5.414E-03	-10525.77	42	3105	0.960	4.199E-03	-11699.72	20.9	2630	1.025	5.580E-04	-3519.52	12.4
3021	0.990	6.583E-03	-7943.28	7.2	20051	0.997	1.235E-02	-7482.06	7.2	2631	1.026	5.140E-04	-3414.45	10.8
3024	1.005	6.734E-03	-6763.43	24.7	20052	0.997	2.473E-02	-7395.53	7.2	2640	1.023	6.700E-04	-3537.08	12.4
3027	0.997	1.886E-03	-6708.73	24.7	20151	1.000	1.834E-02	-6518.14	21.9	2641	1.022	6.600E-04	-3555.05	12.4
3030	0.993	2.010E-03	-6924.12	25.1	20152	1.000	2.358E-02	-6485.12	21.9	2650	1.023	7.150E-04	-3536.92	12.4
3033	0.999	7.015E-03	-6856.44	26	2000	1.026	5.770E-04	-3424.57	12.6	2651	1.022	7.060E-04	-3553.89	12.4
3036	0.996	2.457E-03	-6903.46	26	2001	1.029	4.600E-04	-3139.36	7.2	** 5140	0.990	0.000E+00	**0**	Slack bus
3039	0.993	2.355E-03	-6998.26	23.8	2010	1.021	7.230E-04	-3991.6	21.9	5148	1.030	4.240E-04	-3018.14	0
3042	0.990	1.411E-02	-10173.06	24.3	2011	1.021	7.230E-04	-3979.78	22	5149	1.030	4.240E-04	-3018.62	0
3045	0.969	4.576E-03	-9871.46	24.3	2020	1.022	6.940E-04	-3540.3	12.4	5150	1.030	4.240E-04	-3016.33	0
3048	1.030	2.864E-02	-9631.73	55.9	2021	1.021	6.840E-04	-3562.52	12.4	** 5151	0.990	3.200E-08	**0**	0
3051	0.965	1.006E-02	-11119.51	55.9	2025	1.000	3.401E-03	-4107.25	12.4	** 5152	0.990	3.210E-08	**0**	0
3054	0.991	2.146E-02	-9106.06	19.7	2026	0.996	3.515E-03	-4700.21	12.4	5153	1.030	3.030E-04	-1512.72	0
3057	0.981	3.045E-03	-9086.27	19.7	2027	0.996	3.516E-03	-4700.4	12.4	5154	1.030	3.100E-04	-1513.33	0
3060	0.992	1.352E-02	-8397.77	27.1	2030	1.030	5.030E-04	-3012.41	0	20251	1.000	3.891E-02	-3967.65	12.4
3063	0.964	6.461E-03	-8484.11	27.1	2031	1.030	4.480E-04	-3014.5	0	20262	0.996	3.932E-02	-4544.34	12.4
3066	0.987	2.803E-02	-9834.89	16.6	2032	1.030	5.120E-04	-3012.01	0	20351	1.012	1.328E-01	-2647.33	0
3069	0.969	3.743E-03	-10889.65	16.6	2033	1.030	4.570E-04	-3014.06	0	20352	1.012	1.328E-01	-2647.33	0
3072	0.992	1.299E-02	-8386.57	15.6	2035	1.012	3.157E-03	-3038.15	0	20373	1.011	1.257E-01	-2639.22	0
3075	0.996	4.143E-03	-8124.19	15.6	2036	1.012	3.158E-03	-3038.13	0	20374	1.011	1.255E-01	-2639.78	0
3078	0.994	4.467E-03	-8201.04	15.6	2037	1.011	2.897E-03	-3012.61	0	20451	0.991	3.815E-02	-3595.6	10.8
3081	1.000	3.115E-02	-8173.9	50.3	2040	1.026	5.710E-04	-3416.27	10.8	20472	0.992	3.816E-02	-3623.59	12.4

During MVAr nodal injections, there were not limits reached. It should be noted that the range of nodal voltage limits with contingency factors considered is less than that without contingency factors considered. This factor leads to more nodal credits for CF LRIC-voltage network charges than LRIC-voltage network charges. It should also be noted that the nodal credits follow the same pattern as the case without considering the contingency factors (in the previous chapter, table 4.7) but only increased credits, therefore bus 3084 attracts the most credit while the slack bus and buses 5151 and 5152 attract nothing.

Table 5.14: CF LRIC-Voltage Network Charges due to 1 MW injections at each node on Pembroke distribution test system.

Bus	Initial Voltage (pu)	Voltage Difference (pu)	LRIC-V Charges (£/MVAr/yr)	Distance from slack Bus (km)	Bus	Initial Voltage (pu)	Voltage Difference (pu)	LRIC-V Charges (£/MVAr/yr)	Distance from slack Bus (km)	Bus	Initial Voltage (pu)	Voltage Difference (pu)	LRIC-V Charges (£/MVAr/yr)	Distance from slack Bus (km)
2005	0.997	3.540E-04	-1483.35	7.2	3084	0.958	6.875E-03	-6618.24	50.3	2041	1.025	1.220E-04	-515.92	12.4
2015	1.000	2.350E-04	-1161.56	21.7	3087	0.998	2.757E-03	-4374.11	24.3	2045	0.991	2.420E-04	-508.07	10.8
3003	1.002	4.687E-03	-6150.28	37.8	3090	0.976	1.662E-03	-3470.97	24.3	2046	0.991	2.420E-04	-508.06	10.8
3006	0.964	3.470E-03	-5565.85	37.8	* 3093	0.999	5.948E-03	**-7519.21**	20.9	2047	0.992	2.400E-04	-515.32	12.4
3009	0.992	4.311E-03	-7375.5	42.8	3096	0.954	3.887E-03	-6503.8	20.9	2048	0.992	2.400E-04	-515.32	12.4
3012	0.958	2.807E-03	-5942.34	42.8	3099	0.995	6.830E-04	-1487.8	23.8	2620	1.025	8.200E-05	-514.78	12.4
3015	1.009	5.096E-03	-6034.45	42	3102	0.965	3.454E-03	-5551.61	37.9	2621	1.025	8.200E-05	-514.94	12.4
3018	0.962	3.816E-03	-5258.43	42	3105	0.960	2.692E-03	-5931.46	20.9	2630	1.025	9.800E-05	-515.34	12.4
3021	0.990	1.242E-03	-2575.15	7.2	20051	0.997	2.770E-04	-1399.79	7.2	2631	1.026	7.600E-05	-452.73	10.8
3024	1.005	1.415E-03	-2055.33	24.7	20052	0.997	3.400E-05	-1299.47	7.2	2640	1.023	1.480E-04	-542.78	12.4
3027	0.997	9.410E-04	-1315.88	24.7	20151	1.000	6.200E-05	-1043.44	21.9	2641	1.022	1.430E-04	-551.83	12.4
3030	0.993	1.108E-03	-1547.39	25.1	20152	1.000	-5.500E-05	-1006.46	21.9	2650	1.023	1.670E-04	-542.61	12.4
3033	0.999	1.645E-03	-2387.4	26	2000	1.026	1.070E-04	-476.64	12.6	2651	1.022	1.640E-04	-551.24	12.4
3036	0.996	8.740E-04	-1459.82	26	2001	1.029	5.300E-05	-321.91	7.2	** 5140	0.990	0.000E+00	**0**	Slack bus
3039	0.993	9.690E-04	-1605.86	23.8	2010	1.021	1.710E-04	-766.51	21.9	5148	1.030	3.500E-05	-254.34	0
3042	0.990	4.923E-03	-5177.46	24.3	2011	1.021	1.710E-04	-751.42	22	5149	1.030	3.500E-05	-254.43	0
3045	0.969	3.354E-03	-4351.75	24.3	2020	1.022	1.580E-04	-547.17	12.4	5150	1.030	3.600E-05	-254.11	0
3048	1.030	1.235E-02	-6457.12	55.9	2021	1.021	1.540E-04	-558.56	12.4	** 5151	0.990	1.520E-09	**0**	0
3051	0.965	7.284E-03	-5608.24	55.9	2025	1.000	4.690E-04	-1131.48	12.4	** 5152	0.990	1.523E-09	**0**	0
3054	0.991	5.967E-03	-4930.58	19.7	2026	0.996	6.130E-04	-1385.97	12.4	5153	1.030	1.300E-05	-78.1	0
3057	0.981	1.404E-03	-3046.33	19.7	2027	0.996	6.130E-04	-1386.12	12.4	5154	1.030	1.200E-05	-78.15	0
3060	0.992	6.730E-03	-4402.79	27.1	2030	1.030	6.500E-05	-255.8	0	20251	1.000	-3.420E-04	-977.02	12.4
3063	0.964	4.543E-03	-3375.52	27.1	2031	1.030	5.100E-05	-254.17	0	20262	0.996	-2.190E-04	-1203.42	12.4
3066	0.987	6.992E-03	-6664.61	16.6	2032	1.030	6.500E-05	-255.81	0	20351	1.012	-1.118E-02	-46.77	0
3069	0.969	2.137E-03	-4884.8	16.6	2033	1.030	5.000E-05	-254.18	0	20352	1.012	-1.118E-02	-46.77	0
3072	0.992	3.023E-03	-2505.45	15.6	2035	1.012	2.810E-04	-505.55	0	20373	1.011	-9.980E-03	161.05	0
3075	0.996	1.501E-03	-1883.15	15.6	2036	1.012	2.810E-04	-505.54	0	20374	1.011	-9.936E-03	160.1	0
3078	0.994	3.047E-03	-2276.49	15.6	2037	1.011	1.360E-04	-265.76	0	20451	0.991	-5.450E-04	-368.86	10.8
3081	1.000	1.149E-02	-7105.86	50.3	2040	1.026	1.010E-04	-454.07	10.8	20472	0.992	-5.470E-04	-375.12	12.4

During MW nodal injections, there were not limits reached. It should be noted that the range of nodal voltage limits with contingency factors considered is less than that without contingency factors considered. This factor leads to more nodal credits for CF LRIC-voltage network charges than LRIC-voltage network charges. It should also be noted that the nodal credits follow the same pattern as the case without considering the contingency factors (in the previous chapter, table 4.8) but only increased credits, therefore, bus 3081 attracts the most credit while the slack bus and buses 5151 and 5152 attract nothing.

5.5 Chapter Conclusions

In this chapter, the CF LRIC-voltage network charges are presented and tested on the IEEE 14 bus test system and the practical distribution test system. The CF LRIC-v network charges are an extension of the LRIC-v network charges, in which the physical reality of n-1 contingency conditions is considered, as per the statutory requirement. When considering these aforementioned contingencies, the security and reliability of the network are enhanced and, as such, this has to be factored into the LRIC-v charging principle model since the respective nodal voltage limits would be reduced to accommodate the contingencies.

The CF LRIC-voltage network charges follow the same pattern as the LRIC-v network charges but the difference is that the former charges are determined with reduced nodal voltage margins and, therefore, more than the latter. Consequently, the CF LRIC-voltage charges reflect correct price signals than LRIC-voltage charges as they consider n-1 contingencies, therefore, they are better able to direct siting and sizing of future demand and generation for the efficient and effective utilization of the network VAr compensation assets. Also, the network users are able to exercise an economic choice, of whether to source VAr from the network or provide their own VAr. Finally, this in turn, would work towards bettering the overall network voltage profile.

Compared with proposed LRIC-voltage network charges in chapter 4, the CF LRIC-voltage network charges are more than the former. This is due to the fact that the resulting network nodal margins are reduced, that is, the network lower and upper nodal limits are tightened to accommodate the n-1 contingencies. It should be noted that, it is a statutory requirements for network operators to operate the network to be able to withstand n-1 contingencies for the network to attain reasonable degree of security and reliability. The CF LRIC-voltage network charges have all the features that exist in the proposed LRIC-voltage network charges but the former charges reflect the physical reality of the network to accommodate n-1 contingencies and, therefore, the resulting charges in this chapter are of an actual practical nature.

Chapter 6

LRIC-Voltage Network Charges Considering Different Network Circuit R/X Ratios and Demand Growth Rates

In this chapter, studies were performed to analyses the trend of LRIC-voltage network charges on different types of networks and different demand growth rates. This provided insights into how charges would change with different network circuit resistance/reactance (R/X) ratios and different demand load growth rates. For the former study, a 9-bus test network which is a subset of the practical Western Power Distribution (WPD) network was used, while for the latter study, IEEE-14 bus test system and the practical 87-bus distribution test system developed, operated and maintained by Western Power Distribution (WPD) network were used.

For the former study, the results show that when the network circuit Xs are atleast ten times more than their R counterparts, only MVAr nodal perturbations should be considered. When the network circuit Rs, on the other hand, are atleast ten folds more than their Xs counterparts, then, only MW nodal perturbations should be considered. Finally, when the network circuit Xs and their corresponding Rs are comparable, both MVAr and MW nodal perturbations should be considered. On the other hand, for the latter study, the results show that the LRIC-v network charges given different load growth rates are a function of the system nodal voltage loading levels.

6.1 Introduction

In this chapter, studies were performed to analyse the trend of LRIC-voltage network charges on different types of networks and different demand growth rates. These provided insights into how charges would change with different network circuit resistance/reactance (R/X) ratios and different demand growth rates [77]. The LRIC-voltage network charges are different for different network types. On the different types of network front, what set networks apart is the nature of R/X ratios on network circuits. This, in turn, would guide into how the MVAr and MW nodal perturbations could be treated in the context of LRIC-voltage network charges. In transmission networks, the circuit R/X ratio, is usually lower than 0.5 while on distribution networks, the ratio ranges from 0.5 to 7 [78]. On the other front, different demand load growth rates provide different LRIC-voltage network charges. As the demand load grows on the system, it is imperative to have insights into how it would impact the whole system, technically and economically. This, in turn, would enable the network planners to make appropriate investment decisions in the long-term network development. In this study, an economical analysis aspect was looked into, relating to how LRIC-voltage charges varied in comparison to demand load growth.

On different types of networks, the 9-bus test network which is a subset of the practical Western Power Distribution (WPD) network was chosen for this study as a result of the ease at which, its circuit R/X ratios could be varied ranging from, when Rs was ten folds more than the corresponding Xs to when the Xs were 10 times more than the corresponding Rs. Varying this network's R/X ratios is a practical representation which ranges from transmission to distribution systems. Otherwise, if not varying this network's R/X ratios, then, it would mean performing separate runs on transmission and distribution networks, each in turn. On the other hand, for the different demand growth rates, the IEEE-14 bus test system and the practical 87-bus distribution test system developed, operated and maintained by Western Power Distribution (WPD) network were used. It should be noted the different demand load growth rates considered for this study were 1%, 1.6% and 2%.

The results of these studies are presented and analysed in the next section.

6.2 Results and Analysis

The results are presented and analysed below, to demonstrate the trend the LRIC-voltage network charges followed given different circuit R/X ratios and different demand growth rates.

6.2.1 Different Types of Networks

1. 9-Bus Test System

As it can be observed, below on figure 6.1, the 9-Bus network is a subset of the practical Western Power Distribution (WPD) network with only demand connected at the 11-kV voltage level. The line distances between the buses are depicted in red. Where the line distances are not shown, then the line distance is zero. The VAr compensation assets (SVCs) have the investment costs of £58, 050.00 and £174, 240.00 at the 11-kV and 33-kV voltage levels, respectively. Bus 1 is the slack bus. The nodal voltage limits are assumed to be $1 \pm 6\%$ pu. The use of power flow was employed to capture the nodal voltages while performing nodal withdrawals/injection on the system.

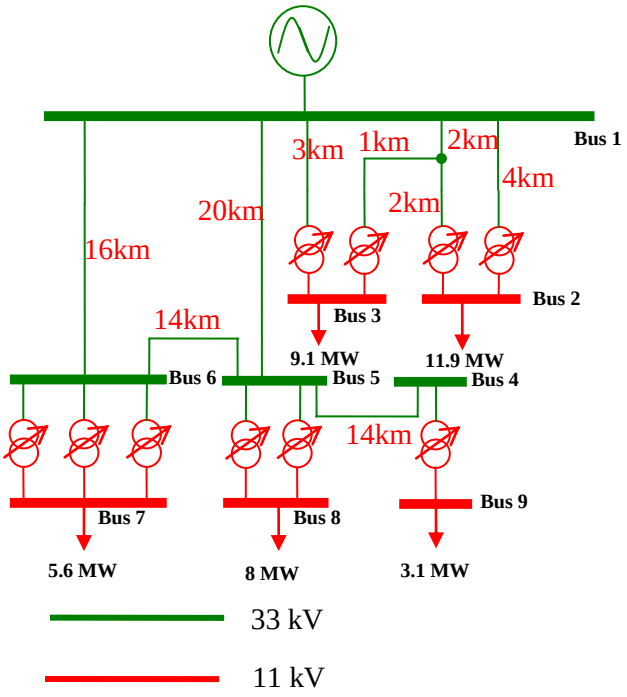

Figure 6.1: 9-bus practical network

The annual load growth rate for this practical network is assumed to be 1.6% while the discount rate is assumed to be 6.9%. To demonstrate the value of the proposed LRIC-voltage network charging methodology three cases have been used to show the cost/benefit to the network when the resistance/reactance (R/X) ratios of circuits are varied from when R and X are comparable, to where X dominates R and finally where R dominates X given the nodal withdrawal/injection. Case 1 involves nodal withdrawals of 1 MVAr and 1 MW, and nodal injections of 1 MVAr and 1 MW when the network circuit R/X ratios are slightly less than unity, each of these perturbations are performed each in turn. Case 2 and case 3 follow with the same set of perturbations as those of case 1 but case 2 having network circuit R/X ratios being equal to 0.1 while finally case 3 having network circuit ratios being equal to 10.

Case 1: This case involves a 1 MVAr nodal withdrawal and secondly a 1 MW nodal withdrawal when circuit reactances are slightly more than resistance counterparts. Figure 6.2, and tables 6.1 and 6.2 show the nodal LRIC-voltage network charges and the shortest distances for each node from the slack bus during 1 MVAr and 1 MW withdrawals, respectively. In addition, tables 6.1 and 6.2 show the voltages after each perturbation and voltage differences (voltages after nodal perturbations – voltages before nodal perturbations). On the other hand, figure 6.3, and tables 6.3 and 6.4 show the nodal LRIC-voltage network charges and the shortest distances for each node from the slack bus during 1 MVAr and 1 MW injections, respectively. In addition, tables 6.3 and 6.4 show the voltages after each perturbation and voltage differences (voltages after nodal perturbations – voltages before nodal perturbations).

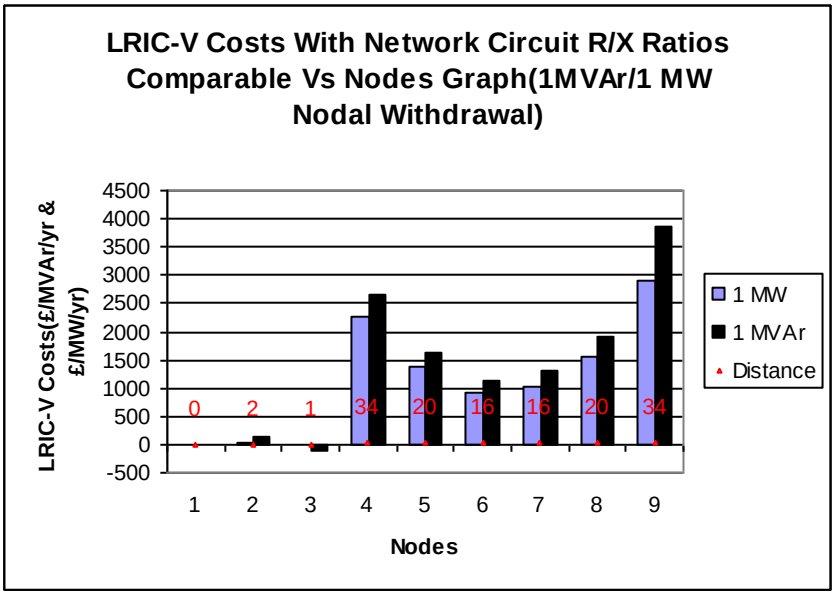

Figure 6.2: LRIC-voltage network charges due to 1 MVAr and 1 MW withdrawals at each node on the 9-bus test system

Table 6.1: LRIC-voltage network charges due to 1 MVAr withdrawal at each node on the 9-bus test system.

Bus	Initial Voltage(pu)	Voltage Difference(pu)	LRIC-V £/MVAr/yr	Distance (km)
1	1.03	0.000E+00	0	0
2	0.992	-5.760E-03	152.11	2
3	1.020	-5.460E-03	-95.06	1
4	0.971	-8.650E-03	2651.19	34
5	0.983	-3.800E-03	1634.77	20
6	0.993	-3.390E-03	1139.25	16
7	0.989	-9.486E-03	1323.58	16
8	0.978	-9.425E-03	1897.64	20
9	0.985	-2.966E-02	3853.97	34

Table 6.2: LRIC-voltage network charges due to 1 MW withdrawal at each node on the 9-bus test system.

Bus	Initial Voltage(pu)	Voltage Difference(pu)	LRIC-V £/MW/yr	Distance (km)
1	1.03	0.000E+00	0	0
2	0.992	-5.760E-03	27.47	2
3	1.020	-5.460E-03	-18.45	1
4	0.971	-8.650E-03	2250.35	34
5	0.983	-3.800E-03	1374.45	20
6	0.993	-3.390E-03	925.21	16
7	0.989	-9.486E-03	1033.56	16
8	0.978	-9.425E-03	1570.06	20
9	0.985	-2.966E-02	2899.9	34

Since the circuit reactances are slightly more than the corresponding circuit resistances, it can be observed from figure 6.2, and tables 6.1 and 6.2 that the nodal costs due to 1 MVAr withdrawals are more than those due to 1 MW withdrawals. Generally for both tables 6.1 and 6.2, it can also be observed that the costs increase as the nodal distance increase from the slack bus. For both 1 MVAr and 1 MW withdrawals, it can be seen that at bus 3 a credit is attracted since voltage is more than the target voltage of 1 pu and that means that the higher voltage limit is critical. When a withdrawal occurs at this node the higher voltage limit margin is increased, therefore, an overall credit has to be earned at this node since other nodes due to the disturbance at this node earn less costs as disturbance propagated become even less with distance from this disturbed bus.

On the other hand, other buses except for the slack bus have initial voltages less than the target voltage of 1 pu and, therefore, for these it means that the lower voltage limit is critical. For these buses, during withdrawal these attract costs since the already critical lower voltage limit margin is degraded further and, therefore, the overall results are costs at these buses as their investment horizon on VAr compensation assets are brought forward. It should also be noted that at buses 6 and 7, their respective distances from the slack bus are the same but the costs for bus 7 are more than that of bus 6 since the former is connected to the latter through three parallel transformer set, therefore, there is a voltage drop across this set. The same applies to pairs of buses 5 and 8, and buses 4 and 9. It should be further noted that, for buses 5 and 8, two transformers are involved while one transformer is involved between buses 4 and 9.

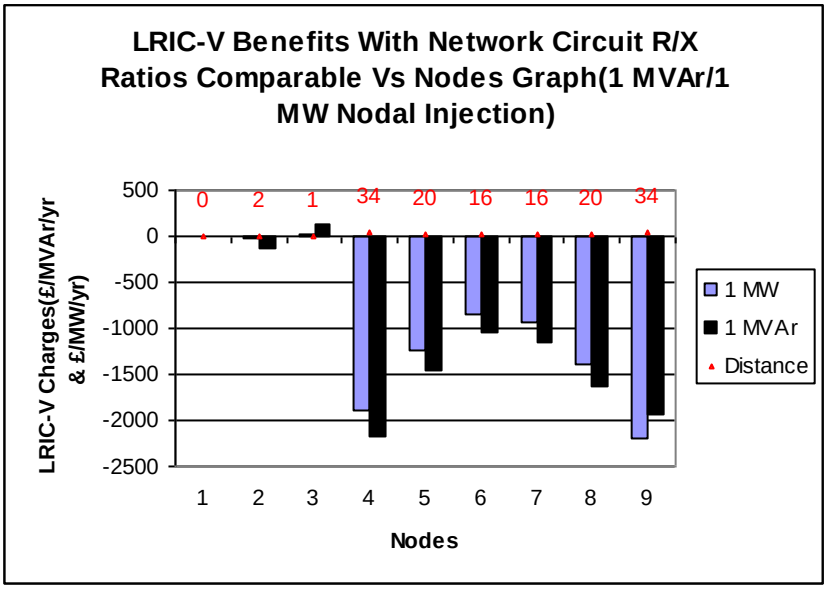

Figure 6.3: LRIC-voltage network charges due to 1 MVAr and 1 MW injection at each node on the 9-bus test system

Table 6.3: LRIC-voltage network charges due to 1 MVAr injection at each node on the 9-bus test system.

Bus	Initial Voltage(pu)	Voltage Difference(pu)	LRIC-V £/MVAr/yr	Distance (km)
1	1.03	0.000E+00	0	0
2	0.992	6.240E-03	-121.72	2
3	1.020	5.540E-03	136.44	1
4	0.971	8.350E-03	-2167.48	34
5	0.983	4.200E-03	-1454.58	20
6	0.993	3.610E-03	-1037.87	16
7	0.989	8.514E-03	-1143.44	16
8	0.978	9.575E-03	-1626.9	20
9	0.985	2.734E-02	-1938.91	34

Table 6.4: LRIC-voltage network charges due to 1 MW injection at each node on the 9-bus test system.

Bus	Initial Voltage(pu)	Voltage Difference(pu)	LRIC-V £/MW/yr	Distance (km)
1	1.03	0.000E+00	0	0
2	0.992	1.240E-03	-25.3	2
3	1.020	5.400E-04	19.33	1
4	0.971	7.350E-03	-1882.87	34
5	0.983	3.200E-03	-1240.76	20
6	0.993	2.610E-03	-854.69	16
7	0.989	3.514E-03	-932.28	16
8	0.978	4.575E-03	-1381.58	20
9	0.985	1.234E-02	-2203.7	34

During nodal injections, it is also observed that the credits consequent to 1 MVAr injections are more than the credits for their 1 MW injection counterparts since the network circuit R/X ratios remain unchanged as the case resulting from withdrawals. It can further be observed that the credits increase as the nodal distances increase from the slack bus as can be observed from figure 6.3 and, tables 6.3 and 6.4. Bus 3 attracts an overall cost for both injections of real and reactive power since the initial voltage at this bus is more than the target voltage of 1 pu and, therefore, during injection the voltage increases as such degrading the already critical higher bus voltage limit margin further, thereby, advancing the investment horizon of VAr compensation asset investment at this bus. Even though other individual buses due to the disturbance at bus 3 attract credits but those are smaller in magnitudes resulting in overall costs at this bus.

On the other hand, other buses have their respective voltages below the target voltage and, as such, their lower busbar voltage limits are the ones critical. When injections occur at these buses their respective lower busbar limit margins are increased, thereby, deferring the VAr compensation asset investments. The same situation holds for bus pairs, buses 6 and 7, buses 5 and 8 and, buses 4 and 9 where buses 7, 8 and 9 attract more the credits than their counterparts, respectively, as is the case as the situation above.

Case 2: This case involves a 1 MVAr nodal withdrawal and, secondly, a 1 MW nodal withdrawal when circuit reactances are 10 times more than resistance counterparts. Figure 6.4 and, tables 6.5 and 6.6 show the nodal LRIC-voltage network charges and the shortest distances for each node from the slack bus during 1 MVAr and 1 MW withdrawals, respectively. In addition, tables 6.5 and 6.6 show the voltages after each perturbation and voltage differences (voltages after nodal perturbations – voltages before nodal perturbations). On the other hand, figure 6.5, and tables 6.7 and 6.8 show the nodal LRIC-voltage network charges and the shortest distances for each node from the slack bus during 1 MVAr and 1 MW injections, respectively. In addition, tables 6.7 and 6.8 show the voltages after each perturbation and voltage differences (voltages after nodal perturbations – voltages before nodal perturbations).

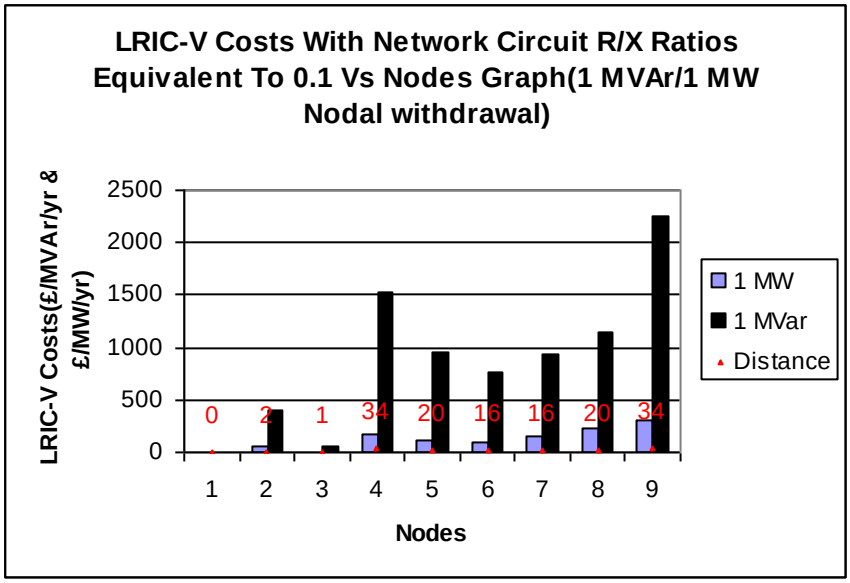

Figure 6.4: LRIC-voltage network charges due to 1 MVAr and 1 MW withdrawal at each node on the 9-bus test system.

Table 6.5: LRIC-voltage network charges due to 1 MVAr withdrawal at each node on the 9-bus test system.

Bus	Initial Voltage(pu)	Voltage Difference(pu)	LRIC-V £/MVAr/yr	Distance (km)
1	1	0.000E+00	0	0
2	0.967	5.809E-03	392.2	2
3	0.995	5.839E-03	52.53	1
4	0.990	8.267E-03	1535.32	34
5	0.992	4.184E-03	951.73	20
6	0.994	3.950E-03	765.92	16
7	0.990	9.048E-03	943.03	16
8	0.988	8.867E-03	1154.5	20
9	1.005	2.903E-02	2243.09	34

Table 6.6: LRIC-voltage network charges due to 1 MW withdrawal at each node on the 9-bus test system.

Bus	Initial Voltage(pu)	Voltage Difference(pu)	LRIC-V £/MW/yr	Distance (km)
1	1	0.000E+00	0	0
2	0.967	8.090E-04	58.1	2
3	0.995	8.390E-04	6.2	1
4	0.990	1.267E-03	180.83	34
5	0.992	1.840E-04	122.08	20
6	0.994	-5.000E-05	88.88	16
7	0.990	1.048E-03	158.92	16
8	0.988	1.867E-03	225.25	20
9	1.005	6.032E-03	314.22	34

Since the circuit reactances dominate the corresponding circuit resistances, it can be observed from figure 6.4 and, tables 6.5 and 6.6 that the nodal costs due to 1 MVAr withdrawals are significantly more than those due to 1 MW withdrawals. Generally, for both tables 6.5 and 6.6, it can also be observed that the costs increase as the nodal distances increase from the slack bus. From bus 2 to bus 8, the initial bus voltages are all less than the target voltage of 1 pu, therefore, during the nodal withdrawals the already critical lower bus voltage limits are degraded further and, as such, those earn costs as the investment horizons for their respective VAr compensation assets are advanced. At bus 9, the initial voltage is more than 1 pu and after withdrawal the final voltage is less than 1 pu. This bus earns credit from 1.005 pu to 1 pu and earns a cost from 1 pu to 0.999 pu. This results in the overall cost at this node a bit reduced.

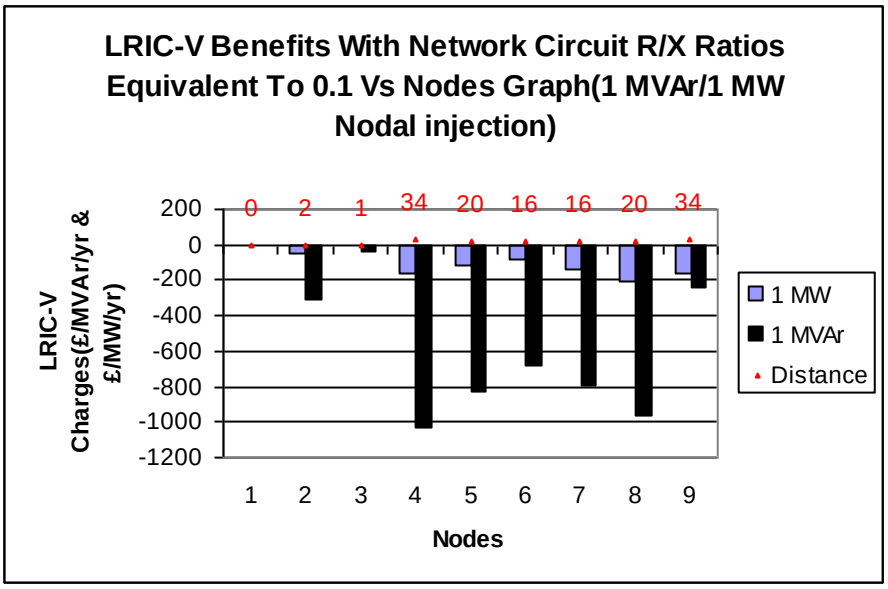

Figure 6.5: LRIC-voltage network charges due to 1 MVAr and 1 MW injections at each node on the 9-bus test system.

Table 6.7: LRIC-voltage network charges due to 1 MVAr injection at each node on the 9-bus test system.

Bus	Initial Voltage(pu)	Voltage Difference(pu)	LRIC-V £/MVAr/yr	Distance (km)
1	1	0.000E+00	0	0
2	0.967	-6.191E-03	-312.32	2
3	0.995	-5.161E-03	-34.29	1
4	0.990	-8.733E-03	-1034.2	34
5	0.992	-3.816E-03	-830.1	20
6	0.994	-4.050E-03	-686	16
7	0.990	-8.952E-03	-790.92	16
8	0.988	-9.133E-03	-967.39	20
9	1.005	-2.697E-02	-239.93	34

Table 6.8: LRIC-voltage network charges due to 1 MW injection at each node on the 9-bus test system.

Bus	Initial Voltage(pu)	Voltage Difference(pu)	LRIC-V £/MW/yr	Distance (km)
1	1	0.000E+00	0	0
2	0.967	-1.191E-03	-53.84	2
3	0.995	-1.161E-03	-5.68	1
4	0.990	-7.330E-04	-161.84	34
5	0.992	-8.160E-04	-115.95	20
6	0.994	-5.000E-05	-84.48	16
7	0.990	-9.520E-04	-142.71	16
8	0.988	-1.133E-03	-203.7	20
9	1.005	-4.968E-03	-163.79	34

Since the circuit R/X ratio remains the same as before, it can be observed from figure 6.5 and, tables 6.7 and 6.8 that the nodal costs due to 1 MVAr withdrawals are significantly more than those due to 1 MW withdrawals. Generally for both tables 6.7 and 6.8, it can also be observed that the costs increase as the nodal distances increase from the slack bus. From bus 2 to bus 8, the initial bus voltages are all less than the target voltage of 1 pu, therefore, during the nodal injections the critical lower bus voltage limit margins are increased and, as such, those earn credits as the investment horizons for their respective VAr compensation assets are deferred. At bus 9, the initial voltage is more than 1 pu and after injection the final voltage is further increased, thereby, reducing the already critical higher bus voltage limit margin. This bus earns a cost as the investment horizon of the VAr compensation asset at this bus is advanced closer. The overall result for both 1 MVar and 1 MW injections at bus 9 is the reduced overall credit as other buses earn credits due to perturbations on this bus. For both 1 MVar and 1 MW injections the credits earned at bus 9 are less than those earned at bus 4.

Case 3: This case involves a 1 MVAr nodal withdrawal and, secondly, a 1 MW nodal withdrawal when circuit resistances are 10 times more than reactance counterparts. Figure 6.6 and, tables 6.9 and 6.10 show the nodal LRIC-voltage network charges and the shortest distances for each node from the slack bus during 1 MVAr and 1 MW withdrawals, respectively. In addition, tables 6.9 and 6.10 show the voltages after each perturbation and voltage differences (voltages after nodal perturbations – voltages before nodal perturbations). On the other hand, figure 6.7 and, tables 6.11 and 6.12 show the nodal LRIC-voltage network charges and the shortest distances for each node from the slack bus during 1 MVAr injection and, secondly, 1 MW injection, respectively. In addition, tables 6.11 and 6.12 show the voltages after each perturbation and voltage differences (voltages after nodal perturbations – voltages before nodal perturbations).

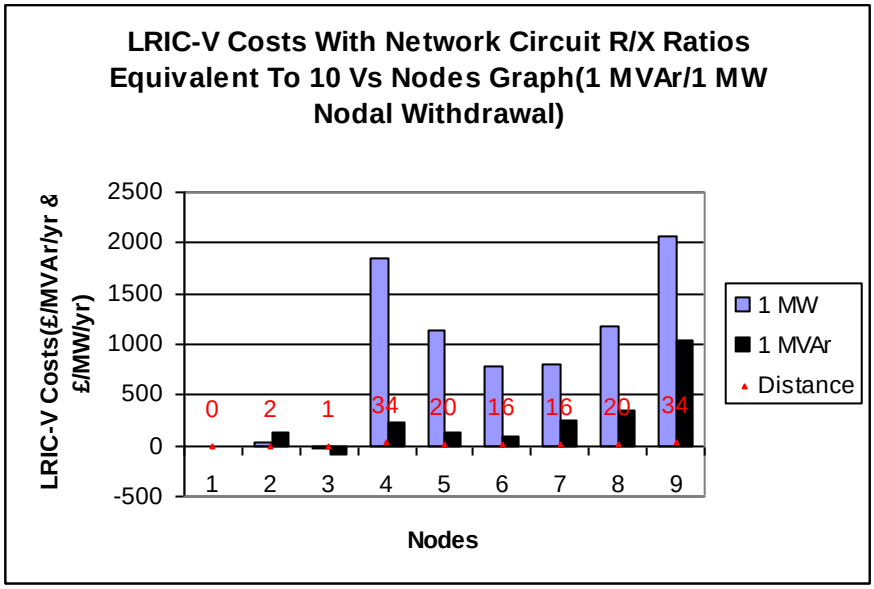

Figure 6.6: LRIC-voltage network charges due to 1 MVAr and 1 MW withdrawals at each node on the 9-bus test system.

Table 6.9: LRIC-voltage network charges due to 1 MVAr withdrawal at each node on the 9-bus test system.

Bus	Initial Voltage(pu)	Voltage Difference(pu)	LRIC-V £/MW/yr	Distance (km)
1	1.03	0.00E+00	0	0
2	0.992	5.11E-03	137.37	2
3	1.021	5.58E-03	-94.26	1
4	0.975	9.39E-04	224.78	34
5	0.986	2.52E-04	141.04	20
6	0.996	2.10E-05	99.44	16
7	0.992	6.13E-03	241	16
8	0.982	5.90E-03	348.2	20
9	0.989	2.01E-02	1029.95	34

Table 6.10: LRIC-voltage network charges due to 1 MW withdrawal at each node on the 9-bus test system.

Bus	Initial Voltage(pu)	Voltage Difference(pu)	LRIC-V £/MW/yr	Distance (km)
1	1.03	0.00E+00	0	0
2	0.992	1.11E-03	25.69	2
3	1.021	5.84E-04	-18.39	1
4	0.975	6.94E-03	1839.58	34
5	0.986	3.25E-03	1136.16	20
6	0.996	3.02E-03	774.75	16
7	0.992	4.13E-03	808.91	16
8	0.982	3.90E-03	1185.99	20
9	0.989	1.11E-02	2072.22	34

Since the circuit resistances dominate the corresponding circuit reactances, it can be observed from figure 6.6 and, tables 6.9 and 6.10 that the nodal costs due to 1 MW withdrawals are significantly more than those due to 1 MVAr withdrawals. Generally, from both tables 6.9 and 6.10, it can also be observed that the costs increase as the nodal distances increase from the slack bus. For both 1 MVAr and 1 MW withdrawals, it can be seen that at bus 3 a credit is attracted since voltage there is more than the target voltage of 1 pu and that means that the higher voltage limit is critical. Due to this latter fact, during withdrawal at this bus, the higher voltage limit margin is increased from 1.021 pu to 1.02 pu, thereby, a credit has to be earned as a reward and, thereby, contributing to the overall credit at the bus.

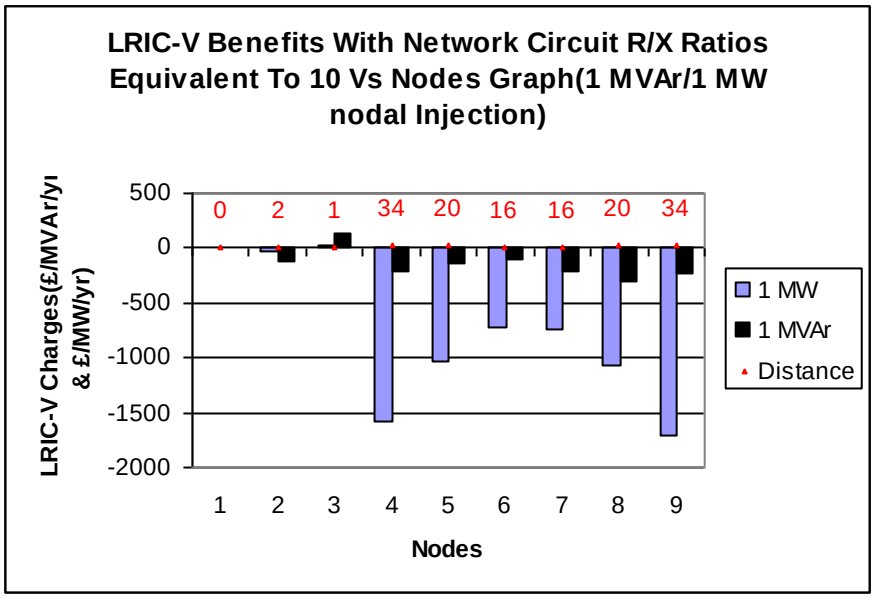

Figure 6.7: LRIC-voltage network charges due to 1 MVAr and 1 MW injections at each node on the 9-bus test system.

Table 6.11: LRIC-voltage network charges due to 1 MVAr injection at each node on the 9-bus test system.

Bus	Initial Voltage(pu)	Voltage Difference(pu)	LRIC-V £/MW/yr	Distance (km)
1	1.03	0.00E+00	0	0
2	0.992	-4.89E-03	-112.8	2
3	1.021	-5.42E-03	130.91	1
4	0.975	-1.06E-03	-206.96	34
5	0.986	-7.48E-04	-136	20
6	0.996	2.10E-05	-96	16
7	0.992	-5.87E-03	-207.58	16
8	0.982	-5.10E-03	-311.43	20
9	0.989	-1.99E-02	-224.27	34

Table 6.12: LRIC-voltage network charges due to 1 MW injection at each node on the 9-bus test system.

Bus	Initial Voltage(pu)	Voltage Difference(pu)	LRIC-V £/MW/yr	Distance (km)
1	1.03	0.00E+00	0	0
2	0.992	-8.86E-04	-23.81	2
3	1.021	-1.42E-03	19.23	1
4	0.975	-7.06E-03	-1579.55	34
5	0.986	-2.75E-03	-1039.63	20
6	0.996	-2.98E-03	-723.36	16
7	0.992	-3.87E-03	-748.78	16
8	0.982	-4.10E-03	-1077.78	20
9	0.989	-1.09E-02	-1705.54	34

During nodal injections, it is also observed that the credits consequent to 1 MW injections are more than the credits due to their 1 MVAr injection counterparts since the R/X ratio remain unchanged. It can further be observed that the credits increase as the nodal distances increase from the slack bus as can be observed from figure 6.7 and, tables 6.11 and 6.12. Bus 3 attracts an overall cost for both injections of real and reactive power since the initial voltage at this bus is more than the target voltage of 1 pu and, therefore, during injection the voltage increases as such degrading the already critical higher bus voltage limit margin further, thereby, advancing the investment horizon of VAr compensation asset investment at this bus. During 1 MVAr injection at bus 9, from voltage 0.989 pu to 1 pu, this bus earns a credit and from 1 pu to 1.009 pu this bus attracts a cost and, as such, the overall credit at this bus is reduce and it is consequently less than credit earned at bus 8. On the other hand, during 1 MW injection at bus 9, from 0.989 pu to 1 pu this bus earn a credit and this results in bus 9 earning the largest credit than any other bus.

6.2.2 Different Demand Growth Rates

1. IEEE-14 Bus Test System

The IEEE-14 bus test system was introduced in chapter 4. All the data used here is the same as in the previous chapters, 4 and 5.

Figure 6.8 shows the LRIC-voltage network costs owing to 1 MVAr nodal withdrawals considering 1%, 1.6% and 2% load growth rates while figure 6.9 shows these costs but given 1 MW nodal withdrawals considering the same respective load growth rates, as mentioned earlier.

On the other hand, figure 6.10 shows the LRIC-voltage network credits at each node given 1 MVAr injections considering 1%, 1.6% and 2% load growth rates while figure 6.11 shows these credits given 1 MW nodal injections considering the same respective aforementioned load growth rates.

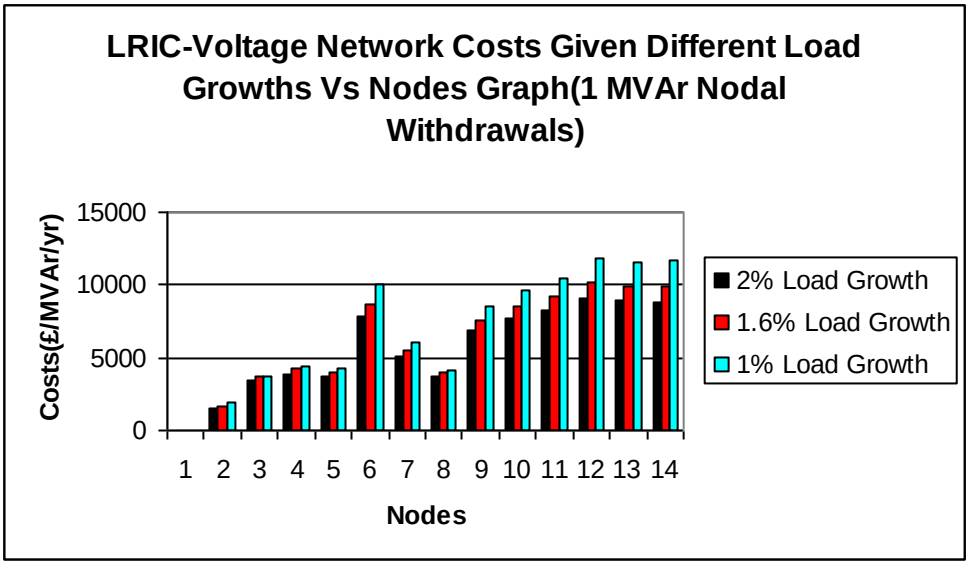

Figure 6.8: LRIC-voltage network costs owing to 1 MVAr nodal withdrawals considering different load growth rates on IEEE 14 bus test system.

As it can be observed, from figure 6.8, the results show that the more the load growth rate the less are the charges. For a higher load growth rate, the present values before and after MVAr withdrawals are more than the corresponding present values before and after MVAr withdrawals with a less load growth rate. The former present values are such that their differences are smaller than the corresponding differences in the latter present values (PVs), for buses with bus voltage loadings before withdrawals in excess of 66.5% with respect to the lower voltage limit. These buses are 6, 9, 10, 11, 12, 13 and 14 with bus voltage loadings of 66.6%, 67.8%, 74.8%, 73.6%, 79.5%, 83% and 90.9%, respectively, which also have very high charges. Elsewhere, the few buses with critical lower voltage limits (buses 3, 4 & 5) and having voltage loadings less than 66.5%, the reverse is true as their respective differences in (PVs) are more for the more load growth rate. Buses 2, 7 and 8 have critical upper voltage limits and they attract credits during their respective nodal withdrawals, but since the lower bus voltage limits dominate and these tend to influence the results and hence resulting costs at nodes. The overall result is, the more the LRIC-voltage network costs are the descending load growth rates.

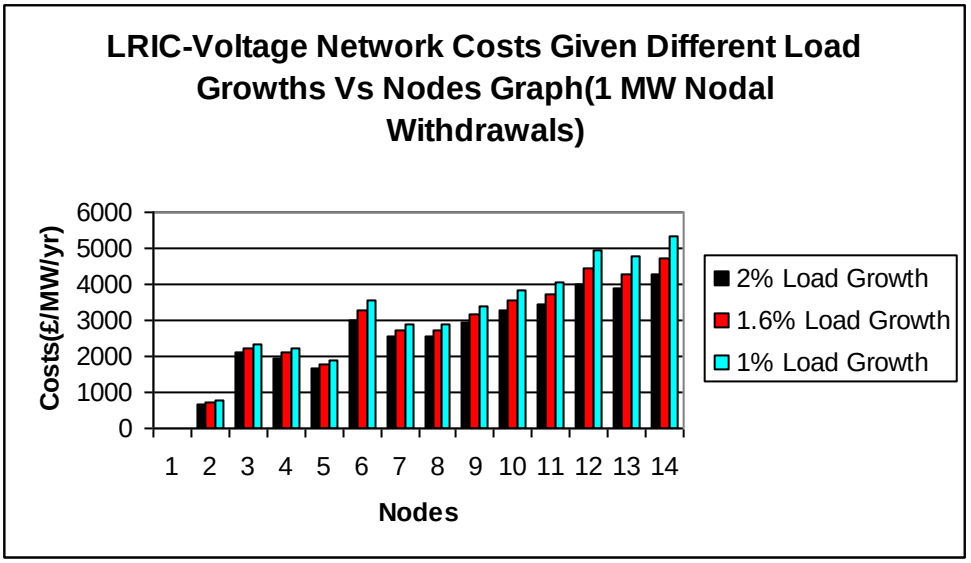

Figure 6.9: LRIC-voltage network costs owing to 1 MW nodal withdrawals considering different load growth rates on IEEE-14 bus test system.

As it can be observed, from figure 6.9, the results show the same pattern as those shown above, in figure 6.8, and for the same reasons advanced in the aforementioned case, the less the load growth rate the more the LRIC-voltage network costs. The only differences are the reduced LRIC-voltage network costs, in this case, since this network's circuit Xs are more than the corresponding circuit Rs.

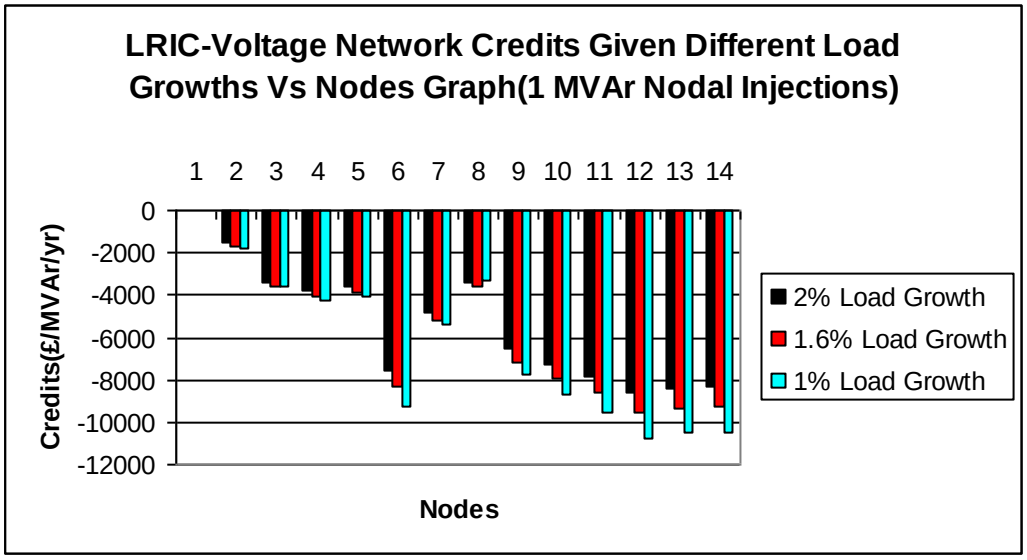

Figure 6.10: LRIC-voltage network costs owing to 1 MVAr nodal injections considering different load growth rates on IEEE-14 bus test system.

It can be observed, from figure 6.10, that the credits follow the same pattern as the, above two cases, in that the less the load growth rate the more are the LRIC-voltage network credits, the same reasons as outlined in the above two cases hold.

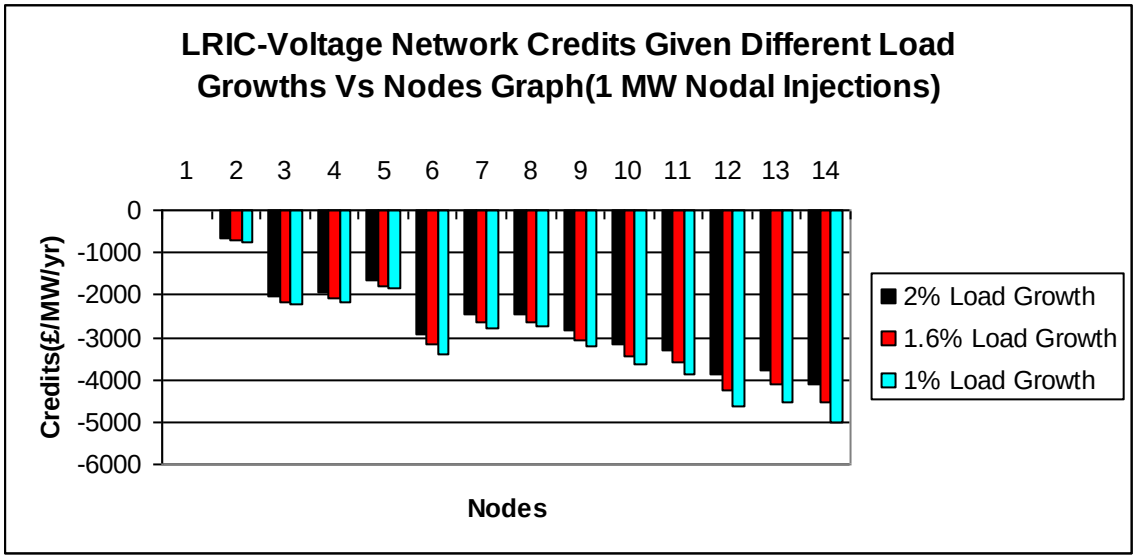

Figure 6.11: LRIC-voltage network costs owing 1 MW nodal injections considering different load growth rates on IEEE-14 bus test system.

The results show the same pattern as that in figure 6.10 but with reduced nodal credits as this network's circuit Xs are more than the corresponding circuit Rs.

2. Distribution Test System

The distribution practical test system, under the ownership of WPD, was introduced in chapter 4. All the data used here is the same as in the aforementioned chapter. The demand growth rates utilized for this study were also 1%, 1.6% and 2%.

Table 6.13 shows the LRIC-voltage network costs due to 1 MVAr nodal withdrawals considering 1%, 1.6% and 2% load growth rates (LGRs) while table 6.14 shows these costs but given 1 MW nodal withdrawals considering the same respective load growth rates, as mentioned above.

On the other hand, table 6.15 shows the LRIC-voltage network credits at each node given 1 MVAr injections considering 1%, 1.6% and 2% load growth rates while table 6.16 shows these credits given 1 MW nodal injections considering the same respective aforementioned load growth rates.

Table 6.13: LRIC-voltage network costs given 1 MVAr nodal withdrawals considering different load growth rates on 87-bus Pembroke practical distribution test system test system.

Bus	1% LGR LRIC-V Charges (£/MVAr/yr)	1.6% LGR LRIC-V Charges (£/MVAr/yr)	2% LGR LRIC-V Charges (£/MVAr/yr)	Bus	1% LGR LRIC-V Charges (£/MVAr/yr)	1.6% LGR LRIC-V Charges (£/MVAr/yr)	2% LGR LRIC-V Charges (£/MVAr/yr)	Bus	1% LGR LRIC-V Charges (£/MVAr/yr)	1.6% LGR LRIC-V Charges (£/MVAr/yr)	2% LGR LRIC-V Charges (£/MVAr/yr)	Bus	1% LGR LRIC-V Charges (£/MVAr/yr)	1.6% LGR LRIC-V Charges (£/MVAr/yr)	2% LGR LRIC-V Charges (£/MVAr/yr)
2005	860.57	1018.78	1035.06	3066	2135.62	2342.21	2301.42	2021	426.67	501.55	493.23	2650	425.73	500.07	491.44
2015	869.68	1015.9	1019.13	3069	1665.11	1798.59	1763.15	2025	458.95	553.98	554.28	2651	426.34	501.01	492.55
3003	2198.46	2387.74	2327.25	3072	895.22	1117.35	1173.55	2026	475.49	580.36	583.67	5140	0	0	0
3006	2163.34	2332.25	2264.58	3075	867.86	1046.5	1078.45	2027	475.5	580.38	583.68	5148	361.6	424.9	418.35
3009	2034.58	2143.46	2081.91	3078	870	1053.22	1087.74	2030	361.83	424.92	417.97	5149	361.67	424.98	418.43
3012	1964.77	2050.95	1985.14	3081	3195.99	3326.21	3199.95	2031	361.47	424.66	418	5150	361.4	424.66	418.11
3015	2050.47	2223.72	2168.17	3084	2862.35	2917.79	2786.04	2032	361.83	424.91	417.95	5151	0	0	0
3018	2026.16	2184.6	2118.57	3087	1069.84	1352.31	1402.41	2033	361.47	424.66	417.98	5152	0	0	0
3021	881.52	1060.16	1087.14	3090	1043.78	1302.14	1342.08	2035	373.92	429.31	413.56	5153	179.62	211.35	208.29
3024	882.21	1041.27	1055.65	3093	2340.83	2412.1	2328.71	2036	373.92	429.31	413.56	5154	179.72	211.47	208.41
3027	871.57	1021.01	1027.04	3096	2237.62	2271.58	2180.13	2037	363.34	425.78	417.24	20251	488.7	594.72	597.41
3030	875.83	1036.84	1051.13	3099	875.09	1034.81	1048.19	2040	411.56	483.54	476.13	20262	514.93	629.7	634.02
3033	892.42	1069.05	1092.72	3102	2161.09	2329.7	2262.1	2041	424.52	498.71	491.06	20351	508.82	576.54	557.47
3036	875.13	1031.67	1042.89	3105	1988.71	2072.49	2005.39	2045	418.41	498.07	499.52	20352	508.82	576.54	557.47
3039	877.79	1042.65	1059.64	20051	870.76	1031.6	1048.78	2046	418.41	498.07	499.52	20373	488.44	563.22	552.95
3042	1205.01	1538.74	1596.05	20052	884.46	1049.79	1068.46	2047	422.68	502.99	504.29	20374	488.2	562.95	552.68
3045	1126.86	1411.18	1454.43	20151	886.49	1036.58	1040.97	2048	422.68	502.99	504.29	20451	445.37	536.93	542.39
3048	2471.48	2541.62	2425.55	20152	892.25	1044.05	1049	2620	424.24	498.4	490.93	20472	449.41	541.57	546.89
3051	2466.01	2583.68	2478.62	2000	409.87	481.84	475.31	2621	424.53	498.74	491.27				
3054	1190.46	1531.13	1594.28	2001	375.66	441.52	435.06	2630	424.52	498.71	491.1				
3057	996.97	1240.75	1280.4	2010	489.2	574.56	568.22	2631	411.47	483.41	476.03				
3060	1394.95	1613.6	1608.56	2011	488.18	573.36	567	2640	425.71	500.1	491.61				
3063	1320.73	1508.07	1496.5	2020	425.94	500.43	491.92	2641	426.32	501.05	492.72				

During MW and MVAr nodal withdrawals, across all the load growth rates, the overall effect is that all the nodes attract costs since majority of lower bus voltage limits are critical (many bus voltages are below 1 pu). This signifies that the overall effect is that most lower nodal voltage margins are reduced thus advancing closer the investment horizons on these buses. It should be noted that for smaller load growth rate, the smaller the present values (PVs) before and after withdrawals. It should be further noted that the difference between the aforementioned PVs might be more or less for the smaller load growth rate as compared to the ones for the more load growth rates. This latter effect has a bearing in the overall charges as they can be either more or less for either of the load growth rates.

Specifically, during MVAr nodal withdrawals (as it can be observed from table 6.13), generally, the costs increase as the load growth rates increases when considering load growth rates 1% and 1.6%. Considering growth rates 1.6% and 2%, it can be observed that there are some mixed messages since some buses have 1.6% load growth rate costs more than those of the 2% load growth rate and at other buses the reverse is true. Where the nodal costs for 1.6% load growth rate exceed the corresponding costs for 2% load growth rate, then the nodal perturbations occurred at or near buses which had their initial bus voltage loading levels were atleast 80% loaded with respect to their lower voltage limits. This resulted in their respective differences in their PVs being significantly large and resulting in, overall, more costs than the 2% load growth rate case.

Table 6.14: LRIC-voltage network costs given 1 MW nodal withdrawals considering different load growth rates on 87-bus Pembroke practical distribution test system test system.

Bus	1% LGR LRIC-V Charges (£/MVAr/yr)	1.6% LGR LRIC-V Charges (£/MVAr/yr)	2% LGR LRIC-V Charges (£/MVAr/yr)	Bus	1% LGR LRIC-V Charges (£/MVAr/yr)	1.6% LGR LRIC-V Charges (£/MVAr/yr)	2% LGR LRIC-V Charges (£/MVAr/yr)	Bus	1% LGR LRIC-V Charges (£/MVAr/yr)	1.6% LGR LRIC-V Charges (£/MVAr/yr)	2% LGR LRIC-V Charges (£/MVAr/yr)	Bus	1% LGR LRIC-V Charges (£/MVAr/yr)	1.6% LGR LRIC-V Charges (£/MVAr/yr)	2% LGR LRIC-V Charges (£/MVAr/yr)
2005	154.36	186.68	190.77	3066	1154.03	1245.19	1218.34	2021	65.72	77.58	76.53	2650	64.61	76.11	74.94
2015	151.72	178.48	178.06	3069	783.27	827.79	802.45	2025	130.03	155.68	154.74	2651	65.17	76.86	75.76
3003	1367.47	1472.72	1424.51	3072	215.13	280.25	302.4	2026	154.2	185.47	184.81	5140	0	0	0
3006	1207.1	1299.72	1255.64	3075	164.54	208.27	220.56	2027	154.22	185.49	184.83	5148	30.12	35.4	35.29
3009	1349.77	1383.45	1327.65	3078	168.9	226.27	248.5	2030	30.65	35.93	35.66	5149	30.13	35.41	35.3
3012	1068.2	1089.33	1042.08	3081	2107.17	2160.5	2062.38	2031	30.29	35.54	35.36	5150	30.1	35.37	35.26
3015	1318.83	1411.1	1358.75	3084	1711.39	1755.05	1671.96	2032	30.66	35.94	35.67	5151	0	0	0
3018	1126.82	1209.38	1164.7	3087	441.91	588.38	620.08	2033	30.3	35.55	35.36	5152	0	0	0
3021	278.73	337.91	346.61	3090	326.07	439.63	464.76	2035	62.52	72.95	71.54	5153	9.27	10.86	10.85
3024	251.8	303.87	310.23	3093	1560.28	1558.42	1483.92	2036	62.52	72.95	71.54	5154	9.28	10.87	10.86
3027	160	191.64	194.5	3096	1279.02	1272.35	1208.04	2037	33.48	39.26	38.91	20251	146.91	176.18	175.29
3030	171.44	212.42	220.86	3099	168.25	206.27	212.78	2040	54.38	64.06	63.5	20262	171.99	207.31	206.83
3033	287.17	350.68	361.06	3102	1203.72	1295.97	1252	2041	61.8	72.81	72.1	20351	117.58	136.28	132.43
3036	169.31	204.39	208.45	3105	1070.61	1090.59	1043.08	2045	60.9	72.15	72.03	20352	117.58	136.28	132.43
3039	176.29	218.24	226.75	20051	163.4	197.48	201.78	2046	60.9	72.15	72.03	20373	83.6	98.22	96.64
3042	539.23	721.28	758.68	20052	174.25	210.45	214.99	2047	61.92	73.33	73.15	20374	83.48	98.09	96.51
3045	427	575.58	606.46	20151	166.53	196	195.68	2048	61.92	73.33	73.15	20451	76.01	90.21	90.13
3048	1746.43	1808.76	1721.28	20152	171.17	201.49	201.21	2620	61.78	72.8	72.17	20472	77.18	91.56	91.42
3051	1378.34	1449.03	1384.35	2000	55.25	65.34	65.25	2621	61.8	72.83	72.2				
3054	493.55	660.09	698.41	2001	37.57	44.3	44.24	2630	61.8	72.81	72.13				
3057	280.93	377.19	399.15	2010	95.33	112.4	112.18	2631	54.26	63.92	63.37				
3060	762.3	878.89	872.07	2011	93.56	110.29	110.01	2640	64.59	76.12	75.01				
3063	568.44	654.97	648.56	2020	65.03	76.66	75.54	2641	65.15	76.87	75.82				

Specifically, during MW nodal withdrawals, it can be observed, from table 6.14, that the results follow the same pattern as in the MVAr perturbation case, the only difference is that the costs are smaller and this is due to the fact that the network circuit Xs are more than the corresponding network circuit Rs.

Table 6.15: LRIC-voltage network costs given 1 MVAr nodal injections considering different load growth rates on 87-bus Pembroke practical distribution test system test system.

Bus	1% LGR LRIC-V Charges (£/MVAr/yr)	1.6% LGR LRIC-V Charges (£/MVAr/yr)	2% LGR LRIC-V Charges (£/MVAr/yr)	Bus	1% LGR LRIC-V Charges (£/MVAr/yr)	1.6% LGR LRIC-V Charges (£/MVAr/yr)	2% LGR LRIC-V Charges (£/MVAr/yr)	Bus	1% LGR LRIC-V Charges (£/MVAr/yr)	1.6% LGR LRIC-V Charges (£/MVAr/yr)	2% LGR LRIC-V Charges (£/MVAr/yr)	Bus	1% LGR LRIC-V Charges (£/MVAr/yr)	1.6% LGR LRIC-V Charges (£/MVAr/yr)	2% LGR LRIC-V Charges (£/MVAr/yr)
2005	-791.66	-953.41	-978.7	3066	-1333.28	-1529.97	-1544.83	2021	-410.05	-481.84	-477.55	2650	-409.08	-480.4	-475.8
2015	-798.63	-943.89	-953.73	3069	-1379.97	-1585.88	-1595.22	2025	-432.19	-510.82	-509.92	2651	-409.74	-481.31	-476.88
3003	-1564.39	-1798.74	-1785.2	3072	-786.91	-966.69	-1010.9	2026	-448.13	-542.52	-549.32	5140	0	0	0
3006	-1590	-1844.04	-1836.77	3075	-792.44	-967.99	-1005.91	2027	-448.13	-542.53	-549.33	5148	-349.84	-410.34	-408.01
3009	-1584.15	-1802.35	-1807.59	3078	-792.7	-971.1	-1011.03	2030	-349.99	-410.25	-407.5	5149	-349.91	-410.42	-408.08
3012	-1571.4	-1767.7	-1761.59	3081	-1593.49	-1794.13	-1766.89	2031	-349.7	-410.08	-407.63	5150	-349.65	-410.11	-407.78
3015	-1458.14	-1693.82	-1689.37	3084	-1813.41	-2082.31	-2062.85	2032	-349.99	-410.24	-407.47	5151	0	0	0
3018	-1492.37	-1746.45	-1746.26	3087	-915.45	-1155.67	-1205.81	2033	-349.69	-410.08	-407.6	5152	0	0	0
3021	-798.5	-972.99	-1006.91	3090	-926.91	-1181.56	-1234.23	2035	-358.11	-407.56	-394.81	5153	-176.67	-206.67	-205.87
3024	-794.92	-932.89	-939.91	3093	-1641.36	-1793.55	-1768.2	2036	-358.11	-407.55	-394.81	5154	-176.77	-206.79	-205.99
3027	-798.76	-946.23	-958.45	3096	-1702.05	-1887.32	-1869.98	2037	-349.71	-408.57	-403.76	20251	-417.36	-491.81	-489.95
3030	-801.71	-958.84	-978.52	3099	-801.61	-957.85	-976.77	2040	-396.27	-465.2	-461.92	20262	-432.49	-522.15	-527.97
3033	-799.76	-946.21	-960.92	3102	-1588.98	-1842.66	-1835.36	2041	-408.21	-479.32	-475.79	20351	-266.64	-310.52	-299.91
3036	-800.52	-954.08	-970.95	3105	-1582.4	-1779.36	-1773.29	2045	-400.18	-474.45	-478.19	20352	-266.64	-310.52	-299.91
3039	-802.51	-962.92	-984.99	20051	-783.68	-943.77	-968.8	2046	-400.18	-474.45	-478.19	20373	-260.92	-313.33	-309.63
3042	-969.63	-1265.19	-1336.88	20052	-774.53	-932.49	-956.97	2047	-404.1	-479.02	-482.61	20374	-260.98	-313.4	-309.71
3045	-971.07	-1253.27	-1313.45	20151	-785.8	-928.34	-937.97	2048	-404.1	-479.02	-482.61	20451	-386.91	-458.65	-462.45
3048	-774.77	-1278.61	-1379.19	20152	-781.96	-923.65	-933.17	2620	-408.03	-479.16	-475.83	20472	-390.71	-463.08	-466.72
3051	-1533.34	-1853.15	-1871.15	2000	-394.78	-463.88	-461.59	2621	-408.3	-479.48	-476.15				
3054	-872.83	-1103.01	-1157.53	2001	-362.98	-426.03	-423.8	2630	-408.27	-479.39	-475.91				
3057	-895.09	-1134.47	-1185.87	2010	-467.53	-549.48	-547.83	2631	-396.24	-465.14	-461.92				
3060	-1051.02	-1281.91	-1309.83	2011	-466.6	-548.38	-546.69	2640	-409.1	-480.5	-476.04				
3063	-1057.32	-1284.81	-1305.53	2020	-409.27	-480.77	-476.29	2641	-409.76	-481.4	-477.12				

On the other hand, during MW and MVAr nodal injections, across all the load growth rates, the overall effect is opposite to that of nodal withdrawal perturbations as all the nodes attract credits since majority of lower bus voltage limits are critical (many lower bus voltage bounds are below 1 pu). This signifies that the overall effect is that most lower nodal voltage margins are increased thus deferring the investment horizons on these buses.

Specifically, during MVAr nodal injections, it can be observed, from table 6.15, that the results follow the same pattern as in the MVAr withdrawal case (table 6.13), the main difference is that in this case we are dealing with credits at nodes as opposed to costs.

Table 6.16: LRIC-voltage network costs given 1 MW nodal injections considering different load growth rates on 87-bus Pembroke practical distribution test system test system.

Bus	1% LGR LRIC-V Charges (£/MVAr/yr)	1.6% LGR LRIC-V Charges (£/MVAr/yr)	2% LGR LRIC-V Charges (£/MVAr/yr)	Bus	1% LGR LRIC-V Charges (£/MVAr/yr)	1.6% LGR LRIC-V Charges (£/MVAr/yr)	2% LGR LRIC-V Charges (£/MVAr/yr)	Bus	1% LGR LRIC-V Charges (£/MVAr/yr)	1.6% LGR LRIC-V Charges (£/MVAr/yr)	2% LGR LRIC-V Charges (£/MVAr/yr)	Bus	1% LGR LRIC-V Charges (£/MVAr/yr)	1.6% LGR LRIC-V Charges (£/MVAr/yr)	2% LGR LRIC-V Charges (£/MVAr/yr)
2005	-149.8	-181.38	-186.31	3066	-899.03	-1014.45	-1011.24	2021	-64.96	-76.15	-75.77	2650	-63.84	-74.68	-74.16
2015	-148.29	-172.85	-175.02	3069	-694.64	-761.54	-749.42	2025	-125.73	-149.43	-150.06	2651	-64.4	-75.42	-74.98
3003	-1024.36	-1159.11	-1144.07	3072	-187.19	-243.66	-264.67	2026	-149.12	-178.09	-179.35	5140	0	0	0
3006	-940.71	-1062.25	-1048.37	3075	-155.09	-196.21	-208.76	2027	-149.14	-178.11	-179.37	5148	-29.9	-35.08	-35.06
3009	-1094.12	-1197.49	-1177.87	3078	-157.17	-208.72	-229.8	2030	-30.37	-35.54	-35.36	5149	-29.91	-35.1	-35.07
3012	-909.14	-979.49	-955.94	3081	-1255.08	-1394.94	-1364.45	2031	-30.05	-35.21	-35.1	5150	-29.87	-35.05	-35.03
3015	-981.74	-1125.51	-1116.96	3084	-1163.14	-1294.01	-1267.02	2032	-30.37	-35.54	-35.36	5151	0	0	0
3018	-875.15	-999.47	-991.2	3087	-394.08	-531.77	-568.19	2033	-30.05	-35.21	-35.1	5152	0	0	0
3021	-260.19	-316.28	-326.86	3090	-301.62	-411.21	-439.88	2035	-60.1	-69.7	-68.86	5153	-9.2	-10.78	-10.76
3024	-234.36	-280.77	-291	3093	-1182.03	-1262.9	-1235.74	2036	-60.1	-69.7	-68.86	5154	-9.2	-10.78	-10.77
3027	-154.83	-183.62	-189.01	3096	-1036.97	-1102.8	-1077.45	2037	-31.48	-36.83	-36.62	20251	-109.31	-129.61	-129.96
3030	-165.42	-202.88	-213.82	3099	-162.94	-197.9	-207.03	2040	-53.85	-63.04	-62.98	20262	-131.95	-157.1	-157.95
3033	-267.08	-324.23	-338.34	3102	-938.63	-1059.71	-1045.83	2041	-61.15	-71.55	-71.47	20351	-5.81	-7.94	-8.81
3036	-162.91	-194.88	-201.63	3105	-909.61	-980.69	-956.94	2045	-57.98	-68.23	-68.67	20352	-5.81	-7.94	-8.81
3039	-169.62	-208.02	-219.14	20051	-141.05	-170.91	-175.54	2046	-57.98	-68.23	-68.67	20373	18.3	21.13	20.81
3042	-443.61	-614	-659.09	20052	-130.55	-158.34	-162.61	2047	-58.95	-69.33	-69.74	20374	18.19	21	20.68
3045	-371.07	-516.06	-553.73	20151	-133.92	-155.93	-157.73	2048	-58.95	-69.33	-69.74	20451	-43.06	-50.56	-50.74
3048	-967.02	-1173.67	-1185.45	20152	-129.42	-150.64	-152.31	2620	-61.21	-71.64	-71.64	20472	-43.88	-51.5	-51.65
3051	-913.95	-1077.6	-1078.67	2000	-54.72	-64.41	-64.72	2621	-61.23	-71.67	-71.66				
3054	-410.1	-555.56	-596.23	2001	-37.28	-43.83	-43.94	2630	-61.2	-71.61	-71.55				
3057	-263.29	-355.99	-380.37	2010	-94.06	-109.94	-111.04	2631	-53.78	-62.95	-62.9				
3060	-580.48	-715.79	-731.7	2011	-92.31	-107.89	-108.9	2640	-63.86	-74.73	-74.28				
3063	-456.15	-558.28	-569.24	2020	-64.27	-75.24	-74.78	2641	-64.42	-75.47	-75.1				

Finally, during MW nodal injections, it can be observed, from table 6.16, that the results follow the same pattern as in the MVAr nodal injection case, the only difference is that the credits are smaller and this is due to the fact that the network circuit Xs are more than the corresponding network circuit Rs.

6.3 Chapter Conclusions

In this chapter, the studies were performed to analyse the trend of LRIC-voltage network charges on different types of networks and different demand growth rates, providing insights into how charges given those. The former study was carried-out on a 9-bus test network which is a subset of the practical Western Power Distribution (WPD) network. This study was, specifically, intended to provide an insight into how to treat the LRIC-voltage network charges in relations to real and reactive power nodal withdrawals/injections in transmission and distribution systems. To represent a fair degree of systems ranging from transmission to distribution networks, the aforementioned 9-bus test system, at first, had its circuit reactances (Xs) 10 times more than their corresponding resistance (Rs) counterparts. The second case was when the network circuit Xs and Rs were comparable and, finally, the case when the network circuit Rs were 10 times more than their corresponding X counterparts. On the other hand, the latter study, was carried-out on the IEEE-14 bus test system and, finally, on a practical 87-bus distribution test system developed, operated and maintained by Western Power Distribution (WPD) network.

Involving different types of networks, the results show that when the network circuit Xs are atleast ten times more than their R counterparts, only MVAr nodal perturbations should be considered. When the network circuit Rs, on the other hand, are atleast ten folds more than their Xs counterparts, then, only MW nodal perturbations should be considered. Finally, when the network circuit Xs and their corresponding Rs are comparable, both MVAr and MW nodal perturbations should be considered. On the other hand, involving different growth rates, the results show that the LRIC-v network charges given different load growth rates are a function of the power system nodal voltage loading levels. This means that, there is a nodal bus voltage loading threshold above which if most buses are loaded at in a power system, the least load growth rate would have more charges. On the other hand, below the aforementioned nodal bus voltage loading threshold and if most power system buses are involved, then the larger load growth rate would generate more charges.

Chapter 7

LRIC-Voltage Network Pricing For Existing Network SVCs

In this chapter, the LRIC-voltage network charging principle for pricing the use of future SVCs which was discussed in chapter 4, is extended to price also for the use of existing network SVCs. This new extension is tested on a IEEE-14 bus test system and, to prove its practical applicability, is also tested on a practical distribution test system developed, operated and maintained by WPD. The results show that the existing network SVCs can be successfully priced despite the fact that the nodal voltages where these aforesaid devices are sited do not vary.

7.1 Chapter Introduction

In chapter 4, the LRIC-voltage network charging principle was proposed and explained. This aforementioned charging principle was utilised to price the network nodal voltage degradations for future SVCs as the nodal reinforcements. However, this proposed charging principle failed to price for the use of existing network SVCs since where these existing devices are sited the corresponding bus voltages do not vary. The reason why the bus voltage does not vary is because the existing network SVCs would be preset to keep the corresponding nodal voltages at constant values and, therefore, since the proposed LRIC-voltage charging principle depicted its strength upon the network voltage variations, this approach can not be applied in this regard.

In this chapter, the LRIC-voltage network charging principle would be extended to cover for the pricing of the existing network SVCs. The reactive power loading of the SVC varies in keeping the bus voltage, where this device is sited, at a preset value given variations in power system demand and generation loading conditions. In this regard, this new extension involves the mapping of the SVCs' reactive power loading limits to the nodal voltage limits at the buses where these SVCs' are sited. For example, if the SVC reactive power lower and upper limits are $Q_{\min}$ and $Q_{\max}$, respectively. While, on the other hand, if the nodal voltage lower and upper limits, where this SVC is sited, are V_L and V_H, respectively. To that end, $Q_{\min}$ would be mapped to V_L while $Q_{\max}$ would be mapped to V_H. With this limit mapping exercise completed, then, it would be possible to price for the use of the existing network SVCs.

In this next section, the mapping exercise involving the mapping of SVC reactive power limits to nodal voltage limits where this device is sited shall be formulated and explained. Thereafter, this new extension would be tested on the IEEE-14 bus test system and finally on the practical distribution test system. Both of these test systems were introduced in chapter 4. Finally, the results would be presented and analysed.

7.2 Mapping SVC VAr limits to nodal voltage limits and charging for use of existing network SVCs

Since the existing network SVC is meant to continuously adjust its reactive power output to regulate the voltages at the controlled bus to a preset value (e.g. 1 pu), therefore, the bus voltage at which this SVC exists remain constant and, only, the device's reactive power output varies accordingly. Owing to this factor, the LRIC-voltage network charging approach can not be applied without any modification, therefore, this aforementioned approach is modified as detailed below to accommodate the behaviour of the existing network SVC.

If a network node b, has lower voltage limit, V_L and upper voltage limit, V_H, and on this bus if there exist an SVC having minimum reactive power capacity, $Q_{\min}$ and maximum

reactive power capacity, $Q_{\max}$. Then $Q_{\min}$ can be mapped to V_L while $Q_{\max}$ can be mapped to V_H and, therefore, the relation below by equation (7.1) holds

$$V_{b_{SVC}} = \left(\frac{V_H + V_L}{2}\right) + \left(\frac{V_H - \left(\frac{V_H + V_L}{2}\right)}{Q_{\max} - \left(\frac{Q_{\max} + Q_{\min}}{2}\right)}\right) * \left(Q_{gen} - \left(\frac{Q_{\max} + Q_{\min}}{2}\right)\right) \quad (7.1)$$

With the mapped voltage, $V_{b_{SVC}}$, known, then V_b in equations (4.1-4.4) and (4.6-4.7) in chapter 4 can be replaced by the former voltage to price the contribution of the existing network SVC at the node where it is sited.

7.3 Results and Analysis

The results are presented and analysed below, consequent to the modified LRIC-voltage network pricing approach being tested on the IEEE-14 bus test system and a distribution test system chosen from the South Wales distribution network, in the UK.

7.3.1 IEEE-14 Bus Test System

The IEEE-14 bus test system was first introduced in chapter 4 and used in the subsequent chapters. As it is now the norm, this test system is once again used but with two SVCs, one existing at bus 4 and the other at bus 12. These SVCs were randomly installed to exist at these respective buses. It is emphasized that, the reactive power planning (RPP) exercise determines the optimal allocation of VAr compensation assets through-out the entire power system to ensure network security and reliability at the least possible costs. To this end, it can be said that, the random existence of SVCs at the aforementioned buses is just meant to demonstrate the concept of charging for the use of existing network SVCs.

Both the SVCs at buses 4 and 12 have the same specification of maximum and minimum VAr capabilities of 100 MVAr and -50 MVAr, respectively. Both these SVCs have their voltages preset at 1 pu, so as the voltage settings for synchronous condensers at buses 3, 6 and 8. The nodal lower and upper voltage limits remain to be 0.94V and 1.06V, respectively.

Figure 7.1 shows the 1 MVAr and 1 MW nodal withdrawals to reflect the LRIC-V network charges for the use of these existing network SVCs. On the other hand, Figure 7.2 shows the 1 MVAr and 1 MW nodal injections to reflect the LRIC-V network charges for the use of the above mentioned existing network SVCs.

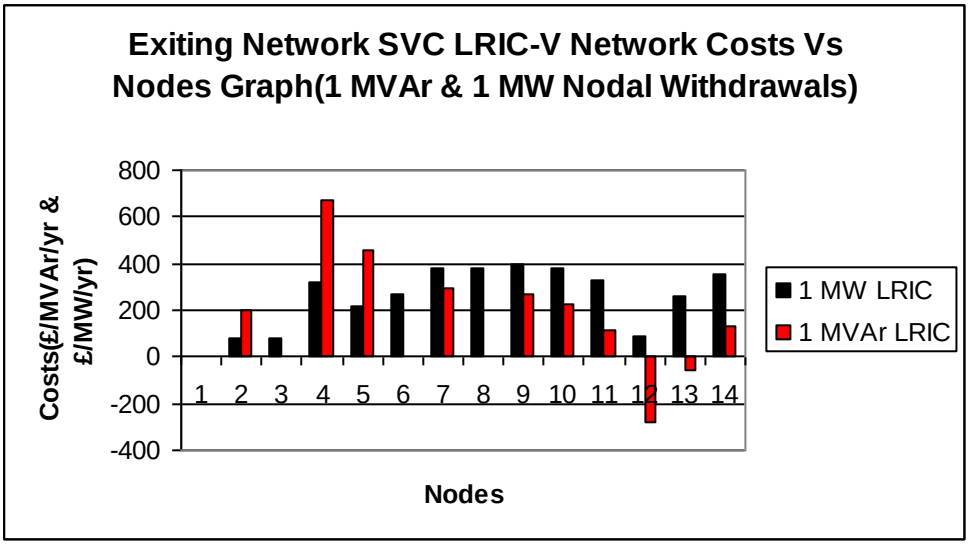

Figure 7.1: LRIC-v network costs consequent to 1 MVAr and 1 MW nodal withdrawals to reflect the use of existing network SVCs.

It should be noted that, the initial VAr loadings of SVCs at buses 4 and 12 were 40.987 MVAr and 11.365 MVAr, respectively. These VAr loadings translated to 1.013V and 0.989V for buses 4 and 12, respectively, owing to the SVC VAr limit/nodal voltage limit mapping exercise. In this regard, during nodal withdrawals, bus 4 was attracting a cost since reactive power had to be injected into the network and that represented a voltage increase in the mapping exercise context and, therefore, a degradation of this bus upper voltage limit margin. This latter effect meant the investment horizon of the concerned SVC was brought closer and, therefore, a penalty imposed in the context of a cost. On the other hand, for bus 12, the reverse was true and hence a credit during nodal withdrawals as its already critical bus lower voltage margin (voltage from the context of transforming node SVC VAr loading to node voltage) is increased and, therefore, its investment horizon was deferred as a result.

Specifically, during 1 MVAr nodal withdrawals, it can be observed that buses 3, 6 and 8 attract no charges as the synchronous condensers at these buses absorbed all the shock resulting from these particular withdrawals, by supplying reactive power into the network. However, bus 2 attracts a cost even though a generator is connected at this bus since this connected device has reached its VAr capacity. It can be observed that bus 4 attracts the most cost as during MVAr withdrawal at this bus, the existing SVC there makes up all for the withdrawal. Elsewhere, other than buses 12 and 13, the costs reduce as these buses' distances from bus 4 increase, owing to the reduced perturbations impacted on bus 4 and increased perturbations impacted on bus 12 which is attracting credits. On the other hand, bus 12 attracts a credit since it absorbs all the impact resulting from the withdrawal on it. Bus 13 also attracts a credit, since, due to its closeness to bus 12, during MVAr withdrawal at the former bus the voltage at the latter bus is offset only to be restored by the action of the SVC at bus 12 in putting more capacitive reactance into the network.

On the other hand, during 1 MW nodal withdrawals, all buses (excluding slack bus) attract costs since the slack bus has to support these buses with real power as the synchronous compensators and the SVCs do not have their own real power supplies. Also, buses 4 and 12 attract cost and credit for these perturbations, respectively. The costs increase as the bus

distances increase from bus 4 and once again decrease when their relative distances decrease with relation to bus 12 which is attracting a credit. As such bus 9 is attracting the most cost. In this case, bus 12 attracts a cost since during withdrawal at it, it attracts a credit but because the real power has to flow from the slack bus, bus 4 attracts a larger cost resulting in the overall being a cost at bus 12. Due to the latter factor, bus 13 attracts a cost as well. Bus 4 attracts the least credit because it is closer to both slack bus and bus 4.

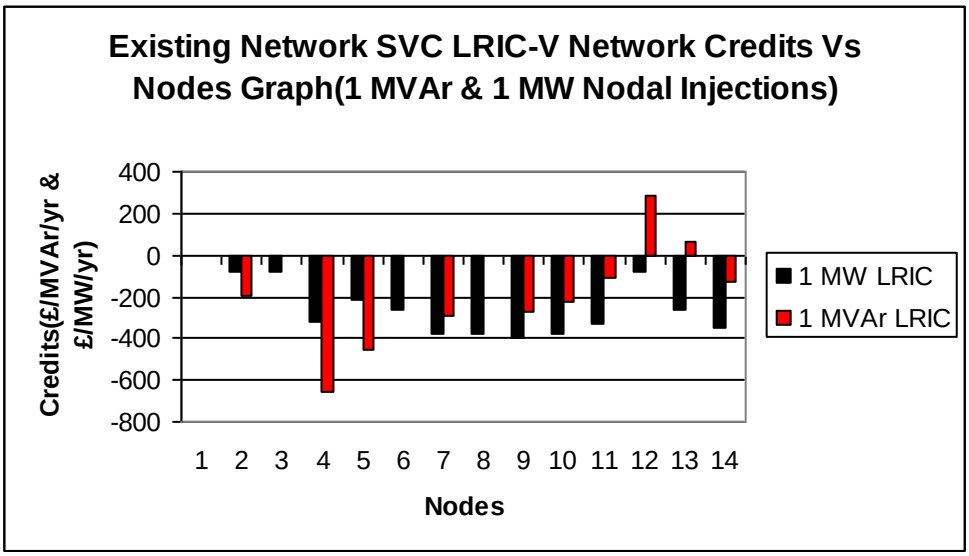

Figure 7.2: LRIC-v network costs consequent to 1 MVAr and 1 MW nodal injections to reflect the use of existing network SVCs.

In the contrary, during nodal injections, buses 4 and 12 attract credit and cost, respectively. The trend in this case is the same as the earlier case, for both MVAr and MW perturbations, but in the opposite sense. The same reasons as advanced above hold in this case and, therefore, for MVAr nodal injections bus 4 attracts the most credit while buses 12 and 13 attract costs. On the other hand, for MW perturbations, bus 9 attracts the most credit while bus 2 attracts less credit.

7.3.2 Pembroke Practical Test System

This test system was also first introduced in chapter 5 and, subsequently, used in the chapters which followed, thereafter. This test system's economic data, voltage limits and any other system constraints remain the same as introduced in chapter 5. However, in this case, three SVCs exist at buses 2005, 2015 and 2620. These SVCs were randomly installed at these respective buses. It is emphasized that RPP, as mentioned earlier, remains the only process which determines the optimal siting of VAr compensation devices on a given power system and, therefore, the random installation of such devices at the aforementioned buses was purely to demonstrate the concept of charging for these devices.

Both the SVCs at buses 2005 and 2015 have the same specification of minimum and maximum VAr capabilities of -50 MVAr and 100 MVAr, respectively. While, on the other

hand, the SVC at bus 2620 has the minimum VAr capability of -100 MVAr and maximum capacity of 100 MVAr. All the three devices have their respective voltages preset at 1 pu.

Table 7.1 shows the 1 MVAr and 1 MW nodal withdrawals to reflect the LRIC-V network charges for the use of these existing network SVCs. On the other hand, Table 7.2 shows the 1 MVAr and 1 MW nodal injections to reflect the LRIC-V network charges for the use of the above mentioned existing network SVCs.

Table 7.1: LRIC-V network charges for the use of existing network SVCs during MVAr and MW withdrawals on Pembroke test system.

Bus	LRIC-Charges (£/MVAr/yr)	LRIC-Charges (£/MW/yr)	Bus	LRIC-Charges (£/MVAr/yr)	LRIC-Charges (£/MW/yr)	Bus	LRIC-Charges (£/MVAr/yr)	LRIC-Charges (£/MW/yr)
2005	-17.42	-243.33	3084	58.02	-278.08	2041	-2125.16	-363.39
2015	60.14	-261.42	3087	19.45	-265.94	2045	-2077.64	-351
3003	58.94	-273.25	3090	19.48	-265.67	2046	-2077.65	-351
3006	58.75	-274.97	3093	8.19	-273.19	2047	-2106.95	-360.37
3009	12.6	-271.32	3096	8.41	-271.69	2048	-2106.95	-360.38
3012	12.74	-270.02	3099	60.02	-263.16	2620	-2126.85	-363.43
3015	58.85	-272.81	3102	58.76	-274.88	2621	-2125.39	-363.55
3018	58.56	-275.81	3105	8.87	-268.52	2630	-2125.3	-363.5
3021	-17.89	-248.18	20051	-17.6	-243.52	2631	-2039.12	-311.74
3024	60.4	-259.46	20052	-17.84	-243.75	2640	-2133.06	-378.22
3027	59.96	-263.06	20151	61.25	-260.37	2641	-2135.39	-381.04
3030	59.89	-264.22	* 20152	**61.61**	-260.05	2650	-2133.16	-378.33
3033	60.51	-258.56	2000	-1862.11	-242.78	2651	-2135.49	-381.15
3036	60.01	-262.77	2001	-1734.69	-171.58	*** 5140	**0**	**0**
3039	59.97	-263.77	2010	-1808.07	-245.87	5148	-1694.71	-147.88
3042	18.88	-269.77	2011	-1812.97	-254.26	5149	-1695.67	-147.98
3045	18.93	-269.5	2020	-2134.02	-380.52	5150	-1694.22	-147.79
3048	58.11	-272.46	2021	-2136.81	-383.99	*** 5151	**0**	**0**
3051	57.61	-275.2	2025	-2263.52	-725.64	*** 5152	**0**	**0**
3054	5.06	-264.89	2026	-2318.02	-851.24	5153	-854.03	-44.94
3057	6.09	-259.16	2027	-2318.05	-851.33	5154	-854.29	-44.97
3060	58.73	-271.31	2030	-1695.92	-150.62	20251	-2356.25	-815.11
3063	58.34	-274.8	2031	-1694.58	-148.78	** 20262	**-2414.46**	**-943.96**
3066	-1.52	-266.78	2032	-1695.94	-150.66	20351	-2153.15	-587.62
3069	-0.42	-261.64	2033	-1694.6	-148.82	20352	-2153.15	-587.62
3072	-18.22	-247.59	2035	-1761.17	-310.68	20373	-2047.7	-416.9
3075	-17.71	-244.54	2036	-1761.17	-310.68	20374	-2046.58	-416.34
3078	-18.07	-245.61	2037	-1703.28	-164.81	20451	-2161.54	-432.49
3081	58.58	-275.75	2040	-2039.61	-312.46	20472	-2192.01	-443.06

The initial VAr loadings for SVCs before any MVAr/Mw nodal perturbations on buses 2005, 2015 and 2620 are 15.422 MVAr, 32.704 MVAr and – 92.263 MVAr, respectively. These initial SVC VAr loadings translated into 0.992V, 1.006V and 0.908V for buses 2005, 2015 and 2620, respectively. Based on these initial SVC loading conditions, during MVAr/MW nodal withdrawals, buses 2005 and 2620 would attract credit as they would have their already critical lower bus voltage margins increased, thereby, deferring the investment horizon on these buses. It should be noted that, in essence, the respective SVC voltages has being preset to 1 pu so during the above mentioned nodal perturbations, the real voltages at these buses remain 1 pu. Therefore, only the translated voltage at these buses, relating to the already aforementioned mapping exercise, vary with varying respective bus SVC VAr loading. On the other hand, during MVAr/MW nodal withdrawals, the reverse is true for bus 2015 as it attracts a cost consequent to the fact that the SVC's investment horizon is advanced forward.

Specifically, during MVAr nodal withdrawals, the charges range from being costs to credits as the distances of node perturbations increase from bus 2015 and getting closer to buses 2005 and 2620. Since the SVC at bus 2620 is heavily loaded towards its minimum loading capacity, nodal perturbations closer to it attract significant credits resulting in the overall charges being significant credits. Bus 20152 (highlighted in bolded font and the corresponding bus number preceded by an asterisk) attracts most cost as it is closer to bus 2015 and a distance away from both buses 2005 and 2620. This is because during the MVAr perturbation at this bus, the perturbations propagated to bus 2015 (which attracts a cost) are more significant than those to buses 2005 and 2620 which attract credits and, therefore, results in an overall cost. Bus 20262 (highlighted in bolded font and the corresponding bus number preceded by double asterisk) attracts the most credit. Although, this bus is not closest to bus 2620, but it is connected to bus 2620 through a series of two transformers, one transforming from 0.415 kV to 11 kV and the other from 11 kV to 132 kV from the side of bus 20262. This voltage transformer series result in increased perturbations at bus 2620 and, therefore, significant overall credit. The slack bus, buses 5151 and 5152 (highlighted in bolded font and the corresponding bus number preceded by triple asterisk) attract attracts no costs since the voltage at the slack bus does not vary and the voltages at the two latter buses changes a little since they are both closer to the slack bus.

On the other hand, during nodal MW withdrawals, the slack bus has to supply real power as opposed to the earlier case when the SVCs at buses supplied the reactive power. The result being increased propagation of perturbations to buses 2005, 2015 and 2620 from other buses. With SVC at bus 2620 heavily loaded, this increase results in the overall charges being credits at all buses. Again, bus 20262 (highlighted in bolded font and the corresponding bus number preceded by double asterisk) attracts the most credit but less than that caused by MVAr withdrawals due to aforementioned increased perturbations resulting in SVC at 2015 attracting an increased cost, therefore, reduced overall credit at this bus and other buses.

Table 7.2: LRIC-V network charges for the use of existing network SVCs during MVAr and MW nodal injections on Pembroke test system.

Bus	LRIC-Charges (£/MVAr/yr)	LRIC-Charges (£/MW/yr)	Bus	LRIC-Charges (£/MVAr/yr)	LRIC-Charges (£/MW/yr)	Bus	LRIC-Charges (£/MVAr/yr)	LRIC-Charges (£/MW/yr)
2005	18.41	242.25	* 3084	**-58.84**	275.78	2041	2296.17	366.54
2015	-58.58	261.62	3087	-19.42	265.56	2045	2226.95	341.04
3003	-58.17	272.66	3090	-19.42	265.3	2046	2226.95	341.04
3006	-58.26	274.04	3093	-9.49	271.09	2047	2260.87	350.34
3009	-13.2	270.1	3096	-9.43	269.93	2048	2260.86	350.34
3012	-13.21	268.96	3099	-58.61	263.23	2620	2298.63	367.05
3015	-58.14	272.18	3102	-58.26	273.96	2621	2296.93	367.17
3018	-58.2	274.73	3105	-9.31	267.41	2630	2296.63	366.93
3021	18.57	246.81	20051	18.21	242.06	2631	2196.32	314.13
3024	-58.57	260	20052	17.99	241.83	2640	2305.11	381.49
3027	-58.68	262.98	20151	-57.61	262.66	2641	2307.88	384.43
3030	-58.68	264.08	20152	-57.31	262.98	2650	2304.99	381.39
3033	-58.66	259.15	2000	1991.76	243.54	2651	2307.76	384.33
3036	-58.62	262.81	2001	1846.87	171.78	*** 5140	**0**	**0**
3039	-58.63	263.76	2010	1931.21	246.15	5148	1801.67	147.95
3042	-19.71	268.47	2011	1936.78	254.69	5149	1802.75	148.05
3045	-19.7	268.27	2020	2306.12	383.74	5150	1801.11	147.85
3048	-58.53	270.77	2021	2309.43	387.36	*** 5151	**0**	**0**
3051	-58.77	272.66	2025	2443.25	729.29	*** 5152	**0**	**0**
3054	-6.15	263.05	2026	2506.29	861.5	5153	880.05	44.68
3057	-5.97	258.59	** 2027	**2506.32**	**861.58**	5154	880.32	44.7
3060	-58.19	270.47	2030	1802.74	150.43	20251	2351.97	635.38
3063	-58.19	273.46	2031	1801.43	148.77	20262	2411.32	763.45
3066	-0.11	264.1	2032	1802.73	150.43	20351	1641.5	21.09
3069	0.23	260.49	2033	1801.42	148.78	20352	1641.5	21.09
3072	17.65	244.91	2035	1865.87	303.48	20373	1595.52	-98.75
3075	18.07	242.81	2036	1865.87	303.48	20374	1595.88	-98.18
3078	17.66	243.11	2037	1801.8	156.06	20451	2145.32	257.61
3081	-58.45	274.48	2040	2196.62	314.59	20472	2177.93	265.63

In contrast to the earlier case of nodal withdrawals, during MVAr/MW nodal injections, buses 2005 and 2620 attract costs while bus 2015 attracts credit. This is as a result of the fact that buses 2005 and 2620 have their investment horizons advanced forward while that of bus 2015 is deferred as opposed to the earlier case of MVAr withdrawals.

Generally, the results echo the same message as in the case of MW/MVAr nodal withdrawals, but in an opposite sense. The difference, in this case, is that the charges are more on the other side of the aforementioned transformers of case with nodal withdrawals. This is as result of the MW/MVAr injections being significant on the aforementioned side of transformers. Therefore, during MVAr injections, bus 3084 (highlighted in bolded font and the corresponding bus number preceded by an asterisk) attracts most credit while bus 2027 (highlighted in bolded font and the corresponding bus number preceded by double asterisks) attracts the most cost. On the other hand, during MW injections, all the nodes attract costs and the most cost is registered at bus 2027 (highlighted in bolded font and the corresponding bus number preceded by double asterisk). Also, in this case, the slack bus, buses 5151 and 5152 (highlighted in bolded font and the corresponding bus number preceded by triple asterisk) attract attracts no costs since the voltage at the slack bus does not vary and the voltages at the two latter buses changes a little since they are both closer to the slack bus.

7.4 Chapter Conclusions

In this chapter, LRIC-voltage network charging principle to price for the use of existing network SVCs is presented and tested on the IEEE standard test system and the practical distribution test system. This aforementioned formulation is the extension of the earlier formulation, in chapter 5, which dealt with the pricing of future SVCs on the network. This latter formulation could not be used for pricing the existing network SVCs since it depicted its strength from the nodal voltage variations during MVAr and MW perturbations and, with existing network SVCs, the nodal voltages do not change as the devices' voltages would be preset at a constant level. Only the SVCs VAr loading levels would change consequent to the aforementioned perturbations and, therefore, it was imperative to map the SVCs' VAr limits to the nodal voltage limits where the device was connected and, thereafter, be able to charge for the use of these existing network SVCs.

It should be noted that, physically on a network, there would be existing network SVCs and at the buses where these exist, the formulation for pricing their use would be used. On the other hand, at the nodes without SVCs, the formulation of chapter 4 would be utilized to price the future network SVCs. This would therefore create a comprehensive and appropriate pricing framework that could account for the overall impact caused by the network users on the network.

Finally, the results show that the existing network SVCs can be successfully priced despite the fact that the nodal voltages where these aforesaid devices are sited do not vary.

Chapter 8

Improved Implementation For LRIC-Voltage Network Charges

This chapter presents an improved version of the LRIC-v network charges. This improvement emanates from the premise that the voltage change at a node and its corresponding power (MVA) change are related to each other by the P-V curve. As such, the best approximation of this relationship was used to execute the nodal voltage degradation rates resulting from the load growth rate and, finally, the Improved LRIC-v network charges were sought. This formulation was once again tested on the IEEE 14 bus test system and on the practical 87-bus distribution test system developed, operated and maintained by Western Power Distribution (WPD) network. The results show that improved LRIC-v network charges are less than the earlier computed LRIC-v network charges since the nodal voltage degradation rates for the latter are less than those of the former.

8.1 Chapter Introduction

In chapter 4, the LRIC-voltage network charging principle was proposed and tested on both the IEEE-14 bus and the practical 87-bus distribution test systems. In computing these charges, the respective nodal voltage degradation rates were considered as a constant rate following a constant load growth and reflecting network configurations. However, the nodal voltage degrading rate consequent upon a constant load growth rate closely follows the nodal P-V curve, which in fact, is of quadratic nature. Therefore, this raised a need to establish an approximate behaviour along this P-V curve that would enable the computation of the most representative nodal voltage degradation rates. Since it is a formidable task to accurately formulate this aforementioned behaviour, then it becomes apparent to approximately express this behaviour in simple terms, the idea being to provide a good compromise between accuracy and simplicity in determining the voltage degradation rates. Thereafter, the improved version of the LRIC-v network charges could be sought. This modified version to reflect improved LRIC-v network charges is finally tested on the IEEE 14 bus test system and, lastly, on the distribution practical test system. Finally, the results are presented and analyzed.

8.2 Approximating The Behavior Of The Nodal Voltage Change Resulting From Nodal Power Change

The P-V curve relates the nodal voltage change due to nodal power (MVA) change in a quadratic form, as shown in figure 8.1 below.

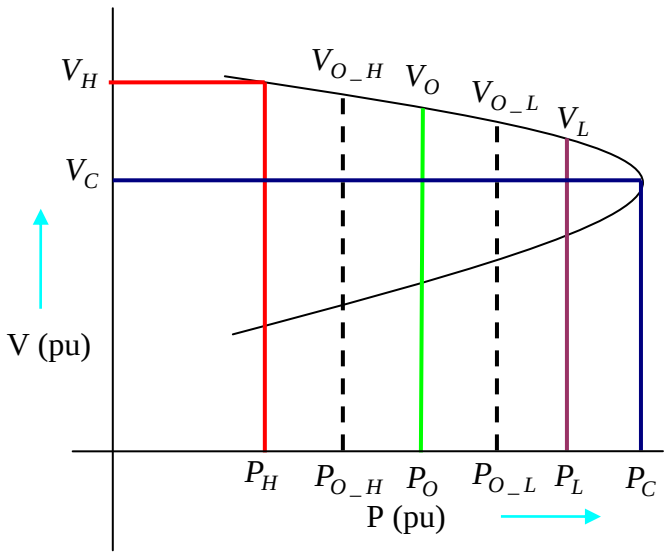

Figure 8.1: Nodal P-V curve

The P-V curve approach was used in the work in [79]-[80] to approximate the respective nodal voltage collapse points at the corresponding specific load points, among other things. In this work, this P-V curve formulation is extended to feature buses without load also. Thereafter, the nodal voltage changes consequent to the corresponding nodal load changes for all buses would be determined.

The idea is to approximate the most reasonable behavior of the nodal voltage change owing to the nodal power change along the P-V curve. The P-V curve is represented by the quadratic equation, below, over the limits ranging from $V = V_O$ to $V = V_L$, assuming that load would grow from V_O to V_L over the years:

$$P_1 = a_1 V^2 + b_1 V + c_1 \tag{8.1}$$

Then, the behavior of the nodal voltage change to nodal power change can be approximated along the P-V curve by the use of the linear relationship, below, over the limits ranging from $V = V_O$ to $V = V_L$:

$$P_2 = a_2 V + b_2 \tag{8.2}$$

Also, the behavior of the nodal voltage change to nodal power change can be approximated along the P-V curve by the use of the piecewise linear relationship, below, over the two separate limits, ranging from $V = V_O$ to $V = V_{O\_L}$ and from $V = V_{O\_L}$ to $V = V_L$:

$$P_3 = a_3 V + b_3 \quad V_O \le V_{O\_L} \tag{8.3}$$

$$P_4 = a_4 V + b_4 \quad V_{O\_L} \ge V_L \tag{8.4}$$

The quadratic representation of the nodal voltage degradations consequent to load growth rate would be the most accurate approach to adopt but it would be most complex to construct and, therefore, a need to seek for other options of constructing a compromise between accuracy and simplicity to represent this mentioned behaviour, namely, piece-wise linear approximation. In that light, the resulting calculated charges consequent to utilizing improved nodal voltage degradation rates would be better in terms of accuracy than the earlier charges achieved with the linear approach, since this approximation would follow the p-v curve more closely than the linear dispensation.

8.3 Results and Analysis

The results are presented and analysed below, to demonstrate the improved version of the LRIC-voltage network charges. Once more, this study is tested on the IEEE-14 bus test system and a distribution test system chosen from the South Wales distribution network, in the UK. Both of these test systems were introduced in chapter 4 and have been used in the

subsequent chapters. It should be noted that, in this chapter, the LRIC-v and the Improved LRIC-v network charges are compared and the issue of analyzing why the charges follow a certain specific trend at particular nodes was executed in chapter 4, therefore, reference should be made to that chapter regarding the same.

8.3.1 IEEE-14 Bus Test System

This test system was introduced in chapter 4 and was subsequently used in the chapters which followed, thereafter. All the data introduced earlier remains the same, namely, the nodal voltage limits, economic data and, loading and generation conditions of this test system. It should be noted that, in this chapter, a revised version of the nodal voltage degradations consequent to nodal load growth rate was sought, based on the nodal P-V curves. These new nodal voltage degradation rates were employed to determine the improved LRIC-v network charges.

Firstly, to ensure that all nodes are within voltage limits, the power loadings along the respective nodal P-V curves of the IEEE 14 test system were increased arbitrarily, in steps of 3.5%, from initial loading levels, up to 14%. This assumption was adopted since all the buses remained within their voltage limits and the idea was to view how the nodal voltages considering the linear, piece-wise linear and quadratic approaches varied in comparison to the simulated results. Therefore, as a result, while performing the respective load increments, the resulting voltages due to the aforementioned quadratic, piecewise and linear curves were noted. Thereafter, the aforementioned voltages were compared to the simulated results, which were used as a benchmark, to establish the respective nodal percentage voltage errors. These percentage errors are shown in figures 8.2(a)-8.2(d). The nodal voltage degradation rates would be calculated from the curve that would offer a good compromise between accuracy and simplicity and, thereafter, these would be also used in determining the LRIC-v network charges.

Finally, to demonstrate the value of the improved LRIC-voltage network charges four cases have been used to show the effects to the network when connecting various demands and generations at each node. Case 1 involves a withdrawal of 1 MVAr at each node, case 2 involves a withdrawal of 1 MW at each node, case 3 involves an injection of 1 MVAr at each node and, finally, case 4 involves an injection of 1 MW at each node.

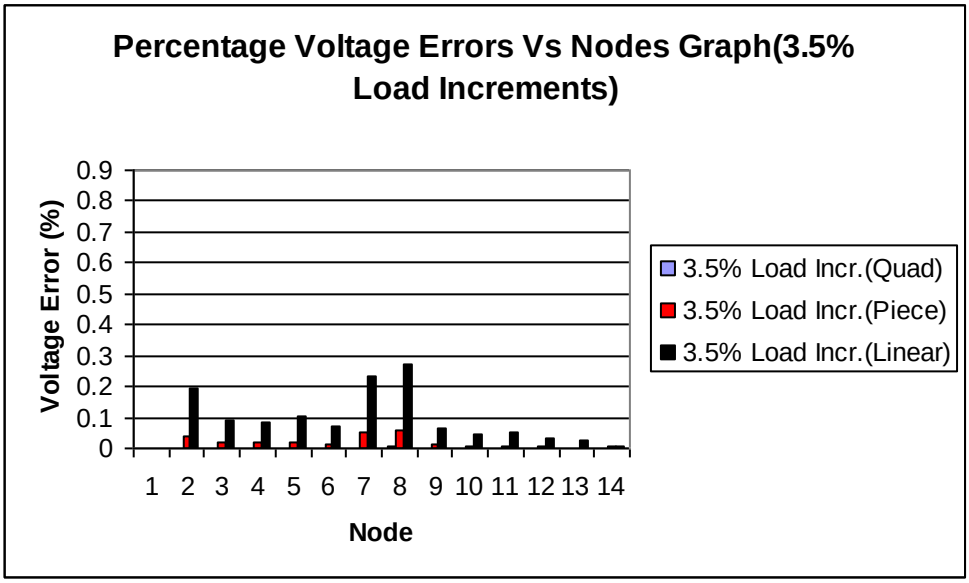

Figure 8.2(a): Percentage voltage errors against nodes graph due to 3.5% load increments on IEEE-14 bus test system

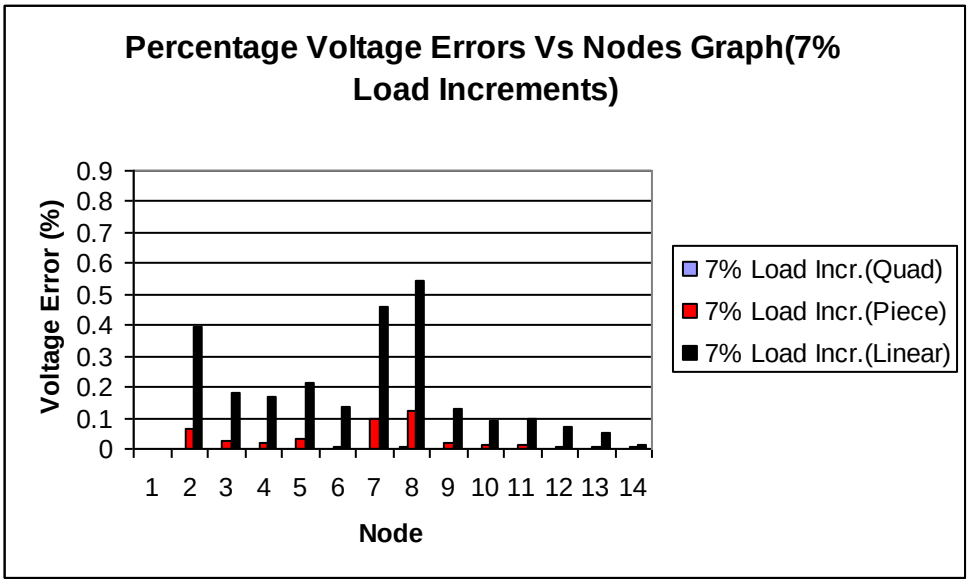

Figure 8.2(b): Percentage voltage errors against nodes graph due to 7% load increments on IEEE-14 bus test system

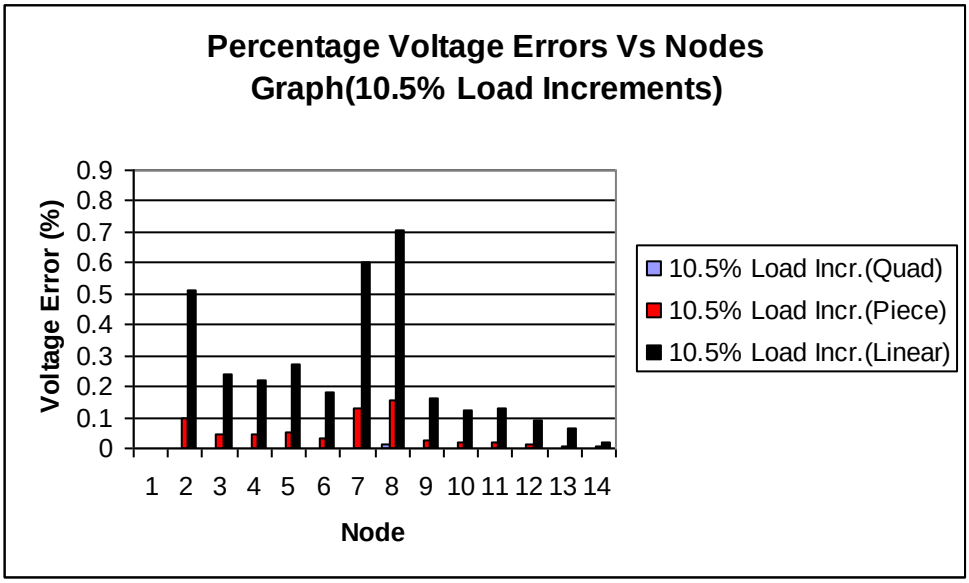

Figure 8.2(c): Percentage voltage errors against nodes graph due to 10.5% load increments on IEEE-14 bus test system

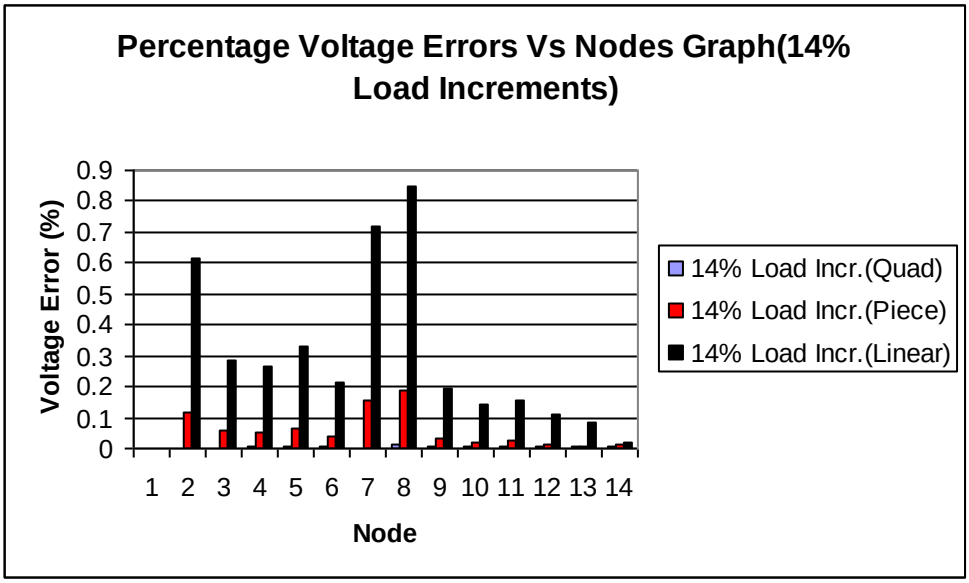

Figure 8.2(d): Percentage voltage errors against nodes graph due to 14% load increments on IEEE-14 bus test system

Figure 8.2: Illustration of the three approaches to approximate nodal voltage changes consequent upon the nodal power increment.

The results in figures 8.2(a)-8.2(d), show that the nodal voltage changes closely follow the PV curves since percentage voltage errors as a result of the quadratic function are all very small. Then follows the piece-wise linear curves in terms of being the second best with regard to bus voltage percentage errors and with linear curves offering the worst voltage errors. The voltage percentage errors, across all the cases, are significant at buses 8, 7 and

2 since their initial voltages were 1.048 pu, 1.008 pu and 1.006 pu, respectively. This latter observation is due to the fact that, the less closer the initial bus voltages to the lower bus limit, the more the error during load increments. On the other hand, the closer the initial bus voltages to the lower bus limit the less the percentage voltage errors. It is against this latter background that the initial voltage at bus 14 was 0.954 pu which is closer to the lower bus voltage limit, 0.94 pu. Further, the results show that piecewise linear function provides the second best approximation to the nodal voltage changes while the linear function provides the worst approximation. This is backed by the fact that, during 3.5% load increment, the percentage voltage error at bus 8 is 0.0125, 0.05 and 0.28 for piecewise linear, linear and quadratic functions, respectively. These errors keep on increasing following that pattern owing to the load increments, for these respective functions, such that during 14% load increments the errors became 0.025%, 0.2% and 0.84% for piecewise linear, linear and quadratic functions, respectively. This shows that, the percentage voltage errors increased as the load deviated, increasing from the initial loading level to 14% load increments. It should be notes across all cases, bus 1 registered 0% voltage errors for all the functions since the voltage at this bus does not change because this bus is the slack bus. Also, it should be noted that, the rest of the buses other than buses 2, 7 and 8 have their initial voltages less than 1 pu, hence, they have less percentage voltage errors than buses 2, 7 and 8. Since the piecewise linear function offers a good compromise between accuracy and simplicity, it would be used as a reasonable approximation in determining the nodal voltage degradation rates given the load growth rates and, consequently those would be used to calculate the nodal LRIC-voltage network charges in the next phase as earlier stated.

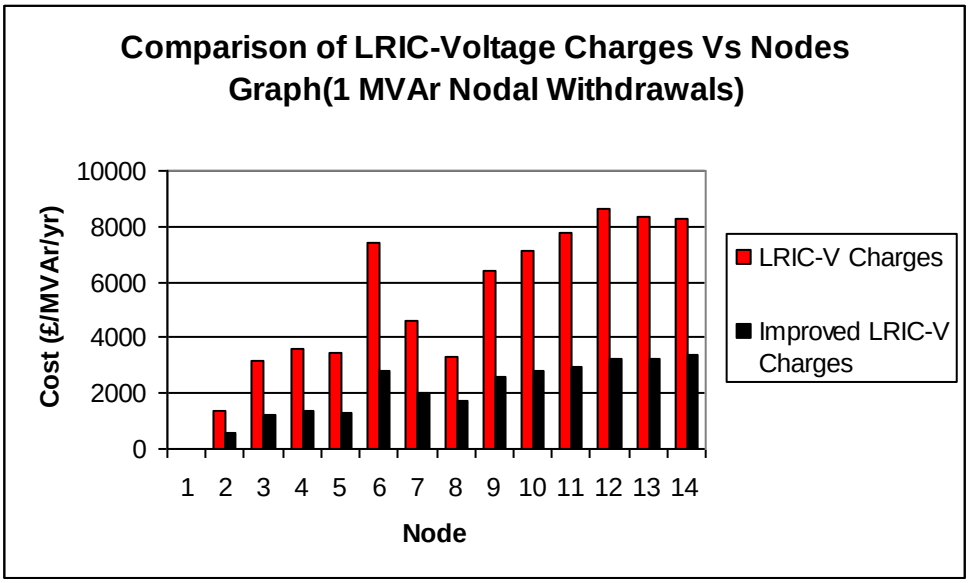

Figure 8.3: Comparison of LRIC-v and Improved LRIC-v network charges due to 1 MVAr nodal withdrawals on the IEEE 14 bus test system.

Figure 8.3 shows LRIC-v and Improved LRIC-v network charges for each node of the IEEE-14 bus test system.

It can be observed that, the Improved LRIC-v charges follow the same pattern as the previously computed LRIC-v charges. The only difference is that, the improved LRIC-v charges are less than the original at every node since the nodal voltage degradation rates

for the improved version are smaller in better approximating the PV curve. From the results it can be concluded that, the more accurate nodal voltage degradation rates derived from better PV approximations would give smaller LRIC-v charges for this system at this particular initial network loading level.

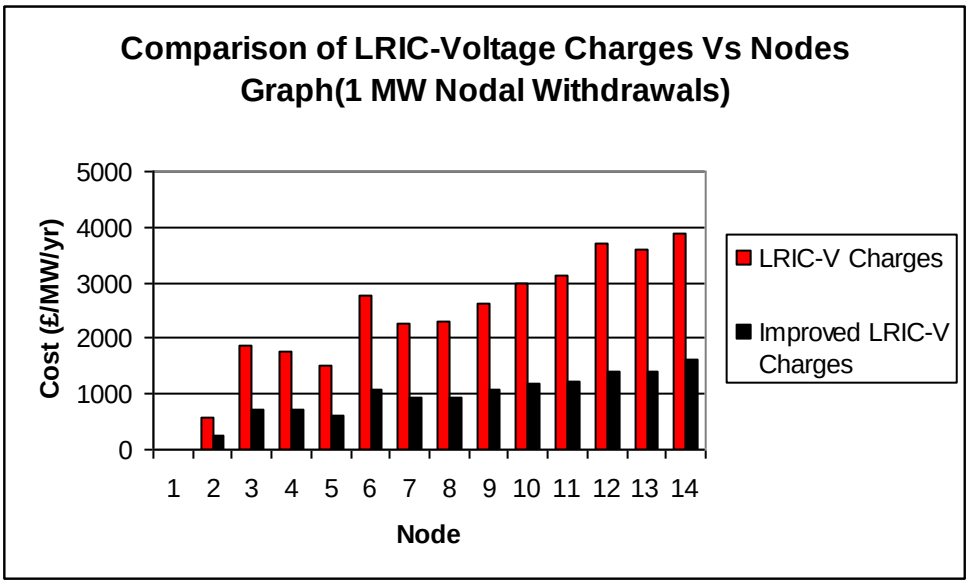

Figure 8.4: Comparison of LRIC-v and Improved LRIC-V network charges due to 1 MW nodal withdrawals on the IEEE 14 bus test system.

During 1 MW nodal withdrawals, it can also be observed from figure 8.4, that the Improved LRIC-v network charges follow the same pattern as the LRIC-v network charges. Again, the LRIC-v charges are higher than those of the improved version since the nodal voltage degradation rates are less than the corresponding nodal rates of the improved version.

It should be noted, as was established in chapter 4, that the charges for 1 MVAr nodal withdrawals are higher that those of the corresponding 1 MW nodal withdrawals since the network's circuit reactances are larger than its corresponding resistances.

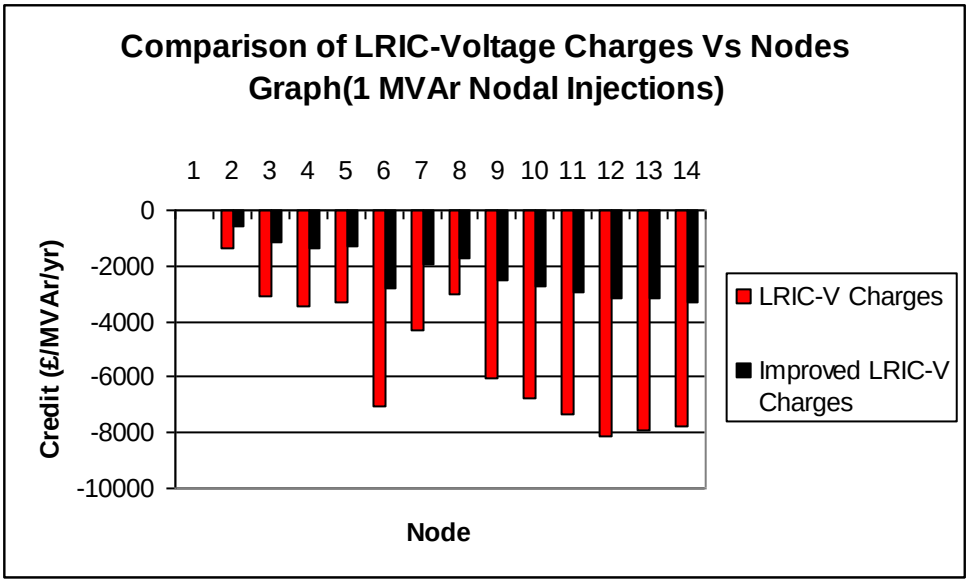

Figure 8.5: Comparison of LRIC-v and Improved LRIC-v network charges due to 1 MVAr nodal injections on the IEEE 14 bus test system.

During 1 MVAr nodal injections, it can also be observed from figure 8.5, that the Improved LRIC-v network credits follow the same pattern as the LRIC-v network credits. Again, the LRIC-v charges are more than those of the improved version since the nodal voltage degradation rates are less than the corresponding nodal rates of the improved version.

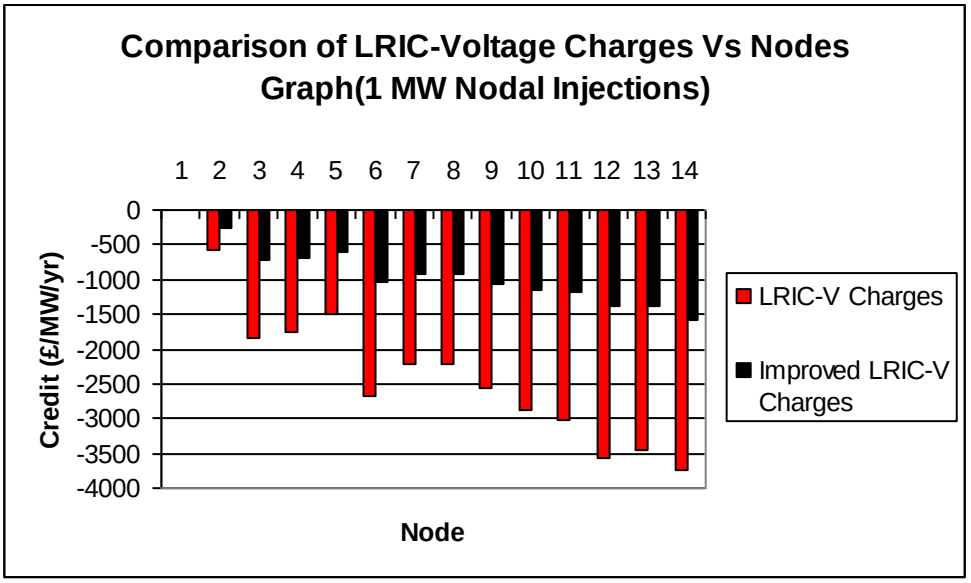

Figure 8.6: Comparison of LRIC-v and Improved LRIC-v network charges due to 1 MW nodal injections on the IEEE 14 bus test system.

During 1 MW nodal injections, it can also be observed from figure 8.6, that the Improved LRIC-v network credits follow the same pattern as the LRIC-v network credits. Again, the

LRIC-v charges are more than those of the improved version since the nodal voltage degradation rates are less than the corresponding nodal rates of the improved version.

It should be noted that, as was established in chapter 4, that the credits for 1 MVAr nodal injections are more that those of the corresponding 1 MW nodal injections since the respective network circuit reactances are more than the corresponding network circuit resistances.

8.3.2 Practical Distribution System

As explained earlier, this particular test system was introduced in chapter 4 and used in the chapters that followed, thereafter. As in the last section, this section aims to illustrate the voltage error for approximating the nodal PV curve from the three approaches, namely, quadratic, linear and piece-wise linear functions. This is followed by the charges comparison between the enhanced busbar voltage degrading rate and the original linear approximation.

In this subsection, to ensure that all the nodes are within their respective voltage limits, the power loadings along the respective nodal P-V curves of this practical test system were increased in steps 2.5%, from initial loading levels, up to 10%. Also, this assumption was motivated by the fact that all the nodal voltages remained within their respective limits as the busbar loading was varied as indicated. In addition, while performing the respective load increments, the resulting voltages due to the aforementioned quadratic, piecewise and linear curves were noted. Thereafter, the aforementioned voltages were compared to the simulated results, which were used as a benchmark, to establish the respective nodal percentage voltage errors. These percentage errors are shown in tables 8.1(a)-8.1(d). The nodal voltage degradation rates would be calculated from the curve that would offer a good compromise between accuracy and simplicity and, thereafter, these would be also used in determining the Improved LRIC-v network charges.

Again, four distinct cases were utilized to demonstrate the value of the improved LRIC-voltage network charges to show the cost/benefit to the network when connecting various demands and generations at each node. Case 1 involves a withdrawal of 1 MVAr at each node, case 2 involves a withdrawal of 1 MW at each node, case 3 involves an injection of 1 MVAr at each node and, finally, case 4 involves an injection of 1 MW at each node. All theses cases are shown in tables 8.2-8.5, respectively.

Table 8.1 (a): Percentage voltage errors at each node resulting from 2.5% load increments on the Pembroke practical test system.

Bus	Linear % Volt. Error	PieceWise % Volt. Error	Quadratic % Volt. Error	Bus	Linear % Volt. Error	PieceWise % Volt. Error	Quadratic % Volt. Error	Bus	Linear % Volt. Error	PieceWise % Volt. Error	Quadratic % Volt. Error	Bus	Linear % Volt. Error	PieceWise % Volt. Error	Quadratic % Volt. Error
2005	0.111	0.039	0.000	3066	0.054	0.023	0.000	2021	1.300	0.090	0.003	2650	0.110	0.100	0.000
2015	0.097	0.030	0.006	3069	0.020	0.007	0.004	2025	0.067	0.028	0.000	2651	0.236	0.112	0.112
3003	0.068	0.029	0.000	3072	0.081	0.031	0.000	2026	0.054	0.023	0.000	5140	0.000	0.000	0.000
3006	0.019	0.007	0.002	3075	0.098	0.036	0.001	2027	0.054	0.023	0.000	5148	0.275	0.208	0.001
3009	0.056	0.024	0.000	3078	0.090	0.033	0.001	2030	0.374	0.209	0.002	5149	0.373	0.203	0.002
3012	0.012	0.003	0.003	3081	0.062	0.026	0.000	2031	0.415	0.200	0.002	5150	0.258	0.215	0.001
3015	0.077	0.032	0.000	3084	0.012	0.003	0.003	2032	0.515	0.198	0.000	5151	0.000	0.000	0.000
3018	0.017	0.006	0.002	3087	0.070	0.029	0.000	2033	0.561	0.191	0.000	5152	0.000	0.000	0.000
3021	0.080	0.031	0.000	3090	0.037	0.015	0.002	2035	0.107	0.037	0.000	5153	0.269	0.074	0.001
3024	0.110	0.040	0.000	3093	0.063	0.027	0.000	2036	0.412	0.134	0.134	5154	0.270	0.074	0.001
3027	0.097	0.035	0.001	** 3096	**0.008**	**0.003**	**0.001**	2037	0.853	0.070	0.000	20251	0.240	0.054	0.001
3030	0.082	0.031	0.001	3099	0.090	0.033	0.002	2040	0.397	0.190	0.001	20262	0.220	0.034	0.001
3033	0.091	0.035	0.000	3102	0.019	0.006	0.003	2041	0.541	0.162	0.001	20351	0.412	0.134	0.134
3036	0.090	0.032	0.002	3105	0.011	0.006	0.001	2045	0.112	0.035	0.000	20352	0.412	0.134	0.134
3039	0.079	0.030	0.002	20051	0.469	0.151	0.151	2046	0.104	0.100	0.000	20373	0.086	0.080	0.000
3042	0.055	0.023	0.000	20052	0.469	0.151	0.151	2047	0.110	0.034	0.001	20374	0.086	0.080	0.000
3045	0.027	0.011	0.001	20151	0.569	0.251	0.171	2048	0.110	0.034	0.001	20451	0.069	0.040	0.000
3048	0.113	0.045	0.000	20152	0.569	0.251	0.171	2620	2.351	0.099	0.006	20472	0.066	0.050	0.000
3051	0.024	0.010	0.000	2000	0.839	0.110	0.006	2621	3.417	0.096	0.006				
3054	0.059	0.025	0.000	2001	0.317	0.159	0.006	2630	0.441	0.091	0.016				
3057	0.041	0.015	0.004	2010	0.814	0.080	0.006	2631	0.844	0.113	0.005				
3060	0.056	0.024	0.000	2011	0.875	0.080	0.006	** 2640	**5.847**	**0.092**	**0.007**				
3063	0.018	0.006	0.003	2020	3.122	0.090	0.007	2641	1.785	0.093	0.003				

Table 8.1 (b): Percentage voltage errors at each node resulting from 5% load increments on the Pembroke practical test system.

Bus	Linear % Volt. Error	PieceWise % Volt. Error	Quadratic % Volt. Error	Bus	Linear % Volt. Error	PieceWise % Volt. Error	Quadratic % Volt. Error	Bus	Linear % Volt. Error	PieceWise % Volt. Error	Quadratic % Volt. Error	Bus	Linear % Volt. Error	PieceWise % Volt. Error	Quadratic % Volt. Error
2005	0.221	0.078	0.000	3066	0.107	0.046	0.000	2021	2.601	0.181	0.006	2650	0.221	0.201	0.014
2015	0.193	0.060	0.012	3069	0.040	0.014	0.009	2025	0.135	0.055	0.014	2651	0.472	0.225	0.224
3003	0.136	0.057	0.000	3072	0.162	0.063	0.000	2026	0.109	0.046	0.006	5140	0.000	0.000	0.000
3006	0.039	0.014	0.005	3075	0.195	0.071	0.001	2027	0.109	0.046	0.000	5148	0.550	0.415	0.003
3009	0.112	0.048	0.000	3078	0.179	0.066	0.002	2030	0.747	0.418	0.003	5149	0.746	0.407	0.004
3012	0.024	0.006	0.006	3081	0.124	0.053	0.001	2031	0.830	0.401	0.003	5150	0.515	0.431	0.001
3015	0.155	0.065	0.000	3084	0.024	0.006	0.005	2032	1.030	0.396	0.001	5151	0.000	0.000	0.000
3018	0.034	0.011	0.005	3087	0.140	0.058	0.000	2033	1.122	0.382	0.001	5152	0.000	0.000	0.000
3021	0.159	0.062	0.000	3090	0.074	0.029	0.004	2035	0.214	0.075	0.001	5153	0.538	0.148	0.003
3024	0.220	0.081	0.005	3093	0.126	0.054	0.000	2036	0.825	0.268	0.268	5154	0.540	0.149	0.003
3027	0.195	0.069	0.002	** 3096	**0.017**	**0.005**	**0.003**	2037	1.705	0.140	0.000	20251	0.480	0.109	0.003
3030	0.164	0.062	0.001	3099	0.180	0.065	0.003	2040	0.794	0.380	0.001	20262	0.440	0.069	0.002
3033	0.181	0.070	0.003	3102	0.037	0.012	0.006	2041	1.083	0.324	0.001	20351	0.825	0.268	0.268
3036	0.180	0.064	0.004	3105	0.022	0.011	0.002	2045	0.223	0.071	0.001	20352	0.825	0.268	0.268
3039	0.159	0.059	0.003	20051	0.938	0.303	0.302	2046	0.209	0.201	0.002	20373	0.173	0.161	0.000
3042	0.109	0.047	0.004	20052	0.938	0.303	0.302	2047	0.219	0.069	0.001	20374	0.173	0.161	0.088
3045	0.054	0.022	0.003	20151	1.138	0.503	0.342	2048	0.219	0.069	0.001	20451	0.139	0.081	0.000
3048	0.225	0.091	0.000	20152	1.138	0.503	0.342	2620	4.702	0.198	0.012	20472	0.133	0.101	0.000
3051	0.049	0.021	0.003	2000	1.678	0.220	0.012	2621	6.834	0.193	0.012				
3054	0.119	0.050	0.000	2001	0.635	0.319	0.011	2630	0.882	0.183	0.032				
3057	0.083	0.030	0.008	2010	1.627	0.159	0.012	2631	1.689	0.226	0.010				
3060	0.111	0.047	0.000	2011	1.750	0.161	0.012	** 2640	**11.694**	**0.184**	**0.013**				
3063	0.037	0.012	0.007	2020	6.245	0.180	0.013	2641	3.570	0.186	0.006				

Table 8.1 (c): Percentage voltage errors at each node resulting from 7.5% load increments on the Pembroke practical test system.

Bus	Linear % Volt. Error	PieceWise % Volt. Error	Quadratic % Volt. Error	Bus	Linear % Volt. Error	PieceWise % Volt. Error	Quadratic % Volt. Error	Bus	Linear % Volt. Error	PieceWise % Volt. Error	Quadratic % Volt. Error	Bus	Linear % Volt. Error	PieceWise % Volt. Error	Quadratic % Volt. Error
2005	0.332	0.118	0.000	3066	0.161	0.069	0.000	2021	3.901	0.271	0.009	2650	0.331	0.301	0.021
2015	0.290	0.090	0.018	3069	0.060	0.021	0.013	2025	0.202	0.083	0.021	2651	0.708	0.337	0.337
3003	0.203	0.086	0.000	3072	0.242	0.094	0.000	2026	0.163	0.069	0.009	5140	0.000	0.000	0.000
3006	0.058	0.020	0.007	3075	0.293	0.107	0.002	2027	0.163	0.069	0.000	5148	0.824	0.623	0.004
3009	0.168	0.072	0.000	3078	0.269	0.099	0.002	2030	1.121	0.627	0.005	5149	1.119	0.610	0.006
3012	0.036	0.010	0.008	3081	0.185	0.079	0.002	2031	1.245	0.601	0.005	5150	0.773	0.646	0.002
3015	0.232	0.097	0.000	3084	0.036	0.010	0.008	2032	1.545	0.594	0.001	5151	0.000	0.000	0.000
3018	0.051	0.017	0.007	3087	0.211	0.087	0.000	2033	1.683	0.573	0.001	5152	0.000	0.000	0.000
3021	0.239	0.093	0.000	3090	0.111	0.044	0.006	2035	0.321	0.112	0.001	5153	0.807	0.223	0.004
3024	0.330	0.121	0.008	3093	0.189	0.080	0.000	2036	1.237	0.402	0.401	5154	0.809	0.223	0.004
3027	0.292	0.104	0.004	* 3096	**0.025**	**0.008**	**0.004**	2037	2.558	0.210	0.000	20251	0.719	0.163	0.004
3030	0.246	0.093	0.002	3099	0.269	0.098	0.005	2040	1.191	0.570	0.002	20262	0.659	0.103	0.003
3033	0.272	0.105	0.004	3102	0.056	0.018	0.010	2041	1.624	0.486	0.002	20351	1.237	0.402	0.401
3036	0.269	0.097	0.006	3105	0.032	0.017	0.003	2045	0.335	0.106	0.002	20352	1.237	0.402	0.401
3039	0.238	0.089	0.005	20051	1.408	0.454	0.453	2046	0.313	0.301	0.002	20373	0.259	0.241	0.000
3042	0.164	0.070	0.006	20052	1.408	0.454	0.453	2047	0.329	0.103	0.002	20374	0.259	0.241	0.133
3045	0.081	0.032	0.004	20151	1.708	0.754	0.513	2048	0.329	0.103	0.002	20451	0.208	0.121	0.000
3048	0.338	0.136	0.000	20152	1.708	0.754	0.513	2620	7.053	0.296	0.018	20472	0.199	0.151	0.000
3051	0.073	0.031	0.005	2000	2.517	0.330	0.018	2621	10.251	0.289	0.017				
3054	0.178	0.075	0.000	2001	0.952	0.478	0.017	2630	1.323	0.274	0.048				
3057	0.124	0.046	0.012	2010	2.441	0.239	0.018	2631	2.533	0.339	0.016				
3060	0.167	0.071	0.000	2011	2.625	0.241	0.018	** 2640	**17.541**	**0.276**	**0.020**				
3063	0.055	0.017	0.010	2020	9.367	0.270	0.020	2641	5.356	0.278	0.009				

Table 8.1 (d): Percentage voltage errors at each node resulting from 10% load increments on the Pembroke practical test system.

Bus	Linear % Volt. Error	PieceWise % Volt. Error	Quadratic % Volt. Error	Bus	Linear % Volt. Error	PieceWise % Volt. Error	Quadratic % Volt. Error	Bus	Linear % Volt. Error	PieceWise % Volt. Error	Quadratic % Volt. Error	Bus	Linear % Volt. Error	PieceWise % Volt. Error	Quadratic % Volt. Error
2005	0.431	0.153	0.000	3066	0.209	0.089	0.000	2021	5.071	0.352	0.011	2650	0.431	0.392	0.027
2015	0.377	0.118	0.023	3069	0.077	0.028	0.017	2025	0.263	0.108	0.027	2651	0.920	0.438	0.438
3003	0.264	0.112	0.000	3072	0.315	0.122	0.000	2026	0.212	0.090	0.012	5140	0.000	0.000	0.000
3006	0.076	0.026	0.010	3075	0.381	0.138	0.002	2027	0.212	0.090	0.000	5148	1.072	0.810	0.006
3009	0.218	0.093	0.000	3078	0.349	0.129	0.003	2030	1.457	0.815	0.006	5149	1.454	0.793	0.008
3012	0.047	0.013	0.011	3081	0.241	0.103	0.002	2031	1.618	0.782	0.006	5150	1.005	0.840	0.002
3015	0.302	0.126	0.000	3084	0.047	0.013	0.010	2032	2.009	0.772	0.001	5151	0.000	0.000	0.000
3018	0.067	0.022	0.009	3087	0.274	0.114	0.000	2033	2.188	0.745	0.002	5152	0.000	0.000	0.000
3021	0.310	0.122	0.000	3090	0.144	0.057	0.008	2035	0.417	0.146	0.001	5153	1.049	0.289	0.005
3024	0.429	0.157	0.010	3093	0.245	0.105	0.000	2036	1.608	0.523	0.522	5154	1.052	0.290	0.005
3027	0.380	0.135	0.005	* 3096	**0.032**	**0.010**	**0.005**	2037	3.326	0.274	0.000	20251	0.935	0.212	0.005
3030	0.320	0.121	0.003	3099	0.350	0.127	0.006	2040	1.548	0.741	0.002	20262	0.857	0.134	0.004
3033	0.354	0.136	0.005	3102	0.073	0.024	0.013	2041	2.112	0.632	0.003	20351	1.608	0.523	0.522
3036	0.350	0.126	0.007	3105	0.042	0.022	0.004	2045	0.436	0.138	0.002	20352	1.608	0.523	0.522
3039	0.309	0.115	0.006	20051	1.830	0.590	0.589	2046	0.407	0.392	0.003	20373	0.337	0.313	0.000
3042	0.213	0.091	0.008	20052	1.830	0.590	0.589	2047	0.428	0.134	0.003	20374	0.337	0.313	0.172
3045	0.105	0.042	0.006	20151	2.220	0.980	0.667	2048	0.428	0.134	0.003	20451	0.270	0.157	0.000
3048	0.439	0.177	0.000	20152	2.220	0.980	0.667	2620	9.169	0.385	0.023	20472	0.259	0.196	0.000
3051	0.095	0.040	0.006	2000	3.272	0.429	0.023	2621	13.327	0.376	0.022				
3054	0.232	0.098	0.000	2001	1.238	0.622	0.022	2630	1.719	0.357	0.063				
3057	0.161	0.059	0.016	2010	3.173	0.311	0.023	2631	3.293	0.441	0.020				
3060	0.217	0.092	0.000	2011	3.413	0.314	0.024	** 2640	**22.804**	**0.358**	**0.026**				
3063	0.071	0.023	0.013	2020	12.177	0.351	0.026	2641	6.962	0.362	0.011				

The results in tables 8.1(a)-8.1(d), show that the nodal voltage changes closely follow the PV curves since percentage voltage errors as a result of the quadratic function are all very small. The voltage percentage errors, across all the cases, are significant at bus 2640 (results in bolded font and bus number preceded by double asterisk) since its initial voltage was 1.02 pu. This latter observation is due to the fact that, the less closer the initial bus voltages to the lower bus limit, the more the error during load increments. On the other hand, the closer the initial bus voltages to the lower bus limit the less the percentage voltage errors. It is against this latter background that the initial voltage at bus 3096 (results in bolded font and bus number preceded by an asterisk) was 0.951 pu which is closer to the lower bus voltage limit. Further, the results show that piecewise linear function provides the second best approximation to the nodal voltage changes while the linear function provides the worst approximation. This is backed by the fact that, during 2.5% load increment, the percentage voltage error at bus 2640 was 5.847, 0.092 and 0.007 for piecewise linear, linear and quadratic functions, respectively. These errors keep on increasing following that pattern owing to the load increments, for these respective functions, such that during 10% load increments the errors became 22.804%, 0.358% and 0.026% for piecewise linear, linear and quadratic functions, respectively. Likewise, these kinds of errors increased at bus 3096. This shows that, the percentage voltage errors increased as the load deviated, increasing from the initial loading level to 10% load increments. Furthermore, the percentage voltage errors increased as the load deviation increased from the initial loading level. It should be noted that, buses 5140, 5151 and 5152 registered 0% voltage errors since bus 5140 is the slack bus, therefore, its voltage does not change across all cases. While, on the other hand, buses 5151 and 5152 are less affected by load changes because they do not have load directly connected to them and also they are closer to the slack bus. Since the piecewise linear function offers a good compromise between accuracy and simplicity, it would be used as a reasonable approximation in determining the nodal voltage degradation rates given the load growth rates and, consequently those would be used to calculate the nodal LRIC-voltage network charges to provide an improved version of this charging methodology.

Table 8.2: Comparison of LRIC-v and Improved LRIC-V network charges due to 1 MVAr nodal withdrawals on the Pembroke practical test system.

Bus	Improved LRIC-V Charges (£/MVAr/yr)	LRIC-V Charges (£/MVAr/yr)	Bus	Improved LRIC-V Charges (£/MVAr/yr)	Base LRIC-V Charges (£/MVAr/yr)	Bus	Improved LRIC-V Charges (£/MVAr/yr)	LRIC-V Charges (£/MVAr/yr)	Bus	Improved LRIC-V Charges (£/MVAr/yr)	LRIC-V Charges (£/MVAr/yr)
2005	2323.29	2843.64	3066	5612.53	6633.58	2021	720.61	1269.07	2650	738.39	1271.68
2015	2189.65	2795.95	3069	4161.18	5053.04	2025	853.55	1379.12	2651	717.79	1267.56
3003	5374.7	6566.01	3072	2782.43	3100.48	2026	899.18	1425.73	5140	0	0
3006	5184.34	6394.27	3075	2482.95	2919.98	2027	899.21	1425.76	5148	602.33	1069.03
3009	4958.59	6008.73	3078	2510.17	2935.46	2030	584.31	1063.56	5149	602.4	1069.23
3012	4689.92	5745.4	3081	7475.22	9209.59	2031	596.29	1066.67	5150	601.72	1068.33
3015	4721.42	5898.11	3084	6436.83	8011.74	2032	583.3	1063.25	5151	0	0
3018	4693.49	5860.04	3087	3393.35	3939.08	2033	595.24	1066.34	5152	0	0
3021	2521.75	3029.79	3090	3193.36	3762.26	2035	500.17	1050.86	5153	265.29	516.98
3024	2280	2868.71	3093	5598.11	6763.53	2036	500.15	1050.85	5154	264.75	517.06
3027	2220.77	2812.24	3096	5178.05	6367.47	2037	592.35	1070.05	20251	909.76	1450.9
3030	2328.73	2885.6	3099	2318.77	2880.05	2040	708.61	1227.53	20262	963	1506.14
3033	2494.9	3027.7	3102	5179.05	6388.06	2041	740.95	1270.02	20351	679.97	1346.27
3036	2282.58	2849.49	3105	4746.11	5809.63	2045	879.88	1320.08	20352	679.97	1346.27
3039	2359.92	2903.78	20051	2352.79	2877.57	2046	879.9	1320.09	20373	776.35	1345.58
3042	3918.01	4495.97	20052	2392.24	2922.22	2047	890.22	1333.73	20374	775.93	1344.86
3045	3496	4088.92	20151	2238.04	2854.32	2048	890.24	1333.74	20451	944.98	1398.7
3048	4865.67	6275.63	20152	2254.53	2874.29	2620	744.96	1269.96	20472	955.44	1412.5
3051	5273.02	6660.56	2000	720.52	1226.68	2621	745.79	1270.95			
3054	3944.67	4486.25	2001	641	1116.22	2630	743.89	1270.58			
3057	3042.32	3584.32	2010	959.23	1495.86	2631	711.61	1227.89			
3060	3689.03	4538.01	2011	942.16	1488.68	2640	738.35	1271.62			
3063	3394.75	4208.93	2020	737.33	1271.88	2641	721.14	1268.4			

Table 8.2 shows the LRIC-v and Improved LRIC-v network charges following 1 MVAr nodal withdrawals. It should be noted that the LRIC-v network charges for this test network were established in chapter 4. What set apart the LRIC-v and Improved LRIC-v network charges is the manner in which the nodal voltage degradation rates were determined owing to network load growth rate. Other parameters, as expressed in chapter 4, remain equal. For the LRIC-v network charges, first, the nodal voltages before and after load increments were noted and, thereafter, the respective nodal voltage degradation rates were calculated. While for the Improved LRIC-v network charges, the respective nodal voltage degradation rates were based on the piecewise linear formulation along the respective nodal P-V curves detailed in section 8.2. The aforementioned piecewise formulation provided a good compromise between accuracy and simplicity, as shown in the earlier part of results in this subsection.

As can be observed in table 8.2, the Improved LRIC-v charges follow the same pattern as the previously computed LRIC-v charges. The only difference is that, the latter is more than the former at every node since the nodal voltage degradation rates for the latter are less than those of the former. This is consequent to the fact that the final nodal voltages, resulting from 1.6% system load growth rate, are more for the LRIC-v network charge case than the other case. It should be noted that the initial nodal voltages, before the system loads are increased at a rate of 1.6%, are equal. Therefore, it can be concluded that, the more nodal voltage degradation rates the less are the LRIC-v charges for this system at this particular initial network loading level.

Table 8.3: Comparison of LRIC-v and Improved LRIC-V network charges due to 1 MW nodal withdrawals on the Pembroke practical test system.

Bus	Improved LRIC-V Charges (£/MW/yr)	LRIC-V Charges (£/MW/yr)	Bus	Improved LRIC-V Charges (£/MW/yr)	LRIC-V Charges (£/MW/yr)	Bus	Improved LRIC-V Charges (£/MW/yr)	LRIC-V Charges (£/MW/yr)	Bus	Improved LRIC-V Charges (£/MW/yr)	LRIC-V Charges (£/MW/yr)
2005	394.84	507.81	3066	2902.51	3471.09	2021	97.25	187.64	2650	103.36	186.6
2015	311.43	453.33	3069	1913.71	2314.88	2025	211.37	375.74	2651	95.47	185.86
3003	3222.92	3961.97	3072	700.33	758.86	2026	251.14	445.2	5140	0	0
3006	2831.51	3489.16	3075	492.17	566.54	2027	251.17	445.25	5148	44.66	85.38
3009	3139.25	3835.05	3078	590.55	613.19	2030	38.48	84.56	5149	44.67	85.41
3012	2479.56	3030.16	3081	4758.87	5881.11	2031	41.21	84.61	5150	44.61	85.3
3015	2924.44	3672.85	3084	3839.63	4756.23	2032	38.49	84.58	5151	0	0
3018	2504.92	3145.47	3087	1491.82	1712.88	2033	41.22	84.63	5152	0	0
3021	740.4	926.77	3090	1133.11	1293.92	2035	80.57	172.78	5153	12.95	26
3024	615.43	801.02	3093	3534.21	4327.63	2036	80.57	172.78	5154	12.97	26.03
3027	361.49	491.56	3096	2890.84	3544.78	2037	44.51	93.28	20251	241.69	425.64
3030	451.07	564.13	3099	427.65	548.85	2040	86.65	157.06	20262	283.53	497.53
3033	748.9	941.52	3102	2823.38	3479.42	2041	101.76	179.65	20351	149.08	324.76
3036	396.19	528.08	3105	2489.3	3038.47	2045	108.04	180.66	20352	149.08	324.76
3039	464.5	581.38	20051	418.92	537.54	2046	108.04	180.67	20373	123.05	239.33
3042	1870.06	2114.41	20052	447.8	573.19	2047	110.35	183.81	20374	122.87	239
3045	1510.19	1701.16	20151	346.8	499.75	2048	110.36	183.81	20451	138.32	227.45
3048	3518.42	4488.24	20152	357.9	514.3	2620	103.98	180.03	20472	140.94	231.03
3051	2859.96	3631.54	2000	98.87	163.82	2621	104.01	180.1			
3054	1689.86	1922.21	2001	62.83	109.34	2630	103.13	179.93			
3057	967.17	1109.92	2010	197.67	288.2	2631	87.9	157.02			
3060	1961.96	2429.75	2011	187.03	280.91	2640	103.33	186.54			
3063	1454.3	1806.69	2020	103.19	187.54	2641	96.97	186.21			

During 1 MW nodal withdrawals, it can also be observed from table 8.3, that the Improved LRIC-v network charges follow the same pattern as the LRIC-v network charges. Again, the LRIC-v charges are more than those of the improved version since the nodal voltage degradation rates are less than the corresponding nodal rates of the improved version.

It should be noted that, as was established in chapter 4, that the charges for 1 MVAr nodal withdrawals are more that those of the corresponding 1 MW nodal withdrawals since the respective network circuit reactances are more than the corresponding network circuit resistances.

Table 8.4: Comparison of LRIC-v and Improved LRIC-V network charges due to 1 MVAr nodal injections on the Pembroke practical test system.

Bus	Improved LRIC-V Charges (£/MVAr/yr)	LRIC-V Charges (£/MVAr/yr)	Bus	Improved LRIC-V Charges (£/MVAr/yr)	LRIC-V Charges (£/MVAr/yr)	Bus	Improved LRIC-V Charges (£/MVAr/yr)	LRIC-V Charges (£/MVAr/yr)	Bus	Improved LRIC-V Charges (£/MVAr/yr)	LRIC-V Charges (£/MVAr/yr)
2005	-2089.61	-2602.09	3066	-3288.81	-4072.92	2021	-613.39	-1175.44	2650	-631.22	-1178.22
2015	-1861.58	-2479.5	3069	-3578.09	-4351.44	2025	-647.96	-1233.9	2651	-610.79	-1174.03
3003	-3811.39	-4801.13	3072	-2188.13	-2621.34	2026	-719.81	-1286.01	5140	0	0
3006	-3991.06	-4961.93	3075	-2201.31	-2641.74	2027	-719.83	-1286.03	5148	-529.76	-1003.88
3009	-3991.5	-4867.17	3078	-2217.31	-2647.94	2030	-510.79	-997.77	5149	-529.79	-1004.04
3012	-3963.14	-4844.7	3081	-3722.34	-4660.56	2031	-523.52	-1001.39	5150	-529.22	-1003.24
3015	-3550.08	-4467.4	3084	-4560.89	-5616.43	2032	-509.73	-997.42	5151	0	0
3018	-3724.85	-4660.03	3087	-2610.44	-3184.02	2033	-522.42	-1001.02	5152	0	0
3021	-2229.81	-2717.94	3090	-2767.45	-3311.93	2035	-398.65	-959.12	5153	-246.8	-499.05
3024	-1818.77	-2461.32	3093	-3899.66	-4889.21	2036	-398.63	-959.11	5154	-246.23	-499.09
3027	-1883.55	-2487.66	3096	-4239.48	-5191.26	2037	-516	-999.08	20251	-623.62	-1191.59
3030	-1962.5	-2537.33	3099	-1955.86	-2534.73	2040	-611.33	-1141.35	20262	-693.45	-1241.72
3033	-1801.04	-2407.29	3102	-3987.97	-4958.26	2041	-637.35	-1178.33	20351	-304.73	-801.37
3036	-1903.05	-2491.57	3105	-4001.34	-4885.2	2045	-751.91	-1209	20352	-304.73	-801.37
3039	-1972.75	-2539	20051	-2068.66	-2575.96	2046	-751.92	-1209	20373	-410.1	-840.98
3042	-2998.2	-3529.32	20052	-2044.14	-2545.87	2047	-760.11	-1220.82	20374	-410.19	-841.17
3045	-3004.7	-3545.23	20151	-1828.99	-2437.77	2048	-760.12	-1220.83	20451	-726.44	-1168.81
3048	-3021.26	-3593.66	20152	-1818.99	-2425.06	2620	-642.16	-1178.89	20472	-734.33	-1180.23
3051	-4023.27	-4987.73	2000	-628.67	-1144.41	2621	-642.86	-1179.75			
3054	-2473.34	-3010.14	2001	-563.28	-1046.42	2630	-640.7	-1179.19			
3057	-2684.69	-3202	2010	-828.11	-1377.13	2631	-614.79	-1142.06			
3060	-2720.98	-3414.05	2011	-810.71	-1370.06	2640	-631.25	-1178.27			
3063	-2829.46	-3522.7	2020	-629.55	-1178.17	2641	-614.41	-1175.08			

During 1 MVAr nodal injections, it can also be observed from table 8.4, that the Improved LRIC-v network credits follow the same pattern as the LRIC-v network credits. Again, the LRIC-v charges are more than those of the improved version since the nodal voltage degradation rates are less than the corresponding nodal rates of the improved version.

Table 8.5: Comparison of LRIC-v and Improved LRIC-V network charges due to 1 MW nodal injections on the Pembroke practical test system

Bus	Improved LRIC-V Charges (£/MW/yr)	LRIC-V Charges (£/MW/yr)	Bus	Improved LRIC-V Charges (£/MW/yr)	LRIC-V Charges (£/MW/yr)	Bus	Improved LRIC-V Charges (£/MW/yr)	LRIC-V Charges (£/MW/yr)	Bus	Improved LRIC-V Charges (£/MW/yr)	LRIC-V Charges (£/MW/yr)
2005	-381.9	-492.36	3066	-2352.83	-2789.93	2021	-92.34	-182.47	2650	-98.61	-181.48
2015	-293.02	-433.53	3069	-1751.21	-2105.67	2025	-189.76	-354.45	2651	-90.58	-180.67
3003	-2475.36	-3064.54	3072	-605.35	-657.49	2026	-225.2	-420.06	5140	0	0
3006	-2275.7	-2809.94	3075	-460.88	-532.39	2027	-225.23	-420.1	5148	-43.9	-84.45
3009	-2693.9	-3259.99	3078	-538.42	-564.15	2030	-37.57	-83.4	5149	-43.91	-84.48
3012	-2210.51	-2679.19	3081	-2983.9	-3675.4	2031	-40.4	-83.6	5150	-43.85	-84.37
3015	-2359.12	-2935.18	3084	-2804.88	-3440.04	2032	-37.57	-83.41	5151	0	0
3018	-2095.11	-2604.98	3087	-1330.22	-1529.26	2033	-40.4	-83.6	5152	0	0
3021	-688.12	-864.53	3090	-1071.74	-1215.77	2035	-74.15	-163.57	5153	-12.83	-25.79
3024	-547.37	-726.23	3093	-2816.17	-3447.69	2036	-74.15	-163.57	5154	-12.85	-25.81
3027	-336.78	-465.1	3096	-2473.51	-3014.8	2037	-40.85	-87.08	20251	-165.19	-308.18
3030	-421.37	-532.95	3099	-401.5	-520.85	2040	-83.19	-153.36	20262	-197.48	-371.21
3033	-629.06	-823.97	3102	-2270.17	-2803.2	2041	-97.43	-175.05	20351	-11.78	-17.63
3036	-368.19	-497.41	3105	-2213.43	-2681.66	2045	-99.68	-169.36	20352	-11.78	-17.63
3039	-433.52	-548.2	20051	-358.78	-463.7	2046	-99.68	-169.36	20373	33.34	54.73
3042	-1642.67	-1824.85	20052	-331.04	-429.32	2047	-101.78	-172.25	20374	33.17	54.42
3045	-1392.57	-1544.39	20151	-259.66	-389.24	2048	-101.78	-172.25	20451	-71.07	-124.16
3048	-2516.08	-3087.78	20152	-249.22	-375.38	2620	-99.82	-175.69	20472	-72.87	-126.63
3051	-2287.75	-2823.25	2000	-95.91	-160.57	2621	-99.85	-175.75			
3054	-1440.9	-1625.49	2001	-61.51	-107.81	2630	-98.91	-175.48			
3057	-919.68	-1050.58	2010	-189.14	-279.14	2631	-84.55	-153.48			
3060	-1634.09	-1988.32	2011	-178.65	-272.05	2640	-98.63	-181.54			
3063	-1276	-1554.26	2020	-98.41	-182.43	2641	-92.16	-181.15			

During 1 MW nodal injections, it can also be observed from table 8.5, that the Improved LRIC-v network credits follow the same pattern as the LRIC-v network credits. Again, the LRIC-v charges are more than those of the improved version since the nodal voltage degradation rates are less than the corresponding nodal rates of the improved version.

It should be noted that, as was established in chapter 4, that the credits for 1 MVAr nodal injections are more that those of the corresponding 1 MW nodal injections since the respective network circuit reactances are more than the corresponding network circuit resistances.

8.4 Chapter Conclusions

In this chapter, the improved version of the LRIC-v network charges is presented. This improvement emanates from the premise that the voltage change at a node and its nodal power (MVA) change are related to each other by the P-V curve. Consequently, the piecewise linear formulation provided a good compromise between accuracy and simplicity and, therefore, it was utilized to calculate the nodal voltage degradation rates resulting from the load growth rate and, finally, the Improved LRIC-v network charges were sought and compared to those of the earlier proposed LRIC-v network charging version. This formulation was once again tested on the IEEE 14 bus test system and on the practical 87-bus distribution test system developed, operated and maintained by Western Power Distribution (WPD) network.

The results show that improved LRIC-v network charges are less than the earlier computed LRIC-v network charges since the nodal voltage degradation rates for the latter are less than those of the former. This is consequent to the fact that the final nodal voltages, resulting from 1.6% system load growth rate, are more for the LRIC-v network charge case than the other case. It should be noted that the nodal voltages, before the system loads are increased at a rate of 1.6%, are equal. From the results it can be concluded that, the more nodal voltage degradation rates the less are the LRIC-v charges for this system at this particular initial network loading level. Moreover, this improved version provided best results since the charges were processed based on nodal voltage degradation rates calculated to reflect the correct physical relationship of the nodal voltages consequent to the system load growth rate.

Chapter 9

Conclusions and Future Work

Based upon the previous chapter discussions and the observations emanating from the case studies presented, conclusions are drawn. Ultimately, there would be some suggestions regarding the future work to extend this research work further and, as a result, make it more refined.

9.1 Conclusions

The current power industry environment entails that countries around the globe commit or set them in the process of introducing more competition into their power industry regimes. Upon moving from monopolies to competitive electricity markets, it was deemed imperative to ensure open access to transmission and distribution networks in an effort to promote effective competition in the electricity supply sector. In that regard, the charges for the use of network asset set by network companies are the central element in providing efficient economic signals for guiding the siting and sizing of oncoming demands and generators, and incentivizing the efficient use of these network assets. These network assets refer to lines, transformers, VAr compensation assets, protection assets, e.t.c.

In the UK and the rest of the world, there are many such economic use of network asset pricing approaches (network charging methodologies), for transmission and distribution networks, reflecting investment cost incurred in the network circuits and transformers to support real and reactive power flow, as mentioned in chapters 3 and 4. However, to reflect the investment cost for maintaining network voltages in network charges has received very little attention in network charges. Currently, power factor penalty approach is used to recover costs of operation, mainly generator fuel related cost, and does not provide for those of network VAr compensation assets for maintaining network voltages. This power factor penalty approach has been criticized by many researchers as it is not based on economic principle and, moreover, it is regarded as inconsistent and inadequate. Furthermore, with the increasing penetration of embedded generators (EGs) in the UK, there is a growing need to formulate pricing methodologies based on economic principle to ensure that network assets are effectively and efficiently utilised [6]. Since the existing approach does not provide correct economic efficient price signals, EGs may potentially locate at sites which may result in considerable network investment. Therefore, it is against this background that, this research work is directed to address this issue of recovering network costs associated with maintaining the network voltages. Therefore, Long-Run Incremental Cost (LRIC)-voltage network charging principle was proposed and it is one of the major contributions in this research work.

LRIC-v network charging principle is based on the use of spare nodal voltage capacity or headroom of an existing network voltages to provide time to invest in VAr compensation devices. The VAr compensation devices, in question, are particularly SVCs given the issue of encouraging EGs penetration into the network. EGs mainly are wind turbines and they introduce voltage variations into the network and, therefore, for smooth system operation fast acting SVCs would be ideal to be introduced [6, 22, 23, 24]. The LRIC-v network charging principle was at first proposed to price for the future network VAr compensation assets and extended until it became comprehensive to be able to price for the existing network VAr compensation assets, among others. The evolution of this proposed novel pricing methodology over the course of the research is as follows:

1. LRIC-Voltage Network Pricing Reflecting Future VAr Compensation Assets

Firstly, this approach was proposed utilizing network voltage variations to reflect the future network VAr compensation asset prices resulting from nodal withdrawals/injections [63]. The most attraction of this approach is that for the first time a method to evaluate long-run incremental cost is proposed based on the spare nodal voltage capacity of an existing network. The resulting network voltage charging model is able to provide locational forward-looking economic signals, reflecting the extent of the impact to busbar voltages by a connected party, i.e. whether they accelerate or delay the need for future network compensation devices. In the event of a network user accelerating the requirement for future network compensation assets, that user shall be penalized for that action. Otherwise, if the network user delays the requirement for future network compensation asset reinforcement(s), such a user shall be rewarded for that action. In addition, this approach considers both real and reactive power nodal withdrawals/injections. These economic messages will, in turn, influence generation/demand in order to minimize the cost of future investment in VAr compensation.

2. LRIC-Voltage Charges On The System With Different R/X Ratios

A fundamental study was performed to analyses the trend of LRIC-voltage network charges on different types of networks [77], providing insights into how charges would change with different network circuit resistance/reactance (R/X) ratios. The results showed that when the network circuit Xs are at least ten times more than their R counterparts, only MVAr nodal perturbations should be considered. When the network circuit Rs, on the other hand, are at least ten folds more than their Xs counterparts, then, only MW nodal perturbations should be considered. Finally, when the network circuit Xs and their corresponding Rs are comparable, both MVAr and MW nodal perturbations should be considered. In a nutshell, this meant that for transmission networks, only MVAr nodal perturbations should be considered while for distribution networks both MW and MVAr nodal perturbations should be considered.

3. How the LRIC-Voltage Network Charges Varies With Different Demand Load Growth

Another fundamental study was carried-out to analyse the trend of LRIC-voltage network charges on different demand load growths, providing insights into how charges would change given different demand load growths. The results showed that the LRIC-v network charges given different load growth rates are a function of the system nodal voltage loading levels. This means that, there is a nodal bus voltage loading threshold above which if most buses are loaded at in a power system, the least load growth rate would have more charges. On the other hand, below the aforementioned nodal voltage loading threshold and if most power system buses are involved, then the larger load growth rate would generate more charges.

4. LRIC-Voltage Network Pricing To Support Network Voltages Under N-1 Contingencies

The LRIC-voltage network pricing previously proposed was extended to consider n-1 contingencies, as it is a requirement that these types of contingencies should be considered to ensure acceptable network security and reliability. The investment cost-related pricing (ICRP) charging model [72] used in the UK, for recovering investment costs of network circuits and transformers, does not consider the network security requirement in their pricing model, but, it relies on post-processing through a full-contingency analysis to give an average security factor of 1.86 for all concerned network assets. On other works related to investment costs of circuits and transformers, authors of [65] demonstrated a simplistic approach to network security based on the assumption that reinforcement is required when a branch reaches 50% utilization. Authors of [66]-[73] considered the n-1 contingency analysis into their charging principles and all of these were for pricing of network circuits and transformers. In this regard, it was imperative to factor n-1 contingencies into the LRIC-v network charges. The results showed that the respective charges follow the same pattern as the original approach, but are increased since the nodal busbar voltage margins are reduced to accommodate n-1 contingencies. This, in turn, provides correct economic price signals since the network operators are required to operate their networks physically to accommodate n-1 contingencies.

5. LRIC-Voltage Network Pricing For Existing Network SVCs

The LRIC-voltage network pricing approach, for pricing future network SVCs, was extended to cover for pricing the existing network SVCs, where SVCs were installed in the network. The earlier proposed charging principle failed to price for the use of existing network SVCs since where these existing devices are sited the corresponding bus voltages do not vary. The reason why the bus voltage does not vary is because the existing network SVCs would be preset to keep the corresponding nodal voltages at constant values and, therefore, since the proposed LRIC-voltage charging principle depicted its strength upon the network voltage variations, this approach could not be applied in this regard. It is true that the reactive power loading of the SVC varies in keeping the bus voltage, where this device is sited, at a preset value given variations in power system demand and generation loading conditions. In this regard, this new extension involved the mapping of the SVCs' reactive power loading limits to the nodal voltage limits at the buses where these SVCs' are sited. For example, if the SVC reactive power lower and upper limits are $Q_{\min}$ and $Q_{\max}$, respectively and, on the other hand, if the nodal voltage lower and upper limits, where this SVC is sited, are V_L and V_H, respectively. To that end, $Q_{\min}$ was mapped to V_L while $Q_{\max}$ was mapped to V_H. With this limit mapping exercise completed, then, it was possible to price for the use of the existing network SVCs.

6. Improved Implementation For LRIC-Voltage Network Charges

This entails an improved version of the LRIC-v network charges. This improvement emanates from the premise that the voltage change at a node and its corresponding power (MVA) change are related to each other by the P-V curve. As such, the best approximation of this relationship was used to execute the nodal voltage degradation rates resulting from

the load growth rate and, finally, the improved LRIC-v network charges were sought. In the earlier proposed basic LRIC-v network charging approach, the respective nodal voltage degradation rates were computed by noting the nodal voltages before and after annual network load growth and fixed these nodal voltage degradation rates to signify the constant rates at which the voltage would be varied from the current voltage levels down to the respective nodal voltage limits. This improved version resulted in processing the charges based on nodal voltage degradation rates calculated to reflect the correct physical relationship of the nodal voltages consequent to the system load growth rate.

Overall, LRIC-v network charging principle is intended to allocate the network VAr asset costs based on the usage of the network nodal voltage capacities from study nodes. It achieves this by evaluating the future network VAr compensation asset investment requirements and fairly allocates the future network VAr compensation costs to users. The strong points of the LRIC-v network charging principle incorporate the ability to reflect the forward-looking charges, to distinguish the charges at different locations, to consider both real and reactive powers, and to derive charges for both demand and generation users.

Finally, the LRIC-v network charging approach appeal to all stakeholders, namely, network owners, and network demand and generation users. From the perspective of network owners, it can reduce the future VAr compensation asset costs while at the same time improving the overall network voltage profile. From the perspective of demand and generation users, it can provide the lowest possible use of system charges. Moreover, the reduced electricity prices for the end consumers.

9.2 Future Work

In this section, some fundamental extensions to the work done in this thesis shall be recommended to ensure that the developed work can be more suitable in real world network charging methodologies. Those shall be briefly expressed, each in turn, below.

1. The use of electrical distance concept for effective voltage control

Given the densely meshed nature of the power networks nowadays and the recent voltage problems in a number of power network establishments, it is apparent that to solve the voltage problem, the concerned network ought to be divided into voltage control zones as explained in Appendix A. This approach entails the use of electrical distance concept to identify effective distinct network voltage control zones to independently master the voltage control in each zone as need arises. What set apart this approach from the rest, is that, it deals with the physical structure of the network as opposed to the trial and error method entailed in the conventional approaches. In Appendix A, a rigorous literature review was undertaken and, as a result, the use of electrical distance concept complimented by GA, as the decision-making tool, was found to be the most attractive integrated framework given the aforementioned current power industry conditions, for the siting of

SVCs to achieve an overall effective network voltage control. Therefore, this approach should be ventured into and, thereafter, all possible contingencies should be considered to ensure the proper sizing of the SVCs, which would constitute the whole exercise of RPP process.

2. Interaction between thermal and voltage network charges

The upgrading of the network consequent to either power withdrawal / injection can be dealt with by either constructing a new line / installing a transformer (resulting from LRIC-thermal network charges) or installing a reactive power compensation device (resulting from LRIC-voltage network charges). It should be noted that this exercise can also, at times, be achieved by either installing a higher rating of any of the aforementioned devices. Both of these approaches, in turn, can improve the overall network circuit power carrying capacity and its voltage profile. In this regard, a comprehensive spot-on interaction between these two approaches has to be established to strike a balance between cost effectiveness and the most effective way to ensure network security and reliability as per statutory requirement. Therefore, it is against this background that, a rigorous study has to be instituted to establish this aforementioned interaction between thermal and voltage network charges.

3. Improving more the LRIC-voltage network charges

The load growth was assumed to be 1.6% in determining the LRIC-V charges. This factor compromise the accuracy of the charges as in reality different buses have different load growths. In future if the respective load at every load bus can be sought then the charges can be more accurate. Ultimately, this would institute some accuracy in the LRIC-voltage network charges.

4. Proper selection of the slack bus

It is recommended that before the LRIC-voltage network charges can be evaluated for any given network, the correct location of the slack bus should be established to represent the physical reality of the concerned particular network relating to the same. LRIC-voltage network charges are different at every different slack bus position on any chosen network, therefore if the slack bus is wrongly placed, incorrect economic signals would be sought and those would not be reflective of the situation on the ground.

5. Factoring n-2 contingencies into the LRIC-voltage network charging approach

In this research work the network security is assessed given n-1 circuit contingencies. This means that each circuit is outaged and replaced back in its intact state, each in turn, to ensure that the network can withstand this kind of situation. Specifically, the effective network nodal voltage limits are established given the worst possible n-1 circuit contingency to ensure that the proper network nodal voltage ranges are established in order to evaluate the correct LRIC-voltage network charges which reflect the aforementioned contingency scenario. This emanates from the fact that, in reality, the network is expected

to be able to withstand this kind of contingency scenario to ensure that voltage instability is not experienced. Given the aforementioned, this contingency situation should be reflected in the LRIC-voltage network charges. On the other hand, P2/6 involves the assessment of the system security contribution from distributed generation given n-1 and n-2 circuit outages. The latter outage situation involves removing any two network circuits at a time and replacing them back, in turn, while assessing the concerned system security contribution from the distributed generation. Since in the UK, the government made commitment to encourage the distributed generations to connect onto the system, then it would suitable to factor into the n-2 circuit contingency situation in the LRIC-voltage network charges which is recommended for future work.

Finally, it is hoped that this thesis would raise attention in the area covered and, ultimately, stimulate further research in the aforementioned area.

Appendices

A - Reactive Power Compensation Devices, Optimization Techniques and Planning

The reactive power compensation planning is briefly introduced and explained in the context of being a mix of various VAr compensation devices and, siting and sizing of these devices on a power system employing any suitable optimization technique. Next, VAr compensation devices and some fundamental optimization techniques, for siting the VArs compensation devices would be reviewed alongside the advantages and disadvantages of each of them. Finally, the RPP problem would be discussed, in detail.

A-1 Introduction

The issue of reactive power compensation planning or reactive power planning (RPP) involves two functions: a mix of various VAr compensation devices and the appropriate optimization technique(s) to guide the siting and sizing of these VAr compensation devices on a particular power system, optimally as described by [81-95]. It should be noted that the problem formulation is upon the discretion of the power system operator in determining the factors which are fundamental and the bias grounded on those factors, subject to satisfying the required power network criteria of reliability, security and quality of supply.

In this chapter, VAr compensation devices, some fundamental optimization techniques, for siting the VAr compensation devices would be discussed. In addition, other important issues such as SVC siting using voltage collapse critical modes, other RPP developments and practical examples of VAr compensation planning existing in real world, are discussed. Finally, reactive power compensation planning problem, which comprises of the mix of VAr compensation devices and any suitable optimization technique, would be discussed.

A-2 Reactive Power Compensation Devices

All power system plant absorbs or produces reactive power (VArs), but this particular reactive power is of no use in the compensation context since the system operator has no direct control over it. What is of paramount importance is to be able to control VArs at particular nodes, as may be required. Since economic viability of transmitting VArs degrades as distance and kW loading increase, it therefore may be necessary to support VArs at the receiving-end bus [1].

Reactive power compensation devices come in distinct characteristics to serve different purposes owing to their designs and operational specifications. These can be classified into three groups owing to the technologies they represent, which are first, second and third generation compensation devices. These are outlined below.

A-2.1 First generation compensation devices [1, 96, 97]

Table A.1: First generation compensation devices.

Name of Device	Abbreviation
Fixed shunt reactor	FR
Fixed shunt capacitor	FC
Mechanically switched shunt reactor	MSR
Mechanically switched shunt capacitor	MSC
Saturated reactor	SR
Series capacitor	SC
Quadrature booster	QB
Phase shifting transformer	PST
Synchronous compensator	condenser

Table A.1, shows the first generation compensation devices which are the earliest and simplest technology designs. Their behaviour and characteristics will be outlined below.

A-2.1.1 Fixed shunt devices (FR & FC)

These devices are connected across the system to give constant voltage support at respective busbars. They lack in that the voltage is proportional to the reactive power output, such that, as the voltage drops the reactive power output drops, at the time when it is most required. In addition, during the system light loading conditions the voltage suffers from the effect of being increased since the reactive power output from the capacitors will increase.

A-2.1.2 Series capacitors

These devices are connected in series with connected lines to cancel out the effect of natural inductance in these lines. These have the effects on the stability of the system in assisting to maintain the steady power transfer capacity and voltage stability. Their major setback is that, when there is a short-circuit these devices are severely affected by overvoltages.

A-2.1.3 Switched shunt devices

These devices operate the same way as the fixed shunt devices but the difference is that they comprise of one or more reactive power elements which may be mechanically switched on or off therefore offering variable amounts of discrete compensation. Even

though these offer flexibility to some extend, they suffer from bearing enough speed of operation as opposed to switches. They also suffer from having limited switching operations to be carried-out during their life-time.

All the shunt devices best perform during steady-state conditions to minimize losses and maintain the voltage profile of the distribution system.

A-2.1.4 Synchronous compensator

This device is a synchronous motor not connected to a mechanical load and it is used to either generate or absorb VArs by varying its field excitation (under-excited generating VArs and over-excited absorbing VArs). The control action is achieved by controlling excitation in reference to the system voltage, creating a character that has voltage-VAr characteristic. This action offers advantages entailed in dynamic compensation devices. This action enables capacitive VArs to be injected in to the system when voltage is low, therefore, increase the voltage. On the other hand, inductive VArs will be injected when the voltage is high and, therefore, the voltage would be reduced to the required level. This behaviour is depicted in fig. A.1 below.

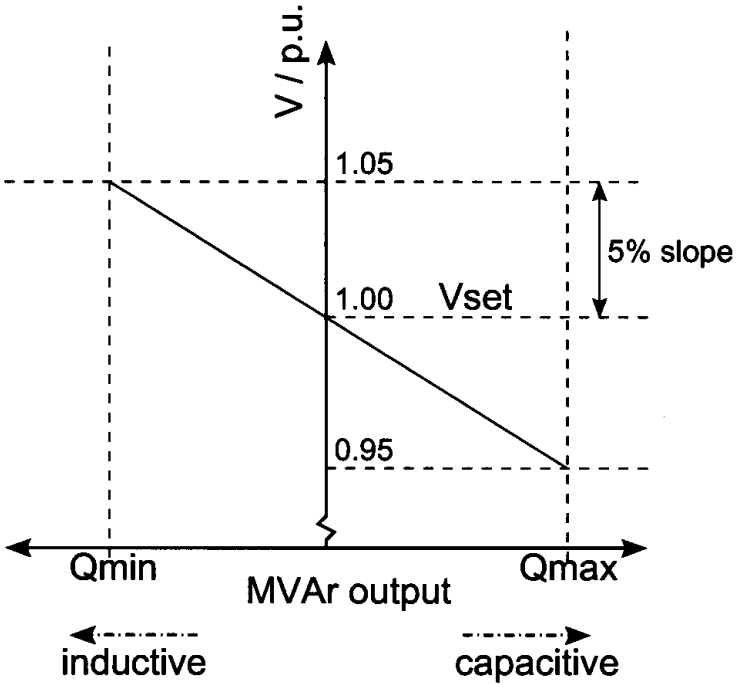

Figure A.1: Voltage-VAr characteristic of a voltage control devices [1]

The most fundamental aspect about the synchronous condenser is that it introduces dynamic reactive power output which inherently can deal effectively with transient and dynamic effects due to daily load cycles, repetitive impact loads (arc furnaces) and sudden loading changes. The device also enhances transient stability of the system which in turn reduces the effect of oscillatory dynamic instability [96].

A-2.2 Second generation compensation devices

Table A.2: Second generation compensation devices.

Name of Device	Abbreviation
Thyristor controlled reactor	TCR
Thyristor switched capacitor	TSC
Static VAr compensator	SVC
Thyristor controlled series compensator	TSSC / TSSR
Thyristor switched series compensator	TCSC / TCSR
Thyristor controlled braking resistor	TCBR
Thyristor controlled phase shifting transformer	TCPST
Line commutated converter compensator	LCC

Table A.2 shows the family of second generation compensation devices. These devices are consequent to the invention of a thyristor. A thyristor has characteristics matching those of a diode and it is a silicon device with a PNPN structure. It differs with a diode in that it has an additional characteristic of a gate in which this device only conducts when the current is applied to this gate. As long as the gate current is applied, this device will conduct continuously until the field voltage returns to zero, then it will switch off.

A triac can be created by connecting back to back thyristors in parallel. If this arrangement has a reactor connected in series to it, as shown in fig. A.2, a new device can be created which has a variable reactive power.

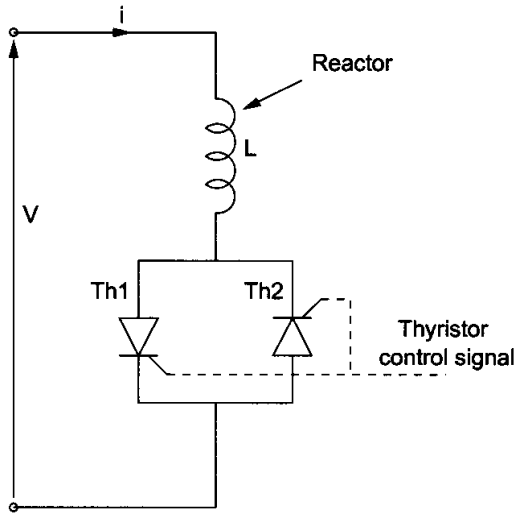

Figure A.2: Circuit created by two thyristors and a reactor [1]

The operation of the above device is that, in each cycle, one thyristor may be switched on (fired), allowing a current to pass through. If the firing angle of the thyristors is varied, then the actual reactance can be varied. The firing angle is the phase difference between

the beginning of the cycle and firing the thyristor. In essence, the thyristor in this regard, is employed to represent the mechanical switch.

This arrangement is the basis for the FACTS devices, in which the compensation devices described in the first generation compensation devices are combined with the thyristor circuits to form these second generation compensation devices.

A-2.2.1 Static VAr compensator (SVC)

Since this device is to be employed in this project work to achieving the required compensation, it is worthwhile to analyse it in more pronounced details. Some of the main achievements that the SVC can impose on a power system when sited for compensation are as follows [1]:

- Reactive power flow control during power system steady state conditions:
  - maintain required voltage profile on a power system
  - minimise system losses
- Monitor and control voltage change as a result of:
  - synchronising power flow swings
  - dynamic changes in high voltage DC conveters
  - daily load cycles
  - repetitive impact loads causing voltage flicker (e.g arc furnances)
  - load shedding to maintain the system balance
- Enhancement of power system stability to:
  - prevent transient instability
  - prevent oscillatory dynamic instability
  - prevent voltage instability or voltage collapse
  - maintain steady state power transfer capability

SVC plant comes in a number of design specifications to achieve a range of useful characteristics. In one design, the control output can be either completely passive or active (as in saturable reactors which are static components). Also, thyristors or conventional (non-solid state) switches can be employed to achieve switching [96]. Figure A.3 shows a typical design of an SVC.

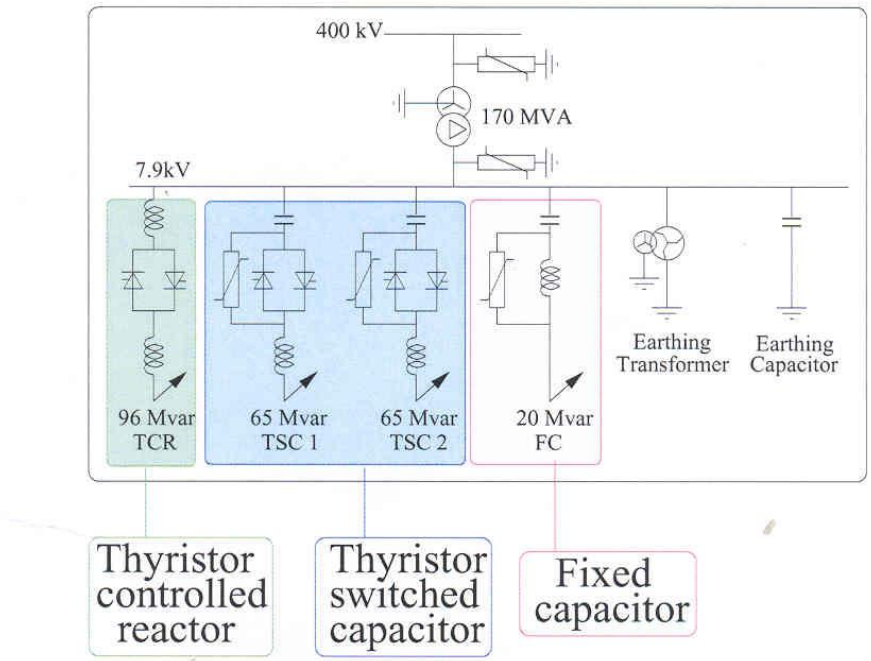

Figure A.3: Typical SVC [1]

This device has voltage regulator feed-back control (active control) and more than one thyristor switch assemblies to control the output. Figure A.3 shows the SVC control characteristic.

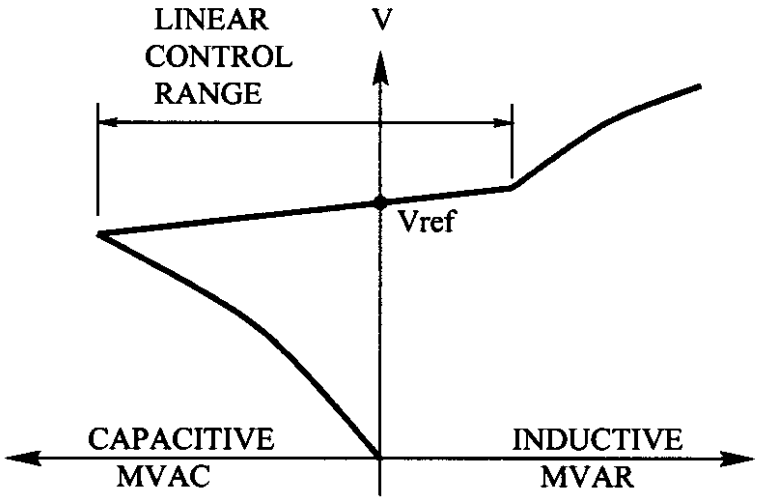

Figure A.4: SVC control characteristic [1]

As shown by fig. A.4, the thyristors control the current through the SVC reactors and / or SVC capacitor banks when the device is operating in the linear region of the steady state control characteristic. Any range from minimum to maximum inductive and capacitive VAr output can be achieved, should it be required. Also, the fine tuning of the device's

respective thyristor firing angles can result in respective outputs being fine-tuned, as may be needed. Harmonic filtering is achieved by fixed capacitor assemblies.

There are a range of SVC configurations as outlined by [97, 98] and they are as follow:

- **Thyristor-controlled reactor (TCR), fixed capacitor (FC)**

  Generally the TCR is rated larger than the total fixed capacitance to compensate this capacitance and offer net negative VArs. Two or more fixed capacitor banks supply positive VArs. This setup provides reasonable flexibility in control and up-rating terms. The setback with this assembly is that, there is high generation of high losses and, harmonics and therefore extensive filtering is required.

- **Segmented TRC-FC**

  This arrangement is the same as the one above, but the single large TRC is replaced by two or more smaller TRC segments. The result is the reduced harmonics in the output but with increased cost and reduced efficiency.

- **12-pulse TCR-FC**

  The twelve pulse setup results in further reduction of harmonics as compared to the segmented TRC-FC. Effective cancellation of all but twelfth harmonics is achieved by employing two coupling transformers, or one with secondary windings (one star connected and the other delta connected) and dividing the reactive elements between these windings, a 30˚ phase shift is created between the outputs of the two halves.

- **High impedance thyristor controlled transformer (TCT)**

  The impedance of a specially designed transformer is employed in place of air core reactors to provide a controlled reactance. The transformer bears a leakage reactance of around 100% and a delta connected thyristor on the secondary winding controls the short circuit current flow through its impedance. This offers the whole setup a built-in overhead capacity, that is, during severe transient over-voltages the TCT has the capability for excessive short term VAr absorption. This setup is very costly.

- **Thyristor switched capacitor (TSC), TCR**

  This device is similar compared to the TCR-FC fixed configuration, only the capacitor banks are in series with a solid state switch. The capacitor rating is only a portion of the total output and capacitance is varied in discrete steps in order to keep the operation of the reactor bank within its normal control range. This device offers reduced operating losses and improved performance during large system

perturbations especially when the demand for compensation exceeds the linear control range of the SVC. Fixed capacitor type compensators act as parallel LC circuits and oscillations can be established between the system and the LC circuit, and this arrangement helps during large disturbances. Oscillations can be avoided by switching in or out capacitor banks (TSC-TCR) rapidly as this minimises the perturbations. The setback is that this arrangement is costly and has a complex control circuitry.

- **Mechanically switched capacitors (MSC), TCR**

  This device is similar to the TSC-TCR arrangement but only less expensive. In place of thyristors, conventional switches are employed to control current through the capacitors. The mechanical switching can be effected in four cycles as opposed to half and one cycle for thyristor switches. The life of mechanical switches and slower response discourages the use of this device for steady-state voltage regulation.

- **Saturable reactor (SR)**

  This device does not use any solid state switches or active control. It responds to variations in its terminal voltage by self regulating itself. This regulation of the SR compensator is dependent on the natural saturation characteristics of the iron-core reactor. SR type compensators have the best harmonic character of any commercially available SVC. Series slope-correction capacitors are in place to change the voltage regulation characteristics and these slow down the time response to a state comparable to solid-state SVCs, and introduce harmonic effects. Control and uprating are less flexible. Load-tap changing coupling transformers are needed to change the voltage reference point (saturation point). SRs cost more or less to solid-state devices and are associated with more losses than switched capacitor devices, as at zero net VAr output, losses are still observed in the coupling transformer of the reactor itself.

A-2.3 Third generation compensation devices

These devices have an added dimension to the second generation devices, in that with the latter devices, once the thyristor is switched on there is no way to switch it off unless when the voltage return to zero. This limitation has the effect of limiting the operating speed of the device to twice the frequency of the system voltage (in UK is 100Hz). The third generation devices resulted because of the availability of the gate turn off (GTO) thyristors in the nineties. This thyristor could also operate at high ratings. Table A.3 shows the third generation compensation devices.

Table A.3: Third generation compensation devices.

Name of Device	Abbreviation
Static synchronous compensation	STATCOM
Solid-state series compensator	SSSC
Unified power flow converter	UPFC
Self-commutated converter compensator	SCC

The basis of the third generation compensation devices is the Solid-State Synchronous Voltage Source (SVS), which is similar to a rotating synchronous condenser. One fundamental character of SVS is that it maintains capacitive output at low system voltages and has less harmonic resonances. Other characteristics are that, it does not suffer from low short circuit impedance, high maintenance cost, rotational instability and the mechanical limitation associated with inertia limited response. Moreover, it dynamically exchange real power with the AC system if it is coupled to an appropriate source to supply or absorb the power it absorbs from, or supplies to, the AC system. Figure A.5 depicts the structure of SVS.

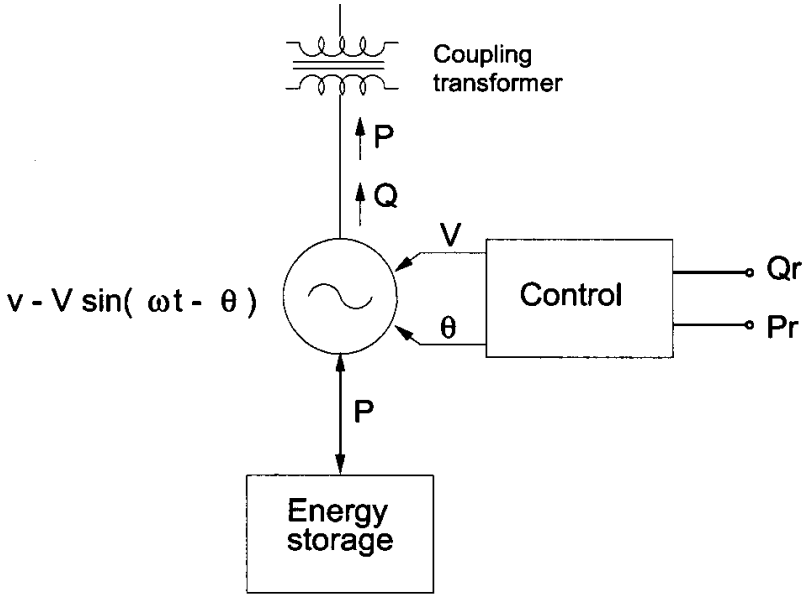

Figure A.5: Synchronous voltage source [1]

The control signals for voltage (V) and phase angle (θ) are due to control device reference inputs Qr and Pr. In turn, V and θ define the output voltage of the SVS. Lagging reactive current is drawn when the voltage source of the device is smaller that the line voltage. When the reverse is true, as regard to voltage, leading reactive current is drawn from the line and the equipment acts as a capacitor. By adjusting the phase of the generated voltage, real power can be exchanged with the line. This device absorbs power when lagging the line voltage, otherwise, it generates power when leading the line voltage.

The implementation of the SVS voltage source comprises the DC energy storage and the AC distribution system interfaced by switching power converters. Figure A.6 shows this arrangement.

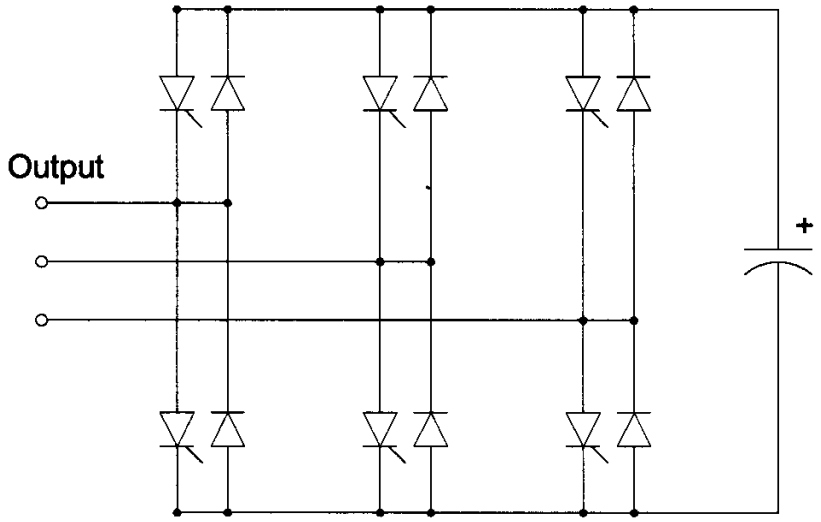

Figure A.6: Simple six-pulse two-level Voltage Source Converter [1]

Each phase (figure A.6) is supplied with two level square wave, shifted in phase by 120˚, producing three-level line to line voltage. A smoother AC signal outputs can be produced combining multiple converters of slightly different amplitudes and voltages.

A-2.3.1 Static Synchronous Compensator (STATCOM) [98]

This device is a voltage sourced converter (VSC) connected to a busbar through an inductance from the coupling transformer to supply shunt reactive compensation.

The STATCOM has a number of advantages over SVC as related below.

- Has the ability to act as a voltage source in starting other converter devices.
- May be used with other compensation devices.
- They do not need harmonic filters.
- Magnitude order better performance than SVC in:
    - unbalanced operation
    - flicker reduction

  - damping system oscillation

- Needs (15-35)% less MVA rating to produce equal support for:
  - dynamic voltage support
  - transient stability performance
  - system steady-state power transfer
- It is smaller in size than an equivalent SVC.
- Can deliver VARs over its full range no matter what the system voltage is.
- It has a 20% short term overload capacity
- It does not:
  - introduce resonances
  - add to fault level other than rating
  - have electromechanical oscillations
  - contribute to system resonances

A-2.3.2 Solid-State Series Compensation (SSSC)

This device controls power flow by controlling the angle and impedance of the line. This real power exchange capability enables to enhance dynamic stability. The implementation of this device comprises of the VSC connected in series to a line through a coupling transformer.

A-2.3.3 Unified Power Flow Converter (UPFC)

This device is a combination of SSSC and STATCOM which share the same energy storage device. This device can operate as a separate SSSC and STATCOM or a double rated STATCOM.

A-2.4 Tap-changing transformers

By employing this device, voltage can be controlled [9, 10]. The turns ratio of this device can be varied by varying the tap setting. To minimize large perturbations at consumer

busbars, the respective voltage change must be as well small and, usually, it is in the region of 1.25% of the nominal voltage between successive tap settings.

One fundamental type of tap-changing transformer is automatic tap-changing transformer. Automatic tap-changing transformer automatically adjusts its tap setting to be equal to preset voltage value at one of the busbars to which is connected (control busbar). When the voltage is below the preset value, the tap setting is increased to increase the control busbar voltage. On the other hand, if the voltage is above the preset value, the tap setting is decreased.

A-3 Compensation Placement Approaches

VAr compensation is fundamental to maintain the quality, reliability and security of the network. However, siting compensation is an expensive undetaking as described by [1]. Badly formulated siting plans can be highly suboptimal, and the substantial amount of money involved make the matter of optimal placement very essential for network operators (NOs). Further, the magnitude of the problem space is equivalent to the size of the network and the contingency state numbers considered. Also, the problem dimension is discrete, nonlinear, non differentiable and multimodal [99].

The RPP problem, as one of the most challenging optimisation undertaking in the power systems, has received considerable attention in the context of optimisation algorithms. Various optimisation algorithms that can be found in the literature are detailed in this section.

A-3.1 Siting Techniques For SVCs

To solve reactive power allocation problems, many optimisation techniques have been utilized. In this section, the most commonly used algorithms would be described and these would be ordered in terms of the date in which they start to appear in the literature.

1. Algebraic Techniques

Author of [100] came-up with the first paper mentioning a structured scheme to the siting of reactive power compensation. The author indicated the drawbacks of the then existing techniques, that an improperly sited fixed capacitor can lead to increased energy loss in a line. Consequently, the author presented an analysis of the results of fixed capacitors on radial circuits consisting of distributed loads considering the effects of a periodic load cycle. In doing so, the author, presented a set of curves indicating the optimum positions and most economical ratings of fixed capacitors on the radial circuit. Further, the author extended this approach to cover for both fixed and switched capacitors [101]. However, the author's analytical approach is suitable only for an individual circuit, but problems are encountered when applying it to a network since every time extra compensation is installed

on a line the state of the network varies and, therefore, previous sitings require to be re-examined to take account of this change.

2. Gradient techniques

Authors of [102] presented an optimal reactive power siting technique. It was achieved by formulating the load flow problem in a linearised manner and a gradient scheme is utilized to guide the optimisation. In a nutshell, it means that a linear approximation to the problem space is devised, with the algorithm performing hill climbing to optimise the control variables, that is, the amount of VAr compensation to be added at each node.

Gradient or hill climbing algorithms operate by inspecting the local area surrounding solutions to realize better solutions. This is achieved by making small variations to the solutions and re-examining its performance. Any variation producing a better solution (performance) is kept. However, even though extremely fast and easy to implement, their setback is that they can find improved solutions while one exists in the locality and can, as a result, easily get trapped in the local minima or maxima during minimisation or maximisation, respectively.

3. Linear Programming (LP) technique

Authors of [103] presented an approach for planning VAr compensation which incorporated the then new SVC. The technique aimed to realize the minimum amount of additional VAr needed to maintain the nodal voltages within required acceptable limits. A linear programming (LP) technique is utilized by the algorithm to optimize the control parameters. Solutions are validated by steady state and dynamic modelling. Also, the authors presented a paradigm for simulating a thyristor-controlled static device used with a linear programming approach.

LP technique, as the name implies, search an optimal solution to a linear representation of a problem. A set of quantified variables or decision variables is the problem solution. At the optima, these aforementioned variables are the unknown values to be determined. In the context of these variables, three sets of linear equations (namely constraints, variable limits and objective functions) are then needed for the formulation of the LP problem. Constraints combine the variables to define bounds on possible solutions, variable limits define the bounds on the parameters that variables may take and objective functions are mathematical formulations of the objectives of the optimisation.

Combined, these equations create the problem space or hyper-space upon which each dimension is a variable having two regions, namely, feasible and infeasible regions. Unlike a point in the feasible region, that in the infeasible region violates at least one variable limit or constraint. There exist hyper-planes or flat surfaces within this problem space such that each point is related to the same objective function value and these, for simplicity, could be imagined as hyper-contours of the objective function. The optimum solutions exist within the feasible region and are those points which lie on the best possible objective function hyper-contour.

Consequent to the notion that the problem has been formulated from linear equations, two imperative issues of LP theory can be raised. Firstly, it can be demonstrated that this optimum intersection lies on the very edge of the feasible region as the objective function must increase as it moves away to infinity. Secondly, since the feasible region is bounded by flat planes, any other flat plane touching the edge of this region must be touching it at the corner-points. Any other contact points, resulting from more than one optimum corner-points such that edge connecting them must lie on the same hyper-contour, must have the same objective function value. In this regard, an optimum solution to the problem must be one of the corner-points. Therefore, the LP algorithm only has to establish these points to find the optima.

LP is a powerful approach that has been used in many engineering problems successfully. However, it has two major setbacks when applied to the problem of RPP. Firstly, all variables are regarded as non-discrete or continuous. Whilst being a substantial tool for a number of applications, this is not the case in the context of the RPP problem as the variables therein are not continuous. Many VAr compensation assets are only available in specific sizes and variable transformer taps can only operate within a discrete set of values.

To mitigate this setback, there have been many algorithms established premised on LP that deal with such discrete problems better. They include integer programming and 0-1 programming. Integer programming, as is the case with mixed integer programming, is intended to completely support integer values by retaining constant integer values and performing LP on any continuous variables. Adjusted by plus/minus one, would be one of the integer values before repeating the LP optimisation. Further approximations are introduced to speed up optimisation [104] as the LP optimisation is a recursive process which is extremely time consuming. On the other hand, 0-1 programming utilises additional variables that can either take a zero or a one to represent “on-off” switching for other variables, which in essence would be to control whether a device is installed or not installed.

Finally, another setback to all LP based approaches is that even though an optimum solution can be often quickly attained, in fact, it is actually an optimum solution to an approximation of the problem (that is, the performance of such a solution may or may not be near optimal when applied to the original problem).

Further, LP premised approaches continued to receive attention as reflected in [105] where Opuku utilised duplex simplex linear programming approach along with relaxation and contingency analysis to solve the problem of RPP. This approach was applied to IEEE 30-bus and 118-bus networks. The author described the necessary modification to promote convergence in LP techniques when attending to large, highly stressed or contingent systems. In another work in [106], the authors utilised an LP technique for coordinated optimisation of preventive transformer taps and reactive power compensation device installation.

4. Decomposition

Authors of [107] segregated the planning problem into a master and two sub-problems. The master problem is responsible for the investment in VAr compensation assets and it represents this investment as the investment to be effected for each year of the planning

horizon. This approach is contrary to other planning approaches which entail that all compensation would be installed simultaneously. This may not necessarily be the issue but if maybe the network operator can only afford one asset per year then the order in which these devices should be installed becomes imperative. This approach presents the optimal solution as the annual siting plan. On the other hand, the two sub-problems achieve the optimal operation of the network under normal conditions in the context of real and reactive power. It should be noted that the more objectives an optimisation algorithm is provided with, the more compromises the algorithm may have to make. This means that the algorithm may opt for a solution that gives improved incremental performance at the expense of the final performance.

Also, authors of [108] employed a decomposition scheme which aimed specifically at the location of FACTS (Flexible AC Transmission Systems) devices, particularly static phase shifters and variable series capacitors. They tested the approach on a number of test systems up to and including a thirty node system.

Thereafter, a number of innovative approaches developed in the area of SVC expansion planning followed. It should be noted most of such modern approaches use some form of artificial intelligence.

5. Simulated Annealing (SA)

SA depicts its strength from drawing similarities between the cooling of molten metal and a minimization process. Resulting from the cooling metal, the corresponding molecules are reconfigured such that the molecular structure potential energy of the metal is minimal after the cooling process is complete. This approach basically takes the form of gradient algorithm operation, in that, solutions constitute small downhill movements, but on top of this process is a measure of temperature. At each iteration, the temperature starts from being high and decreases until it ends at some lower cool point. There is a random opportunity that the uphill movement can be allowed, at each iteration, as opposed to the downhill movement. The probability of such movement to be allowed is proportional to the temperature. Initially, the search point remains fairly unconstrained and evolves freely around the problem space. With temperature dropping, the search point would start to settle into minima, however, it would be still be able to get out of local minima to attain global minima. The search point would be unable to move uphill once the minimum temperature has been reached and, therefore, search would concentrate on finding minimum optimal point in the locality that it is in [109 and 110].

A scheme for optimal multi-objective SVC planning was devised by authors in [101]. This approach employs the use of a Lagrange multiplier and parallel SA to optimize for voltage stability enhancement. The system VAr margin, voltage depressions at critical points and system I^2 R losses were represented by a defined fuzzy performance index hence transforming the multi-objective problem into a single objective one. The compensation siting constraints are the overall capacity to be installed, the number of SVCs and the SVC controller characteristics. The approached was tested on the IEEE14-bus network given normal and credible contingent conditions.

A similar optimisation to [111] was performed in [110] and it was based on SA. The optimisation constraints were minimisation of SVC investment cost, reduction of the

voltage deviation of the system, system security margin robustness and active power loss reduction. Further, the formulation of a number of the main constraints and objectives commonly used regarding SVC placement problem were discussed in detail. The proposed approach was tested on the AEP 14-bus network.

SA alongside a hybrid expert system was utilized by [109]. Busbars were removed from the list of candidate busbars by the expert system thus reducing the problem space. The removal is effected after a unit of compensation is sited at a bus and it results into no improvement in the context of network voltage profile. Also, expert system setup the SA level with an initial solution from which to start optimisation process. This integrated approach solves a problem consisting of a multi-objective function by replacing each objective function a fuzzy score. The multi-objective optimisation is translated into a single minimisation or maximisation optimisation by adding up the fuzzy scores. The approach is tested on the modified IEEE 30-bus network. A slight cost reduction and considerable CPU time reduction are demonstrated as compared to SA.

6. Tabu search

Tabu search technique is similar to SA as it is also an extended gradient technique as expressed in [112 and 113]. The optimal solutions are achieved by moving the search point to a better solution in the neighbourhood of the current search point by performing a simple hill climbing. The most attraction with the tabu search is in the utilization of its tabu list, which retains all the solutions previously attained, and does not permit the search point to revisit those. This results in permitting the search point to move uphill, if only the existing solutions in the current neighbourhood are worse. Consequent to this controlled uphill movement, the search point may move out of the local optima and, as a result, the algorithm has the ability to establish optimal solutions in multi-modal problem dimensions.

7. Evolutionary Algorithms (EAs)

The area of evolutionary algorithms started with the invention of the genetic algorithm (GA) as shown in [114]. GAs is the search algorithm premised upon the mechanics of natural selection and genetics. Over the recent years, the growing tendency has been the application of EA premised techniques to the siting problem. A siting algorithm utilizing GAs was presented in [115]. The GA function utilized an interbreeding/crossover algorithm that uses system structure and objective function heuristics, in addition to expert system stochastic if-then rules. This approach was tested on practical 51-bus and 224-bus networks.

Evolutionary programming was work done by [116, 117] employing an evolutionary based approach. This approach was tested on the IEEE 30-bus test network and it optimised for reactive power installation cost and total energy loss. The latter two objectives were combined employing a weighted approach, which used a simple proportionate selection scheme. In [116], the authors utilized a GA with an adaptive mutation rate, the performance of which is compared to the popular technique referred to as Broyden's method. The approach begins by utilizing a high mutation rate and reduces it as the solution converges. The idea is to trigger greater initial exploration and then progressively encourage greater exploration. This approach utilized the population's convergence by

comparing the minimum and maximum fitness. In this regard, this technique is applicable for problems where there is almost zero probability of infeasibility or extremely bad solutions being routinely produced from the converged population, as solutions would confuse the monitoring of convergence. The results strongly indicate that the evolutionary techniques are superior over LP approaches, registering up to a fifty percent solution cost improvement.

Also, [117] assumed optimisation of network contingencies. Major disadvantage of their approach was that the reactive power requirement for each contingency network state is separately optimized and each state, consequently, needed a different set of new VAr sources. In this regard, there is no way of generating an individual siting plan that is near optimal for all cases. This means that, if all the VAr sources needed for all cases were installed, then, the results would be suboptimal.

Authors of [118] analysed the performance of the three main evolutionary algorithms, namely, GAs, evolutionary programming and evolutionary strategy. Although the evolutionary strategy and evolutionary programming techniques are based on GAs, they do not involve the use of crossover operator, but, instead rely solely on mutation to achieve diversity. These approached were bench marked against a linear programming technique. On the IEEE 30-bus test network, optimization was performed to minimise fuel consumption. The conclusion drawn by authors was that, the three evolutionary techniques perform in a similar comparable manner, however, all outperformed the LP technique. Further, the authors discussed the results of different mutation rates, in which lower rates provided faster convergence but with a higher probability of converging on local optima.

There are many studies regarding the problem of siting capacitors on distribution networks, namely, the field of the network between the Supergrid substations and the customers. Authors in [119] investigated the utilization of GAs for the aforementioned problems. Even though successful results were presented, however, since the results emanated from a 5-bus test system, therefore concrete conclusions could not be readily drawn about the GAs in the context of it being applied to real-world sized problems. Similarly, in [120], the capacitor siting results were presented on a 9-bus network. The approach attempted to minimise the compensation cost subject to the limits of harmonic distortion. Also, authors in [121], implemented capacitor placement utilizing GAs and that was in particular reference to the dynamic performance of the network and authors in [122] presented results for individual case studies of the bus Italian network utilizing a combination of GA and LP techniques.

An integrated framework entailing GAs and LP was presented by [123] and [124] to solve the operational sub-problem. Authors of [124] utilized a sub-problem premised technique, applying GA to optimise the discrete aspects of the problem, namely, capacitor allocation and transformer taps. Then, they used the LP algorithm to optimise the continuous variables associated with the system operating state. They tested the approach on the IEEE 30-bus and a practical 309-bus networks and the study only involved the intact state of these respective test networks. In their study, the algorithm involved the use of integer coded GA with a proportional selection scheme. The mismatch penalty and VAr installation costs were combined to formulate a single objective function. Their findings were focussed on looking into the effects of changing the GA parameters, namely, crossover probability, mutation rate and population size. Conclusion drawn from this study

was that, the crossover of one in two, a mutation probability of one in ten thousand and a population of three-hundred and eighty generated best results.

8. Decomposing The Power Network Into Manageable Subsystems

Consequent to deregulation and competitive power markets around the globe in recent years, the networks became very large in size, however, the system still had to be effectively handled by system operators in the context of power quality and security, as required. The drawback was that the problem space involved was so massive that the then used approaches took a lot of time and effort to converge to the global optimum solution. The currently used approaches then, were such that they involved the evolvement through the search space to attain a global optimum to achieve efficient and effective network security in the context of ensuring that network nodal voltages are within required limits. Given that drawback, it became apparent to decompose a network into manageable subsystems and gain decentralised control in these in the context of voltage / VAr was an ideal solution. Consequently, the concept of decomposing a network into distinct manageable voltage control zones was introduced. This concept involves the defining of the proximity of all network nodes with reference to each other using electrical distance (fully explained in chapter 9) concept which defines the physical network structure. The electrical distance concept defines the sensitivity of the VAr change to voltage change at a given node(s) found in the Jacobian matrix in the Newton-Raphson load flow. After defining the electrical distances between all network nodes and owing to the distribution of all the network VAr sources, then the distinct voltage control zones would be determined such that these sources would be balanced throughout the zones and, ultimately, independent voltage control in each zone would be realised.

Resulting from the increasingly meshed character of the French system, Lagonotte et al [125] proposed an approach combining the use of electrical distance concept and the experience of the system operator to sought uncoupled distinct voltage control zones in this particular network. This decomposition advocated for decentralized voltage and VAr control relating to the generating sets throughout the power system. These different voltage control zones corresponded to those already physically defined for this French network. The setback with this approach was that it required the knowledge of the system operator to finalize on the number of resulting voltage control subsystems.

Irving et al [126] used simulated annealing algorithm to segregate a power system network model into a number of subnetworks in order to optimise the use of parallel computer systems for network analysis. This approach was compared to iterative improvement method and tested on IEEE 30, IEEE 118 and 734 node test networks. The results showed that simulated annealing algorithm had the effect of significant improvement in cost function but with the limitation of increased computer time required.

Quintana and Muller [127] proposed a formulation to partition a power network into groups of nodes, transmission elements e.t.c. based on the concept of electrical distances among the nodes of the particular network. Strongly connected nodes, that is, nodes with complex voltage and power injections interdependent to each other, are grouped together. On the other hand, weakly connected nodes are assigned to separate clusters. Thereafter, the authors combined this network partitioning approach with equivalencing techniques in

a security-control algorithm for addressing system emergencies (voltage violations and thermal overloads) by shunt device switching operations and transmission branches, and real and reactive power generation rescheduling. Their approach was tested on IEEE 24, IEEE 118 and the Mexican power network 256 bus test networks. The results showed that the combined network partitioning and equivalencing techniques may reduce the computing time of other application algorithms like online VAr control, contingency analysis e.t.c.

A-3.2 SVC siting utilizing voltage collapse critical modes

A totally different approach to the compensation siting problem was taken by the authors in [128]. This methodology involved the use of analytical technique as opposed to optimization technique. The siting was premised upon an analysis of the power system power flows at the state of maximum loadability (the power system loaded to its near collapse point) and modal analysis was carried-out on this stressed network. Then, SVCs were sited at vulnerable nodes to voltage collapse. Results were presented for the Canadian B.C system.

A-4 Other RPP developments

Further advances in the specific planning algorithm developments to address the generic issues of the RPP problem have been recorded and shall be outlined in this section.

Optimisation of existing plant, which is an imperative placement problem consideration, was highlighted by the authors of [129]. The authors argued that, any placement algorithm (ranging from heuristic to artificial intelligence methodologies) requires to evaluate the performance of each potential or candidate solution. The argument they raised was that, to make a reliable assessment, all plant attributable to the system performance requires to be taken into account. This increased the problem space and the authors discussed how conventional power flow approaches may be insufficient for evaluating solutions. The aforementioned power flow evaluates system conditions, namely, power flows, voltage angles e.t.c., from the physical parameters of the system and, the demand and generation patterns as the input. Therefore, this refers that the system equations are only evaluated for one particular set of equipment settings.

This means that, if an inadequate solution is achieved, then various settings like tap settings and so on, must be adjusted and power flow re-run. This approach needs the user heuristic knowledge and, therefore, as the network dimension increases the complexity of this problem also increases. It is apparent that optimal power flow (OPF) software becomes imperative in these circumstances. OPF is a power flow function which both solves the power flow equations and optimally adjusts system control variables to achieve required results. Like with the conventional power flow software, the system data is specified and, also, additional data is needed to specify constraints, limits and control limits. The handling of these system control variables can be regarded as a sub-problem of the placement problem, when using the OPF software. The optimal-siting algorithm only requires to devise the proposed siting plan, not the entire system specification. The entire

system specification is only achieved while evaluating the performance of the siting plan, utilizing the OPF software.

Authors of [130] attended to the problem of the discrete issue to the specification of reactive power source installation. The problem emanates from the notion that commercially available compensation assets are not available in continuous sizes as pointed out in [131]. For example, SVCs at 400 kV level, typical operate at 75 MVArs inductive and 150 MVAr capacitive. It should be noted that potentially more than one SVC may be placed at a single node. When selecting the optimisation algorithm, the discreet issue of the problem is imperative. Algorithms like LP, assume that all variables are continuous. The optimal solution presented by the LP algorithm must be translated into a realisable siting plan and the natural way of performing this is by rounding up the sizes of the compensation assets to the next commercially available size. This may effect in a sub-optimal solution. Let us consider two competing siting algorithms to illustrate this point. The first, a continuous approach, establishes a solution involving two 10 MVAr SVC for buses A and B. The second algorithm, a discrete approach, establishes a solution at bus C involving 100 MVAr SVC. Assuming that the commercially available devices are in units 100 MVArs, implementing the first solution would mean two 100 MVAr SVCs would be considered and the solution may be sub-optimal. Consequently, the authors presented an approach employing the use of mixed integer programming algorithm that regarded capacitors as discrete entities in real practical systems.

An algorithm for simplifying the problem space of VAr placement problems by distinguishing weak nodes was proposed by authors in [132]. The weak nodes are those at which the nodal voltage is already closer to the limit and are more likely to be candidates for VAr compensation.

Furthermost, authors in [133] showed that existing VAr/OPF planning applications could be accurately utilised to deal with voltage stability constrained reactive power planning and voltage stability applications, alongside the traditional feasibility criteria of acceptable voltage profile.

A-5 Practical examples of VAr compensation planning existing in real-world

The “Application of a static VAr system to regulate system voltages in Western Nebraska” was reported in detail by authors in [134]. The location and size of the reactive power devices were selected through a combination of reiterated load flow studies and heuristic knowledge. In addition, the new reactive power approach for the Ohio electricity network was looked at by [129], a GA for siting VAr sources on the Israeli power system was utilised by Levitin et al [135] and the B.C. system in Canada was examined by Mansour et al [128]. All these papers, the considerations of a utility system planner contemplating controllable shunt VAr compensation devices for their system were described.

A-6 Reactive Power Compensation Planning Problem

The reactive power compensation benefits, devices and optimisation techniques for siting these compensation devices were discussed in sections 1.1, A.2 and A.3, respectively. Consequently, it would be very important to define the reactive power compensation planning or reactive power planning (RPP) problem.

The basis of the VAr compensation planning problem is guided by the underlying basic principle: "*define the specification for the installation of new reactive sources which achieves the maximum benefit at the least possible cost, while satisfying system and operational constraints* [1]". This statement represents the complete scope of the problem:

- *define the specification for the installation of new reactive sources*. The specification requires to define the types of compensation to be installed, the compensation device parameters, namely, their size, location and any control parameters.

- *maximum benefit*. The network planner requires to establish measures to evaluate the particular siting plan benefits. Consequent to the massive scope of effects involved regarding modifications to the network, planning algorithms presented as discussed earlier, generally focus on a certain subset of effects. Usually, the planning exercise considers steady-state effects, thereby, reducing the problem space of the planning exercise.

- *least cost*. "Maximum benefit" is mainly realized by considering the cost. The issue of how much it should cost is mainly upon the discretion of the network operator: factors associated to network losses and voltages can be regarded as indirect cost while the capital cost of installing new sources is a direct cost. Practically, if all the effects considered can be expressed as costs and can be all added together to offer one value for the network performance measure. If it is impossible to express the costs as such, then more complicated multi-objective techniques require to be used to compare competing siting plans. Some of those multi-objective problems were discussed section A.3.

- *satisfying all constraints*. Mainly the constraints can be classified as expansion constraints – the physical limitations with reference to the number of device placement – and operational constraints- power balance; voltage magnitude limits; transformer tap limits, real and generation limits; line flow limits, reactive power compensation limits; and voltage phase angle difference limits.

As mentioned earlier, the constructing of the problem is upon the choice of the power system operator, resulting from the factors they regard important.

The overall solution to the problem requires to encompass more than just the plan for the placement of devices. The problem can be regarded as comprising two sub-problems: firstly, establishing the optimum siting plan and, secondly, establishing how to optimise the system to realize maximum benefit from the siting plan. The set of equations below depicts the power system operating constraints and are as follows:

1. Load Flow Equations

$$P_{gi} - P_{di} = \sum_{j=1}^{N} |V_i||V_j||Y_{ij}| \cos(\theta_{ij} + \delta_j - \delta_i) \quad for\, i = 1,....., N \qquad (A.1)$$

$$Q_{gi} - Q_{di} = -\sum_{j=1}^{N} |V_i||V_j||Y_{ij}| \sin(\theta_{ij} + \delta_j - \delta_i) \quad for\, i = 1,....., NG \qquad (A.2)$$

$$Q_{gi} - Q_{di} + Q_{ci} = -\sum_{j=1}^{N} |V_i||V_j||Y_{ij}| \sin(\theta_{ij} + \delta_j - \delta_i) \quad for\, i = 1,....., NL \qquad (A.3)$$

2. Generating Limits

$$P_{gi}^{\min} \le P_{gi} \le P_{gi}^{\max} \quad for\, i = 1,....., NG \qquad (A.4)$$

$$Q_{gi}^{\min} \le Q_{gi} \le Q_{gi}^{\max} \quad for\, i = 1,....., NG \qquad (A.5)$$

3. Voltage Limits

$$|V_i| = cons\tan t \quad for\, i = 1,....., NG \qquad (A.6)$$

$$|V_i^{\min}| \le |V_i| \le |V_i^{\max}| \quad for\, i = 1,....., NL \qquad (A.7)$$

4. Transmission Limits

$$P_{ij} \le P_{T\max} \quad \forall i, j, i \ne j \qquad (A.8)$$

5. VAr injection limits

$$C_{ci} \le C_{c\max} \quad for\, i = 1,....., NL \qquad (A.9)$$

A-6 Conclusions

The following were discussed:

- VAr compensation devices
- Optimization techniques
- SVC siting utilizing voltage collapse critical modes
- Practical examples of VAr compensation planning existing in real world
- RPP problem

Since the optimisation techniques are the driver for siting various VAr compensation devices in what is referred to as RPP problem formulation, the approach of decomposing the power network into manageable subsystems for the effective and efficient voltage/VAr control was found to be most attractive for the following reasons:

- for larger and more integrated systems, the already existing approaches involve a very large problem space, therefore, takes a lot of computational effort to converge to the global optimum
- the use of the concept of electrical distance involves defining the actual structure of the network and, therefore, the various VAr compensation devices could be balanced across the entire network for the simple effective and efficient voltage/VAr control in resulting different zones

While expressing the electrical distances among the network buses define the close proximity of these in the context of the sensitivity of the Var change at bus(es) to the voltage change at the same bus(es), there should be some decision-making tool to ensure that the network is divided into manageable subsystems comprising of a balanced number of VAr compensation assets for the effective and efficient voltage / VAr control. In this regard, a novel approach involving the combined exploitation of the electrical distance concept and GA algorithm (as the decision-making tool) was recommended for future work in this research work. What set the GAs apart from other optimisation techniques are the following:

- GAs perform a parallel search. This enables them to be more tolerant of the local minima. Due to this feature, the GAs can effective deal with multi-modal problems to attain global optimum
- GAs exploit probabilistic transition rules, not deterministic rules to select the next generation. This feature enables them to explore complicated and uncertain areas to converge to global optimum, as such making them more flexible and robust than conventional approaches

- GAs utilize payoff information (objective or fitness functions) directly for search direction as opposed to auxiliary knowledge or derivatives. This ensures that the GAs deal with non-differentiable, non-smooth and discontinuous problem space, without relying on approximations as other appraches.

- GAs are usually integer based methods. This feature is suitable as the RPP problem

The aforementioned features make GAs robust, parallel algorithms which adaptively explore the global optimal point and have been discovered to produce excellent results when applied to various problem, however, their combined use with the electrical distance concept, as decision-making tool is yet to be explored. In this regard, this research work recommends the investigation of the application of the combined exploitation of the electrical distance concept and the simple GA.

B LRIC and Yardstick Approaches

B-1 LRIC Approach

Example of LRIC method

Taking a simple two feeder network as follows:

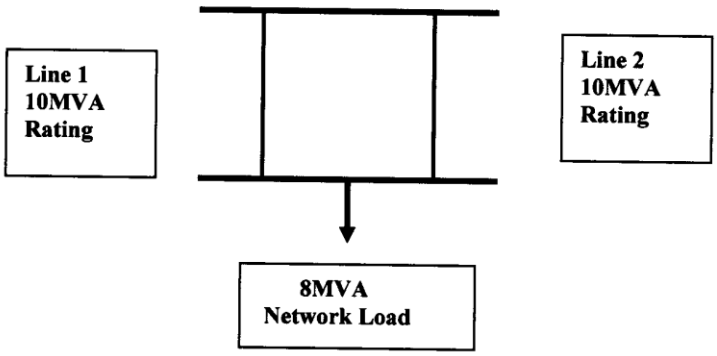

The long run incremental cost is given by:

$LRIC_N = \sum_l \Delta U_l = 2 \times 4{,}465 = £8{,}950/MVA$

Where:

ΔU_l is the change in the net present value of the future reinforcement cost of each feeder as a result of the incremental injection of 1MVA (ΔP_{ln}) (this will be shared equally by the two feeders) given by the equation

$$\Delta U_l = A \times V \times \left(\frac{1}{(1+d)^{n2}} - \frac{1}{(1+d)^{n1}}\right) = 0.0831 \times 200{,}000 \times \left(\frac{1}{(1+0.069)^{10.6}} - \frac{1}{(1+0.069)^{22.4}}\right)$$

= £4,465/MW

Where:

A is a 40 year annunity calculated as

$$A = \frac{d}{\left(1-\left(\frac{1}{(1+d)^{40}}\right)\right)} = \frac{0.069}{\left(1-\left(\frac{1}{(1+0.069)^{40}}\right)\right)} = 0.07414 \text{ i.e. } 7.41\% \text{ plus a } 0.9\% \text{ O\&M uplift} = 8.31\%$$

V is the cost of the reinforcement when the asset becomes overloaded, £200,000

d is the discount rate (the regulatory cost of capital of 6.9% is used)

n1 is the original number of years to reinforcement given by

$$n1 = \frac{\log C_l - \log D_l}{\log(1 + r))} = \frac{\log 5 - \log 4}{\log(1+0.01)} = 22.4 \text{ years}$$

Where:

Cl is the capacity of asset l, 10MVA

Dl is the power flow in asset l , 4MVA and

r is the expected growth rate, 1%

and n2 is the new number of years to reinforcement following a change in the flow of 0.5MVA (as increase in load at node of 1MW will be equally shared between the two feeders) (ΔP_l) through asset l as a result of the injection at node N is given by

$$n2 = \frac{\log C_l - \log (D_l + \Delta P_l)}{\log(1 + r)} = \frac{\log 5 - \log(4+0.5)}{\log(1+0.01)} = 10.6 \text{ years}$$

B-2 Yardstick Approach

Example of Yardstick	**Profile 1**		**WPD Wales**	
kWh/kW	3662			
			£/kW/yr	p/kWh
33/11kV Substation			29.32	0.729
33/11kV S/S Losses	@	4.97%		0.036
11kV System			19.23	0.478
11kV System Losses	@	4.19%		0.020
11kV/LV Substation			3.98	0.103
11kV/LV S/S Losses	@	2.86%		0.003
LV System			7.36	0.191
LV System Losses	@	0.93%		0.002
Total 500MW Model Costs				1.562
Power Factor Deviation Cost				-0.078
Service Cost			2.08	0.057
Subtotal				1.541
Total Network Costs				1.541
Plus Working Capital	@	0.773%		0.012
Operational Rates (attributed to the LRIC part of the model)				0.092
Operational Rates (attributed to the DRM part of the model)				0.095
Total Yardstick				1.740
Scaling (Not applied to the LRIC parts of the model)		149%		
Scaled Yardstick				2.17

Note: An adjustment for customer contributions has been applied at the LV system level and has a value of 50%.

C Test System Data

C-1 IEEE 14 Bus Test System

Figure C.1 is showing the standard IEEE-14 bus test system. The bus data, line data and transformer data are given in Tables C.1, C.2 and C.3, respectively.

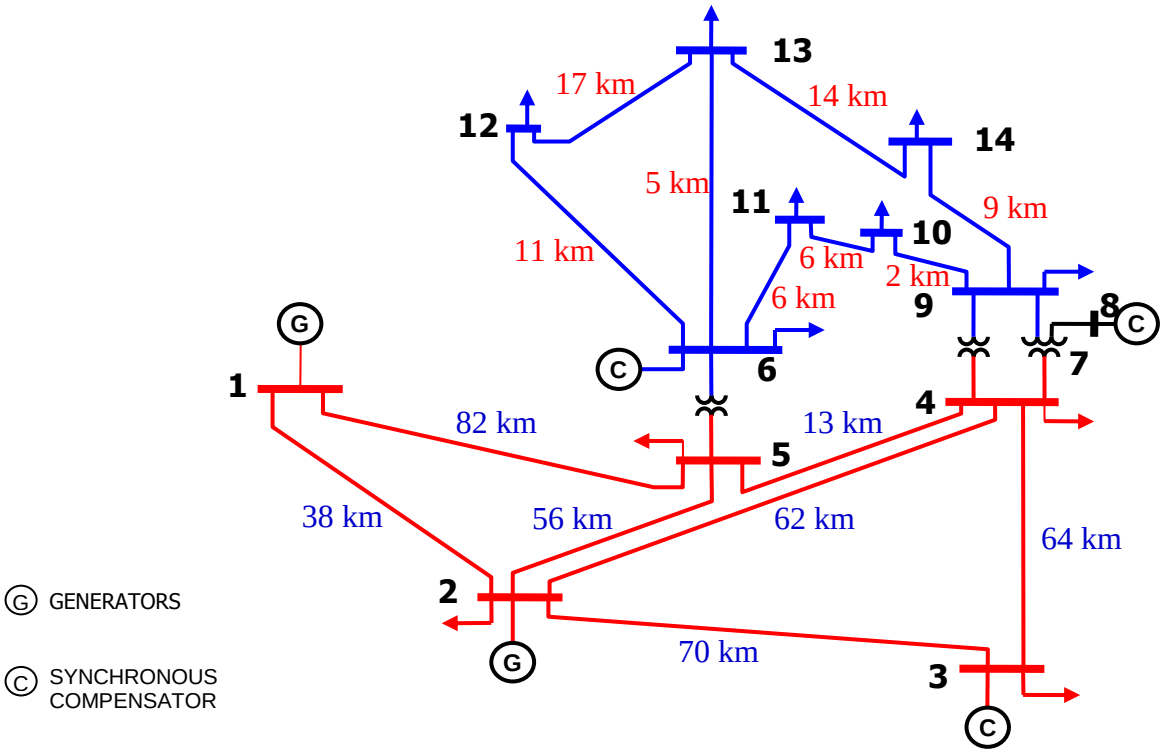

Figure C.7: IEEE-14 bus test system.

Table C.4: Bus data

Bus no.	Bus Name	Base kV	Type	Demand		Generator/Condenser		SVC Cost
				P(MW)	Q(MVAr)	P(MW)	Q(MVAr)	(£)
1	BUS001	275	Slack	0	0	-	-	1,452,000
2	BUS002	275	Generator	21.7	12.7	40	50	1,452,000
3	BUS003	275	Condenser	94.2	19	0	40	1,452,000
4	BUS004	275	Load	47.8	-3.9	-	-	1,452,000
5	BUS005	275	Load	7.6	1.6	-	-	1,452,000
6	BUS006	132	Condenser	11.2	7.5	0	24	696,960
7	BUS007	132	Load	0	0	-	-	696,960
8	BUS008	132	Condenser	0	0	0	24	696,960
9	BUS009	132	Load	29.5	16.6	-	-	696,960
10	BUS010	132	Load	9	5.8	-	-	696,960
11	BUS011	132	Load	3.5	1.8	-	-	696,960
12	BUS012	132	Load	6.1	1.6	-	-	696,960
13	BUS013	132	Load	13.5	5.8	-	-	696,960

14	BUS014	132	Load	14.9	5	-	-	696,960

Table C.5: Line data

From	To	Base kV	Resistance R	Resistance X	Susceptance Ch	Rating (A)
1001	1002	275	0.01938	0.05917	0.0528	590
1001	1005	275	0.05403	0.22304	0.0492	590
1002	1003	275	0.04699	0.19797	0.0438	590
1002	1004	275	0.05811	0.17632	0.034	590
1002	1005	275	0.05695	0.17388	0.0346	590
1003	1004	275	0.06701	0.17103	0.0128	590
1004	1005	275	0.01335	0.04211	0	590
1006	1011	132	0.09498	0.1989	0	1455
1006	1012	132	0.12291	0.25581	0	1455
1006	1013	132	0.06615	0.13027	0	1455
1007	1008	132	0	0.17615	0	1455
1007	1009	132	0	0.11001	0	1455
1009	1010	132	0.03181	0.0845	0	1455
1009	1014	132	0.12711	0.27038	0	1455
1010	1011	132	0.08205	0.19207	0	1455
1012	1013	132	0.22092	0.19988	0	1455
1013	1014	132	0.17093	0.34802	0	1455

Table C.6: Transformer data

From	Base kV	To	Base kV	Resistance R	Resistance X	Susceptance Ch	Rating (A)
1004	275	1007	132	0	0.20912	0	120
1004	275	1009	132	0	0.55618	0	120
1005	275	1006	132	0	0.25202	0	120

The power flow result of IEEE- 14 bus test system is as given below.

Bus Data

Bus Number	Bus Name	Voltage (pu)	Voltage (kV)	V Angle (deg)	Pg (MW)	Qg (MVAr)	Pd (MW)	Qd (MVAr)	Load pf
1001	BUS001	1.03	283.25	0	233.383	-27.786	0	0	----
1002	BUS002	1.019915	280.477	-5.3806	40	50	21.7	12.7	0.86
1003	BUS003	0.995546	273.775	-13.6972	0	40	94.2	19	0.98
1004	BUS004	0.988379	271.804	-10.9303	0	0	47.8	-3.9	1
1005	BUS005	0.995019	273.63	-9.3398	0	0	7.6	1.6	0.98

1006	BUS006	0.982493	129.689	-15.6401	0	24	11.2	7.5	0.83
1007	BUS007	1.007998	133.056	-14.4379	0	0	0	0	----
1008	BUS008	1.048325	138.379	-14.4379	0	24	0	0	----
1009	BUS009	0.981343	129.537	-16.3431	0	0	29.5	16.6	0.87
1010	BUS010	0.973582	128.513	-16.5603	0	0	9	5.8	0.84
1011	BUS011	0.974327	128.611	-16.2631	0	0	3.5	1.8	0.89
1012	BUS012	0.967309	127.685	-16.6346	0	0	6.1	1.6	0.97
1013	BUS013	0.963172	127.139	-16.7332	0	0	13.5	5.8	0.92
1014	BUS014	0.953884	125.913	-17.6898	0	0	14.9	5	0.95

Line Data

From (Bus i)	To (Bus j)	Branch Code	Rated V (kV)	Pij (MW)	Qij (MVAr)	Pji (MW)	Qji (MVAr)	P Loss (MW)	% Util	Status
1001	1002	L1	275	157.856	-29.126	-153.18	37.863	4.67857	56.6333	IN
1001	1005	L1	275	75.5267	1.3399	-72.614	5.6401	2.91305	26.3982	IN
1002	1003	L1	275	74.2604	-1.9567	-71.769	8.0034	2.49115	26.0653	IN
1002	1004	L1	275	56.0921	0.6667	-54.331	1.2474	1.76094	19.6498	IN
1002	1005	L1	275	41.1247	0.7271	-40.195	-1.4018	0.92941	14.4739	IN
1003	1004	L1	275	-22.4308	12.9966	22.897	-13.0673	0.4658	9.3029	IN
1004	1005	L1	275	-63.1312	5.3306	63.68	-3.6003	0.54854	22.6203	IN
1006	1011	L1	132	5.8406	1.2733	-5.8054	-1.1997	0.03516	1.7895	IN
1006	1012	L1	132	7.5365	2.2667	-7.4576	-2.1025	0.07886	2.3475	IN
1006	1013	L1	132	16.9522	6.0964	-16.73	-5.6584	0.2224	5.3622	IN
1007	1008	L1	132	0	-23.077	0	24	0	7.0759	IN
1007	1009	L1	132	29.8939	24.9207	-29.894	-23.2807	0	11.5447	IN
1009	1010	L1	132	6.7283	6.4885	-6.6995	-6.4118	0.02886	2.7988	IN
1009	1014	L1	132	10.5375	5.1078	-10.357	-4.7228	0.18099	3.4709	IN
1010	1011	L1	132	-2.3005	0.6118	2.3054	-0.6003	0.00491	0.7159	IN
1012	1013	L1	132	1.3576	0.5025	-1.3527	-0.498	0.00495	0.4342	IN
1013	1014	L1	132	4.5824	0.3564	-4.5435	-0.2772	0.03892	1.375	IN

Transformer Data

From (Bus i)	To (Bus j)	Branch Code	Pij (MW)	Qij (MVAr)	Pji (MW)	Qji (MVAr)	P Loss (MW)	% Util	Tap Ratio	Status
1004	1007	T1	29.8939	3.6901	-29.894	-1.8439	0	25.0298	0.975	IN
1004	1009	T1	16.8719	6.6992	-16.872	-4.9156	0	14.8861	0.975	IN
1005	1006	T1	41.5292	-2.2379	-41.529	6.8637	0	34.8675	1.025	IN

C-2 Distribution Test System

Figure C.2 shows the distribution test system in South Wales area of England.

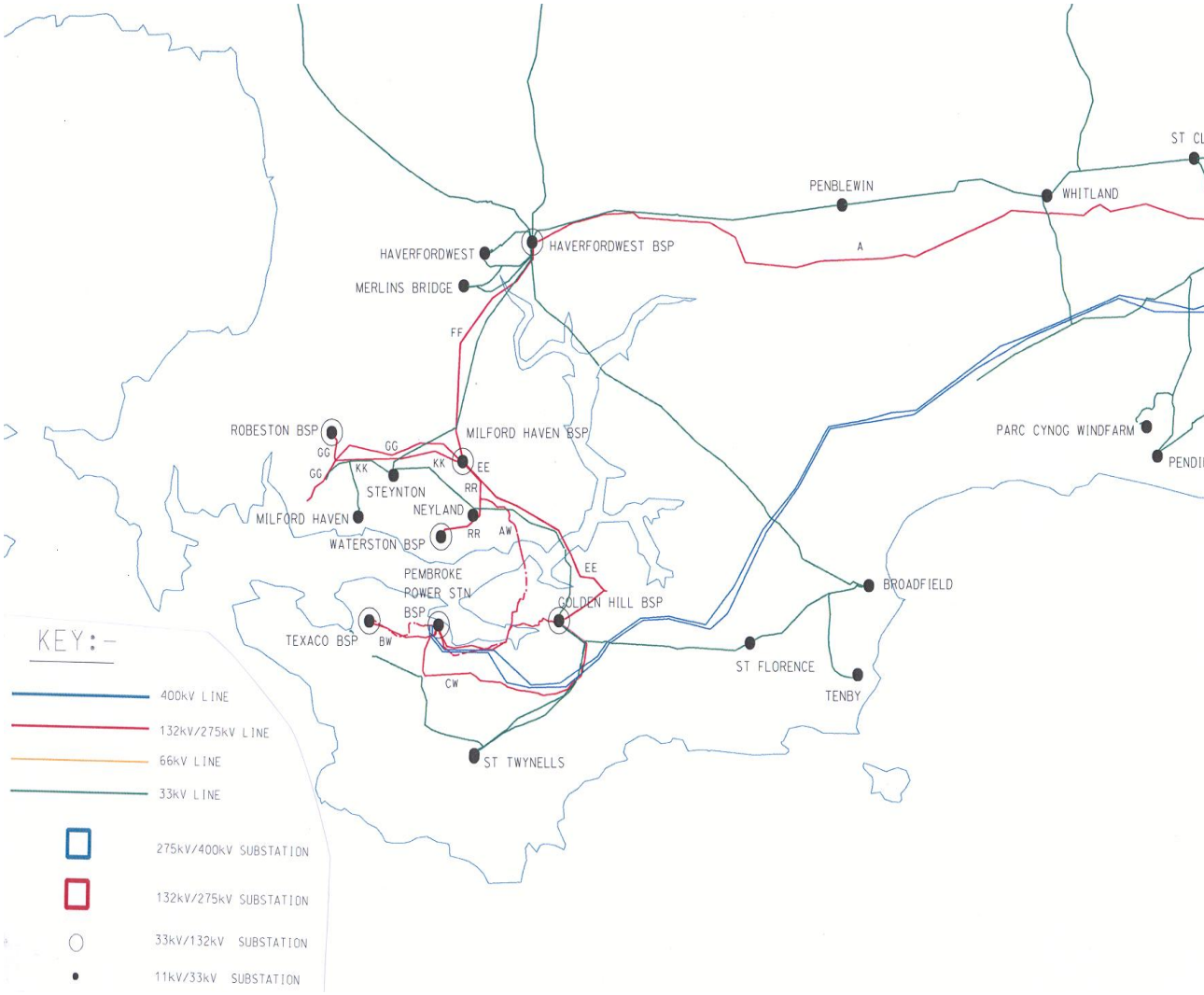

Figure C.8: Geographic map of distribution test system

The bus data, line data and transformer data are given in Tables C.4, C.5 and C.6, respectively.

Table C.7: Bus data

Bus no.	Bus Name	Base kV	Type	Demand		Generator/Condenser		SVC Cost
				P(MW)	Q(MVAr)	P(MW)	Q(MVAr)	(£)
2005	2005	33	Load	2	2	-	-	55,305.58
2015	2015	33	Load	0	0	-	-	55,305.58
3003	3003	11	Load	5.6	0	-	-	18,435.19
3006	3006	33	Load	0	0	-	-	55,305.58
3009	3009	11	Load	10.5	0	-	-	18,435.19
3012	3012	33	Load	0	0	-	-	55,305.58

3015	3015	11	Load	8	0	-	-	18,435.19
3018	3018	33	Load	0	0	-	-	55,305.58
3021	3021	11	Load	14.1	0	-	-	18,435.19
3024	3024	11	Load	9.1	0	-	-	18,435.19
3027	3027	33	Load	0	0	-	-	55,305.58
3030	3030	33	Load	0	0	-	-	55,305.58
3033	3033	11	Load	11.9	0	-	-	18,435.19
3036	3036	33	Load	0	0	-	-	55,305.58
3039	3039	33	Load	0	0	-	-	55,305.58
3042	3042	11	Load	4.1	0	-	-	18,435.19
3045	3045	33	Load	0	0	-	-	55,305.58
3048	3048	11	Load	3.1	0	-	-	18,435.19
3051	3051	33	Load	-4	0	-	-	55,305.58
3054	3054	11	Load	4.3	0	-	-	18,435.19
3057	3057	33	Load	0	0	-	-	55,305.58
3060	3060	11	Load	8.6	0	-	-	18,435.19
3063	3063	33	Load	0	0	-	-	55,305.58
3066	3066	11	Load	3.1	0	-	-	18,435.19
3069	3069	33	Load	0	0	-	-	55,305.58
3072	3072	11	Load	2.2	0	-	-	18,435.19
3075	3075	33	Load	0	0	-	-	55,305.58
3078	3078	33	Load	0	0	-	-	55,305.58
3081	3081	11	Load	1.9	0	-	-	18,435.19
3084	3084	33	Load	0	-1	-	-	55,305.58
3087	3087	11	Load	9	0	-	-	18,435.19
3090	3090	33	Load	0	0	-	-	55,305.58
3093	3093	11	Load	4.9	0	-	-	18,435.19
3096	3096	33	Load	0	0	-	-	55,305.58
3099	3099	33	Load	0	0	-	-	55,305.58
3102	3102	33	Load	0	0	-	-	55,305.58
3105	3105	33	Load	0	0	-	-	55,305.58
20051	20051	0.415	Load	0	0	-	-	695.51
20052	20052	0.415	Load	0	0	-	-	695.51
20151	20151	0.415	Load	0	0	-	-	695.51
20152	20152	0.415	Load	0	0	-	-	695.51
2000	2000	132	Load	0	0	-	-	221,222.32
2001	2001	132	Load	0	0	-	-	221,222.32
2010	2010	132	Load	0	0	-	-	221,222.32
2011	2011	132	Load	0	0	-	-	221,222.32
2020	2020	132	Load	0	0	-	-	221,222.32
2021	2021	132	Load	0	0	-	-	221,222.32
2025	2025	11	Load	13.63	3.27	-	-	18,435.19
2026	2026	11	Load	13.72	3.44	-	-	18,435.19
2027	2027	11	Load	16.45	5.97	-	-	18,435.19
2030	2030	132	Load	0	0	-	-	221,222.32
2031	2031	132	Load	0	0	-	-	221,222.32
2032	2032	132	Load	0	0	-	-	221,222.32
2033	2033	132	Load	0	0	-	-	221,222.32
2035	2035	11	Load	16.45	5.97	-	-	18,435.19
2036	2036	11	Load	0	0	-	-	18,435.19
2037	2037	11	Load	1.22	0.46	-	-	18,435.19
2040	2040	132	Load	0	0	-	-	221,222.32

2041	2041	132	Load	0	0	-	-	221,222.32
2045	2045	11	Load	1.22	0.44	-	-	18,435.19
2046	2046	11	Load	0	0	-	-	18,435.19
2047	2047	11	Load	0	0	-	-	18,435.19
2048	2048	11	Load	0	0	-	-	18,435.19
2620	2620	132	Load	0	0	-	-	221,222.32
2621	2621	132	Load	0	0	-	-	221,222.32
2630	2630	132	Load	0	0	-	-	221,222.32
2631	2631	132	Load	0	0	-	-	221,222.32
2640	2640	132	Load	0	0	-	-	221,222.32
2641	2641	132	Load	0	0	-	-	221,222.32
2650	2650	132	Load	0	0	-	-	221,222.32
2651	2651	132	Load	0	0	-	-	221,222.32
5140	5140	400	Slack	0	0	-	-	670,370.68
5148	5148	132	Load	0	0	-	-	221,222.32
5149	5149	132	Load	0	0	-	-	221,222.32
5150	5150	132	Load	0	0	-	-	221,222.32
5151	5151	22	Load	0	0	-	-	36,870.39
5152	5152	22	Load	0	0	-	-	36,870.39
5153	5153	132	Load	0	0	-	-	221,222.32
5154	5154	132	Load	0	0	-	-	221,222.32
20251	20251	0.415	Load	0	0	-	-	695.51
20262	20262	0.415	Load	0	0	-	-	695.51
20351	20351	0.415	Load	0	0	-	-	695.51
20352	20352	0.415	Load	0	0	-	-	695.51
20373	20373	0.415	Load	0	0	-	-	695.51
20374	20374	0.415	Load	0	0	-	-	695.51
20451	20451	0.415	Load	0	0	-	-	695.51
20472	20472	0.415	Load	0	0	-	-	695.51

Table C.8: Line data

From	To	Base kV	Resistance R	Resistance X	Susceptance Ch	Rating (A)
2015	3090	33	0.2804911	0.3633686	0.0005784	300
3090	3045	33	0.1559487	0.1417743	0.000631804	250
3090	3057	33	0.0741644	0.1429089	0.000609816	300
2005	3069	33	0.2102842	0.3082044	0.000913214	380
2005	3078	33	0.3028594	0.2737829	0.001276211	250
2005	3075	33	0.1242435	0.2503286	0.001811532	250
3057	2005	33	0.1356366	0.2710195	0.001212114	400
3069	3105	33	0.1066988	0.1458817	0.000143947	380
3105	3012	33	0.04273663	0.05745091	0.00029077	380
3105	3096	33	0.1025311	0.1438904	0.000147354	400
2015	3012	33	0.5054449	0.6861482	0.002315699	380
2015	3018	33	0.5068371	0.6568535	0.000723623	300
2015	3027	33	0.0739292	0.07004097	0.001086828	219
2015	3063	33	0.365161	0.4992586	0.000492636	300
2015	3036	33	0.06784385	0.1328056	0.000297316	400

2015	3099	33	0.04719853	0.06453119	6.37E-05	300
2015	3102	33	0.3998695	0.5458123	0.000692068	300
3102	3084	33	0.3120676	0.4379501	0.000448492	400
3102	3006	33	0.00319941	0.00449	4.60E-06	410
3006	3018	33	0.352602	0.4569671	0.000503418	395
3018	3051	33	0.350564	0.4543259	0.000500508	395
3099	3030	33	0.04596705	0.01794118	0.000777972	219
3099	3039	33	0.03206136	0.05676101	0.000426348	400
5153	5150	132	0.00081	0.04041	0	918.5
5154	5148	132	0.000795	0.04197	0	1049.7
5150	5149	132	0	0.0001	0	65535
5150	2000	132	0.01263323	0.0274393	0.008690114	590
5150	2031	132	0.00155292	0.00238406	0.05924543	510
5148	2030	132	0.00308127	0.00819203	0.007660742	380
5149	2631	132	0.00485467	0.01444173	0.1393766	770
5149	5148	132	0	0.0001	0	65535
2000	2620	132	0.01068975	0.02424121	0.007287738	547
2001	5148	132	0.00168956	0.00386175	0.1781894	656
2001	2620	132	0.01062701	0.0241023	0.005193462	547
2030	2032	132	0	0.001	0	2000
2031	2033	132	0	0.001	0	2000
2036	2035	11	0	0.0001	0	2000
2621	2010	132	0.00964239	0.02186915	0.004712272	547
2621	2620	132	0	0.0001	0	65535
2621	2630	132	0.00166297	0.00378497	0.00383742	547
2620	2631	132	0.00163417	0.00371299	0.002310984	547
2620	2011	132	0.00972219	0.022046	0.007275515	547
2620	2640	132	0.00643226	0.01519199	0.003003583	585
2620	2641	132	0.00597128	0.01410323	0.002788327	585
2640	2650	132	0.00204977	0.00464893	0.001001731	547
2640	2020	132	0.00103967	0.00235799	0.000508089	547
2641	2651	132	0.00204977	0.00464893	0.001001731	547
2641	2021	132	0.00103967	0.00235799	0.000508089	547
2631	2040	132	0.00258897	0.00587185	0.00126524	547
2630	2041	132	0.00258897	0.00587185	0.00126524	547
2045	2047	11	0	0.48	0	2000
2046	2045	11	0	0.0001	0	2000
2048	2047	11	0	0.0001	0	2000
2025	2026	11	0	0.5	0	2000
2027	2026	11	0	0.0001	0	2000
5152	5151	22	0	0.0001	0	2000

Table C.9: Transformer data

From	Base kV	To	Base kV	Resistance R	Resistance X	Susceptance Ch	Rating (A)
3045	33	3042	11	0.0783	0.945	0	17
3090	33	3087	11	0.0917	1.104	0	13.1
3090	33	3087	11	0.0917	1.1	0	13.1
3057	33	3054	11	0.264	1.84	0	4.5
2005	33	3021	11	0.0625	0.955	0	19.57

2005	33	3021	11	0.0659	0.945	0	19.6
3075	33	3072	11	0.255	1.826	0	4.89
3078	33	3072	11	0.286	2.192	0	3
3069	33	3066	11	0.257	2.44	0	4.7
3096	33	3093	11	0.0826	1	0	18.5
3012	33	3009	11	0.0958	1.12	0	11.4
3012	33	3009	11	0.0969	1.13	0	11.4
3063	33	3060	11	0.157	1.35	0	10
3063	33	3060	11	0.15	1.35	0	10
3084	33	3081	11	0.29	2.18	0	4
3006	33	3003	11	0.257	1.86	0	4
3006	33	3003	11	0.0904	1.113	0	14
3006	33	3003	11	0.338	2.093	0	4
3018	33	3015	11	0.0857	1	0	17.9
3018	33	3015	11	0.0863	1.01	0	17.9
3051	33	3048	11	0.257	1.88	0	4.7
3027	33	3024	11	0.0713	1.057	0	18.47
3030	33	3024	11	0.0714	1.014	0	18.52
3036	33	3033	11	0.0919	1.065	0	17.7
3039	33	3033	11	0.0923	0.997	0	17.7
2005	33	20051	0.415	0	1.07	0	0
2005	33	20052	0.415	0	2.351	0	0
2015	33	20151	0.415	0	1.7493	0	0
2015	33	20152	0.415	0	2.296	0	0
5140	400	5153	132	0.00081	0.04041	0	210
5140	400	5154	132	0.000795	0.04197	0	240
5151	22	5140	400	0	0.03173	0	600
2030	132	2035	11	0.0171	0.5377	0	45
2031	132	2035	11	0.0172	0.5332	0	45
2032	132	2037	11	0.0169	0.4954	0	45
2033	132	2037	11	0.0171	0.4974	0	45
2035	11	20351	0.415	0	14.88	0	0
2035	11	20352	0.415	0	14.88	0	0
2037	11	20373	0.415	0	14	0	0
2037	11	20374	0.415	0	13.97	0	0
2000	132	2005	33	0.0214	0.36	0	30
2001	132	2005	33	0.0117	0.2738	0	45
2040	132	2045	11	0.0255	0.41	0	30
2041	132	2047	11	0.0256	0.411	0	30
2045	11	20451	0.415	0	3.594	0	0
2047	11	20472	0.415	0	3.594	0	0
2010	132	2015	33	0.00405	0.24297	0	90
2011	132	2015	33	0.01005	0.2502	0	90
2010	132	2015	33	0.00405	0.24297	0	90
2011	132	2015	33	0.01005	0.2502	0	90
2020	132	2025	11	0.0188	0.3834	0	30
2021	132	2026	11	0.0185	0.3907	0	30
2025	11	20251	0.415	0	3.702	0	0
2026	11	20262	0.415	0	3.719	0	0

The power flow result of practical test system is as given below.

Bus
Data

Bus Number	Bus Name	Voltage (pu)	Voltage (kV)	V Angle (deg)	Pg (MW)	Qg (MVAr)	Pd (MW)	Qd (MVAr)	load pf
2005		0.997148	32.906	-7.2751	0	0	2	2	0.71
2015		1.000326	33.011	-6.7908	0	0	0	0	----
3003		1.001787	11.02	-10.965	0	0	5.6	0	1
3006		0.964402	31.825	-9.299	0	0	0	0	----
3009		0.992134	10.913	-13.335	0	0	10.5	0	1
3012		0.958048	31.616	-9.9183	0	0	0	0	----
3015		1.008627	11.095	-11.627	0	0	8	0	1
3018		0.962181	31.752	-9.3715	0	0	0	0	----
3021		0.99028	10.893	-11.164	0	0	14.1	0	1
3024		1.004649	11.051	-9.7592	0	0	9.1	0	1
3027		0.996601	32.888	-6.9664	0	0	0	0	----
3030		0.993161	32.774	-7.2208	0	0	0	0	----
3033		0.999053	10.99	-10.794	0	0	11.9	0	1
3036		0.995622	32.856	-7.2251	0	0	0	0	----
3039		0.99313	32.773	-7.3697	0	0	0	0	----
3042		0.990233	10.893	-11.415	0	0	4.1	0	1
3045		0.969389	31.99	-9.1594	0	0	0	0	----
3048		1.030234	11.333	-12.214	0	0	3.1	0	1
3051		0.964663	31.834	-9.0939	0	0	-4	0	-1
3054		0.990592	10.897	-13.072	0	0	4.3	0	1
3057		0.981104	32.376	-8.5141	0	0	0	0	----
3060		0.991733	10.909	-12.61	0	0	8.6	0	1
3063		0.964099	31.815	-9.2545	0	0	0	0	----
3066		0.987423	10.862	-13.569	0	0	3.1	0	1
3069		0.96948	31.993	-9.1684	0	0	0	0	----
3072		0.991832	10.91	-8.7213	0	0	2.2	0	1
3075		0.995721	32.859	-7.4517	0	0	0	0	----
3078		0.994291	32.812	-7.4458	0	0	0	0	----
3081		1.000034	11	-12.149	0	0	1.9	0	1
3084		0.958089	31.617	-9.7905	0	0	0	0	----
3087		0.99794	10.977	-11.658	0	0	9	0	1
3090		0.976217	32.215	-8.8188	0	0	0	0	----
3093		0.998905	10.988	-13.055	0	0	4.9	0	1
3096		0.953947	31.48	-10.255	0	0	0	0	----
3099		0.99521	32.842	-7.1751	0	0	0	0	----
3102		0.964615	31.832	-9.283	0	0	0	0	----
3105		0.959615	31.667	-9.8269	0	0	0	0	----
20051		0.997148	0.414	-7.2751	0	0	0	0	----
20052		0.997148	0.414	-7.2751	0	0	0	0	----
20151		1.000326	0.415	-6.7908	0	0	0	0	----
20152		1.000326	0.415	-6.7908	0	0	0	0	----
2000		1.026063	135.44	-4.0666	0	0	0	0	----
2001		1.029275	135.86	-3.7878	0	0	0	0	----
2010		1.02103	134.78	-4.5938	0	0	0	0	----
2011		1.021248	134.81	-4.5894	0	0	0	0	----
2020		1.022372	134.95	-4.3845	0	0	0	0	----
2021		1.021124	134.79	-4.4124	0	0	0	0	----

2025	1.000266	11.003	-8.3439	0	0	13.63	3.27	0.97
2026	0.995842	10.954	-9.7804	0	0	13.72	3.44	0.97
2027	0.995836	10.954	-9.7813	0	0	16.45	5.97	0.94
2030	1.029711	135.92	-3.6998	0	0	0	0	----
2031	1.030066	135.97	-3.6757	0	0	0	0	----
2032	1.029709	135.92	-3.7001	0	0	0	0	----
2033	1.030064	135.97	-3.6761	0	0	0	0	----
2035	1.0118	11.13	-6.0818	0	0	16.45	5.97	0.94
2036	1.0118	11.13	-6.0818	0	0	0	0	----
2037	1.011435	11.126	-3.8553	0	0	1.22	0.46	0.94
2040	1.02612	135.45	-4.1227	0	0	0	0	----
2041	1.024659	135.26	-4.2302	0	0	0	0	----
2045	0.991449	10.906	-4.3517	0	0	1.22	0.44	0.94
2046	0.991449	10.906	-4.3517	0	0	0	0	----
2047	0.991672	10.908	-4.2859	0	0	0	0	----
2048	0.991672	10.908	-4.2859	0	0	0	0	----
2620	1.024659	135.26	-4.2269	0	0	0	0	----
2621	1.024657	135.26	-4.2287	0	0	0	0	----
2630	1.024663	135.26	-4.2294	0	0	0	0	----
2631	1.026164	135.45	-4.12	0	0	0	0	----
2640	1.022691	135	-4.3635	0	0	0	0	----
2641	1.021644	134.86	-4.3861	0	0	0	0	----
2650	1.022694	135	-4.3636	0	0	0	0	----
2651	1.021646	134.86	-4.3861	0	0	0	0	----
5140	0.99	396	0	165.043	4.645	0	0	----
5148	1.030221	135.99	-3.6664	0	0	0	0	----
5149	1.030217	135.99	-3.6672	0	0	0	0	----
5150	1.030214	135.99	-3.6646	0	0	0	0	----
5151	0.99	21.78	0	0	0	0	0	----
5152	0.99	21.78	0	0	0	0	0	----
5153	1.030205	135.99	-1.8314	0	0	0	0	----
5154	1.030208	135.99	-1.8323	0	0	0	0	----
20251	1.000266	0.415	-8.3439	0	0	0	0	----
20262	0.995842	0.413	-9.7804	0	0	0	0	----
20351	1.0118	0.42	-6.0818	0	0	0	0	----
20352	1.0118	0.42	-6.0818	0	0	0	0	----
20373	1.011435	0.42	-3.8553	0	0	0	0	----
20374	1.011435	0.42	-3.8553	0	0	0	0	----
20451	0.991449	0.411	-4.3517	0	0	0	0	----
20472	0.991672	0.412	-4.2859	0	0	0	0	----

Line Data

From (Bus i)	To (Bus j)	Branch Code	Rated V (kV)	Pij (MW)	Qij (MVAr)	Pji (MW)	Qji (MVAr)	PLoss (MW)	% Util	Status
2015	3090	L1	33	9.2507	-0.3645	-9.01	0.6191	0.24019	53.3309	IN
3090	3045	L1	33	4.1415	0.1278	-4.11	-0.162	0.02811	28.9029	IN
3090	3057	L1	33	-4.1683	-1.195	4.183	1.1647	0.01458	25.3051	IN
2005	3069	L1	33	11.3184	1.3551	-11	-1.0402	0.27508	51.776	IN
2005	3078	L2	33	1.0035	-0.1316	-1	0.0078	0.00308	7.042	IN
2005	3075	L1	33	1.2081	-0.1193	-1.21	-0.0569	0.00182	8.4731	IN
3057	2005	L1	33	-8.5326	-1.5114	8.638	1.6038	0.10557	38.1648	IN

3069	3105	L1	33	7.918	0.7997	-7.85	-0.7148	0.07191	36.4569	IN
3105	3012	L1	33	2.8989	0.4493	-2.89	-0.4707	0.004	13.5045	IN
3105	3096	L1	33	4.9472	0.2655	-4.92	-0.2406	0.02733	21.6071	IN
2015	3012	L1	33	7.9822	0.3758	-7.66	-0.1593	0.32305	36.0309	IN
2015	3018	L1	33	7.0169	0.5072	-6.77	-0.2518	0.25088	40.2568	IN
2015	3027	L1	33	4.7229	0.2875	-4.71	-0.3801	0.01657	37.7604	IN
2015	3063	L1	33	8.9531	0.8639	-8.66	-0.5076	0.2954	51.5162	IN
2015	3036	L1	33	5.9511	0.5093	-5.93	-0.4915	0.0242	26.0683	IN
2015	3099	L1	33	10.5348	0.2567	-10.5	-0.1914	0.05238	61.2988	IN
2015	3102	L1	33	8.202	0.6684	-7.93	-0.3656	0.2708	47.1469	IN
3102	3084	L1	33	1.9229	0.0547	-1.91	-0.0787	0.01242	8.3885	IN
3102	3006	L1	33	6.0083	0.3109	-6.01	-0.3096	0.00124	25.6701	IN
3006	3018	L1	33	0.388	0.1461	-0.39	-0.192	0.00068	1.8754	IN
3018	3051	L1	33	-0.8738	0.1276	0.877	-0.1702	0.00298	3.9334	IN
3099	3030	L1	33	4.4321	-0.0273	-4.42	-0.0461	0.00912	35.3719	IN
3099	3039	L1	33	6.0504	0.2186	-6.04	-0.2398	0.01187	26.4566	IN
5153	5150	S1	132	84.0109	-0.3632	-84	3.0506	0.05387	40.0063	IN
5154	5148	S2	132	80.9296	-0.2693	-80.9	2.8593	0.04906	33.721	IN
5150	5149	L1	132	46.7274	-2.6753	-46.7	2.6774	0	0.3124	IN
5150	2000	L1	132	28.2584	2.2113	-28.2	-2.9216	0.0959	21.0014	IN
5150	2031	L2	132	8.9712	-2.5865	-8.97	-3.6987	0.00118	8.1642	IN
5148	2030	L1	132	8.7283	2.7303	-8.73	-3.5363	0.0025	10.6818	IN
5149	2631	L1	132	60.7798	1.3167	-60.6	-15.5383	0.17245	35.0368	IN
5149	5148	L1	132	-14.052	-3.9941	14.05	3.9943	0	0.0975	IN
2000	2620	L1	132	12.3563	0.1265	-12.3	-0.8575	0.01553	9.8862	IN
2001	5148	L1	132	-58.046	-9.1881	58.1	-9.5839	0.05374	39.2227	IN
2001	2620	L1	132	35.4032	3.9575	-35.3	-4.216	0.12753	28.4463	IN
2030	2032	L1	132	0.5667	0.1984	-0.57	-0.1984	0	0.1313	IN
2031	2033	L1	132	0.6534	0.2658	-0.65	-0.2658	0	0.1543	IN
2036	2035	L0	11	0	0	0	0	0	0	IN
2621	2010	L1	132	31.8354	2.8043	-31.7	-3.0842	0.09393	25.5274	IN
2621	2620	L1	132	-32.071	-2.315	32.07	2.316	0	0.2146	IN
2621	2630	L1	132	0.2354	-0.4892	-0.24	0.0863	0	0.3173	IN
2620	2631	L1	132	-59.564	-15.382	59.62	15.2727	0.05885	49.202	IN
2620	2011	L1	132	31.0303	1.8829	-30.9	-2.4409	0.08964	24.8376	IN
2620	2640	L1	132	18.7194	5.2057	-18.7	-5.4656	0.02323	14.5454	IN
2620	2641	L1	132	25.3595	11.0509	-25.3	-11.2396	0.04371	20.696	IN
2640	2650	L1	132	0	-0.1048	0	0	0	0.0419	IN
2640	2020	L1	132	18.6962	5.5703	-18.7	-5.6149	0.00379	15.6028	IN
2641	2651	L1	132	0	-0.1046	0	0	0	0.0418	IN
2641	2021	L2	132	25.3158	11.3442	-25.3	-11.3798	0.00767	22.1852	IN
2631	2040	L1	132	0.985	0.2656	-0.98	-0.3987	0.00003	0.8327	IN
2630	2041	L1	132	0.2354	-0.0863	-0.24	-0.0465	0	0.1962	IN
2045	2047	L1	11	-0.2354	-0.046	0.235	0.0463	0	0.6294	IN
2046	2045	L0	11	0	0	0	0	0	0	IN
2048	2047	L0	11	0	0	0	0	0	0	IN
2025	2026	L1	11	4.9939	0.9476	-4.99	-0.8185	0	13.31	IN
2027	2026	L0	11	-16.45	-5.97	16.45	5.9703	0	45.9252	IN
5152	5151	L0	22	0	0	0	0	0	0	IN

Transformer Data

From	To	Branch	Pij	Qij	Pji	Qji	P Loss		Tap

(Bus i)	(Bus j)	Code	(MW)	(MVAr)	(MW)	(MVAr)	(MW)	% Util	Ratio		Status
3045	3042	T1	4.1134	0.162	-4.1	0	0.013	24.1665	0.975		IN
3090	3087	T1	4.5105	0.2244	-4.4919	-0	0.019	34.3814	0.973		IN
3090	3087	T2	4.5268	0.2238	-4.5081	7E-04	0.019	34.5056	0.973		IN
3057	3054	T1	4.3497	0.3467	-4.3	0	0.05	96.2616	0.976		IN
2005	3021	T1	7.0453	0.4941	-7.0139	-0.02	0.031	35.9645	1		IN
2005	3021	T2	7.1198	0.4688	-7.0861	0.015	0.034	36.279	1		IN
3075	3072	T1	1.2062	0.0569	-1.2025	-0.03	0.004	24.6467	1		IN
3078	3072	T2	1.0004	-0.0078	-0.9975	0.03	0.003	33.3067	1		IN
3069	3066	T1	3.1253	0.2405	-3.1	0	0.025	66.3252	0.971		IN
3096	3093	T1	4.9199	0.2406	-4.9	0	0.02	26.5561	0.95		IN
3012	3009	T1	5.3004	0.317	-5.2734	-0	0.027	46.418	0.959		IN
3012	3009	T2	5.2535	0.313	-5.2266	6E-04	0.027	46.0063	0.959		IN
3063	3060	T1	4.3282	0.2426	-4.2987	0.011	0.029	43.169	0.964		IN
3063	3060	T2	4.3295	0.2649	-4.3013	-0.01	0.028	43.1942	0.964		IN
3084	3081	T1	1.9105	0.0787	-1.9	0	0.01	47.6511	0.952		IN
3006	3003	2A	1.5768	0.013	-1.5705	0.033	0.006	39.3457	0.959		IN
3006	3003	T1	2.646	0.1709	-2.6397	-0.09	0.006	18.9028	0.959		IN
3006	3003	T2	1.3964	-0.0204	-1.3899	0.061	0.007	34.8464	0.959		IN
3018	3015	T1	4.0335	0.1583	-4.0199	5E-04	0.014	22.504	0.95		IN
3018	3015	T2	3.9936	0.1578	-3.9801	-0	0.013	22.2817	0.95		IN
3051	3048	T2	3.1233	0.1702	-3.1	0	0.023	66.2543	0.928		IN
3027	3024	T1	4.7064	0.3801	-4.6908	-0.15	0.016	25.4869	0.986		IN
3030	3024	T2	4.423	0.0461	-4.4092	0.15	0.014	23.8525	0.986		IN
3036	3033	T1	5.9269	0.4915	-5.8949	-0.12	0.032	33.4557	0.988		IN
3039	3033	T2	6.0385	0.2398	-6.0051	0.121	0.033	34.0385	0.988		IN
2005	20051	E1	0	0	0	0	0	----	1		IN
2005	20052	E2	0	0	0	0	0	----	1		IN
2015	20151	E1	0	0	0	0	0	----	1		IN
2015	20152	E2	0	0	0	0	0	----	1		IN
5140	5153	S1	84.065	2.3241	-84.011	0.363	0.054	40.0258	0.96		IN
5140	5154	S2	80.979	2.3208	-80.93	0.269	0.049	33.7379	0.96		IN
5151	5140	T2	0	0	0	0	0	0	1		IN
2030	2035	G1	8.1591	3.338	-8.1466	-2.94	0.013	19.4196	1		IN
2031	2035	G2	8.3165	3.4329	-8.3034	-3.03	0.013	19.8165	1		IN
2032	2037	G3	0.5667	0.1984	-0.5667	-0.2	0	1.3336	1.017		IN
2033	2037	G4	0.6534	0.2658	-0.6533	-0.26	0	1.5665	1.017		IN
2035	20351	E1	0	0	0	0	0	----	1		IN
2035	20352	E2	0	0	0	0	0	----	1		IN
2037	20373	E3	0	0	0	0	0	----	1		IN
2037	20374	E4	0	0	0	0	0	----	1		IN
2000	2005	G1	15.806	2.7951	-15.752	-1.88	0.054	53.193	1.017		IN
2001	2005	G2	22.643	5.2307	-22.581	-3.79	0.062	51.2619	1.017		IN
2040	2045	G1	0.9849	0.3987	-0.9846	-0.39	0	3.5385	1.033		IN
2041	2047	G2	0.2354	0.0465	-0.2354	-0.05	0	0.7997	1.033		IN
2045	20451	E1	0	0	0	0	0	----	1		IN
2047	20472	E2	0	0	0	0	0	----	1		IN
2010	2015	G1	15.871	1.5421	-15.861	-0.93	0.01	17.6851	1.017		IN
2011	2015	G2	15.47	1.2205	-15.446	-0.62	0.024	17.2096	1.017		IN
2010	2015	G1	15.871	1.5421	-15.861	-0.93	0.01	17.6851	1.017		IN
2011	2015	G2	15.47	1.2205	-15.446	-0.62	0.024	17.2096	1.017		IN
2020	2025	G1	18.692	5.6149	-18.624	-4.22	0.069	64.3551	1		IN
2021	2026	G2	25.308	11.3798	-25.176	-8.59	0.132	90.5844	0.983		IN

2025	20251	E1	0	0	0	0	0	----	1	IN
2026	20262	E2	0	0	0	0	0	----	1	IN

D Published Papers

1. Furong Li and Matlotse E., "Long-run incremental cost pricing based on nodal voltage spare capacity**",** IEEE PES General Meeting, pp. 1-5**,** 20-24 July 2008.

2. Matlotse E. and Furong Li, "Long-run incremental cost pricing for the use of network reactive power compensation devices for systems with different R/X ratios", IEEE PES General Meeting, pp. 1-8**,** 26-30 July 2009.

Long-run Incremental Cost Pricing Based on Nodal Voltage Spare Capacity

Furong Li and E. Matlotse

Abstract— This paper proposes long-run incremental cost (LRIC) pricing to reflect the investment cost in network to maintain the quality of supply, i.e. ensuring that nodal voltages are within limits. The proposed approach makes use of spare nodal voltage capacity or headroom of an existing network (distribution and transmission systems) to provide the time to invest in reactive power compensation devices. A nodal reactive power withdrawal or injection will impact on system voltages, which in turn defer or accelerate the future network investment, the LRIC-voltage network charge aims to reflect the impact on network voltage profiles as the result of nodal reactive power perturbation. This approach provides forward-looking signals that reflect both the voltage profiles of an existing network and the indicative future cost of VAr compensation assets. The forward-looking LRIC-voltage charges can be used to influence the location of future generation/demand for bettering network quality.

Index Terms—LRIC-voltage charges, Long-run incremental cost pricing and RPP problem.

I. Introduction

The deregulation of the electric power systems has generated new effort to tackle "green house" effects and binding statutory requirements in encouraging efficient utilization of network assets. Maintaining the quality of supply is one of the key goals required from the network operators. This can be achieved by the use of the reactive power compensation devices in supporting the nodal voltages whilst transporting real power thus improving the efficiency of the network.

The investment costs of maintaining network voltages within statutory limits should be recovered from generators, large industrial customers and suppliers. An approach for network charging to reflect potential impact on network voltages needs to satisfy to purposes:

1) to recover capital, operation and maintenance costs of the network VAr compensation assets thus enabling the concerned network establishments to gain a reasonable rate of return on the capital invested;
2) to provide forward-looking, economically efficient signals that reflect both the extent of the network VAr compensation assets required to service withdrawal and/or injection and at the degree of network VAr compensation asset use. This aims to influence the future use of the system by network users to benefit the system voltage profiles.

The majority of the network charging methodologies reflect the investment cost incurred in circuits and transformers to support real and reactive power flow. To reflect investment cost incurred for maintaining network voltages in network charges has received very little attention in network charges [5-9]. Paper [1] presents the first integrated framework for VAr planning and spot-pricing based on marginal costs but it does not have the ability to influence the future use of the system to benefit the network. Other approaches in reactive power pricing tend to reflect the operational cost from new customers, i.e. how they might change network losses [2, 3, 4]. They do not reflect the capital investment cost.

The usage-based MW-Miles or MVA-Miles charging methodologies [7] reflect the extent of the use of the network by network users. The usage-based methodologies were found inefficient as they cannot discriminate between network users who incur additional operating costs or network reinforcement and expansion, and those who reduce otherwise needed network upgrades. It was against this background that the concept of incremental charging methodologies was preferred [5, 6]. The approaches of [8, 9] were employed and they successfully addressed the concerns found lacking in the usage-based methodologies.

This paper proposes an LRIC approach to price the capital cost incurred in the network to support nodal voltages. The approach employs the unused nodal voltage capacity or headroom within an existing network to provide an economically efficient forward-looking pricing signal to direct the siting of future demand and generation. A nodal injection/withdrawal of reactive power will impact on the nodal voltage, the impact will be further propagated over the entire network. The impact on the nodal voltage will affect the investment horizon of network compensation devices. As the LRIC aims to give indicative future investment cost in maintaining system voltage profiles, each study node is a candidate for a reactive compensation device. Depending on the headroom of each study node, the investment horizon for each nodal can be inferred. For a nodal reactive perturbation, there will be a related benefit if the system wide investment can be deferred otherwise there will be a cost if it can be advanced. Then the LRIC-voltage charges are the sum of the

Furong Li is with the Department of Electronic & Electrical Engineering, University of Bath, Bath, BA2 7AY U.K. (e-mail: F.Li@bath.ac.uk).

Edwin Matlotse is a PhD student at the University of Bath, Department of Electronic & Electrical Engineering, Bath, BA2 7AY U.K.(e-mail: em246@bath.ac.uk).

difference in the present value of the future investment with and without the nodal reactive power injection or withdrawal.

II. Mathematical Formulation of Long-run Incremental Cost Pricing Based on DC Power Flow

The voltage charging principle is based upon the premise that for an assumed nodal generation/load growth rate there will be an associated rate of busbar voltage degradation. Given this assumption the time horizon for a busbar to reach its upper /lower voltage limit can be evaluated. Once the limit has been reached there will be a capital cost associated to keep the nodal level within the statutory limits. A nodal demand/generation increment would affect the reinforcement investment horizon. The nodal voltage charge would then be the difference in the present value of the future reinforcement consequent to voltage with and without the nodal power flow.

The proposed charging model can be implemented through the following steps:

1) Evaluating the future cost of network to support an existing customer at node N

If a network node b, has lower voltage limit, V_L and upper voltage limitV_H, and supports a voltage V_b, then the number of years for the voltage to grow from V_b to V_L/V_H for a given voltage degradation rate v can be evaluated from (1.a) or (1.b)

for demand: $V_L = V_b \times (1-v)^{n_{bL}}$ (1.a)

for generation: $V_H = V_b \times (1+v)^{n_{bH}}$ (1.b)

where: n_{bL}/n_{bH} is the number of years V_b takes to reach V_L / V_H

Reconfiguring equations (1.a) and (1.b) constitute:

$$(1-v)^{n_{bL}} = \frac{V_L}{V_b} \quad (2.a)$$

$$(1+v)^{n_{bH}} = \frac{V_H}{V_b} \quad (2.b)$$

Taking the logarithm of equations (2.a) and (2.b) on both sides gives

$$n_{bL} x \log(1-v) = \log V_L - \log V_b \quad (3.a)$$

$$n_{bH} x \log(1+v) = \log V_L - \log V_b \quad (3.b)$$

then the values of n_{bL}/n_{bH} are

$$n_{bL} = \frac{\log V_L - \log V_b}{\log(1-v)} \quad (4.a)$$

$$n_{bH} = \frac{\log V_H - \log V_b}{\log(1+v)} \quad (4.b)$$

The assumption is that when the node is fully loaded the reinforcement will take effect. This means that investment will be effected in n_{bL} / n_{bH} years when the node utilization reaches V_b. At this point an installation of a VAr compensation asset is regarded as the future investment that will be needed at the node to support the voltage.

2) Determining the present value of future investment cost

The function of how far into the future investment can be effected can be determined by evaluating the future investment by discounted it back to its present value. For a set discount rate of d, then the present value of the future investment in n_b years will be:

$$PV_{bL} = \frac{Asset_{CbL}}{(1+d)^{nbL}} \quad (5.a)$$

$$PV_{bH} = \frac{Asset_{CbH}}{(1+d)^{nbH}} \quad (5.b)$$

where $Asset_{CbL}$ / $Asset_{CbH}$ is the modern equivalent asset cost to cater for supporting voltage due to lower voltage limit / upper voltage limit.

3). Deriving the incremental cost of an additional power injection or withdrawal at node N

If the nodal voltage change is ΔV_{bL} consequent upon an additional withdrawal / injection at node N of ΔQ_{in}, will put forward / delay the future investment from year n_{bL} to n_{bnewL}

for withdrawal $V_L = (V_b - \Delta V_{bL}) \times (1-v)^{n_{bnewL}}$ (6.a)

for injection $V_L = (V_b + \Delta V_{bL}) \times (1-v)^{n_{bnewL}}$ (6.b)

for withdrawal $V_H = (V_b - \Delta V_{bH}) \times (1+v)^{nH}$ (6.c)

for injection $V_H = (V_b + \Delta V_{bH}) \times (1+v)^{n_{bnewH}}$ (6.c)

Equations (7.a), (7.b), (7.c) and (7.d) give the new investment horizon as

$$n_{bnewL} = \frac{\log V_L - \log(V_b - \Delta V_{bL})}{\log(1-v)} \quad (7.a)$$

$$n_{bnewL} = \frac{\log V_L - \log(V_b + \Delta V_{bL})}{\log(1-v)} \quad (7.b)$$

$$n_{bnewH} = \frac{\log V_H - \log(V_b - \Delta V_{bH})}{\log(1+v)} \quad (7.c)$$

$$n_{bnewH} = \frac{\log V_H - \log(V_b + \Delta V_{bH})}{\log(1+v)} \quad (7.d)$$

then the present values of the future investments are

$$PV_{bnewL} = \frac{Asset_{CbL}}{(1+d)^{nbnewL}} \quad (8.a)$$

$$PV_{bnewH} = \frac{Asset_{CbH}}{(1+d)^{nbnewH}} \quad (8.b)$$

The changes in the present values as consequent of the nodal withdrawal / injection ΔQ_{In} are given by (9.a) and (9.b)

$$\Delta PV_{bL} = PV_{bnewL} - PV_{Lb} = Asset_{CbL}\left(\frac{1}{(1+d)^{n_{bnewL}}} - \frac{1}{(1+d)^{n_bL}}\right) \quad (9.a)$$

$$\Delta PV_{bH} = PV_{bnewH} - PV_{bH} = Asset_{CbH}\left(\frac{1}{(1+d)^{n_{bnewH}}} - \frac{1}{(1+d)^{n_bH}}\right) \quad (9.b)$$

The annualized incremental cost of the network items associated with component b is the difference in the present values of the future investment due to ΔP_{In} at node N multiplied by an annuity factor

$$IV_{bL} = \Delta PV_{bL} * annuityfactor \quad (10.a)$$

$$IV_{bH} = \Delta PV_{bH} * annuityfactor \quad (10.b)$$

4) Evaluating the long-run incremental cost

The long-run incremental costs to support Node N will be the aggregation of the incremental costs all over the supporting nodes and are

$$LRIC_{NL} = \frac{\sum_{bL} IV_{bL}}{\Delta P_{In}} \quad (11.a)$$

$$LRIC_{NH} = \frac{\sum_{bH} IV_{bH}}{\Delta P_{In}} \quad (11.b)$$

III. IMPLEMENTATION

The 4-bus network shown in Figure 1, has demand D1 supported by one circuit, while D2 is supported by two circuits. All the circuits are assumed to be identical and the potential VAR compensation assets (SVC) at all the buses are also identical assumed to have the same investment cost of £1,450,000. The circuit maximum rating is 45 MVAr and the nodes are at 275kV. The voltage limits are assumed to be $1 \pm 6\%$ pu. The use of an optimal power flow (OPF) was employed to capture the nodal voltages and the circuit utilization while varying the loading condition of the system.

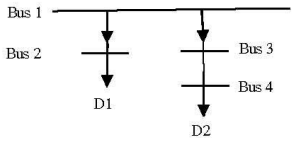

Figure 1. 4-bus network

D1 and D2 were varied from 0 to 45 MVAr, constituting a change of 0% to 100%, while monitoring the respective bus voltages and percentage circuit utilization to support buses 2 and 4. The proposed charging approach provides the LRIC voltage charges for demand connecting at bus 2 as shown by fig. 2 and table 1. The charges at bus 2 monotonically increase with increasing circuit utilization. As can be seen from table 1, the voltages are within specified limits. Further, fig.3 shows the charges at buses 2 and 4, while table 3 shows the charges, the circuit utilization, the voltages at buses 2, 3 and 4. In figure 3, buses 2 and 3 have monotonically increasing charges with increasing circuit utilization. Buses 2 and 3 charges are within for the whole ranges of the respective circuit utilizations and voltage limits. On the other hand, Bus 4 charges increases steadily and towards the lower voltage limit they rise sharply. From table 2 it can be seen that at 100% circuit utilization, the lower voltage limit is exceeded and the charges even rise more sharply. This is because reinforcement was supposed to have been effected when the lower voltage limit was reached.

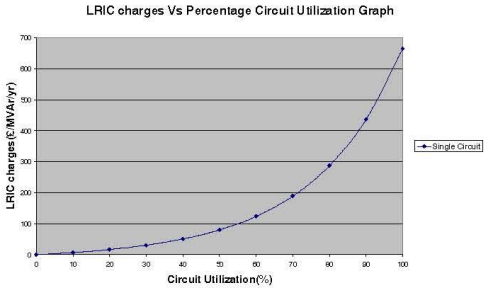

Figure 2. LRIC at bus 2 due to withdrawal.

TABLE 1: LRIC, CIRCUIT UTILIZATION AND VOLTAGE AT BUS 2

% Circuit Utilization	V2	V2 charges (£/MVAr/yr)
0	1.06	0
10	1.055	6.68
20	1.05	16.26
30	1.044	30.13
40	1.039	50.27
50	1.033	79.86
60	1.028	123.61
70	1.022	188.78
80	1.017	287.07
90	1.011	436.08
100	1.005	663.99

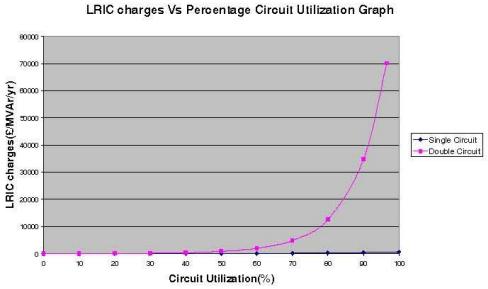

Figure 3. LRIC at bus 2 and bus 4

TABLE 2: LRIC, CIRCUIT UTILIZATION AND VOLTAGE AT BUSES 2, 3 &4

% Cct Util	V2 pu	V3 pu	V4 pu	V2 chrgs £/MVAr/yr	V2 chrgs £/MVAr/yr	V2 chrgs £/MVAr/yr
0	1.06	1.06	1.06	0	0	0
10	1.055	1.055	1.03	6.68	6.81	25.71
20	1.05	1.049	1.039	16.26	17	75.22
30	1.044	1.044	1.028	30.13	32.57	175.48
40	1.039	1.038	1.016	50.27	56.86	389.35
50	1.033	1.031	1.004	79.86	95.66	870.5
60	1.028	1.025	0.991	123.61	159.22	2015.02
70	1.022	1.018	0.978	188.78	266.18	4899.25
80	1.017	1.01	0.964	287.07	451.79	12635.81
90	1.011	1.002	0.95	436.08	784.87	34829.28
100	1.005	0.994	0.935	663.99	1405.57	103 420.16

Flipping the single circuit to the left provides figure 4, where a 0% circuit utilization of the double circuit corresponds to 100% of the single circuit. Figure 4 show that the cost to the network will be the same for a node that is supported by double circuits loaded at 31%, or by a single circuit loaded at 69%.

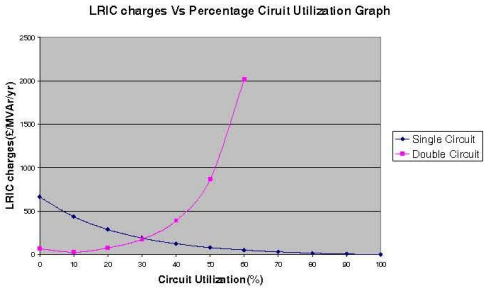

Figure 4: The equilibrium between the nodal extent of use and the degree of circuit utilization.

IV. CONCLUSIONS

This paper presents an approach that prices the capital investment cost incurred in the network for keeping the system voltages within statutory limits. The proposed approach is based on a long-run incremental cost (LRIC) pricing developed in Bath, pricing the use of network circuits and transformers by network customers at each node of the network. The most attraction of the approach is that for the first time a method is proposed to allocate the cost of maintaining the quality of supply based on the spare nodal voltage capacity of an exiting network. The paper demonstrated a very simple approach to determine the indicative cost of LRIC-voltage charges. The resulting network voltage charging model is reflecting the extent of the network buses utilized by a connected party and the degree of the network nodal utilization. This aims to influence future network users to change their utilization patterns to better network voltage profiles.

V. REFERENCES

[1] D. Chattopadhyay, K. Bhattacharya, J. Parikh, "Optimal reactive power planning and its spot-pricing: an integrated approach", IEEE Transactions on Power Systems, Volume 10, no. 4, pp. 2014 – 2020, Nov.1995.

[2] R.A. Fernandes, F. Lange, R.C. Burchett, H.H. Happ, K.A. Wirgau, "Large Scale Reactive Power Planning", IEEE Transactions on Power Apparatus and Systems, Volume 102, no. 5, pp. 1083 – 1088, May 1983.

[3] W. Zhang, F. Li, L.M. Tolbert, "Review of Reactive Power Planning: Objectives, Constraints, and Algorithms", IEEE Transactions on Power Systems, volume 22, no. 4, pp. 2177 – 2186, Nov. 2007.

[4] V. Gopalakrishnan, P. Thirunavukkarasu, R. Prasanna, "Reactive power planning using hybrid evolutionary programming method", Power Systems Conference and Exposition, 2004. IEEE PES, vol.3, pp. 1319 – 1323, Oct. 2004.

[5] D. Shirmohammadi, X.V.Filho, B. Gorenstin, and M.V.P. Pereira, "Some fundamental technical concepts about cost based transmission pricing", IEEE Tran. On Power Systems, vol. 11 no. 2, pp 1001-1008, May, 1996.

[6] H.H. Happ, "Cost of wheeling methodologies", IEEE Tran. On Power Systems, vol. 9 no. 1, pp 147-156, February, 1994.

[7] J. Pan, Y. Teklu, S. Rahman and K. Jun, "Review of usage-based transmission cost allocation methods under open access", IEEE Tran. On Power Systems, vol. 15 no. 4, pp 1218-1224, November, 2000

[8] Furong Li, "Long-run marginal cost pricing based on network spare capacity", IEEE Trans. Power Syst., vol. 22, no.2, pp. 885-886, May 2007.

[9] Furong Li, D.L. Tolly, "Long-run incremental cost pricing based on unused capacity", IEEE Trans. Power Syst., vol. 22, no. 4, pp. 1683-1689, Nov. 2007.

VI. BIOGRAPHIES

Dr. Furong Li (M'2000) was born in Shannxi, China. She received her B.Eng. in Electrical Engineering from Hohai University, China in 1990, and her Ph.D. in 1997 with a thesis on Applications of Genetic Algorithms in Optimal Operation of Electrical Power Systems. She is a senior lecturer in the Power and Energy Systems Group at the University of Bath. Her major research interest is in the area of power system planning, analysis and power system economics.

Mr Edwin Matlosze is a PhD student in the Power and Energy Systems Group at the University of Bath. His major research interest is in the area of reactive power planning, analysis and network charging.

Long-Run Incremental Cost Pricing for the Use of Network Reactive Power Compensation Devices for Systems with Different R/X Ratios

E. Matlotse, *Student Member, IEEE* and Furong Li, *Member, IEEE*

Abstract-- The LRIC-voltage network charging pricing principle is intended to reflect the investment cost of a network to maintain the quality of supply, i.e. ensuring that nodal voltages are within required statutory limits. This charging principle is based on spare nodal voltage capacity or headroom of an existing network (distribution and transmission systems) to provide the time to invest in reactive power (VAr) compensation devices. A nodal reactive power/real power withdrawal/injection will impact on system-wide voltages, which in turn defer or advance the future network investment, the LRIC-voltage network charge aims to reflect the impact on network voltage profiles as the result of nodal reactive power/real power perturbation. This approach also provides forward-looking economically efficient signals that reflect both the voltage profiles of an existing network and the indicative future cost of VAr compensation assets. The forward-looking LRIC-voltage charges can be utilized to influence the location of future generation/demand for bettering the network quality.

The LRIC-voltage network charges are different for different network types. What sets networks apart are the resulting resistance/reactance (R/X) ratios on network circuits.

This paper analyses the trend of LRIC-voltage charges on different types of networks, providing insights into how charges will change with different R/X ratios. These charges provide correct economic signals to potential network users, which help them to make informed decisions as to whether to invest in reactive power devices or pay for the network for reactive power provision. This will ultimately guide towards an effective and efficient usage of the network's reactive power resources. This study is carried-out on a 9-bus network which is a subset of the practical Western Power Distribution (WPD) network. All views presented in this paper are those of the authors and not necessarily those of WPD.

***Index Terms*-- R/X ratios, VAr compensation assets, Long-run incremental cost-voltage network charges and spare nodal voltage capacity.**

I. Introduction

Under the current privatization and deregulation environment, one of the principle requirements are that the network cost should reflect the true economic cost of the service provided, attributable and allocated to all network users. Network operators are charged with the responsibility to maintain the network security and quality of supply at all times. This can be achieved by employing the use of reactive compensation devices in supporting the nodal voltages whilst transporting real power, thereby improving the efficiency of the network.

Reactive power support can be categorized as a component that supports real power shipment, supplies reactive loads and provides reserve for maintaining voltage profiles under steady state and following credible contingencies. To this effect, network operators are required to secure adequate reactive power support to assist real power shipment coupled with improving network security [1]. The reactive power support in a network comes from three sources: 1) generators that can generate reactive power 2) networks for carrying and producing reactive power for maintaining the security and quality of supply 3) suppliers who affect consumers' reactive power consumption [2]. Most research in reactive power pricing [1, 3-14] reflects the benefits from the first source – generation, reflecting the operational cost due to new customers, i.e. how they might change network losses. This paper is concerned with the support from the network, particularly, the pricing of reactive power devices in the network in maintaining the network voltage profiles within acceptable limits given different network R/X circuit ratios to ensure that correct economic signals are attained when employing specific assumptions in determining such.

The investment costs of maintaining network voltages within acceptable limits should be recovered from generators, large industrial customers and suppliers. A scheme for network charging to reflect the potential impact on network voltages needs to satisfy two purposes:

1) to recover capital, operation and maintenance costs of the network VAr compensation assets thus enabling the concerned network establishments to gain a reasonable rate of return on the capital invested;
2) to provide forward-looking, economically efficient signals that reflect both the extent of the network VAr compensation assets required to service withdrawal and/or injection and at the degree of network VAr compensation asset use. This aims to influence the future use of the system by the network users to better the system voltage profiles.

The methodology used in this study, LRIC-voltage network charging pricing principle [15] satisfy both the two purposes outlined above, however, different status of the network R/X circuit ratios ought to be assessed in the context of network practical representation which ranges from transmission to distribution systems. This study will ensure that correct price signals are attained by employing

Furong Li is with the Department of Electronic & Electrical Engineering, University of Bath, Bath, BA2 7AY U.K. (e-mail: F.Li@bath.ac.uk).

Edwin Matlotse is a PhD student at the University of Bath, Department of Electronic & Electrical Engineering, Bath, BA2 7AY U.K.(e-mail: em246@bath.ac.uk).

978-1-4244-4241-6/09/$25.00 ©2009 IEEE

specific assumptions when dealing with either of the systems.

This paper is concerned with a study on varying networks R/X circuit ratios employing LRIC-voltage network charging pricing principle to price the capital investment incurred in the network to support nodal voltages. The used approach employs the use of the unused nodal voltage capacity or headroom within an existing network to provide an economically efficient forward-looking pricing signal to influence the siting of future demand and generation for bettering network voltage profiles. A nodal withdrawal/injection of reactive power/real power will impact on the nodal voltage, which will be further propagated over the entire network. The impact on the nodal voltage will affect the investment horizon of network compensation devices. As the LRIC aims to give indicative future investment cost in maintaining voltage profiles, each study node is a candidate for a reactive power compensation device. Depending on the headroom of each study node, the investment horizon for each node can be inferred. For a nodal reactive power/real power perturbation, there will be a related benefit if the system wide investment can be deferred otherwise there will be a cost if it can be advanced. Then the LRIC-voltage (LRIC-V) network charges are the sum of the difference in the present value of the future investment with and without the nodal reactive power/real power injection or withdrawal.

This paper is organized as follows: Section II details the mathematical model of the used LRIC charging methodology. Section III provides a demonstration of the study carried-out on a 9-bus network which is a subset of the practical WPD network. The paper's conclusions are drawn in Section IV.

II. Mathematical Formulation of Long-run Incremental Cost Pricing Based on Nodal Spare Capacity

The LRIC-V network charging principle is based upon the premise that for an assumed nodal generation/load growth rate there will be an associated rate of busbar voltage degradation. Given this assumption the time horizon for a busbar to reach its upper /lower voltage limit can be evaluated. Once the limit has been reached, a compensation device will be placed at the node as the required network reinforcement to support the network voltage profiles. A nodal demand/generation increment would affect the reinforcement investment horizon. The nodal voltage charge would then be the difference in the present value of the future reinforcement consequent to voltage with and without the nodal increment

The following steps outlined below can be utilized to implement the proposed charging model:

1) Evaluating the future cost of network to support existing customes

If a network node b, has lower voltage limit, V_L and upper voltage limit, V_H, and holds a voltage level of V_b, then the number of years for the voltage to grow from V_b to V_L/V_H for a given voltage degradation rate v_r can be evaluated from (1.a) or (1.b)

when V_L is critical: $V_L = V_b \times (1-v_r)^{n_{bL}}$ (1.a)

when V_H is critical: $V_H = V_b \times (1+v_r)^{n_{bH}}$ (1.b)

where: n_{bL} *and* n_{bH} are the respective numbers of years that takes V_b reach V_L and V_H

Reconfiguring equations (1.a) and (1.b) constitute:

$$(1-v)^{n_{bL}} = \frac{V_L}{V_b} \quad (2.a)$$

$$(1+v)^{n_{bH}} = \frac{V_H}{V_b} \quad (2.b)$$

Taking the logarithm of equations (2.a) and (2.b) on both sides gives

$$n_{bL} x \log(1-v) = \log V_L - \log V_b \quad (3.a)$$

$$n_{bH} x \log(1+v) = \log V_H - \log V_b \quad (3.b)$$

then the values of n_{bL}/n_{bH} are

$$n_{bL} = \frac{\log V_L - \log V_b}{\log(1-v)} \quad (4.a)$$

$$n_{bH} = \frac{\log V_H - \log V_b}{\log(1+v)} \quad (4.b)$$

The assumption is that when the node is fully loaded the reinforcement will take effect. This means that investment will be effected in n_{bL}/n_{bH} years when the node utilization reaches V_L/V_H, respectively. At this point an installation of a VAr compensation asset is regarded as the future investment that will be needed at the node to support the voltage.

2) Determining the present value of future investment cost

For a given discount rate of d, the present value of the future investment in n_{bL}/n_{bH} years will be:

$$PV_{bL} = \frac{Asset_{CbL}}{(1+d)^{nbL}} \quad (5.a)$$

$$PV_{bH} = \frac{Asset_{CbH}}{(1+d)^{nbH}} \quad (5.b)$$

where $Asset_{CbL}$ and $Asset_{CbH}$ are the modern equivalent asset cost to cater for supporting voltage due to lower voltage limit and upper voltage limit violations.

3). Deriving the incremental cost of an additional power injection or withdrawal at node N

If the nodal voltage change is ΔV_{bL} / ΔV_{bH} consequent upon an additional withdrawal/injection at node N due to the VAr magnitude change ΔQ_{In} / ΔP_{In}, this will put forward/delay the future investment from year n_{bL}/n_{bH} to n_{bnewL}/n_{bnewH} and when V_L is critical

for withdrawal $V_L = (V_b - \Delta V_{bL}) \times (1-v)^{n_{bnewL}}$ (6.a)

or

for injection $V_L = (V_b + \Delta V_{bH}) \times (1-v)^{n_{bnewL}}$ (6.b)

when V_H is critical

for withdrawal $V_H = (V_b - \Delta V_{bH}) \times (1+v)^{n_{bnewH}}$ (6.c)

or

for injection $V_H = (V_b + \Delta V_{bL}) \times (1+v)^{n_{bnewH}}$ (6.d)

Equations (7.a), (7.b), (7.c) and (7.d) give the new investment horizon as

$$n_{bnewL} = \frac{\log V_L - \log(V_b - \Delta V_{bL})}{\log(1-v)} \quad (7.a)$$

or

$$n_{bnewL} = \frac{\log V_L - \log(V_b + \Delta V_{bL})}{\log(1-v)} \quad (7.b)$$

$$n_{bnewH} = \frac{\log V_H - \log(V_b - \Delta V_{bL})}{\log(1+v)} \quad (7.c)$$

or

$$n_{bnewH} = \frac{\log V_H - \log(V_b + \Delta V_{bH})}{\log(1+v)} \quad (7.d)$$

then the present values of the future investments are

$$PV_{bnewL} = \frac{Asset_{CbL}}{(1+d)^{nbnewL}} \quad (8.a)$$

$$PV_{bnewH} = \frac{Asset_{CbH}}{(1+d)^{nbnewH}} \quad (8.b)$$

The changes in the present values as consequent of the nodal withdrawal/injection $\Delta Q_{ln} / \Delta P_{ln}$ are given by (9.a) and (9.b)

$$\Delta PV_{bL} = PV_{bnewL} - PV_{bL} = Asset_{CbL}\left(\frac{1}{(1+d)^{n_{bnewL}}} - \frac{1}{(1+d)^{n_b L}}\right) \quad (9.a)$$

$$\Delta PV_{bH} = PV_{bnewH} - PV_{bH} = Asset_{CbH}\left(\frac{1}{(1+d)^{n_{bnewH}}} - \frac{1}{(1+d)^{n_{bH}}}\right) \quad (9.b)$$

The annualized incremental cost of the network items associated with component *b* is the difference in the present values of the future investment due to the reactive power/real power magnitude change $\Delta Q_{ln} / \Delta P_{ln}$ at node N multiplied by an annuity factor

$$IV_{bL} = \Delta PV_{bL} * annuityfactor \quad (10.a)$$

$$IV_{bH} = \Delta PV_{bH} * annuityfactor \quad (10.b)$$

4) Evaluating the long-run incremental cost

If there are a total of *bL* busbars' lower and *bH* busbars' high limits that are affected by a nodal increment from N, then the LRIC-V network charges at node N will be the aggregation of the changes in present value of future incremental costs over all affected nodes:

$$LRIC\_V_{N,L} = \frac{\sum_{bL} IV_{bL}}{\Delta Q_{ln} / \Delta P_{ln}} \quad (11.a)$$

$$LRIC\_V_{N,H} = \frac{\sum_{bH} IV_{bH}}{\Delta Q_{ln} / \Delta P_{ln}} \quad (11.b)$$

III. IMPLEMENTATION

A. 9-BUS PRACTICAL NETWORK

The 9-Bus network shown in figure 1 is a subset of the practical Western Power Distribution (WPD) network with only demand connected at the 11-kV voltage level. All views presented in this paper are those of the authors and not necessarily those of WPD. The line distances between the buses are depicted in red. Where the line distances are not shown, then the line distance is zero. The compensation assets (SVCs) have the investment costs of £58, 050 and £174, 240 at the 11-kV and 33-kV voltage levels, respectively. Bus 1 is the slack bus. The voltage limits are assumed to be $1 \pm 6\%$ pu. The use of power flow was employed to capture the nodal voltages while performing nodal withdrawals/injection on the system.

The annual load growth rate for this practical network is assumed to be 1.6% while the discount rate is assumed to be 6.9%. To demonstrate the value of the proposed LRIC-voltage network charging methodology three cases have been used to show the cost/benefit to the network when the resistance/reactance (R/X) ratios of circuits are varied from when R and X are comparable, to where X dominates R and finally where R dominates X given the nodal withdrawal/injection. Case 1 involves nodal withdrawals of 1 MVAr and 1 MW, and nodal injections of 1 MVAr and 1 MW when the network circuit R/X ratios are slightly less than unity, each of these perturbations are performed each in turn. Case 2 and case 3 follow with the same set of perturbations as those of case 1 but case 2 having network circuit R/X ratios being equal to 0.1 while finally case 3 having network circuit ratios being equal to 10.

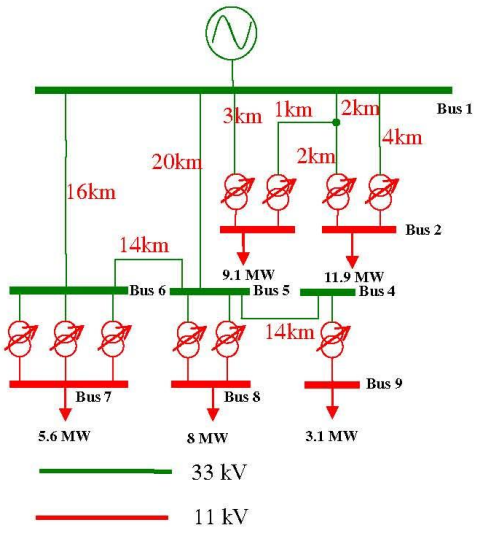

FIGURE 1: 9-BUS PRACTICAL NETWORK

B. RESULTS AND ANALYSIS

Case 1: This case involves a 1 MVAr nodal withdrawal and secondly a 1 MW nodal withdrawal when circuit reactances are slightly more than resistance counterparts. Figure 2 and tables 1and 2 show the nodal LRIC-voltage network charges and the shortest distances for each node from the slack bus during 1 MVAr and 1 MW withdrawals, respectively. In addition, tables 1 and 2 show the initial and final voltages after each withdrawal. On the other hand, figure 3 and tables 3 and 4 show the nodal LRIC-voltage network charges and the shortest distances for each node from the slack bus during 1 MVAr and 1 MW injections, respectively. In addition, tables 3 and 4 show the initial and final voltages after each injection.

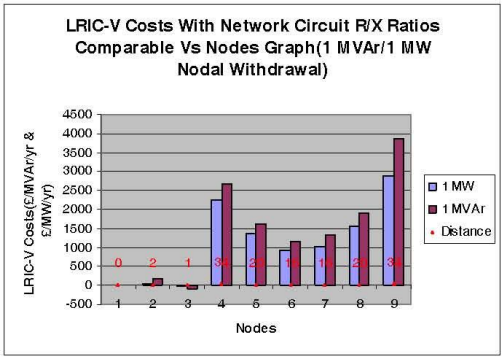

Figure 2: LRIC-voltage network charges due to 1 MVAr and 1 MW withdrawals at each node.

Table 1: LRIC-voltage network charges due to 1 MVAr withdrawal at each node

Bus	Initial Voltage(pu)	Final Voltage(pu)	LRIC-V (£/MVAr/yr)	Distance (km)
1	1.03	1.03	0	0
2	0.992	0.986	152.11	4
3	1.020	1.015	-95.06	3
4	0.971	0.962	2651.19	34
5	0.983	0.979	1634.77	20
6	0.993	0.99	1139.25	16
7	0.989	0.98	1323.58	16
8	0.978	0.969	1897.64	20
9	0.985	0.955	3853.97	34

Table 2: LRIC-voltage network charges due to 1 MW withdrawal at each node

Bus	Initial Voltage(pu)	Final Voltage(pu)	LRIC-V (£/MW/yr)	Distance (km)
1	1.03	1.03	0	0
2	0.992	0.986	27.47	4
3	1.020	1.015	-18.45	3
4	0.971	0.962	2250.35	34
5	0.983	0.979	1374.45	20
6	0.993	0.99	925.21	16
7	0.989	0.98	1033.56	16
8	0.978	0.969	1570.06	20
9	0.985	0.955	2899.9	34

Since the circuit reactances are slightly more than the corresponding circuit resistances, it can be observed from figure 2 and tables 1 and 2 that the nodal costs due to 1 MVAr withdrawals are more than those due to 1 MW withdrawals. Generally for both tables 1 and 2, it can also be observed that the costs increase as the nodal distance increase from the slack bus. For both 1 MVAr and 1 MW withdrawals, it can be seen that at bus 3 a credit is attracted since voltage is more than the target voltage of 1 pu and that means that the higher voltage limit is critical. When a withdrawal occurs at this node the higher voltage limit margin is increased, therefore, an overall credit has to be earned at this node since other nodes due to the disturbance at this node earn less costs as disturbance propagated become even less with distance from this disturbed bus.

On the other hand, other buses except for the slack bus have initial voltages less than the target voltage of 1 pu and therefore for these it means that the lower voltage limit is critical. For these buses, during withdrawal these attract costs since the already critical lower voltage limit margin is degraded further and therefore the overall results are costs at these buses as their investment horizon on VAr compensation assets are brought forward. It should also be noted that at buses 6 and 7, their respective distances from the slack bus are the same but the costs for bus 7 are more than that of bus 6 since the former is connected to the latter through three parallel transformer set therefore there is a voltage drop across this set. The same applies to pairs of buses 5 and 8, and buses 4 and 9. It should be further noted that for buses 5 and 8 two transformers are involved while one transformer is involved between buses 4 and 9.

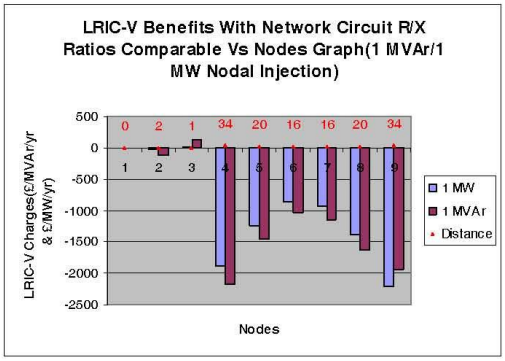

Figure 3: LRIC-voltage network charges due to 1 MVAr and 1MW injection at each node.

Table 3: LRIC-voltage network charges due to 1 MVAr injection at each node

Bus	Initial Voltage(pu)	Final Voltage(pu)	LRIC-V (£/MVAr/yr)	Distance (km)
1	1.03	1.03	0	0
2	0.992	0.998	-121.72	4
3	1.020	1.026	136.44	3
4	0.971	0.979	-2167.48	34
5	0.983	0.987	-1454.58	20
6	0.993	0.997	-1037.87	16
7	0.989	0.998	-1143.44	16
8	0.978	0.988	-1626.9	20
9	0.985	1.012	-1938.91	34

Table 4: LRIC-voltage network charges due to 1 MW injection at each node

Bus	Initial Voltage(pu)	Final Voltage(pu)	LRIC-V (£/MW/yr)	Distance (km)
1	1.03	1.03	0	0
2	0.992	0.993	-25.3	4
3	1.020	1.021	19.33	3
4	0.971	0.978	-1882.9	34
5	0.983	0.986	-1240.8	20
6	0.993	0.996	-854.69	16
7	0.989	0.993	-932.28	16
8	0.978	0.983	-1381.6	20
9	0.985	0.997	-2203.7	34

During nodal injections, it is also observed that the credits consequent to 1 MVAr injections are more than the credits for their 1 MW injection counterparts since the R/X ratio remain unchanged. It can further be observed that the credits increase as the nodal distances increase from the slack bus as can be observed from figure 2 and, tables 3 and 4. Bus 3 attracts an overall cost for both injections of real and reactive power since the initial voltage at this bus is more than the target voltage of 1 pu and therefore during injection the voltage increases as such degrading the already critical higher bus voltage limit margin further, thereby advancing the investment horizon of VAr compensation asset investment at this bus. Even though other individual buses due to the disturbance at bus 3 attract credits but those are smaller in magnitudes resulting in overall costs at this bus. On the other hand, other buses have their respective voltages below the target voltage and as such their lower busbar voltage limits are the ones critical. When injections occur at these buses their respective lower busbar limit margins are increased thereby deferring the VAr compensation asset investments. The same situation holds for bus pairs, buses 6 and 7, buses 5 and 8 and, buses 4 and 9 where buses 7, 8 and 9 attract more the credits than their counterparts, respectively, as is the case as the situation above.

Case 2: This case involves a 1 MVAr nodal withdrawal and secondly a 1 MW nodal withdrawal when circuit reactances are 10 times more than resistance counterparts. Figure 4 and tables 5 and 6 show the nodal LRIC-voltage network charges and the shortest distances for each node from the slack bus during 1 MVAr and 1 MW withdrawals, respectively. In addition, tables 5 and 6 show the initial and final voltages after each withdrawal. On the other hand, figure 5 and tables 7 and 8 show the nodal LRIC-voltage network charges and the shortest distances for each node from the slack bus during 1 MVAr and 1 MW injections, respectively. In addition, tables 7 and 8 show the initial and final voltages after each injection.

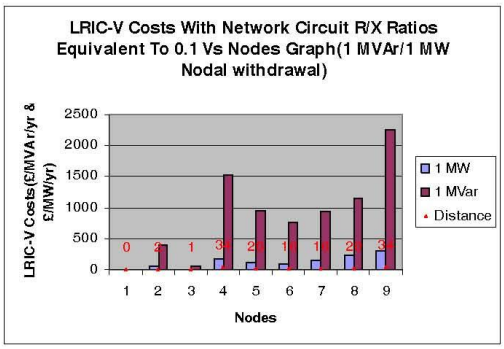

Figure 4: LRIC-voltage network charges due to 1 MVAr and 1MW withdrawal at each node.

Table 5: LRIC-voltage network charges due to 1 MVAr withdrawal at each node

Bus	Initial Voltage(pu)	Final Voltage(pu)	LRIC-V (£/MVAr/yr)	Distance (km)
1	1	1	0	0
2	0.967	0.961	392.2	4
3	0.995	0.989	52.53	3
4	0.990	0.982	1535.32	34
5	0.992	0.988	951.73	20
6	0.994	0.99	765.92	16
7	0.990	0.981	943.03	16
8	0.988	0.979	1154.5	20
9	1.005	0.976	2243.09	34

Table 6: LRIC-voltage network charges due to 1 MW withdrawal at each node

Bus	Initial Voltage(pu)	Final Voltage(pu)	LRIC-V (£/MW/yr)	Distance (km)
1	1	1	0	0
2	0.967	0.966	58.1	4
3	0.995	0.994	6.2	3
4	0.990	0.989	180.83	34
5	0.992	0.992	122.08	20
6	0.994	0.994	88.88	16
7	0.990	0.989	158.92	16
8	0.988	0.986	225.25	20
9	1.005	0.999	314.22	34

Since the circuit reactances dominate the corresponding circuit resistances, it can be observed from figure 4 and tables 5 and 6 that the nodal costs due to 1 MVAr withdrawals are significantly more than those due to 1 MW withdrawals. Generally for both tables 5 and 6, it can also be observed that the costs increase as the nodal distances increase from the slack bus. From bus 2 to bus 8, the initial bus voltages are all less than the target voltage of 1 pu, therefore during the nodal withdrawals the already critical lower bus voltage limits are degraded further and as such those earn costs as the investment horizons for their respective VAr compensation assets are advanced. At bus 9, the initial voltage is more than 1 pu and after withdrawal the

final voltage is less than 1pu. This bus earns credit from 1.005 pu to 1 pu and earns a cost from 1 pu to either 0.999 pu or 0.976 pu. This results in the overall cost at this node a bit reduced.

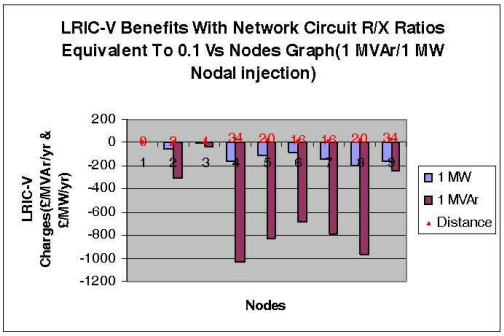

Figure 5: LRIC-voltage network charges due to 1 MVAr and 1 MW injection at each node.

Table 7: LRIC-voltage network charges due to 1 MVAr injection at each node

Bus	Initial Voltage(pu)	Final Voltage(pu)	LRIC-V £/MVAr/yr	Distance (km)
1	1	1	0	0
2	0.967	0.973	-312.32	2
3	0.995	1	-34.29	1
4	0.990	0.999	-1034.2	34
5	0.992	0.996	-830.1	20
6	0.994	0.998	-686	16
7	0.990	0.999	-790.92	16
8	0.988	0.997	-967.39	20
9	1.005	1.032	-239.93	34

Table 8: LRIC-voltage network charges due to 1 MW injection at each node

Bus	Initial Voltage(pu)	Final Voltage(pu)	LRIC-V (£/MW/yr)	Distance (km)
1	1	1	0	0
2	0.967	0.968	-53.84	4
3	0.995	0.996	-5.68	3
4	0.990	0.991	-161.84	34
5	0.992	0.993	-115.95	20
6	0.994	0.994	-84.48	16
7	0.990	0.991	-142.71	16
8	0.988	0.989	-203.7	20
9	1.005	1.01	-163.79	34

Since the circuit R/X ratio remains the same as before, it can be observed from figure 5 and tables 7 and 8 that the nodal costs due to 1 MVAr withdrawals are significantly more than those due to 1 MW withdrawals. Generally for both tables 7 and 8, it can also be observed that the costs increase as the nodal distances increase from the slack bus. From bus 2 to bus 8, the initial bus voltages are all less than the target voltage of 1 pu, therefore during the nodal injections the critical lower bus voltage limit margins are increased and as such those earn credits as the investment horizons for their respective VAr compensation assets are deferred. At bus 9, the initial voltage is more than 1 pu and after injection the final voltage is further increased thereby reducing the already critical higher bus voltage limit margin. This bus earns a cost as the investment horizon of the VAr compensation asset at this bus is advanced further into the future. The overall result for both 1 MVar and 1 MW injections at bus 9 is the reduced overall credit as other buses earn credits due to perturbations on this bus. For both 1 MVar and 1 MW injections the credits earned at bus 9 are less than those earned at bus 4.

Case 3: This case involves a 1 MVAr nodal withdrawal and secondly a 1 MW nodal withdrawal when circuit resistances are 10 times more than reactance counterparts. Figure 6 and tables 9 and 10 show the nodal LRIC-voltage network charges and the shortest distances for each node from the slack bus during 1 MVAr and 1 MW withdrawals, respectively. In addition, tables 9 and 10 show the initial and final voltages after each withdrawal. On the other hand, figure 7 and tables 11 and 12 show the nodal LRIC-voltage network charges and the shortest distances for each node from the slack bus during 1 MVAr injection and secondly 1 MW injection, respectively. In addition, tables 11 and 12 show the initial and final voltages after each injection.

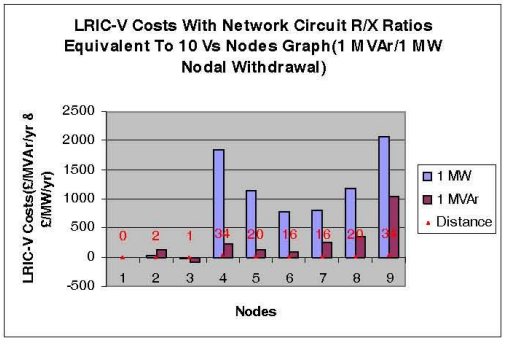

Figure 6: LRIC-voltage network charges due to 1 MVAr and 1 MW withdrawal at each node.

Table 9: LRIC-voltage network charges due to 1 MVAr withdrawal at each node

Bus	Initial Voltage(pu)	Final Voltage(pu)	LRIC-V (£/MVAr/yr)	Distance (km)
1	1.03	1.03	0	0
2	0.992	0.987	137.37	4
3	1.021	1.015	-94.26	3
4	0.975	0.974	224.78	34
5	0.986	0.986	141.04	20
6	0.996	0.996	99.44	16
7	0.992	0.986	241	16
8	0.982	0.976	348.2	20
9	0.989	0.969	1029.95	34

Table 10: LRIC-voltage network charges due to 1 MW withdrawal at each node

Bus	Initial Voltage(pu)	Final Voltage(pu)	LRIC-V (£/MW/yr)	Distance (km)
1	1.03	1.03	0	0
2	0.992	0.991	25.69	4
3	1.021	1.02	-18.39	3
4	0.975	0.968	1839.58	34
5	0.986	0.983	1136.16	20
6	0.996	0.993	774.75	16
7	0.992	0.988	808.91	16
8	0.982	0.978	1185.99	20
9	0.989	0.978	2072.22	34

Since the circuit resistances dominate the corresponding circuit reactances, it can be observed from figure 6 and, tables 9 and 10 that the nodal costs due to 1 MW withdrawals are significantly more than those due to 1 MVAr withdrawals. Generally from both tables 9 and 10, it can also be observed that the costs increase as the nodal distances increase from the slack bus. For both 1 MVAr and 1 MW withdrawals, it can be seen that at bus 3 a credit is attracted since voltage there is more than the target voltage of 1 pu and that means that the higher voltage limit is critical. Due to this latter fact, during withdrawal at this bus, the higher voltage limit margin is increased from 1.021 pu to 1.02 pu thereby a credit has to be earned as a reward and thereby contributing to the overall credit at the bus.

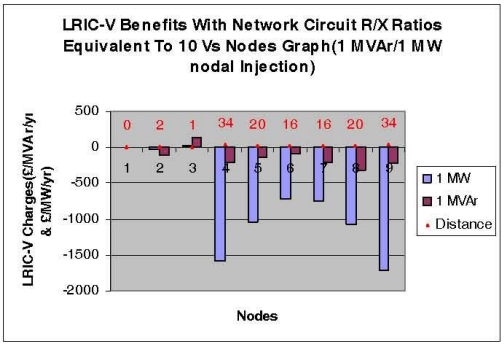

Figure 7: LRIC-voltage network charges due to 1 MVAr and 1MW injection at each node.

Table 11: LRIC-voltage network charges due to 1 MVAr injection at each node

Bus	Initial Voltage(pu)	Final Voltage(pu)	LRIC-V (£/MVAr/yr)	Distance (km)
1	1.03	1.03	0	0
2	0.992	0.997	-112.8	4
3	1.021	1.026	130.91	3
4	0.975	0.976	-206.96	34
5	0.986	0.987	-136	20
6	0.996	0.996	-96	16
7	0.992	0.998	-207.58	16
8	0.982	0.987	-311.43	20
9	0.989	1.009	-224.27	34

Table 12: LRIC-voltage network charges due to 1 MW injection at each node

Bus	Initial Voltage(pu)	Final Voltage(pu)	LRIC-V (£/MW/yr)	Distance (km)
1	1.03	1.03	0	0
2	0.992	0.993	-23.81	4
3	1.021	1.022	19.23	3
4	0.975	0.982	-1579.55	34
5	0.986	0.989	-1039.63	20
6	0.996	0.999	-723.36	16
7	0.992	0.996	-748.78	16
8	0.982	0.986	-1077.78	20
9	0.989	1	-1705.54	34

During nodal injections, it is also observed that the credits consequent to 1 MW injections are more than the credits due to their 1 MVAr injection counterparts since the R/X ratio remain unchanged. It can further be observed that the credits increase as the nodal distances increase from the slack bus as can be observed from figure 7 and, tables 11 and 12. Bus 3 attracts an overall cost for both injections of real and reactive power since the initial voltage at this bus is more than the target voltage of 1 pu and therefore during injection the voltage increases as such degrading the already critical higher bus voltage limit margin further, thereby advancing the investment horizon of VAr compensation asset investment at this bus. During 1 MVAr injection at bus 9, from voltage 0.989 pu to 1 pu, this bus earns a credit and from 1 pu to 1.009 pu this bus attracts a cost and as such the overall credit at this bus is reduce and it is consequently less than credit earned at bus 8. On the other hand, during 1 MW injection at bus 9, from 0.989 pu to 1 pu this bus earn a credit and this results in bus 9 earning the largest credit than any other bus.

IV. CONCLUSIONS

This paper analyses the trend of LRIC-voltage charges on a network, providing insights into how charges will change with different circuit R/X ratios on the network. The different network circuit R/X ratios are meant to establish a network practical representation which ranges from transmission to distribution systems.

The long-run incremental cost (LRIC)-voltage network charging principle is utilized to price the cost of the network for keeping the voltages within statutory limits. This charging principle is based on spare nodal voltage capacity or headroom of an existing network (distribution and transmission systems) to provide the time to invest in reactive power (VAr) compensation devices. The resulting network voltage charging model is able to provide forward-looking economic signals, reflecting the extent of the impact to busbar voltages by a connected party, i.e. whether they accelerate or delay the need for future network compensation devices. These economic messages will in turn influence generation/demand in order to minimize the cost of future investment in VAr compensation.

This analysis was performed on a practical 9-bus network. The major findings are summarized as follows:

) when circuit reactances dominate their resistance counterparts in a network, the charges due to reactive power withdrawals/injections are significantly larger than the corresponding charges due to real power therefore charges due to real power withdrawals/injections can be neglected

2) when circuit reactances and their resistance counterparts in a network are comparable, the charges due to reactive power withdrawals/injections are comparable to the corresponding charges due to real power therefore both types of charges should be considered

3) when circuit resistances dominate their reactance counterparts in a network, the charges due to real power withdrawals/injections are significantly larger than the corresponding charges due to reactive power therefore charges due to reactive power can be neglected

The conclusions drawn from this study can be used in future particularly in the next phase of LRIC-voltage network charging principle which involves the integration of the reactive power planning (RPP) problem with the LRIC pricing approach as the most practical approach to employ. Moreover the study has given an insight into how to realize correct price signals for networks ranging from transmission to distribution systems.

V. REFERENCES

[1] S. K. Parida, S. N. Singh, S. C. Srivastava, "A Value Based Approach towards Reactive Power Cost allocation".

[2] Furong Li, N.P. Padhy, Ji Wang and B. Kuri, "Cost-Benefit Reflective Distribution Charging Methodology", IEEE Trans. Power Systems, Vol. 23, no. 1, pp. 58 – 64, Feb. 2008.

[3] S. Hao, A. Papalexopoulos, "Reactive power pricing and management", IEEE Transactions on Power Systems, Volume 12, no. 1, pp. 95-104, Feb. 1997.

[4] D. Chattopadhyay, K. Bhattacharya, J. Parikh, "Optimal reactive power planning and its spot-pricing: an integrated approach", IEEE Transactions on Power Systems, Volume 10, no. 4, pp. 2014 – 2020, Nov.1995.

[5] K.K. Mandal, B. Kar, D. Pal, M. Basu, N. Chakraborty, "Reactive Power Pricing in a Deregulated Electricity Industry", Power Engineering Conference-7th International, Volume 2, no. 9110484, pp. 853-858, Dec. 2005.

[6] J. Zhong and K. Bhattacharya, "Toward a competitive market for reactive power", IEEE Trans. Power Systems, Vol.17, no.4, pp.1206–1215, Nov.2002.

[7] V.M. Dona and A.N. Paredes, "Reactive power pricing in competitive electric markets using the transmission losses function", IEEE Porto Power Tech Proceedings, Vol. 1, pp. 6,10-13Sept.2001.

[8] Y. Dai, Y.X. Ni, F.S. Wen and Z.X. Han, "Analysis of reactive power pricing under deregulation", IEEE Power Engineering Society Summer Meeting, Vol. 4, pp. 2162 – 2167, 16-20 July 2000.

[9] V. Cataliotti, M.G. Ippolito, F. Massaro, G.Pecoraro and E.R. Sanseverino, "A New Method for the Price Determination of the Reactive Power Supply", UPEC '06. Proceedings of the 41st International Universities Power Engineering, Vol. 1, pp. 242 – 246, 6-8 Sept. 2006.

[10] J.D. Weber, T.J. Overbye, P.W. Sauer and C.L. DeMarco, "A simulation based approach to pricing reactive power", Proceedings of the Thirty-First Hawaii International Conference System Sciences, Vol. 3, pp. 96 – 103, 6-9 Jan. 1998.

[11] A.D. Papalexopoulos and G.A. Angelidis, "Reactive power management and pricing in the California market", IEEE Mediterranean MELECON Electrotechnical Conference, pp.902–905,16-19May 2006.

[12] K.L. Lo and Y.A. Alturki, "Towards reactive power markets. Part 1: reactive power allocation", IEE Proceedings, Generation, Transmission and Distribution, Vol. 153, no. 1, pp. 59 – 70, 12 Jan. 2006.

[13] M.L. Baughman, S.N. Siddiqi, "Real-time pricing of reactive power: theory and case study results", IEEE Transactions on Power Systems, Volume 6, no. 1, pp.23-29, Feb.1991.

[14] J.W. Lamont and J. Fu, "Cost analysis of reactive power support", IEEE Trans. Power Systems,Vol.14, no.3, pp.890–898,Aug.1999.

[15] Furong Lu and E. Matlotse, "Long-Run Incremental Cost Pricing Based on Nodal Voltage Spare Capacity", IEEE Power and Energy Society General Meeting, pp. 1 – 5, 20-24 July 2008.

VI. BIOGRAPHIES

Edwin Matlotse was born in Taung, South Africa in 1969. He received BEng in Electrical and Electronic Engineering at the University of Botswana, Botswana, in 1995 and an MSc in Electrical Power at the Bath University, U.K., in 2001.

Currently, he is pursuing a PhD degree in Electrical Engineering at the Bath University. His major research interest is in the area of system voltage study, analysis and power system economics.

Furong Li (M'2000) was born in Shannxi, China. She received her B.Eng. in Electrical Engineering from Hohai University, China in 1990, and her Ph.D in 1997 with a thesis on Applications of Genetic Algorithms in Optimal Operation of Electrical Power Systems at the university of liverpool. She is a Senior Lecturer with the Power and Energy Systems Group at the University of Bath. Her major research interest include alternative energy generation and its impacts to energy (transmission and distribution) networks, power system planning, operation and management considering uncertainty from intermittent generation, power system analysis (fault current and power quality), power system economics (energy and ancillary market) and network charging methodologies for the use of transmission and distribution networks.

Bibliography

[1] Pilgrim J.D., "Genetic Algorithm for optimal reactive power compensation planning on the national grid system", PhD thesis, Bath University-Bath, 2002.

[2] Williams P. and Andrews P., "Distribution Network Connection: Charging Principles and Options", Department of Trade and Industry (DTI)-UK, 2002.

[3] Charging Team, "The Statement of the Use of System Charging Methodology", National Grid, June 2007.

[4] Northern Electric Distribution Ltd (NEDL), "Use of System Charging Methodology," April 2007.

[5] Western Power Distribution (WPD), "The Statement of the Use of System Charging Methodology", April 2007.

[6] Wang Ji, "Long-Run Marginal Cost Pricing Methodologies in Open Access Electricity Networks", PhD thesis, Bath University-Bath, Feb. 2007.

[7] Ferreira P.J.A., "On the efficiency of the Argentinean Electricity Wholesale Market", http://www.econ.puc_rio.br/PDF/seminario/electr-argentina.pdf, May 2002.

[8] London Business School, "Cross Border Electricity Trading and Market Design: The England-France Interconnector", http://personal.lse.ac.uk/inderst/IFA-case.pdf.

[9] Weedy B.M., "Electrical Power Systems", John Wiley and Sons, 3rd revised edition, 1987.

[10] Saadat H., "Power System Analysis", McGraw-Hill Companies, 1999.

[11] Chebbo et al., "Combined active and reactive dispatch Part 1: Problem formulation and solution algorithm", IEE Proceedings – Generation, Transmission and Distribution, 142(4), pp. 393-400, July 1995.

[12] Shirmohammadi D., Rajagopalan C., Alward E. R. and Thomas C. L., "Cost of transmission transactions: an introduction," IEEE transactions on power systems, Vol. 6, No. 4, PP. 1546-1560, Nov. 1991.

[13] Furong Li, Padhy N.P., Wang Ji and Kuri B., "Cost-Benefit Reflective Distribution Charging Methodology", IEEE Trans. Power Systems, Vol. 23, no. 1, pp. 58 – 64, Feb. 2008.

[14] Chattopadhyay D., Bhattacharya K.and Parikh J., "Optimal reactive power planning and its spot-pricing: an integrated approach", IEEE Transactions on Power Systems, Volume 10, no. 4, pp. 2014 – 2020, Nov.1995.

[15] Baughman M.L.and Siddiqi S.N., "Real-time pricing of reactive power: theory and case study results", IEEE Transactions on Power Systems, Volume 6, no. 1, pp.23-29, Feb.1991.

[16] Berg S.V., Adams J. and Niekum B., "Power factors and the efficient pricing and production of reactive power", The Energy Journal, Vol. 4, pp. 93-102.

[17] Schweppe F.C., Caramanis M.C., Tabors R.D. and Bohn R.E., "Spot pricing of electricity", Kluwer Academic Publishers, 1988.

[18] Muchayi M. and El-Hawary M.E., "A summary of algorithms in reactive power pricing", Canadian Conference on Electrical and Computer Engineering, Vol. 2, pp. 692 – 696, 5-8 Sept. 1995.

[19] Walker S., Hipel K.W. and Inohara T.,"Strategic analysis of the Kyoto Protocol", IEEE International Conference on Systems, Man and Cybernetics, pp.1806 – 1811, 7-10 Oct, 2007

[20] Yu-Tzu Chiu, "Russia and Canada to ratify Kyoto Protocol", IEEE Spectrum, Vol. 39, no. 10, pp. 22 – 23, Oct. 2002.

[21] Mech A.Z. and Rouse S., "Macro and Micro Economic Principles of the Kyoto Protocol Result - Making Money", IEEE-EIC Climate Change Technology, pp.1 – 2, 10-12 May 2006.

[22] Rahman T.K.A., Rahim S.R.A. and Musirin I.,"Optimal allocation and sizing of embedded generators", Power and Energy Conference, pp. 288 – 294, 29-30 Nov, 2004.

[23] Lin Chen, Jin Zhong and Deqiang Gan, "Reactive power planning and its cost allocation for distribution systems with distributed generation", IEEE Power Engineering Society General Meeting, pp. 6, 2006.

[24] UK Government Planning Policy Statement 22: Renewable Energy, The Government Objectives, http://www.greenspec.co.uk/documents/drivers/PlanningState22.pdf.

[25] Hao S. and Papalexopoulos A., "Reactive power pricing and management", IEEE Transactions on Power Systems, Volume 12, no. 1, pp. 95-104, Feb. 1997.

[26] Mandal K.K., Kar B., Pal D., Basu M. and Chakraborty N., "Reactive Power Pricing in a Deregulated Electricity Industry", Power Engineering Conference-7th International, Vol. 2, no. 9110484, pp. 853-858, Dec. 2005.

[27] Zhong J. and Bhattacharya K., "Toward a competitive market for reactive power", IEEE Trans. Power Systems, Vol.17, no.4, pp.1206–1215, Nov.2002.

[28] Dona V.M. and Paredes A.N., "Reactive power pricing in competitive electric markets using the transmission losses function", IEEE Porto Power Tech Proceedings, Vol. 1, pp. 6,10-13Sept.2001.

[29] Dai Y., Ni Y.X., Wen F.S. and Han Z.X., "Analysis of reactive power pricing under deregulation", IEEE Power Engineering Society Summer Meeting, Vol. 4, pp. 2162 – 2167, 16-20 July 2000.

[30] Cataliotti V., Ippolito M.G., Massaro F., Pecoraro G. and Sanseverino E.R., "A New Method for the Price Determination of the Reactive Power Supply", UPEC '06. Proceedings of the 41st International Universities Power Engineering, Vol. 1, pp. 242 – 246, 6-8 Sept. 2006.

[31] Weber J.D., Overbye T.J., Sauer P.W. and DeMarco C.L., "A simulation based approach to pricing reactive power", Proceedings of the Thirty-First Hawaii International Conference System Sciences, Vol. 3, pp. 96 – 103, 6-9 Jan. 1998.

[32] Papalexopoulos A.D. and Angelidis G.A., "Reactive power management and pricing in the California market", IEEE Mediterranean MELECON Electrotechnical Conference, pp.902–905,16-19May 2006.

[33] Lo K.L. and Alturki Y.A., "Towards reactive power markets. Part 1: reactive power allocation", IEE Proceedings, Generation, Transmission and Distribution, Vol. 153, no. 1, pp. 59 – 70, 12 Jan. 2006.

[34] Baughman M.L. and Siddiqi S.N., "Real-time pricing of reactive power: theory and case study results", IEEE Transactions on Power Systems, Volume 6, no. 1, pp.23-29, Feb.1991.

[35] Lamont J.W. and Fu J., "Cost analysis of reactive power support", IEEE Trans. Power Systems,Vol.14, no.3, pp.890–898,Aug.1999.

[36] "Electricity distribution licence - full set of consolidated SLCs", http://epr.ofgem.gov.uk/index.php?pk=doc380969, the Office of Gas and Electricity Markets (OFGEM), U.K., last review at 02 Jan. 2007.

[37] Shirmohammadi et al., "Some fundamental technical concepts about cost based transmission pricing", IEEE transactions on power systems, 11(2), pp. 1002-1008, 1996.

[38] Sood Y. R., Padhy N. P. and Gupta, H. O., "Wheeling of Power under Deregulated Environment of Power System: A Bibilographical Survey", IEEE Power Engineering Review, 7(22), pp. 58 – 58, July 2002.

[39] Yu C.W. and David A.K., "Pricing transmission services in the context of industry deregulation", IEEE transactions on power systems, 1(12), pp. 503 – 510, Feb. 1997.

[40] Kovacs R.R. and Leverett A.L., "A load flow based method for calculating embedded, incremental and marginal cost of transmission capacity", IEEE transactions on power systems, pp. 272-278, 9(1), 1994.

[41] Muchayi M. and El-Hawary M.E., "Wheeling rates evaluation using optimal power flows", IEEE Electrical and Computer Engineering Canadian Conference, (1), pp. 389 – 392, 24-28 May 1998.

[42] Li Y.Z. and David A.K., "Wheeling rates of reactive power flow under marginal cost pricing, Power Systems", IEEE transactions on power systems, 3(9), pp. 1263 – 1269, Aug. 1994.

[43] Caramanis M.C., Roukos N. and Schweppe F.C., "WRATES: a tool for evaluating the marginal cost of wheeling", IEEE transactions on power systems, 2(4), pp. 594 – 605, May 1989.

[44] Merrill H.M. and Erickson B. W., "Wheeling Rates Based on Marginal-Cost Theory", IEEE Power Engineering Review, 11(9), pp. 39 – 40, Nov. 1989.

[45] Li Y.Z. and David, A.K., "Pricing reactive power conveyance, Generation, Transmission and Distribution", [see also IEE Proceedings-Generation, Transmission and Distribution], IEE Proceedings C, 3(140), pp. 174 – 180, May 1993.

[46] Happ H.H., "Cost of wheeling methodologies", IEEE transactions on power systems, 9(1), pp. 147-156, 1994.

[47] Furong Li et al., "Network Benefits from Introducing An Economic Methodology for Distribution Charging", Study commissioned by Ofgem, Bath University, 2005. www.ofgem.gov.uk/**NETWORK**S/ELECDIST/POLICY/.../12617-1206a.pdf

[48] Jing et al., "Review of transmission fixed costs allocation methods", IEEE PES General Meeting, 2003.

[49] Tabors R.D., "Transmission system management and pricing: new paradigms and international comparisons", IEEE transactions on power systems, 9(1), pp. 206-215, 1994.

[50] Yu C., "Long-run marginal cost based pricing of interconnected system wheeling", Electric power systems research, 50(3), pp. 205-212, 1999.

[51] Bakirkzis et al, "Comparison of two methods for long-run marginal cost-based transmission use-of-system pricing", IEEE Generation, Transmission and Distribution Proceedings, 148(5), pp. 477-481, 2001.

[52] Heng H., "Electrical Distribution Network Pricing", MPhil/PhD thesis, Bath University, Bath, 2007.

[53] Charging Team, "The Statement of the Use of System Charging Methodology", National Grid, April 2007.

[54] Zhang et. al., "Neta Approach of Power Transmission Pricing and Its Tryout in Northeastern Power Grid of China", IEEE/PES Transmission and Distribution Conference and Exhibition: Asia and Pacific, 2005.

[55] Lima et al., "Distribution Pricing Based on Yardstick Regulation", IEEE transactions on power systems, vol. 22, no. 1, pp. 68-68, 2000.

[56] Lima J.W.M. and Tanure J.E.S., "Quality of electric supply: Incentives and penalties", Budapest Power Tech. Proc, Budapest-Hungary", Paper BPT99-037-24, Oct. 1999.

[57] Green R., "Electricity transmission pricing: an international comparison, Utilities Policy Transmission Pricing", 6(3), pp.177-184, 1997.

[58] Gronli H., Roma T.G.S. and Marnay C., "TRANSMISSION GRID ACCESS AND PRICING IN NORWAY, SPAIN AND CALIFORNIA – A COMPARITIVE STUDY", Power Delivery Europe, Madrid-Spain, 28-30 September 1999.

[59] Gribik P.R., Angelidis G.A. and Kovacs R.R., "Transmission access and pricing with multiple separate energy forward markets", IEEE transactions on power systems, 14(3), pp. 865-876, 1999.

[60] Braten J., "Transmission Pricing in Norway, Utilities Policy Transmission Pricing", 6(3), pp. 219-226, 1997.

[61] Rudnick H., Soto M. and Palma R., "Use of system approaches for transmission open access pricing", International Journal of Electrical Power & Energy Systems, 21(2), pp. 125-135, 1999.

[62] DLT Consultancy, "Attributes of prospective Distribution Charging Methodologies", http://www.energynetworks.org/spring/regulation/cms02/CMDocuments/contentManDoc_125_b5e54a15-0241-4ebf-81d3-b0e3b403fc42.pdf, Ena COG Workshop, april 2006

[63] Furong Li and Matlotse E., "Long-run incremental cost pricing based on nodal voltage spare capacity**",** IEEE PES General Meeting, pp. 1-5**,** 20-24 July 2008.

[64] "IEEE 14 Bus Test Data", Avalable:http://www.ee.washington.edu

[65] Furong Li and Tolley D.L.,"Long-Run Incremental Cost Pring Based on Unused Capacity", IEEE Transactions on Power Systems, Vol. 22, no. 4, pp. 1683 – 1689, Nov.2007.

[66] Western Power Distribution (WPD) website.

[67] "System Voltage", Available: http://www.westernpower.co.uk/Information-for-Electrical_Installers/Connection-Characteristics/System-Voltage.aspx

[68] Western Power Distribution (WPD), "The Statement of the Use of System Charging Methodology", April 2007.

[69] "Use of System Charging Methodology", Central Networks East, ttp://www.eon-k.com/downloads/CN_East_UoS_methodology_statement_Apr08.pdf, 7th April 2008.

[70] "Statement of charges for use of Scottish Hydro Electric Power Distribution PLC's Electricity Distribution Network", Scottish Hydro Electric Power Distribution plc, http://www.ssepd.co.uk, 1st April 2008.

[71] Berg S.V., Adams J. and Niekum B., "Power factors and the efficient pricing and production of reactive power", The Energy Journal, Vol. 4, pp. 93-102.

[72] The Statement of the Use of System Charging Methodology, The Charging Team. National Grid, U.K. [Online]. Available: http//www. nationalgrid.com/uk/indifo/charging/pdfs.UoSC_Apr_03_(I3R0).pdf.

[73] Hui Yi Heng, Furong Li and Xifan Wang, **"**Charging for Network Security Based on Long-Run Incremental Cost Pricing", IEEE Trans. Power Syst., vol. 24, no. 4, pp. 1686–1693, Nov. 2009.

[74] Strbac G. and Jenkins N., Network Security of the Future UK Electricity System, PIU, U.K., 2001. [Online]. Available: http://www.tyndall. uea.ac.uk /research/theme2/Network_Security_UMIST.pdf.

[75] Mutale J., Strbac G., and Pudjianto D., "Methodology for cost reflective pricing of distribution networks with distributed generation," in Proc. IEEE Power Eng. Soc. General Meeting, 2007.

[76] Pudjianto D., Strbac G. and Mutale J., "Access and pricing of distribution network with distributed generation," in Proc. IEEE Power Eng. Soc. General Meeting, 2007.

[77] Matlotse E. and Furong Li, "Long-run incremental cost pricing for the use of network reactive power compensation devices for systems with different R/X ratios", IEEE PES General Meeting, pp. 1-8**,** 26-30 July 2009.

[78] Blazic B. and Papic I., "Voltage profile support in distribution networks-influence of the network R/X ratio", EPE-PEMC, pp. 2510-2515, 1-3 Sept. 2008.

[79] Hsiao-Dong Chiang, Cheng-Shan Wang, Flueck, A.J., "Look-ahead voltage and load margin contingency selection functions for large-scale power systems" IEEE Trans. Power Systems", Vol. 12, no. 1, pp. 173 – 180, Feb. 1997.

[80] Pama A., Radman G**.,** "A new approach for estimating voltage collapse point based on quadratic approximation of PV-curves" Electric Power Systems Research 79, www.elsevier.com/com/locate/epsr.

[81] Durairaj S., Devaraj and Kannan P.S., "Improved Genetic Algorithm Approach for Multi-Objective contingency constrained Reactive Power Planning", IEEE INDICON, pp. 510 – 515, 11-13 Dec. 2005.

[82] Gopalakrishnan V., Thirunavukkarasu P. and Prasanna R., "Reactive power planning using hybrid evolutionary programming method", IEEE PES Conference and Exposition, vol.3, pp.1319 – 1323, 10-13 Oct. 2004.

[83] Barot H. and Bhattacharya K., "Optimal Reactive Power Planning and Compensation Effects on Transmission Loss Components", IEEE PES General Meeting, pp.1 – 7, 24-28 June 2007.

[84] Chao-Rong C., Hang-Sheng L. and Wenta T., "Optimal Reactive Power Planning Using Genetic Algorithm", IEEE International Conference on Systems, Man and Cybernetics, Vol. 6, pp. 5275 – 5279, 8-11 Oct. 2006.

[85] Thirunavukkarasu P., Prasanna R. and Victoire T.A.A., "Reactive power planning using hybrid method", PowerCon Power System Technology, vol. 2, pp. 1694 – 1698, 21-24 Nov. 2004.

[86] Levi V.A., Popovic D.S.,Levi V.A. and Popovic D.S., "Integrated methodology for transmission and reactive power planning", IEEE Trans. Power Systems, vol. 11, no. 1, pp. 370 – 375, Feb. 1996.

[87] Levi V.A. and Popovic D.S., "Integrated methodology for transmission and reactive power planning", IEEE Power Industry Computer Application Conference, pp. 284 – 289, 7-12 May 1995.

[88] Wenjuan Z., Fangxing Li and Tolbert L.M., "Review of Reactive Power Planning: Objectives, Constraints, and Algorithms", IEEE Trans. Power Systems, vol. 22, no.1, pp. 2177 – 2186, Nov. 2007.

[89] Lee K.Y. and Yang F.F., "Optimal reactive power planning using evolutionary algorithms: a comparative study for evolutionary programming, evolutionary strategy, genetic algorithm, and linear programming", IEEE Trans. Power Systems, vol.13, no. 1, pp. 101 - 108, Feb. 1998.

[90] Behnke M. and Ellis A., "Reactive power planning for wind power plant interconnections", IEEE Power and Energy Society General Meeting, pp. 1 – 4, 20-24 July 2008.

[91] Wenjuan Z., Fangxing Li and Tolbert L., "Review of reactive power planning: objectives, constraints, and algorithms", T&D. IEEE/PES Conference and Exposition, pp. 1, 21-24 April 2008.

[92] Wenjuan Z. and Tolbert L.M., "Survey of reactive power planning methods", IEEE PES General Meeting, vol. 2, pp. 1430 – 1440, 12-16 June 2005.

[93] Lo K.L., Alammari R., El-Khatroushi H. and Tumay M., "Reactive power planning incorporating system security", Electrotechnical Conference, vol. 3, pp. 1567 – 1570, 13-16 May 1996.

[94] Lee K. Y., Ortiz J. L., Park Y. M. and Pond L. G., "An Optimization Technique for Reactive Power Planning of Subtransmission Network under Normal Operation", IEEE Trans. Power Systems, vol.1, no. 2, pp. 153 - 159, May 1986.

[95] Eghbal M., Yorino N., El-Araby E.E. and Zoka, Y., "Multi-load level reactive power planning considering slow and fast VAR devices by means of particle swarm optimisation" IET Generation, Transmission & Distribution, vol.2, no. 5, pp. 743 – 751, , Sep. 2008.

[96] Hauth et al, "The role and benefits of static VAr systems in high voltage power system applications", IEEE Transactions on Power Apparatus and Systems, 101(10) pp. 3761-3770, October 1982.

[97] Byerly et al, "Static reactive power compensation for power transmission systems", IEEE Transactions on Power Apparatus and Systems, PAS-101(10):3761-3770, October 1982.

[98] Johns, A.T. and Song Hua, Y., "Flexible ac transmission systems (FACTS)", The Institution of Electrical Engineers, series 30, 1999.

[99] Pilgrim J.D., Li F. and Aggarwal R.K., "SVCs and SVC siting techniques: Literature synopsis", UPEC 99, Department of Engineering, University of Leicester, Leicester, UK, pp. 115-118, 1999.

[100] Cook R.F., "Analysis of capacitor application as affected by load cycle", AIEE Transactions, pt. III-A Power Apparatus and Systems, pp. 950-957, October 1959.

[101] Cook R.F., "Optimizing the application of shunt capacitors for reactive-volt-ampere control and loss reduction", AIEE Transactions, pt. III-A Power Apparatus and Systems, pp. 430-442, August 1961.

[102] Heydt G.T. and Grady W.M., "A matrix method for optimal VAr siting", IEEE Trans. Power Apparatus and Systems, pp. 1214-1220, July 1975.

[103] Happ H.H. and Wirgau K.A., "Static and dynamic compensation in systems planning", IEEE Trans. Power Apparatus and Systems, pp. 1564-1577, Sept./Oct. 1978.

[104] Aoki K., Fan W. and Nishikori A., "Optimal VAr planning by approximation method for recursive mixed-integer linear programming", IEEE Trans. Power Systems, 3(4), pp. 1741-1747, Nov. 1988.

[105] Opuku G., "Optimal power system VAr planning", IEEE Trans. Power Systems, 5(1), pp. 53-59, Feb.1990.

[106] Ahmed S., Strbac L.Z., Dixon A., Chebbo A. and Ekwue A., "Allocation of reactive support in a competitive environment", 13th PSCC, pp. 368-374, Trondhiem, June 1999.

[107] Lee K.Y., Ortiz J.L., Park Y.M. and Pond L.G., "An optimization technique for reactive power planning of subtransmission network under normal operation", IEEE Trans. Power Systems, 1(2), pp. 153-169, May 1986.

[108] Lie T.T. and Deng W., "Optimal flexible AC transmission systems (facts) devices allocation", Electrical Power & Energy Systems, 19(2), pp. 125-134, 1997.

[109] Jwo W.S., Liu C.W., Liu C.C. and Hsiao Y.T., "Hybrid expert system and simulated annealing approach to optimal reactive power planning", IEE Proceedings - Generation, Transmission and Distribution, 142(4), pp. 381-385, July 1995.

[110] Chen Y.L. and Liu C.C., "Multiobjective VAr planning using the goal attainment method", IEE Proceedings - Generation, Transmission and Distribution, 142(3), pp. 227-232, May 1994.

[111] Chang C.S. and Huang J.S., "Optimal multiobjective SVC planning for voltage stability enhancement", IEE Proceedings - Generation, Transmission and Distribution, 145(2), pp. 203-209, March 1998.

[112] Nara K., Hayashi Y., Ikeda K. and Ashizawa T., "Application of tabu search to optimal placement of distributed generator", IEEE – PES 2001 Winter Meeting, Columbus, Ohio, USA, Jan. 2001.

[113] Mori H., "Optimal allocation of FACTS devices in distribution systems", IEEE Power and Energy Systems, Winter Meeting, 2001.

[114] Holland J.H., "Adaption in Natural and Artificial Systems", University of Michigan Press, Ann Arbor, 1975.

[115] Iba K., "Optimal VAr allocation by genetic algorithm", IEEE Conference on Neural Networks, pp. 163-168, 1993.

[116] Lai L.L. and Ma J.T., "Application of evolutionary programming to reactive power planning – comparison with nonlinear programming approach", IEEE Trans. Power Systems, 12(1), Feb. 1998.

[117] Lai L.L. and Ma J.T., "New approach of using evolutionary programming to reactive power planning with network contingencies", European Transactions – Electrical Power, 7(3), pp. 211-216, May/June 1997b.

[118] Lee K.Y. and Yang F.F., "Optimal reactive power planning using evolutionary algorithms: A comparative study for evolutionary programming, evolutionary strategy, genetic algorithm and linear programming", IEEE Trans. Power Systems, 13(1), Feb. 1998.

[119] Abdullah W.N.W., Saibon H., Mohd A.A. and Lo K.L., "Optimal capacitor placement using genetic algorithm", IPEC, pp. 18-23, Singapore, May 1997.

[120] Chung T.S. and Leung H.C., "A genetic algorithm approach in optimal capacitor selection with harmonic distortion considerations", Electrical Power and Energy Systems, 21, 1999.

[121] Kalyuzhny A., Levitin G., Elmakis D. and Ben-Haim H., "System approach to shunt capacitor allocation in radial distribution systems", Electric Power Systems Research, 56, 5160, 2000.

[122] Delfanti M., Granelli G.P., Marannino P. and Montagna M., "Optimal capacitor placement using deterministic and genetic algorithms", IEEE Trans. Power Systems, 15(3), pp. 1041-1046, Aug. 2000.

[123] Lee K.Y., Ortiz J.L., Park Y.M. and Pond L.G., "An optimisation technique for reactive power planning of subtransmission network under normal operation", IEEE Trans. Power Systems, PWRS-1(2), pp. 153-169, May 1986.

[124] Mantovani J.R.S., Modesto S.A.G. and Garcia A.V., "VAr planning using genetic algorithm and linear programming", IEE Proceedings – Generation, Transmission and Distribution, 148(3), pp. 257-262, May 2001.

[125] Lagonote et al., "Structural analysis of the electrical system: application to secondary voltage control in France", IEEE Trans. Power Systems, 2(4), pp. 479–486, May 1989.

[126] Irving et al, "Optimal network tearing using simulated annealing", IEE Proceedings C- Generation, Transmission and Distribution, 137(1), pp. 69-72, Jan 1990.

[127] Quintana V.H. and Muller N., "Partitioning of power networks and applications to security control", IEE Proceedings-C, 138(6), pp. 535 – 545, 1991.

[128] Mansour Y., Xu W. and Rinzin C., "SVC placement using critical modes of voltage instability", IEEE Trans. Power Systems, 9(2). pp. 757-763, May 1994.

[129] Bridenbaugh C.J., DiMascio D.A. and D'Auila R., "Voltage control improvement through capacitor and transformer tap optimization", IEEE Trans. Power Systems, 7(1), pp. 222-227, Feb. 1992.

[130] Aoki K., Fan W. and Nishikori A., "Optimal VAr planning by approximation method for recursive mixed-integer linear programming", IEEE Trans. Power Systems, 3(4), pp. 1741-1747, Nov. 1988.

[131] Chung T.S. and Leung H.C., "A genetic algorithm approach in optimal capacitor selection with harmonic distortion considerations", Electrical Power and Energy Systems, 21, 1999.

[132] Chen Y.L., Chang C.W. and Liu C.L., "Efficient methods for identifying weak nodes in electrical power networks", IEE Proceedings – Generation, Transmission and Distribution, 142(3), pp. 317-322, May 1995.

[133] Vaahedi E., Tamby J., Mansour Y., Li W. and Sun D., "Large scale voltage stability constrained optimal VAr planning and voltage stability applications using existing OPF/optimal VAr planning tools", IEEE Trans. Power Systems, 14(1), pp. 65-74, Feb. 1999.

[134] Hauth R.L., Humann T. and Newell, "Application of a static VAr systems to regulate system voltage in western Nebraska", Power Application Systems, PAS-97(5), pp. 1955-1964, Sep./Oct. 1978.

[135] Levitin G., Mazal-Tov S. and Reshef B., "Genetic algorithms for optimal planning of transmission system reactive power compensation under security constraints", 9th Mediterranean Electrotechnical Conference, pp. 897-900, 1998.